



Durham E-Theses

The tribological behaviour of cast iron in inert and reducing gas environments

Murray, I

How to cite:

Murray, I (1984) *The tribological behaviour of cast iron in inert and reducing gas environments*, Durham theses, Durham University. Available at Durham E-Theses Online: <http://etheses.dur.ac.uk/7153/>

Use policy

The full-text may be used and/or reproduced, and given to third parties in any format or medium, without prior permission or charge, for personal research or study, educational, or not-for-profit purposes provided that:

- a full bibliographic reference is made to the original source
- a [link](#) is made to the metadata record in Durham E-Theses
- the full-text is not changed in any way

The full-text must not be sold in any format or medium without the formal permission of the copyright holders.

Please consult the [full Durham E-Theses policy](#) for further details.

THE TRIBOLOGICAL BEHAVIOUR OF CAST IRON IN
INERT AND REDUCING GAS ENVIRONMENTS

The copyright of this thesis rests with the author.
No quotation from it should be published without
his prior written consent and information derived
from it should be acknowledged.

by I. Murray B.Sc

A thesis submitted for the degree of Doctor of Philosophy
in the Department of Engineering,
University of Durham.

January 1984



13. APR. 1984

ACKNOWLEDGEMENTS

The author would like to express his gratitude to Dr. A Unsworth for his advice and support during the last three years, and also to all the other members of the staff of Durham University Engineering Department who have helped throughout this project.

The author would also like to thank ICI plc for their financial support, and particularly Dr. D Summers-Smith and Mr O von Bertele for their kind assistance.

SUMMARY

This project was commissioned as a result of a high number of piston ring failures in reciprocating gas compressors. Two sets of experimental apparatus were built. The first was used to study the effect of oxygen and water content on the unlubricated sliding of cast iron against cast iron, as well as the behaviour of a lubricant in non-oxidising environments. The second apparatus investigated the effect of surface temperature on cast iron sliding against cast iron in the presence of a lubricant in an inert gas environment. Electron spectroscopy for chemical analysis (E.S.C.A.) was also used to study the material surfaces.

The experimental results showed that for unlubricated sliding, the partial pressure of water vapour was more important than either the oxygen content or the water vapour flowrate in preventing high friction and wear. For sliding in the presence of a lubricant it was found important not to exceed a certain transition temperature or scuffing would occur.

Recommendations are made for the successful lubrication of reciprocating gas compressors which include a formula relating the discharge pressure to the minimum partial pressure of water vapour required to prevent scuff. It is also recommended that a gradual 'running in' process is adopted and that cylinder wall temperatures are less than 150°C for compressors operating with a discharge pressure over 160 bar.

CONTENTS

	page
Acknowledgements	ii
Summary	iii
List of Figures	x
List of Tables	xiii
Nomenclature	xiv

CHAPTER 1

INTRODUCTION

1.1	Background	1
1.2	Compressor Characteristics	2
1.3	Problem Compressors	3
1.4	Experimental Work	4
1.5	Aims	5
1.6	Lubrication Types	5
1.7	Piston Ring Lubrication	6

CHAPTER 2

LITERATURE REVIEW

2.1	The Nature of Surfaces	13
	2.1.1 Physically Adsorbed Films	13
	2.1.2 Chemisorbed Films (Chemisorption)	14
	2.1.3 Chemical Reaction Films	14
2.2	Wear	
	2.2.1 Adhesive Wear	15
	2.2.2 Abrasive Wear	17
	2.2.3 Corrosive Wear	18
	2.2.4 Surface Fatigue Wear	18
2.3	Effect of Surface Films on Friction and Wear	19
	2.3.1 Friction of Clean Metals	20
	2.3.2 The Mechanical Removal of Surface Films	20
2.4	Frictional Behaviour of Cast Iron	21
2.5	Graphite Lubrication	25
2.6	Friction and Wear in Inert and Reducing Environments	28

	page
2.7 The influence of Temperature on Scuffing	32
2.8 Lubrication of Reciprocating Gas Compressors	33
2.8.1 Lubricant Selection	33
2.8.2 Oil Consumption	34
2.8.3 Effect of Gas Type	34

CHAPTER 3

EXPERIMENTAL APPARATUS

3.1 No 1 Friction Apparatus	
3.1.1 General Description	47
3.1.2 The Friction Test	48
3.1.3 Environmental Chamber	50
3.1.4 Loading Pistons	51
3.1.5 Force Activating Saddle	52
3.1.6 Probe	53
3.1.7 Reciprocating Mechanism	54
3.1.8 Gas Mixing	55
3.1.9 Friction Measurement	56
3.2 Heated Plate Apparatus	57
3.2.1 Plate Heating	57
3.2.2 Loading	57
3.2.3 Friction Measurement	58
3.3 Gas Analysis	59

CHAPTER 4

METHODS AND MATERIALS

4.1 Calibration of Apparatus	
No 1 Friction Apparatus	
4.1.1 Pneumatic Cylinder (Load)	74
4.1.2 Probe (Friction Force)	74
4.1.3 Pin Temperature (Heated Pin Experiments)	75
4.1.4 Oxygen Analyser	75
4.1.5 Dewpoint Hygrometer	75
4.1.6 Rotameter Calibration	76
4.1.7 Speed (R.P.M.)	76
Heated Plate Apparatus	
4.1.8 Load Calibration	77
4.1.9 Friction Calibration	77
4.1.10 Other Calibrations	77

	page
4.2 Specimen Preparation	78
4.2.1 Plate Specimens	78
4.2.2 Pins	78
4.2.3 Specimen Cleaning	79
Experimental Procedures	
4.3 No 1 Friction Apparatus	80
4.3.1 Specimen Loading	80
4.3.2 Setting Up the Environmental Chamber	81
4.3.3 Starting	82
4.3.4 Unlubricated Experiments	82
4.3.5 Lubricated Experiments	83
4.3.6 End of Test	83
4.3.7 E.S.C.A. Experiments	84
4.4 Heated Plate Apparatus	
4.4.1 Start of Test	86
4.4.2 Single Temperature Experiments	86
4.4.3 Incremented Temperature Experiments	87
4.4.4 End of Test	87
4.5 Lubricants	
4.5.1 No 1 Friction Apparatus	88
4.5.2 Heated Plate Apparatus	88
4.6 Experimental Programme	
No 1 Friction Apparatus, Unlubricated Experiments	
4.6.1 Commissioning Tests	89
4.6.2 Effect of Oxygen Content	89
4.6.3 Effect of Water Content	91
No 1 Friction Apparatus, Lubricated Experiments	
4.6.4 CSB 460	93
4.6.5 Shell Risella	93
4.6.6 Heated Plate Apparatus	93
4.7 Data Reading and Processing	97
4.7.1 X-Y Recorder (manual)	97
4.7.2 A-D Convertor (computer)	97
4.7.3 Data Processing	98

CHAPTER 5EXPERIMENTAL RESULTS

5.1	Calibration Results	103
	<u>No 1 Friction Apparatus</u>	
5.1.1	Friction Probe	103
5.1.2	Proving Ring	104
5.1.3	Piston Calibrations	104
5.1.4	Stainless Steel Vs UHMWP Friction Tests	105
	<u>Heated Plate Apparatus</u>	
5.1.5	Friction Calibration	107
5.1.6	Load Calibration	107
	<u>Unlubricated Experiments</u>	
	<u>No 1 Friction Apparatus</u>	
5.2	Introductory Experiments	108
5.2.1	Friction Measurement and Wear Rate	108
5.2.2	Effect of Cleaning	109
5.2.3	Effect of Surface Finish and Hardness	110
5.2.4	Surface Temperature Measurement	110
5.3	Effect of Oxygen Content	112
5.3.1	Effect of Speed	112
5.3.2	Effect of Total Gas Flowrate	113
5.3.3	Effect of Load	113
5.3.4	Comparison of Air and Oxygen	113
5.4	Effect of Water Content	114
	<u>Inert and Reducing Gases</u>	
5.4.1	Hydrogen	114
5.4.2	Nitrogen	115
5.4.3	Argon	115
	<u>Oxidising Gases</u>	
5.4.4	Mixed Gas (83% N , 12% CO , 5% CO)	116
5.4.5	Carbon Dioxide	117
5.4.6	Air	117
5.4.7	Oxygen	118
5.5	E.S.C.A. Tests	119
5.5.1	Wide Scan	119
5.5.2	Iron	119

	page
5.5.3 Oxygen	119
5.5.4 Carbon	119
5.5.5 Other Tests	120
<u>Lubricated Experiments</u>	
5.6 No 1 Friction Apparatus	121
5.6.1 CSB 460	121
5.6.2 Shell Risella	123
5.6.3 Heated Pin Experiments	124
5.7 Heated Plate Friction Apparatus	126
5.7.1 Shell Risella	127
5.7.2 CSB 460	127
5.7.3 E.P. Oil	127
5.7.4 Tests in Air	128
5.8 Mild Steel	129

CHAPTER 6

DISCUSSION

6.1 Errors of Measurement	163
6.1.1 Oxygen Analyser	163
6.1.2 Dewpoint Hygrometer	163
6.1.3 Gas Purity	164
6.1.4 Measurement of Friction	165
6.1.5 Load Measurement	166
6.1.6 Coefficient of Friction	167
6.1.7 Temperature Measurement (Heated Plate Apparatus)	167
6.2 Effect of Surface Finish and Hardness	168
6.3 Effect of Oxygen Content	169
6.4 Effect of Water Content	174
6.4.1 Detrimental Effect of Oxygen	175
6.4.2 Water Flow Vs Vapour Pressure	176
6.4.3 Effect of Load on Transition Vapour Pressure	177
6.5 E.S.C.A.	180
6.6 Lubricated Tests	
6.6.1 No 1 Friction Apparatus	182
6.6.2 Heated Plate Apparatus	183
6.7 Reciprocating Gas Compressors	186

CHAPTER 7CONCLUSIONS AND SUGGESTIONS FOR FURTHER WORK

7.1	Conclusions	
7.1.1	Unlubricated	195
7.1.2	Lubricated	196
7.1.3	Reciprocating Gas Compressors (Recommendations)	197
7.2	Suggestions for Further Work	
7.2.1	Unlubricated	199
7.2.2	Lubricated	200
7.2.3	Reciprocating Gas Compressors	200

APPENDICES

A	I.C.I. Compressor Data	202
B	Maximum Permissible Loads on Friction Probe	204
C	Details of the Experimental Apparatus	206
D	Circuit Diagrams of Motor-Control and Analogue to Digital Convertor	209
E	Reciprocating Mechanism, Motor Selection	211
F	Properties of Cast Iron Specimens	212
G	Calculation of Water Vapour Flowrate	213
H	Piston Calibration Programme	214
J	Properties of Lubricating Oils	220
K	Data Reading Programme	221
L	Calibration Results	228
M	Experimental Results (No 1 Friction Apparatus)	232
N	Experimental Results (Heated Plate Apparatus)	242
P	Properties of Gases	247
Q	Calculation of Oxide Film Depth	249
R	Temperature of Rubbing Surfaces	251
S	Load on Cylinder Wall	253
T	Electron Spectroscopy for Chemical Analysis	256
	REFERENCES	259

LIST OF FIGURES

	page
<u>Plates</u>	
1	8
2	9
<u>Figures</u>	
1.1	10
1.2	11
1.3	11
1.4	12
1.5	12
2.1	37
2.2	37
2.3	38
2.4	38
2.5	39
2.6	40
2.7	40
2.8	41
2.9	41
2.10	42
2.11	42
2.12	43
2.13	43
2.14	44
2.15	44
2.16	45
2.17	45
2.18	46
2.19	46
3.1	61
3.2	62
3.3	62
3.4	62
3.5	63
3.6	64
3.7	65
3.8	66
3.9	67

Figures

page

3.10	Gas mixing	68
3.11	Schematic diagram of friction measurement	69
3.12	Heated plate apparatus, General assembly	70
3.13	Plate heating arrangement	71
3.14	Loading arrangement	72
3.15	Friction measurement	73
4.1	Pneumatic cylinder calibration	99
4.2	Method of probe calibration (Friction force)	100
4.3	Friction calibration (Heated plate apparatus)	101
4.4	Rotameter calibration	102
4.5	Specimen preparation	102
5.1	Friction probe calibration	131
5.2	Proving ring calibrations	131
5.3	Proving ring calibrations (high load)	132
5.4	Piston calibrations (No 1 pistons)	132
5.5	Piston calibrations (No 2 pistons)	133
5.6	Piston calibrations, No 2 pistons at high load	133
5.7	Friction force calibration (heated rig)	134
5.8	Load calibration (heated rig)	134
5.9	Scuff and no scuff friction traces for cast iron	135
5.10	Coefficient of friction to time curve	136
5.11	Effect of pin wear on probe-piston clearance	136
5.12	Effect of hardness on coefficient of friction	137
5.13	Effect of hardness on wear rate	137
5.14	Effect of surface finish on coefficient of friction	138
5.15	Effect of surface finish on wear rate	138
5.16	Effect of speed on friction	139
5.17	Effect of speed on wear rate	139
5.18	Effect of gas flowrate on friction	140
5.19	Effect of gas flowrate on wear rate	140
5.20	Effect of load on coefficient of friction	141
5.21	Effect of load on wear rate	141
5.22	Comparison of air and oxygen (friction coefficients)	142
5.23	Comparison of air and oxygen (wear rates)	142
5.24	Friction-time curves for hydrogen	143
5.25	Friction-water vapour pressure (hydrogen)	144
5.26	Wear rate-water vapour pressure (hydrogen)	144
5.27	Friction-water vapour pressure (nitrogen)	145
5.28	Wear rate-water vapour pressure (nitrogen)	145
5.29	Friction-water vapour pressure (argon)	146
5.30	Wear rate-water vapour pressure (argon)	146
5.31	Scuff load to vapour pressure (argon)	147
5.32	Effect of water flow on coefficient of friction	148
5.33	Effect of water vapour pressure on coefficient of friction	149
5.34	Effect of water flow on wear rate	150
5.35	Effect of water vapour pressure on wear rate	150
5.36	Friction-water vapour pressure (mixed gas)	151
5.37	Wear rate-water vapour pressure (mixed gas)	151
5.38	Friction-water vapour pressure (carbon dioxide)	152

<u>Figures</u>	page	
5.39	Wear rate-water vapour pressure (carbon dioxide)	152
5.40	Friction-water vapour pressure (air)	153
5.41	Wear rate-water vapour pressure (air)	153
5.42	Friction-water vapour pressure (oxygen)	154
5.43	Wear rate-water vapour pressure (oxygen)	154
5.44	Wide scan spectra of unworn and worn plate	155
5.45	Iron spectra of unworn and worn plate	156
5.46	Oxygen spectra of unworn and worn plate	157
5.47	Carbon spectra of unworn and worn plate	158
5.48	Heated pin experiment	159
5.49	Friction-temperature, Shell risella oil	160
5.50	Wear rate-temperature, Shell risella oil	160
5.51	Friction-temperature, CSB 460	161
5.52	Wear rate-temperature, CSB 460	161
5.53	Friction-temperature, E.P. oil	162
5.54	Wear rate-temperature, E.P. oil	162
6.1	Comparison of argon/air mixtures with pure gases	191
6.2	Vapour pressure- μ , Effect if the gas environment	192
6.3	Relationship of pressure to load	193
6.4	Spectra of iron and iron oxide	194
D.1	Circuit diagram for A-D convertor	209
D.2	Circuit diagram for motor cut-off	210
S.1	Force exerted by the piston ring on the cylinder wall	255
T.1	X-ray, Impinging on surface molecule	257
T.2	The chemical shift effect in E.S.C.A.	257

LIST OF TABLES

<u>Tables</u>	page	
1.1	Estimated ring life for selected reciprocating gas compressors	1
1.2	Compressor characteristics, summary of gases handled	2
2.1	Wear constant, ξ , of various sliding combinations	16
2.2	Size of copper wear particles in various environments	16
2.3	Hardness of the cast iron graphite film at various temperatures	23
2.4	Minimum relative humidities for various vapours	26
2.5	Quantity of lube oil required for compressor cylinder lubrication	35
4.1	No 1 Friction apparatus, commissioning tests (unlubricated)	89
4.2	No 1 Friction apparatus, effect of oxygen content (unlubricated)	90
4.3	No 1 Friction apparatus, effect of water content (unlubricated)	92
4.4	No 1 Friction apparatus, lubricated tests using CSB 460 oil	94
4.5	No 1 Friction apparatus, lubricated tests using Shell risella oil	95
4.6	Lubricated tests using heated plate friction apparatus	96
5.1	Results of surface temperature measurement	111
5.2	Lubricated tests, oil flow 2.0 ml/hr	121
5.3	0.5 ml oil, argon environment	122
5.4	Lubricated tests using Shell risella, oil flow 5 ml/hr	123
5.5	Lubricated tests using Shell risella, no oil flow	124
5.6	Lubricated tests in air, heated plate friction apparatus	128
5.7	Mild steel tests	129

NOMENCLATURE

a	Real area of contact	m
b	Half the axial width of a parabolic ring	m
c_p	Specific Heat	KJ/Kg ^o K
d_p	Radial thickness of piston ring	m
d	Particle diameter	m
f	Average rate of film formation or depth of film produced per second	m/s
g	Acceleration due to gravity = 9.81	m/s ²
h	Planck's constant = 6.626×10^{-34}	Js
h_p	Piston clearance	m
k	Thermal conductivity	W/m ^o K
l	Length	m
m_g	Mass flowrate of oxidising gas	Kg/s
m_{H_2O}	Mass flowrate of water vapour	Kg/s
P_m	Hardness	N/m ²
q	Ring gap	m
r	Radius of circular area of contact	m
s	Distance of sliding	m
t	Time	s
u	Velocity	m/s
w	Wear Rate	Kg/m
x	Thermal diffusivity = $k/\rho c$	m ² /s
A	Cross-sectional area	m ²
A_1	Ring face area	m ²
A_2	Ring contact area	m ²
A_3	Ring back area	m ²
A_n	Arrhenius constant for linear oxidation	m ² s/Kg
A_p	Arrhenius constant for parabolic oxidation	m ⁴ s/Kg ²

D	External ring diameter	m
E	Young's Modulus	N/m ²
E _θ	Binding energy	eV
E _K	Kinetic energy	eV
E _n	Modulus of elasticity	N/m ²
F	Friction force	N
F ₀	Euler buckling load	N
F _m	Maximum expected friction force	N
I	Second polar moment	m ⁴
K	Used as a constant	
L	Load	N
P	Pressure	N/m ²
P ₁	Pressure above ring	N/m ²
P _{AV}	Average gas pressure in cylinder	N/m ²
P _{DP}	Saturation pressure for water vapour at corresponding dewpoint	N/m ²
P _e	Ring wall pressure	N/m ²
P _{H₂O}	Partial pressure of water	N/m ²
P _L	Minimum lubricating pressure	N/m ²
P _m	Mean wall pressure	N/m ²
P ₀	Saturation pressure for vapour	N/m ²
P _S	Saturation pressure for water vapour	N/m ²
P _v	Vapour pressure	N/m ²
Q _n	Activation energy for linear oxidation	J
Q _p	Activation energy for parabolic oxidation	J
R	Gas constant for oxidising gas	KJ/Kg ^o K
R _{H₂O}	Gas constant for water vapour	KJ/Kg ^o K
Sc	Speed criterion = ur/2x	
T	Temperature	°C
T	Temperature (absolute)	°K

V	Volume of wear	m^3
V_T	Volumetric gas flow	m^3/s
W	Load per unit width	N/m
W_{ab}	Energy of cohesion of surfaces	J
ϵ	Strain	
η	Dynamic viscosity	Ns/m
ξ	Wear constant	
λ	Frequency	Hz
μ	Coefficient of Friction	
ν_p	Kinematic viscosity of lubricant saturated by gas	cSt
ν_s	Kinematic viscosity of lubricant at pressure P	cSt
ρ	Density	Kg/m^3
ρ	Density of oxide	Kg/m^3
σ	Stress	N/m^2
θ_c	Temperature of real area of contact	$^{\circ}C$
θ_m	Mean rise in temperature of contact area	$^{\circ}C$

CHAPTER 1

INTRODUCTION

1.1 Background

Over a number of years I.C.I. plc have recorded failures in their reciprocating gas compressors relating to piston ring/liner scuffing. Typical examples of the damage caused by such incidents are shown in Plates 1 and 2. An estimate of the repair costs of such failures is in the region of £10,000 to £50,000 (1980 prices). The production losses, which depend upon the reserve capacity available and the current demand for the product, may range from zero to £100,000 for the required period of down-time.

Estimates of the life of the piston rings for ten reciprocating compressors are shown in Table 1.1

Table 1.1 Estimated Ring Life for Selected Reciprocating Gas Compressors

Compressor No	Delivery Pressure	Gas Handled	Ring Life (Months)
1	255	H ₂	4
2	361	CO ₂	4
3	273	H ₂	6
4	600	C ₂ H ₆	4
4	1000+	C ₂ H ₆	4
5	500	C ₂ H ₆	2
5	1000+	C ₂ H ₆	1
6	245	C ₂ H ₆	3
7	72.5	C ₂ H ₄	3
8	290	H ₂	7
9	240	H ₂	7
10	7.6	N ₂	5

Source: I.C.I. plc



Although the figures quoted are only rough estimates, it can be seen that in all cases, the ring life is well under one year.

On the basis of such figures as shown in Table 1.1 and the potential financial losses outlined above, the company decided that it was necessary to increase piston ring life and hence increase compressor reliability. This would lead to lower maintenance costs and production losses. Also, greater reliability would give possible savings in capital expenditure, by reducing the need for reserve capacity (eg. spare compressors).

1.2 Compressor Characteristics

A pictograph of the characteristics of sixty-five I.C.I. compressors is shown in Figure 1.1. A wide range of bore diameters and delivery pressures is shown. A more detailed summary is contained in Appendix A. A summary of the gases handled by these compressors is shown in Table 1.2.

Table 1.2 Compressor Characteristics,
Summary of Gases Handled

Gas Type	No. off
Air	10
Nitrogen (over 95%)	9
Hydrogen (over 95%)	8
Ammonia	12
Hydrocarbon Gases	14
Others	14
<hr/> Total	<hr/> 65

It must be noted that Table 1.2 and Figure 1.1

are by no means complete sets of data for the company. In many cases where there are several of the same compressor units (ie. make, model and service), only one set of data is recorded. Also, Figure 1.1 represents only the final stage characteristics and most of the compressors have multiple stages. In a majority of the compressors, cast iron is used for both the cylinder liners and the piston rings, although some compressors may use other materials.

1.3 Problem Compressors

The compressors most likely to have a piston ring failure were found to be those handling inert or reducing gases, particularly nitrogen and hydrogen. (Hale and Hodge 1969 and Summers-Smith 1975).

A hypothesis was thus put forward that piston ring failure was due to the non-oxidising nature of the gases handled, since boundary lubrication (particularly relevant at T.D.C. (see later)) depended upon the formation of chemi-sorbed films on the contacting surfaces.

"Such films only form as the result of reactions between oxide films on the surface and chemicals in the lubricant. Under boundary conditions the boundary film and the underlying oxide film can be worn off by asperity contacts, but in normal situations where there is free access of oxygen the asperity contact is broken; this allows the re-establishment of the boundary film and a reasonably stable situation is maintained.

On the other hand, however, when boundary lubrication occurs in an inert or reducing atmosphere, a gradual loss of the surface oxide film occurs and eventually severe damage of the surfaces takes place by a scuffing mechanism"

(Summers-Smith 1979).

The evidence to support this theory was the lower incidence of ring failure in air compressors (no data available). Also the apparent success of simple solutions in preventing scuff eg. when the oil reservoir for a nitrogen compressor was altered so that the gas above the oil was atmospheric air instead of nitrogen, scuffing was reduced. (Summers-Smith 1968).

1.4 Experimental Work

Despite the concern about the incidence of scuffing, it was not thought desirable to carry out experimental work using process compressors. The main reasons for this lay in the risk to expensive items of plant and the cost of repairs. In fact, in order to assess the success or failure of any solution, it would be necessary to induce artificial failures; a procedure which was not economically feasible. Another problem lay in the fact that the operation of the compressors varied from plant to plant. In some cases compressors would operate continuously for several months, whilst others would only operate for several hours a week. Also the exact moment of ring failure in a compressor is difficult to assess. Ring failure is only detected when the broken pieces of piston ring cause a failure in the delivery valve (normally indicated by high gas temperatures), which may occur several seconds or even several days after the initial onset of scuffing.

For the above reasons this project was commissioned to investigate the behaviour of cast iron in inert and reducing environments.

1.5 Aims

The main aims of the project were to design and build an apparatus to investigate the behaviour of cast iron rubbing against cast iron in inert and reducing environments. It was decided that the investigation would be restricted to operating conditions in a boundary lubricated regime (see later) and only ambient pressures would be used.

From the previous sections it was felt necessary to assess the amount of oxygen required to prevent scuffing and examine the possibility of using oxidising agents (in lubricants) to produce oxide films. Another subject for investigation was the influence of water vapour on the prevention of scuffing.

The ultimate intention of the project was to propose an acceptable solution to ring scuffing. The method had to be safe to use, particularly in the presence of hydrogen, as well as cost effective. Foremost however, there had to be no contamination of the production gas which in some cases is maintained at a very high level of purity.

1.6 Lubrication Types

As stated in the previous section, the investigation would be restricted to a boundary lubricated regime. However, for a piston ring sliding over a piston liner, other types of lubrication would be available.

If a lubricant were present there would be the possibility of fluid film lubrication similar to one of the types shown in Figure 1.2 (Unsworth 1976). This

Type of lubrication would depend upon the lubricant properties, the load and speed conditions applied, as well as the size, shape and material of the sliding bodies. The magnitude of the coefficient of friction (μ) also depends upon the load, speed and lubricant properties (see Figure 1.3 (Stribeck 1902)). As can be seen from Figure 1.3, high friction can occur when a fluid film is present if the viscosity (η) and/or speed (u) is very high, or the load (W) is very low. On the other hand, friction can be very high; under these conditions it would be very difficult for a fluid film to be maintained, and surface to surface contact (ie. boundary lubrication) would take place (see Figure 1.2).

The most important difference between these two high friction regimes is their likely affect on wear. Whenever a fluid film is present, of a thickness greater than that of the material's surface finish, surface to surface contact will not take place, and hence the wear will be zero. If however, surface to surface contact does take place, wear is inevitable. The amount of wear will depend upon the nature of the rubbing surfaces and the protection of surface films. The effect of surface films on boundary lubrication will be examined in the next chapter.

1.7 Piston Ring Lubrication

Piston ring lubrication has been investigated by many people, particularly those working on internal combustion engines. One aspect which has attracted a great

deal of research is the estimation of the oil film thickness between the piston ring and the cylinder liner. One such estimation is shown in Figure 1.4 (Lloyd 1969). As can be seen from the diagram, the lowest film thickness is encountered at T.D.C. on the compression stroke. This solution is supported by experimental work by Moore et al 1980, who also found that the film thickness at this position was very small and possibly smaller than the known surface finish would allow.

The speed and pressure characteristics of a reciprocating gas compressor are shown in Figure 1.5 (Scheel 1961). It can be seen that at T.D.C. the compressor is operating at its maximum pressure and lowest speed. It can also be seen from equation 2.1 (Eilon 1957)

$$P_m = P_i \left[1 - \frac{2d}{D} - \frac{\mu(d-h_p)}{2bD} (D-d) \right] + P_e \quad 2.1$$

that the higher the delivery pressure (P_i), the higher the pressure on the ring and wall (P_m).

With the low speeds and highly loaded conditions at T.D.C. it is not surprising that the oil film thickness may be very low; in fact it is a relatively safe assumption that at T.D.C. boundary lubrication and therefore surface to surface contact takes place. Thus the most likely position for piston ring scuffing to take place in a reciprocating gas compressor is at T.D.C. It is unlikely that scuffing would be initiated at other parts of the stroke when an adequate fluid film is present. For this reason the investigation was restricted to boundary lubrication.



Plate 1 Scuffed Piston from a Hydrogen Compressor (Courtesy of ICI plc)

Characteristics:- 75mm Diameter, 200mm Stroke, 200 Bar Discharge Pressure

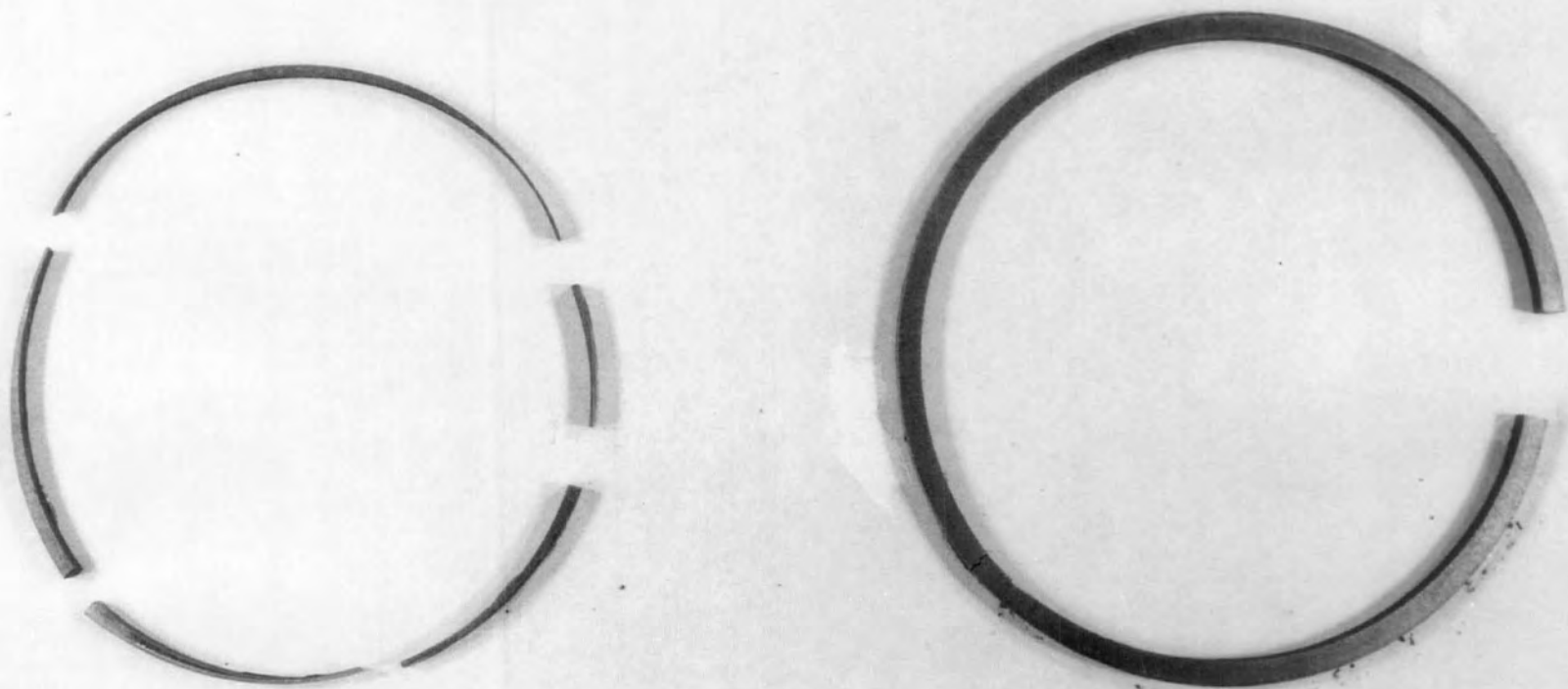


Plate 2 Broken Piston Rings from a Hydrogen Compressor (Courtesy of ICI plc)

Characteristics:- As Plate 1

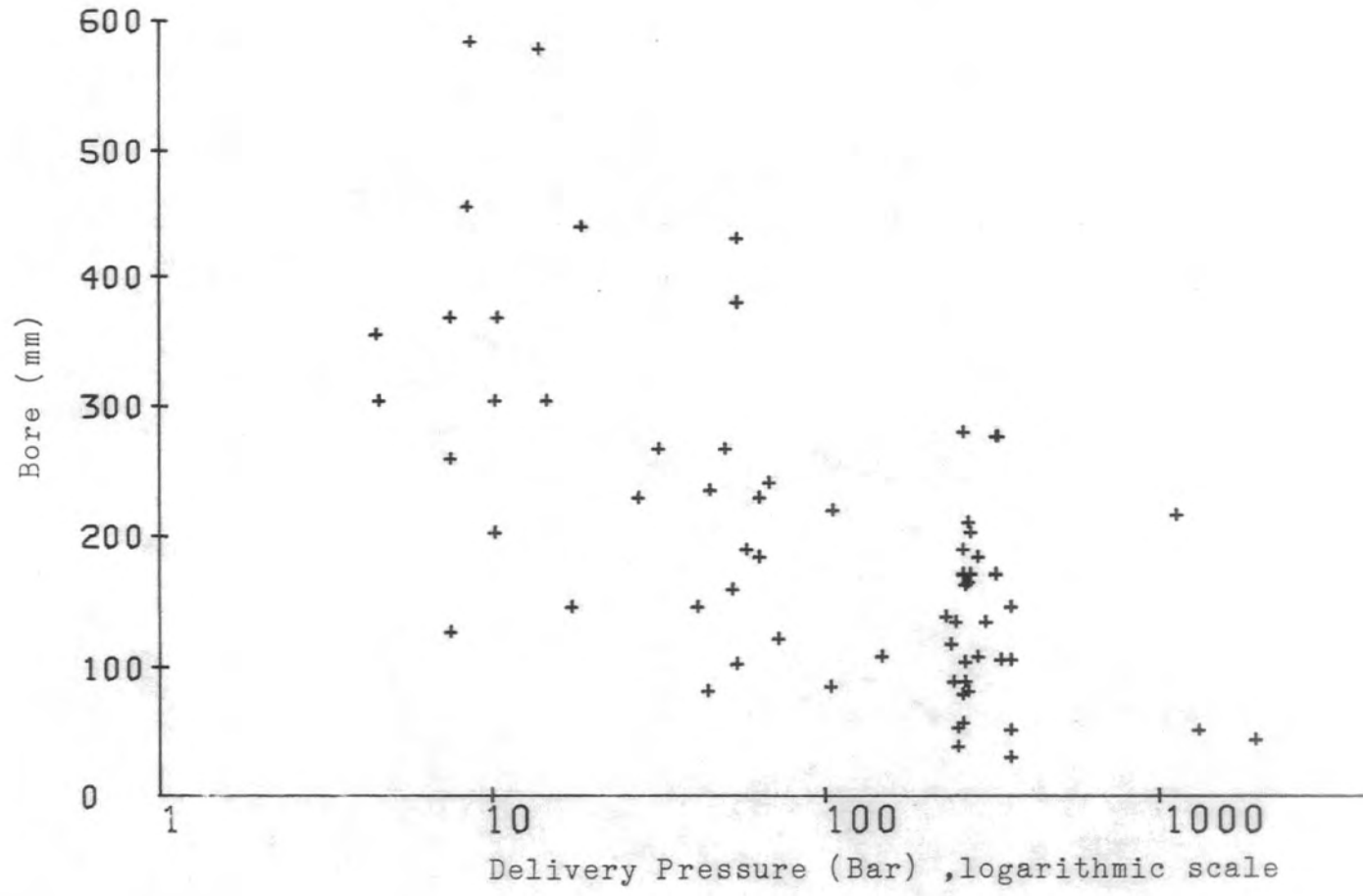
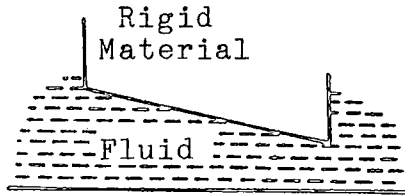


Figure 1.1 ICI Compressor Characteristics

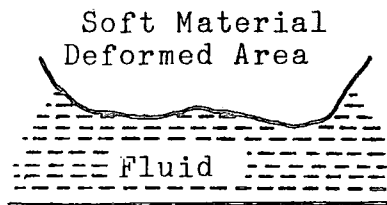
FLUID FILM

Surfaces completely separated by a fluid film

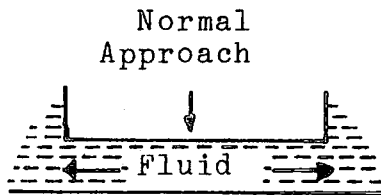
Hydrodynamic



Elasto-hydrodynamic



Squeeze-film



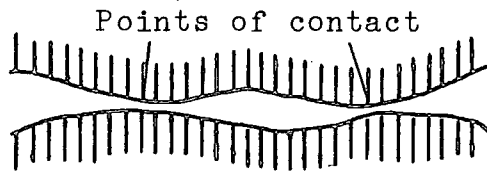
BOUNDARY

Load supported by surface to surface contact

Molecular Protection



Dry Contact



MIXED

Load support shared by fluid film pressure and by boundary contacts

Figure 1.2 Lubrication Types (Unsworth 1975)

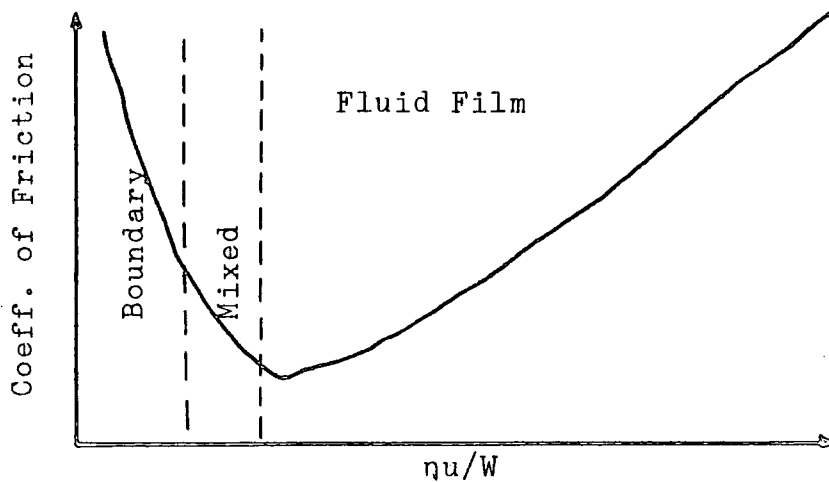
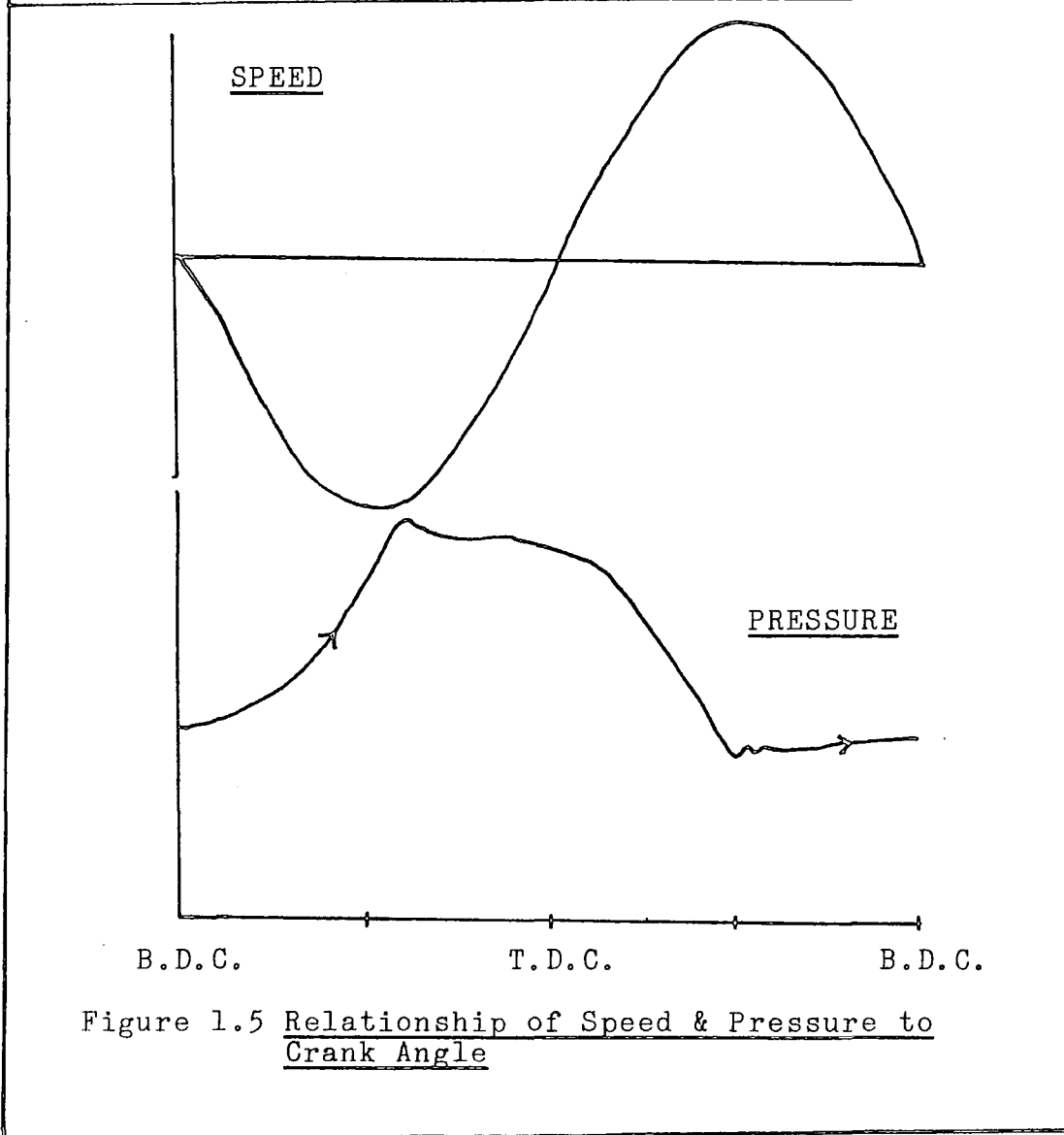
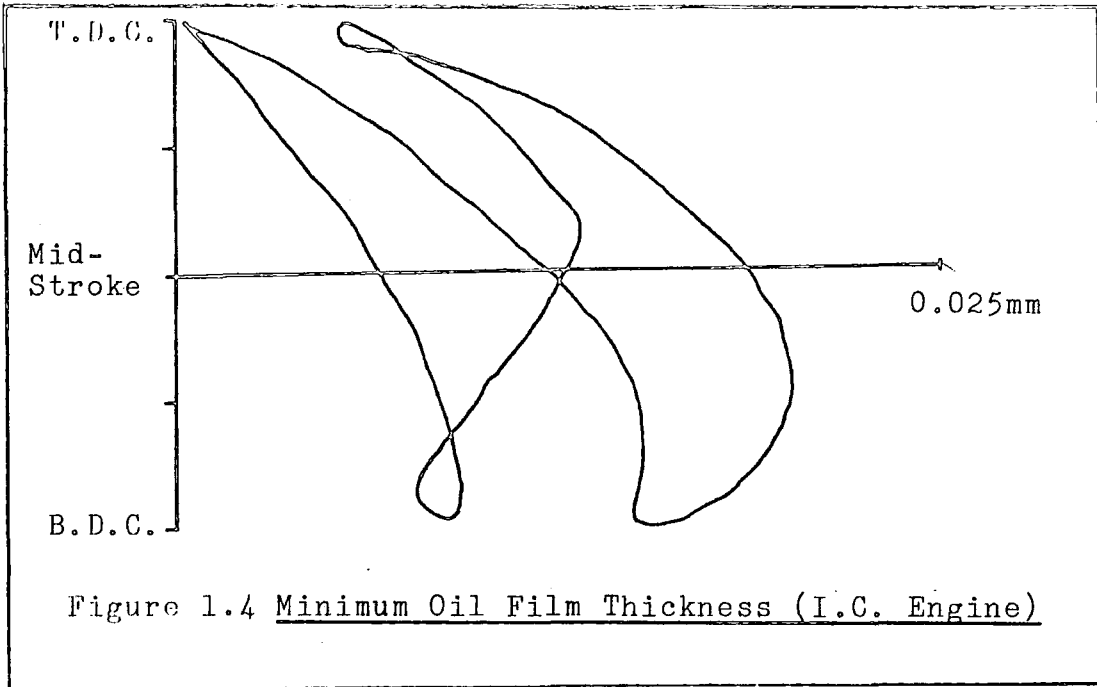


Figure 1.3 Lubrication Regimes for Sliding Surface Pairs (Stribeck 1902)



CHAPTER 2

LITERATURE REVIEW

2.1 The Nature of Surfaces

For most metals, even when in a clean, freshly prepared state, their surfaces rarely consist of pure metal. The surface profile of a typical polished metal specimen is shown in Figure 2.1 (Samuels 1956), where the surface layers are composed of oxide and polishing powder. A depth profile for a carbon steel, Figure 2.2 (Allen and Wild 1981), also shows little iron at the surface. Indeed, the iron concentration is very small until 0.8 μm below the surface.

The type of surface layer of film present on a metal surface will depend upon the nature of the metal itself and the nature of the contaminants which may come into contact with it. The types of film which are likely to be formed are physically adsorbed films, chemisorbed films and chemical reaction films.

2.1.1 Physically Adsorbed Films

A diagrammatic representation of physical adsorption is shown in Figure 2.3 (Godfrey 1975), showing argon adsorbed on platinum. Physical adsorption is characterised by short range Van der Waal forces of attraction giving a low strength film. Films can be more than one molecule thick because one molecule can adsorb on top of another.

If polar molecules (ie. a molecule where there is

an unbalance of its electrical charge) are physically adsorbed, then higher film strengths can be obtained. Polar molecules such as alcohols occur in many lubricating oils.

2.1.2 Chemisorbed Films

Chemisorption is limited to one molecule in thickness, eg. a monomolecular layer of soap formed by a fatty acid reacting with a metal is chemisorbed. Chemisorption shows higher energies of adsorption than physical adsorption, and unlike physical adsorption, is in general, not completely reversible. Frequently adsorption is physical at low temperatures, changing to chemisorption at higher temperatures. Many gases are chemisorbed on metals. In the oxidation of certain metals and graphite, the chemisorption of oxygen is the first process to occur, and it is very fast on clean surfaces.

2.1.3 Chemical Reaction Films

Chemical reaction means that a new compound is formed. The action is irreversible and heating increases the rate of reaction. The type of films formed are inorganic salts of unlimited thickness such as iron sulphide (Figure 2.4). These films have much higher melting points and higher film strengths than either physically adsorbed or chemisorbed films.

2.2 Wear

2.2.1 Adhesive Wear

This is the most common form of wear which occurs when two smooth bodies are slid over each other, and fragments are pulled off one surface to adhere to the other. Later, these fragments may come off the surface on which they are formed and be transferred back to the original surface, or else form loose wear particles.

Adhesive wear arises from the strong adhesive forces set up whenever atoms come into intimate contact. During sliding, a small patch on one of the surfaces comes into contact with a similar patch on the other surface, and there is a probability, small but finite, that when this contact is broken the break will occur, not at the original interface, but within one of the materials. In consequence a transferred fragment may be formed.

The amount of wear is generally proportional to the applied load (L) and to the distance slid (s), and inversely proportional to the hardness (p_m) of the surface being worn away. From Rabinowicz (1966), who uses a model of the sliding process derived by Archard (1953), the volume of transferred fragments formed in sliding through a distance s is:

$$V = \frac{\xi L s}{3 p_m} \quad (2.1)$$

The value of the wear constant ξ , varies depending upon the materials used in the sliding combination (see Table 2.1).

Table 2.1 Wear Constant ξ of Various Sliding Combinations

Combination	Wear Constant ξ $\times 10^3$
Zinc on Zinc	160
Mild Steel on Mild Steel	45
Copper on Copper	32
Stainless Steel on Stainless Steel	21
Copper on Mild Steel	1.5
Bakelite on Bakelite	0.02

Source: Rabinowicz (1966) and Archard (1953)

In equation 2.2 Rabinowicz (1966) gives the condition for loose particle formation:

$$d_p = 60000 \frac{W_{ab}}{P_m} \quad (2.2)$$

It is dependent upon the energy of cohesion (W_{ab}) and the material hardness (p_m). The energy of cohesion (W_{ab}) is affected by the type of surface, which in turn, is affected by the environment. The variation in loose particle size for different environments is shown in Table 2.2.

Table 2.2 Size of Copper Wear Particles in Various Environments

Environment	Average Fragment Diameter (μm)
Nitrogen	480
Helium	380
Carbon Dioxide	300
Dry Air	224
Oxygen	201
Wet Air	144

It can be seen that inert environments, such as nitrogen and helium, which would be expected to leave very clean surfaces, gave the largest wear particles, whereas reactive environments led to the production of much smaller particles.

2.2.2 Abrasive Wear (Rabinwicz 1966)

This form of wear arises when a hard surface slides against a softer surface, digs into it, and ploughs a series of grooves. The material originally in the grooves is normally removed in the form of loose fragments.

Abrasive wear can also arise in a somewhat different situation, when hard abrasive particles are introduced between sliding surfaces and abrade material off each. The mechanism of this form of abrasive wear seems to be that an abrasive grain adheres temporarily to one of the sliding surfaces, or else is embedded in it, and ploughs out a groove in the other. The two forms of wear, one involving a hard rough surface and the other hard, abrasive grains, are generally referred to as the two-body and the three-body abrasive wear process respectively.

Abrasive wear of the two-body kind does not take place when the hard, sliding surface is smooth. Similarly, three-body abrasive wear does not occur when the particles in the system are small, or when they are softer than the sliding materials.

Abrasive wear is widely used in material finishing operations. The two-body type of abrasive wear is made use of

in files, abrasive paper, abrasive cloth and abrasive wheels, whereas the three-body type of wear is used in lapping and polishing.

2.2.3 Corrosive Wear

This form of wear occurs when sliding takes place in a corrosive environment. In the absence of sliding, the products of corrosion would form a film on the surfaces, which would tend to slow down or even arrest the corrosion, but the sliding action wears the film away, so that the corrosive attack can continue.

2.2.4 Surface Fatigue Wear

This form of wear is observed during repeated sliding or rolling over a track. The repeated loading and unloading cycles to which the materials are exposed, may induce the formation of surface or subsurface cracks, which eventually will result in the break-up of the surface with the formation of large fragments, leaving large pits in the surface.

2.3 Effect of Surface Films on Friction and Wear

As suggested in Section 1.6, when two metals come into contact in boundary lubrication, it is the surface films that meet and ultimately decide the frictional forces. The amount of frictional force required will depend upon the shear strengths of the surface film eg. the shear strength of iron is 1300 MN/m compared with 2.4 MN/m for calcium stearate (Moore 1975).

Another important factor in the value of the frictional forces is the thickness of the boundary film. In general, as the thickness of a boundary film increases, the coefficient of friction decreases, as shown in Figure 2.5a (Campbell and Summit 1936). However, continued increase in thickness may result in an increase in friction (Figure 2.5b).

For physically adsorbed or chemisorbed films (see Section 2.1), surface protection is usually enhanced by increasing film thickness (Bowden and Tabor 1971). For thick chemically reacted films there is an optimum thickness for minimum wear, which depends upon the material and the lubricant reactivity. If the material is very reactive, thick films are formed and corrosive wear ensues (see Section 2.2). On the other hand, if reactivity is too low to produce a thick enough film adhesive wear occurs (Jones 1982).

Several experiments have been conducted to examine the effects of surface films on friction and wear, some of which are outlined below.

2.3.1 Friction of Clean Metals

The surface film of a nickel specimen was removed by heating the surface of the metal in a vacuum (Bowden and Rowe 1955). In this way chemical reaction films could also be destroyed and adsorbed gases removed. A friction experiment was then carried out after allowing the surface to cool down to room temperature (see Figure 2.6).

The results showed that the more efficient the film removal (ie. the higher the temperature), the higher the coefficient of friction. A similar result was found for iron sliding on iron (Bowden and Young 1951). The coefficient at ambient temperatures and pressures was 0.4 but rose to 3.5 after degassing at 1000°C in vacuum.

Bowden and Young (1951) also found that when small amounts of oxygen were introduced into a high vacuum system the coefficient of friction of iron could be reduced (see Figure 2.7a). In the case of water vapour, the effect was reversible, in that if the vapour was frozen out, the friction increased but decreased at its reintroduction (Figure 2.7b).

2.3.2 The Mechanical Removal of Surface Films

In machinery the most likely form of film removal is by wear, either adhesive or abrasive, caused by the rubbing together of two surfaces. Davies (1951) carried out experiments at various pressures below atmospheric using a tungsten carbide pin on a mild steel ring at ambient temperatures (see Figure 2.8). The results showed that at a certain pressure (0.16 bar in Air and 0.26 bar

in Nitrogen) there is an increase in the diameter of the wear scar.

Similar results were found by Barnes et al (1977), who found that the coefficient of friction for Fe - 5% Cr was about 0.6 for pressures down to 10^{-6} bar (10^{-1} Pa) but rose to 1.6 or higher at 10^{-11} bar (10^{-6} Pa). The low friction values also corresponded to the formation of smooth raised islands of compacted debris, which was either oxide, oxide covered in metal or a mixture of the two.

From the above two papers it appears that as the amount of gas available is reduced (ie. by lowering the pressure) the friction and wear increases. The amount of gas available must affect the rate at which the protective film can be reformed, and thus ultimately, decide the point at which high friction or wear takes place. A further point worth noting from Figure 2.8 is the effect of nitrogen on wear, although not as good as air, it gives good results for what is normally considered an inert gas.

2.4 Frictional Behaviour of Cast Iron

Cast iron can be classed as a self-lubricating metal-base composite material (Sugishita and Fujiyoshi 1980). The presence of graphite in cast iron plays a major part in reducing its friction and wear. After 'running in' cast iron is covered with a coating of graphite and metal oxide (Fe_2O_3). Montgomery (1969) found that this coating could be up to 1 mm thick, although its exact composition varied from point to point along the surface from 30% to 100% carbon. The coating or 'glaze' gives a resistance to scuffing during momentary contacts between the mating surfaces, but possibly of more importance, is that by covering surface irregularities it produces a smooth surface.

Sugishita and Fujiyoshi (1980) investigated the influence of a number of variables on the formation of graphite films and their subsequent effect on friction for cast iron rubbing against a carbide pin (unlubricated). They found that when the air pressure was reduced, the coefficient of friction increased (see Figure 2.9). Unlike Davies (1951), who found that wear increased dramatically after a certain pressure (see Figure 2.8), the increase in friction was gradual. Humidity was also found to affect the coefficient of friction (see Figure 2.10). At first the coefficient of friction decreased with increasing vapour pressure, but after 8 mbar it increased as the vapour pressure increased. Sugishita suggested from these results that a constant vapour pressure of 8 mbar would seem to be desirable. The effect of surface temperature on the

coefficient of friction depended upon whether the graphite film had been preformed or not (see Figure 2.11). When the graphite film was preformed (by etching in 5% nital), friction rose steadily with temperature, but seizure did not occur. However without a preformed film, seizure occurred at temperatures above 120°C (Sugishita and Fujiyoshi 1980), although Figure 2.11 (from Sugishita and Fujiyoshi 1980) indicates possible seizure below 100°C.

The major reason suggested by Sugishita for the increase in friction with humidity and temperature was a hardening of the graphite layers. Figure 2.12 shows the effect of water vapour on hardness and Table 2.3 shows the variation of hardness with temperature.

Table 2.3 Hardness of the Cast Iron Graphite Film at Various Temperatures

Temperature (°C)	Hardness (HV(0.05N))
25	30.5
50	41.0
75	56.0
100	62.5
120	75.6

Although the effects of pressure, humidity and temperatures are investigated by Sugishita and Fujiyoshi, whilst carrying out experiments with one variable, they give no information on the other two. Whilst it is possible to keep a constant surface temperature for the pressure and humidity tests it is not as easy to keep a constant vapour pressure whilst reducing the air pressure.

In fact, as one might expect, the vapour pressure to be reduced as the air pressure is reduced, Figure 2.9 (μ - pressure) could simply be an extrapolation of Figure 2.10 (μ - vapour pressure) for vapour pressures below 6 mbar.

It is perhaps worth noting that despite the common occurrence of cast iron rubbing against cast iron Sugishita and Fujiyoshi used a cemented carbide pin onto cast iron. In fact there seems to be a scarcity of information regarding the rubbing of cast iron against cast iron despite its wide use in industry.

2.5 Graphite Lubrication

As seen in the previous section, graphite films play an important role in the lubrication of cast iron. In this section we shall look at graphite lubrication and in particular the vapour lubrication of graphite.

Graphite can show high friction and rapid wear ('dusting') in certain environmental conditions. In dry air, hydrogen, nitrogen and inert gases dusting can take place even at atmospheric pressures (Lancaster and Pritchard 1981). Dusting can be prevented by oxygen and carbon dioxide, but only at partial pressures above those at which these gases are normally present in air. By far the most effective way in which dusting can be prevented is by the presence of organic vapours in the environment. Water vapour can also be used but is less effective than organic vapours.

Savage (1955) found that there was a transition from low to high (dusting) wear rates as the vapour pressure decreased (see Figure 2.13), with a hysteresis effect when passing from low pressure (high wear rate) to high pressure (low wear rate). The pressure at which the curve approached zero wear rate was taken as the minimum lubricating pressure (P_L) for that particular vapour (see Figure 2.13). The ratio of this lubricating pressure to the saturation pressure for the vapour over its liquid at the experimental temperature, (P_L/P_0) was defined as the minimum relative humidity for effective lubrication. The values of minimum relative humidity for some vapours are shown in Table 2.4. Savage also showed that there

Table 2.4 Minimum Relative Humidities for Various Vapours

Vapour	P_L Minimum Lubricating Pressure (mbar)	P_0 Saturation Pressure (mbar)	P_L / P_0 Relative Humidity $\times 10^5$	L_m (Å) Effective Molecular Chain Length
Water	4.00	42.3	10000	4.64
Methanol	0.86	212.8	406	6.14
Carbon Tetra- Chloride	0.069	166.3	41.6	7.12
Propane	3.86	13300	29.0	7.72
1-Propanol	0.006	372.4	15.7	9.22
n-Pentane	0.024	904.4	2.6	10.80
1 Bromo-Pentane	0.0004	17.3	2.1	12.35
n-Heptane	0.001	74.5	1.4	13.88

was some correlation between P_L/P_0 and the effective molecular size or chain length of the vapour (see Figure 2.14).

Lancaster and Pritchard (1981) suggested that the vapour lubrication of graphite depended upon a mechanism of physical adsorption of the vapour on the basal planes of the graphite. The adsorbed vapour on the basal planes functioned as a reservoir from which molecules could migrate to neutralise freshly exposed edge sites during a normal low wear regime. The transition to dusting occurred when the basal plane coverage fell below some critical value.

2.6 Friction and Wear in Inert and Reducing Environments

Achieving effective lubrication of moving components in environments other than atmospheric air concerns several industries, such as nuclear power, space exploration, aircraft (reduced pressures) and those industries in which gases are processed (eg. chemicals).

Irving et al (1963), working in conjunction with the nuclear power industry, showed that the bearing life of grease lubricated steel ball bearings was greatly reduced in a hydrogen or helium environment compared with carbon dioxide or air. In addition, he found that hydrogen embrittlement of the steel ball bearings could cause severe damage in a hydrogen environment. Later work by Jones et al found that by adding 5% (wt) sodium stearate and 5% (wt) sodium nitrite to the grease, the bearing life could be increased considerably. The main purpose of these compounds was to provide an oxidising agent that would react with the bearing surface and form a protective oxide layer. Increasing the oxygen and water content of the environment also increased bearing life but not to the extent that sodium stearate and sodium nitrite did.

The test conditions used by the above authors were loads of 2.5 N (radial) and/or 136 N (axial), a speed of 1450 rpm and a temperature range of 150°C to 200°C. Jones et al, when carrying out experiments in which the oxygen and/or moisture content of the helium is increased, did not pay any attention to the gas flowrate and the possible effect of increasing the oxygen or moisture flowrate, as

opposed to increasing their content as a means of producing oxide films.

Jones and Hady (1970) carried out pin-on-disk experiments to study the effect of humidity and a wettability additive (not identified) on boundary lubrication of steel in air and nitrogen. For unlubricated tests they found that nitrogen gave lower wear rates than air, wet nitrogen being better than dry nitrogen. When lubricated (base lubricant only), dry nitrogen gave high wear at 150°C compared with dry air, but gave lower wear than air at 350°C. The wettability additive reduced wear for wet air, dry air and dry nitrogen but made little difference with wet nitrogen.

One significant effect that appears to have been overlooked by the authors is that under all conditions (ie. unlubricated, lubricated with or without additive) wet nitrogen gave the lowest wear rates. In fact, wet nitrogen (50% R.H.) with base lubricant gave a lower wear rate than any other environment, even when the wettability additive was present in the lubricant. Another point about these experiments is that in common with Jones et al (1969) the effect of moisture flowrate was not assessed and only two humidities were considered, dry (100 vpm water) and wet (50% R.H.).

A research programme, for a group of companies consisting of compressor manufacturers and users, was carried out at the National Centre of Tribology at Risley (NCT 1970-73), to investigate the mechanism of lubrication breakdown in non-oxidising gases and to find suitable

additives that would restore the lubricating properties. An experimental rig was built in which two opposed test shoes were loaded against a reciprocating rod fitted with 50 mm diameter test sleeves. The materials used for the shoes and sleeves could be varied. Lubricant was sprayed into the test contact area at a controlled rate and the whole rig was enclosed in a gas tight box that could be filled with the desired gas at atmospheric pressure.

At high flowrates (≈ 250 ml/min) there was no difference in friction or load carrying capacity between atmospheric air and dry nitrogen. However, when the oil flow was lowered (≈ 1 ml/min) there was a variation in the critical loads for air and nitrogen. The critical load was defined as that below which continuous stable operation was achieved, and above which a 'runaway' condition characterised by rising temperature and friction occurred. The critical load for air, using cast iron shoes and sleeve, was 7.2 MN/m^2 compared with 4.4 MN/m^2 for nitrogen. The critical load for nitrogen however could be increased by additives in the lubricant (see Figure 2.15 (Summers-Smith 1975)). The only additives that increased the critical load were benzoyl peroxide and water, deliberately used as oxidising agents to help produce oxide films on the sliding surfaces.

Some criticism may be levelled at these experiments for the way in which 'runaway' was achieved by lowering the oil flowrate. It must be questioned whether 'runaway' was due to the low amount of oil and hence the lack of reactive chemicals or whether the oil flowrate was too

low to guarantee hydrodynamic lubrication. In fact one major finding of the experiments was that provided adequate lubricant was available 'runaway' would not occur whatever the gas environment. No attempt was made to assess the true boundary lubricating properties of the additives by lowering the reciprocating speed to a point at which hydrodynamic lubrication could not take place and then flooding the test area with lubricant to see if the critical load was affected. Summers-Smith (1975) put forward a hypothesis that effective boundary lubrication depends upon surface films eg. oxides. If the oxide film was removed during boundary lubrication it would have to be reformed at the same rate in order to prevent 'runaway'. By lowering the oil flowrate under definite boundary lubricating conditions the minimum rate at which additives should be supplied to prevent 'runaway' (by helping reform the oxide layer) could have been assessed.

Note:- The paper by Summers-Smith (1975) was a summary of the results from the tests carried out by NCT at Risley.

2.7 The Influence of Temperature on Scuffing

In some unlubricated experiments Bowden and Rowe (1955) showed that by heating a metal surface in vacuum the surface film can be removed and increases in friction are recorded (see Section 2.3.1). At much lower temperatures in a lubricated system a transition from high to low friction was found for stainless steel rubbing on stainless steel (see Figure 2.16). Grew and Cameron (1971) found that there was a critical temperature above which there was a marked increase in friction. Similarly, Bailey and Cameron (1973) found that for a modified four ball machine the scuffing load decreased with an increase in temperature (see Figure 2.17).

The critical temperature of scuffing is identified with the desorption of the surface active agent in the lubricant. The critical temperature and its effect depend upon the reactivity of the lubricant and the metal. In the case of an unreactive stainless steel the friction rise is very marked compared with a more reactive tool steel (see Figure 2.16). The effect of this transition can often be overcome by the addition of a reactive agent to the lubricant (eg. an E.P. additive).

2.8 Lubrication of Reciprocating Gas Compressors

When a lubricant is used in a reciprocating gas compressor its function is fourfold. It must prevent wear by a low frictional supporting film between two metal surfaces, one of which is moving with respect to the other (eg. ring and liner). It has to carry away the heat of friction and minute wear particles from the points of bearing. It must minimise corrosion by coating all metallic surfaces, and also, seal by preventing leakage through the minute clearance around the piston and packing rings, the valve and rotor elements (Scheel 1961).

2.8.1 Lubricant Selection

Summers-Smith (1967) defined a range of satisfactory oil viscosity for reciprocating gas compressors. The analysis was based on operating experience with compressors handling a wide range of process gases, using data on gas solubility in lubricating oils and compressor operating parameters. Figure 2.18 gives a plot of effective oil viscosity, defined by

$$\nu_p = \nu_s \left(1 + \frac{P_{AV}}{340} \right)$$

against the maximum pressure drop across the piston.

Satisfactory lubrication can be expected when operating in the region above the shaded area of marginal lubrication.

2.8.2 Oil Consumption

The lubrication of a compressor cylinder is unique in that the supporting film is continually being replenished, there is no lubricant reservoir or circulation, and the lubricant is not consumed, but is lost largely by windage and drainage. Most compressors employ a mechanical force feed lubrication system which provides definite control of the quantity of oil applied and the point of application.

The quantity of oil required for satisfactory lubrication is dependent on the diameter of the compressor cylinder. Table 2.5 gives the quantity of lubricating oil required for compressor lubrication (Scheel 1961).

2.8.3 Effect of Gas Type

The type of gas handled by a compressor must be considered when deciding upon lubricants and materials. Air (oxygen) and carbon monoxide can react with mineral oils. In the case of air, this can lead to carbonaceous deposits which can ignite spontaneously under certain operating conditions leading to fires and explosions, and carbon monoxide can lead to carbon deposits in delivery lines. Chlorine gas presents a materials' problem, especially if moisture is present, and highly corrosive hydrochloric acid is formed.

Wet gases (eg. natural gas from oil fields) can cause problems if hydro-carbon condensate forms in the cylinder, washing off the lubricant and causing excessive

Table 2.5 Quantity of Lube Oil Required for Compressor Cylinder Lubrication

Range of Cylinder Diameters (mm)	Nominal Discharge Pressure (bar)	Film Thickness (μm) $\times 10^3$	Compressor Lube Oil	
			Litres/day	Drops/min
600 - 1000	5.5	406	0.85	13
380 - 600	13.8	432	0.57	9
250 - 380	55.2	580	0.45	7
180 - 250	138.0	610	0.34	5
100 - 180	552.0	1200	0.45	7
75 - 125	1380.0	1450	0.40	6

piston and ring wear. However this problem can often be overcome by increasing the water jacket temperature.

Scheel (1961) and Summers-Smith (1967) differ in opinions on hydrogen and nitrogen. Scheel states that

"extremely high operating pressure is the only special lubrication problem encountered in hydrogen and nitrogen compressors"

whereas Summers-Smith points to the importance of oxide films in boundary lubrication and to problems experienced in operating compressors handling non-oxidising gases (see Chapter 1).

The effect of water content on the effective lubrication of hydrogen compressors was investigated by Summers-Smith (1981). The results of his investigation are shown in Figure 2.19, in which a critical line is shown to divide scuff and no-scuff conditions. Each point marked on the graph corresponds to a compressor stage and not necessarily a separate compressor. Points marked on Figure 2.19 as scuffing problems are compressor stages which in the opinion of Summers-Smith have a higher than normal amount of scuffing incidents. Unlike other workers looking at lubrication in non-oxidising environments (see Section 2.6) Summers-Smith looks at the water flowrate in preference to the water content of the gas environment.

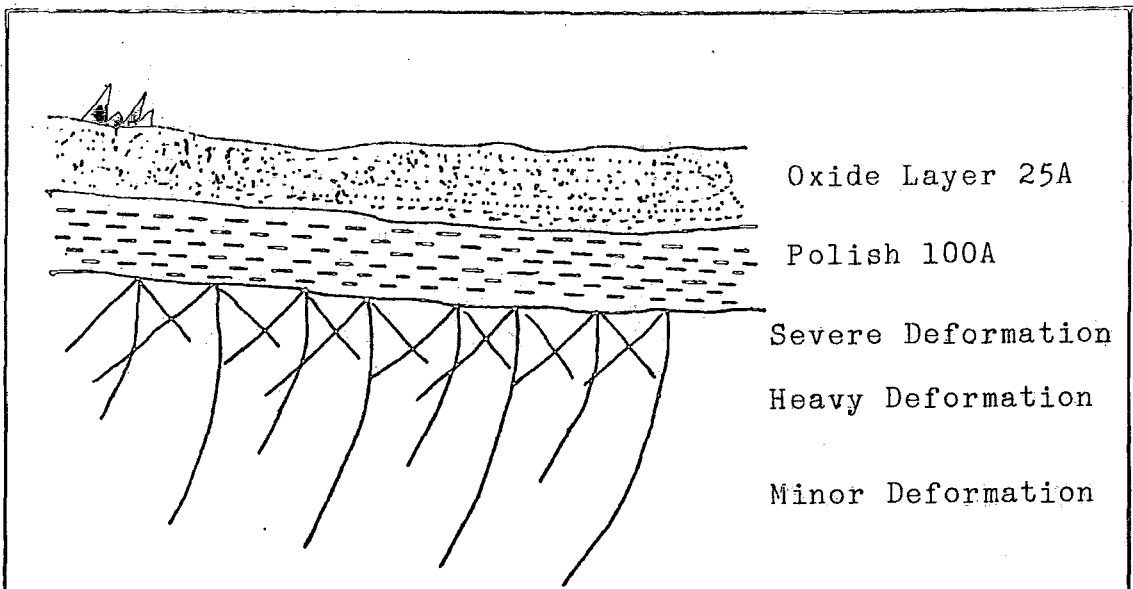


Figure 2.1 Typical Surface After Abrading and Polishing in Air

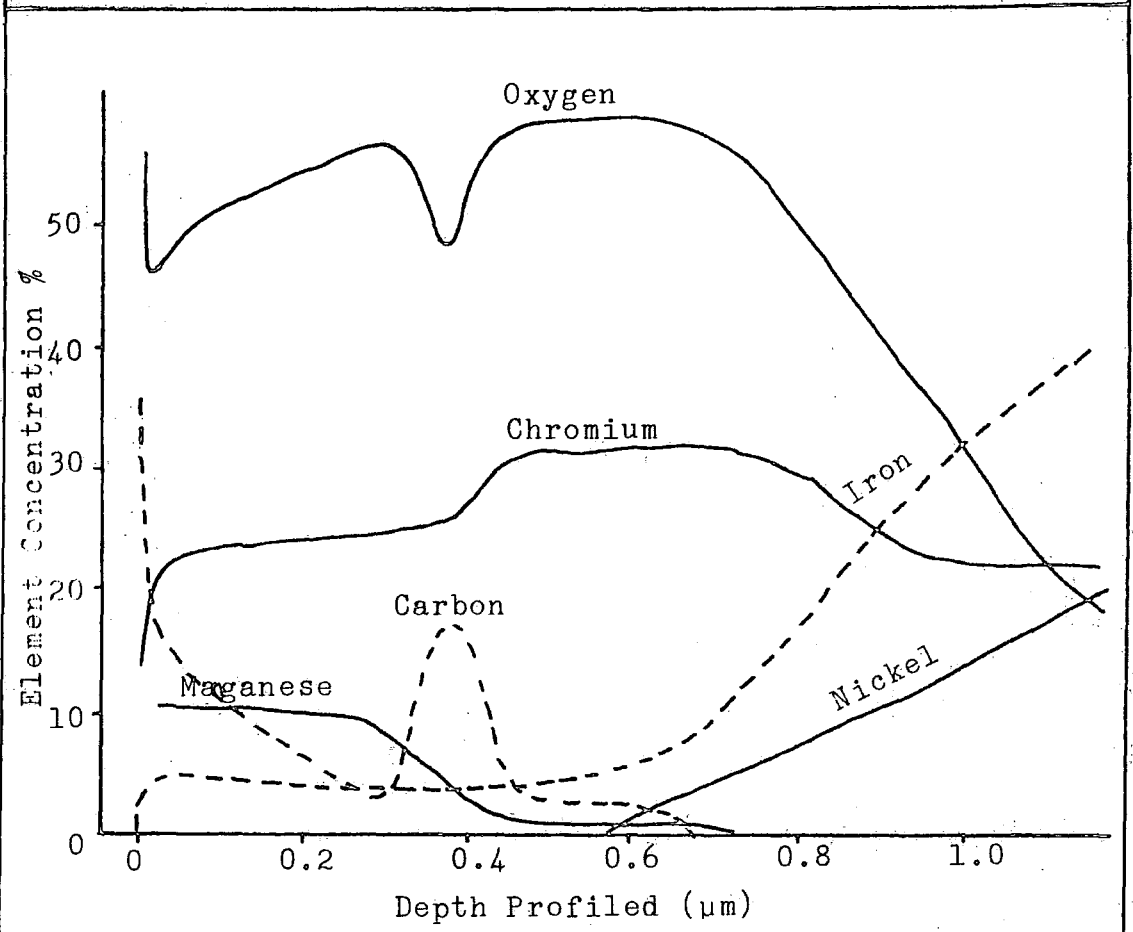
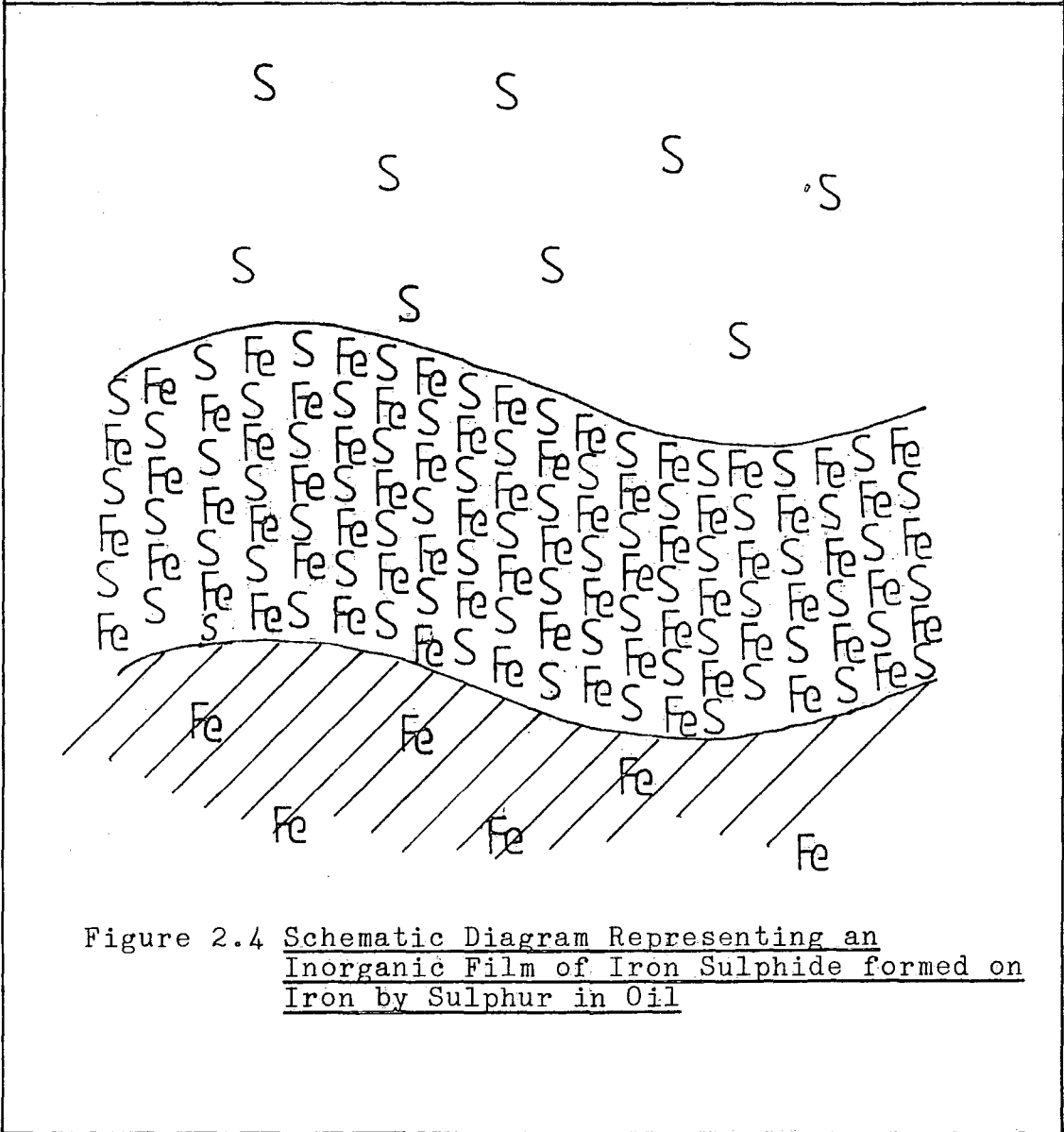
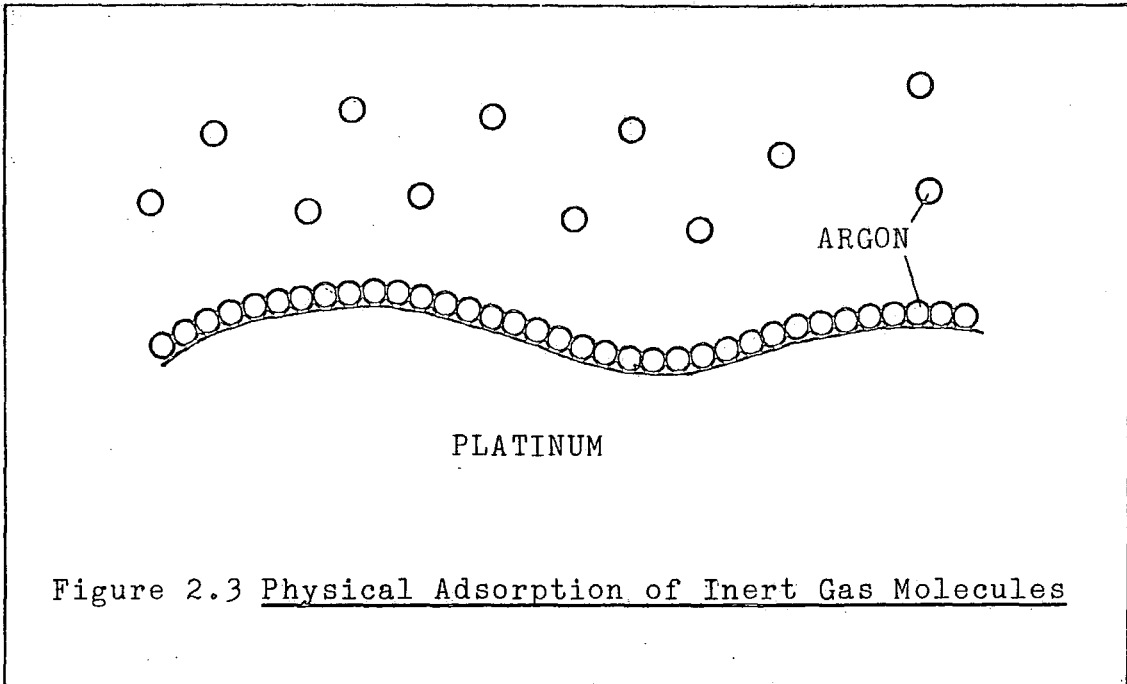


Figure 2.2 Surface Profile of a Carbon Steel



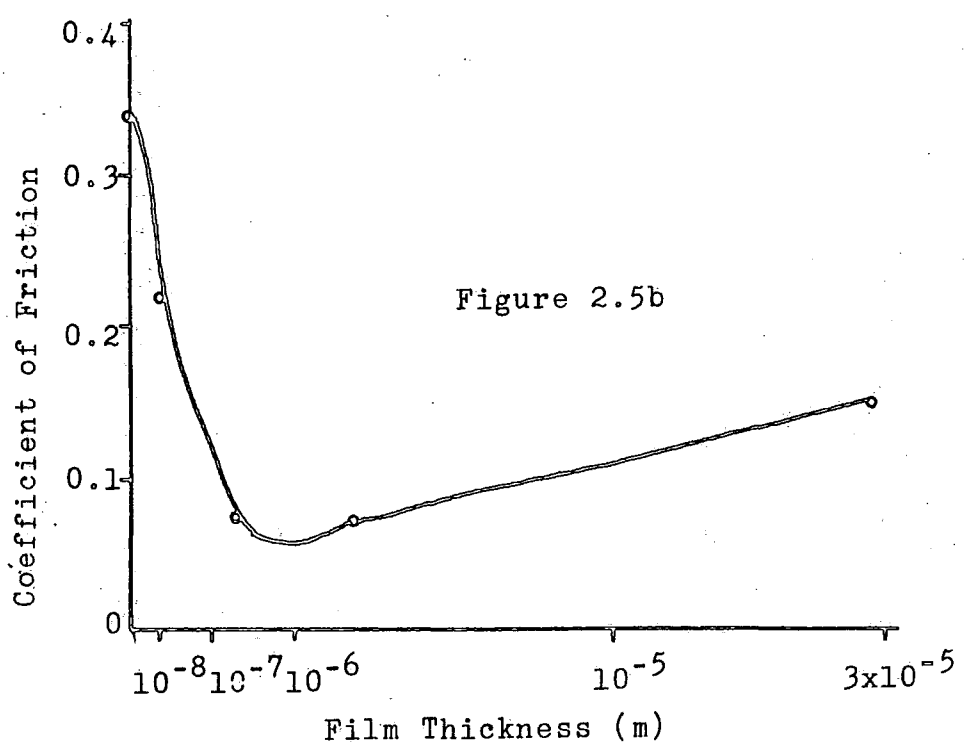
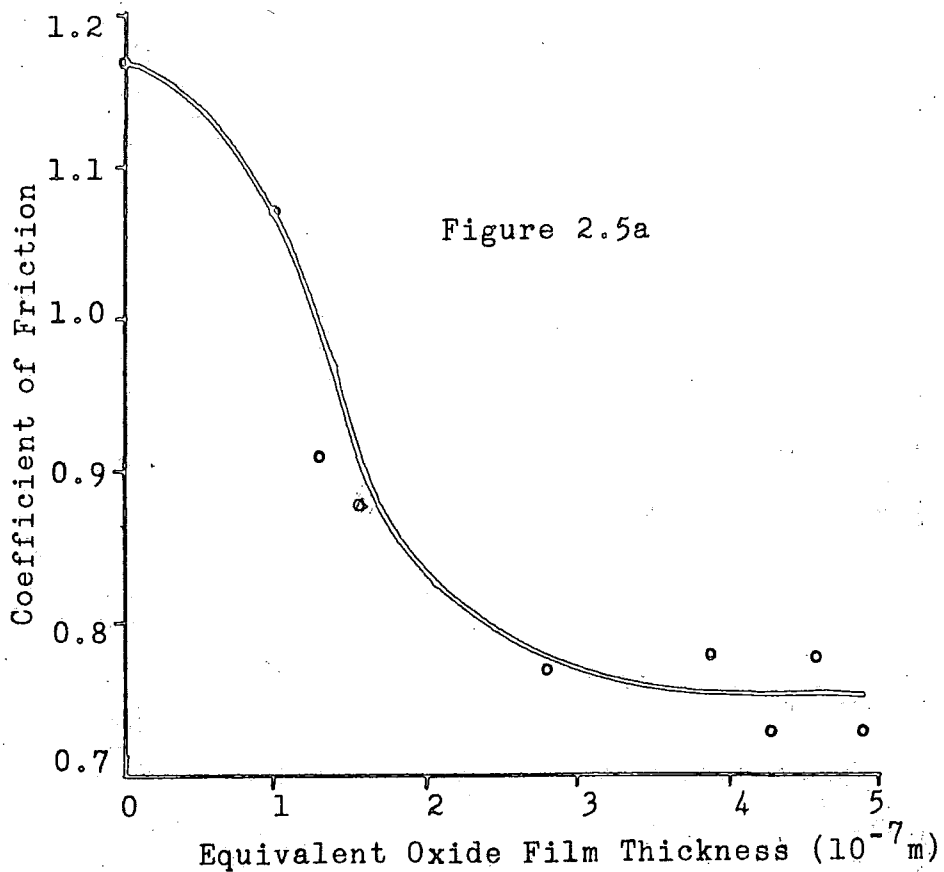


Figure 2.5 Relationship Between Friction & Thickness of Surface Films

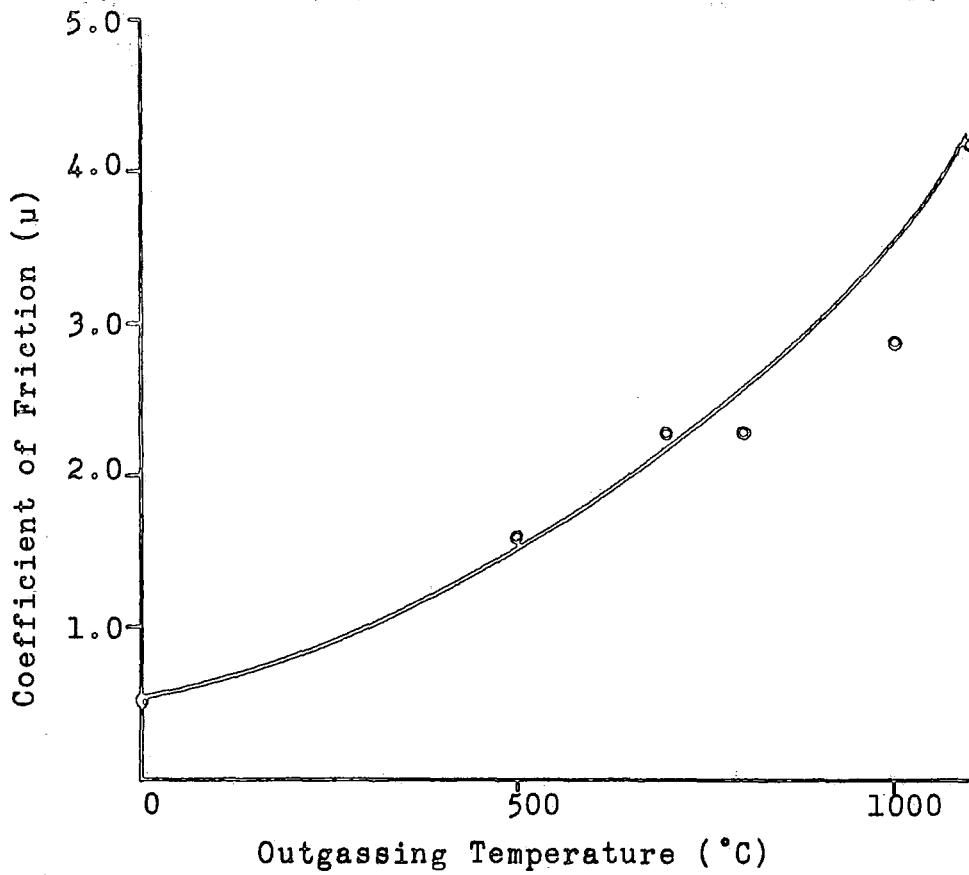


Figure 2.6 Removal of Oxide Film by Heating

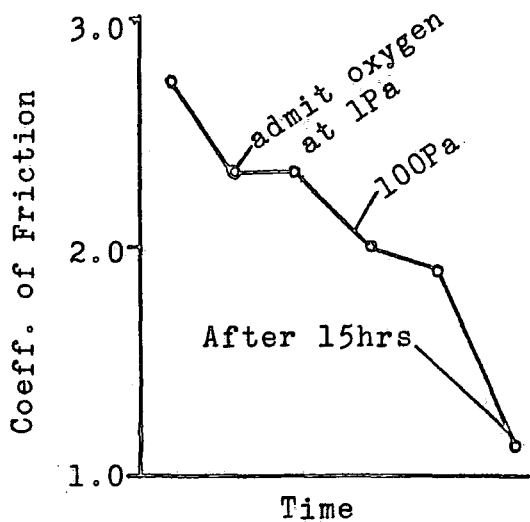


Figure 2.7a

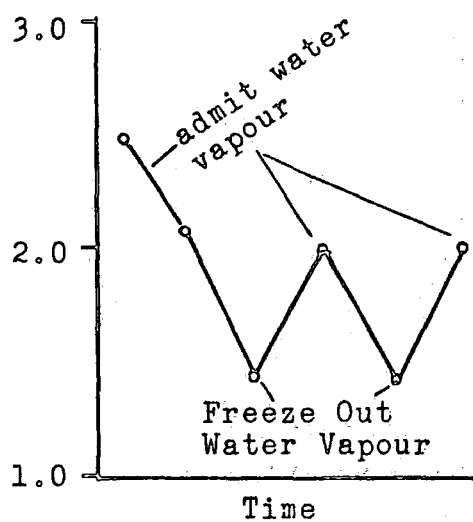


Figure 2.7b

Figure 2.7 Effect of Oxygen & Water on Coefficient of Friction

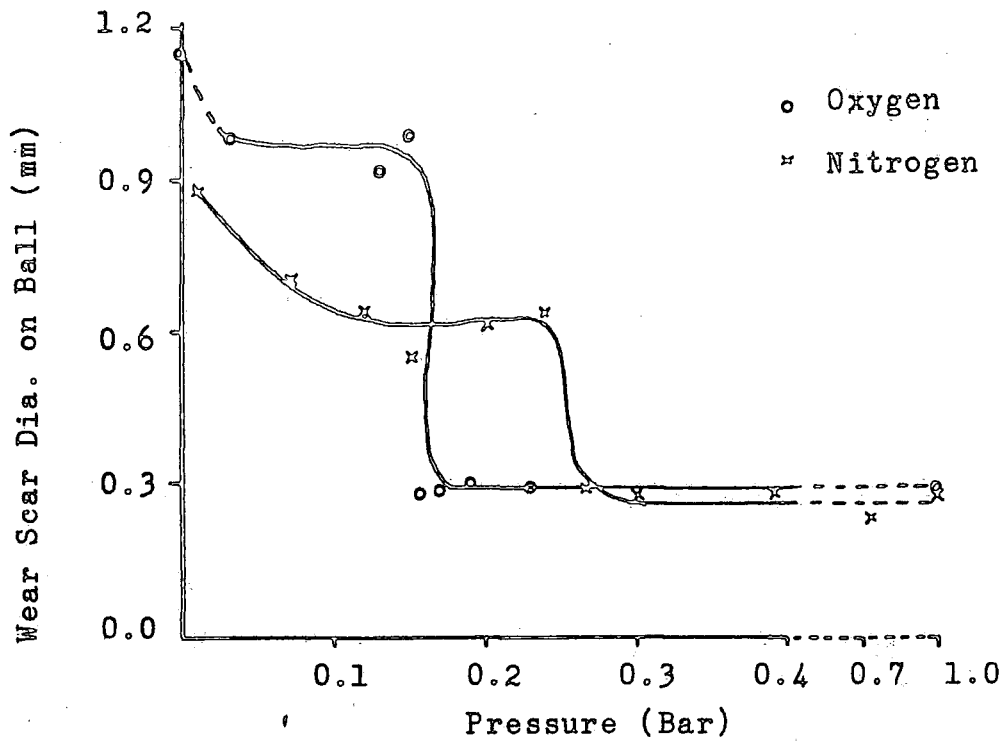


Figure 2.8 Wear in Air & Nitrogen at Various Pressures

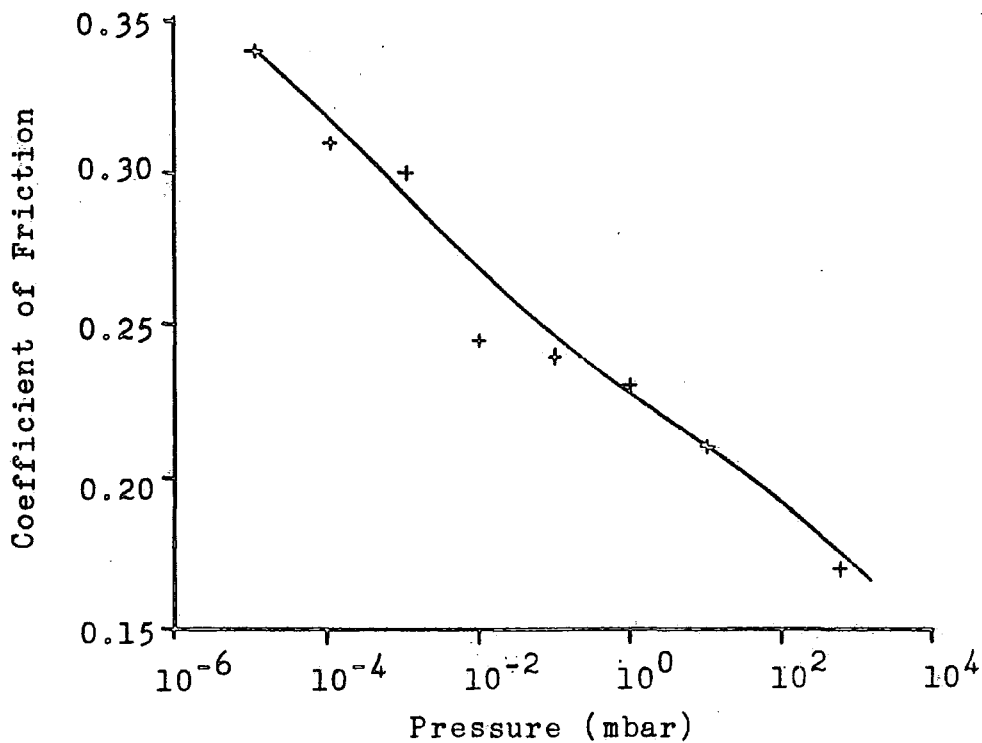


Figure 2.9 Coefficient of Friction v's Air Pressure

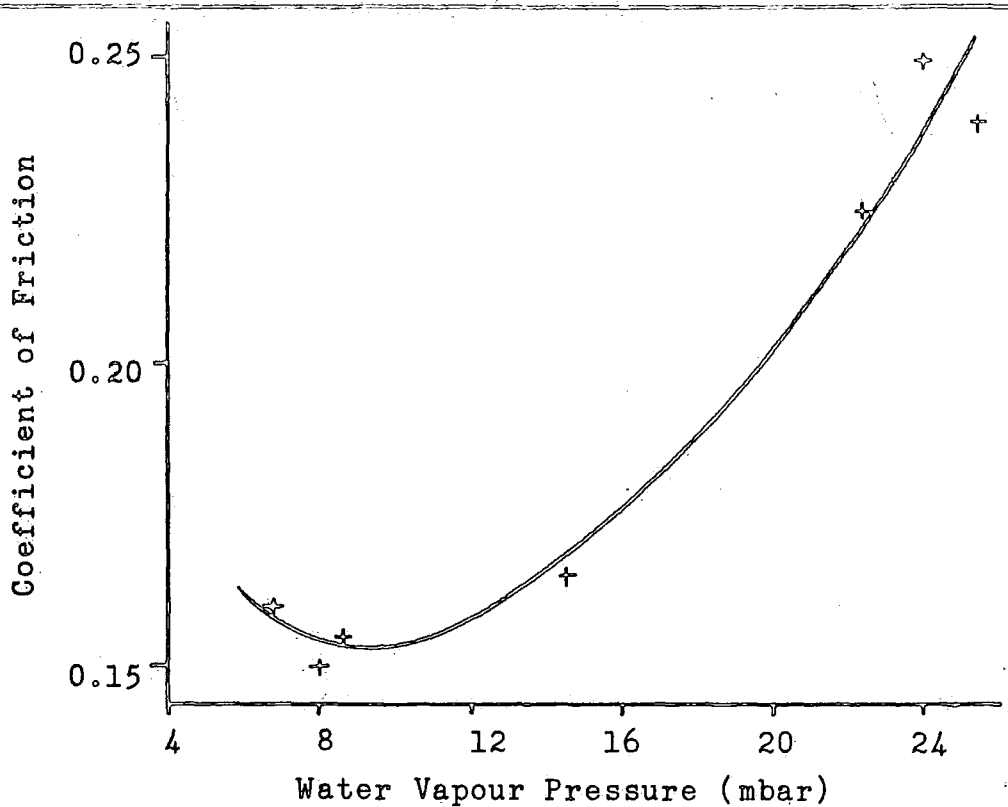


Figure 2.10 Coefficient of Friction v's Water Vapour Pressure

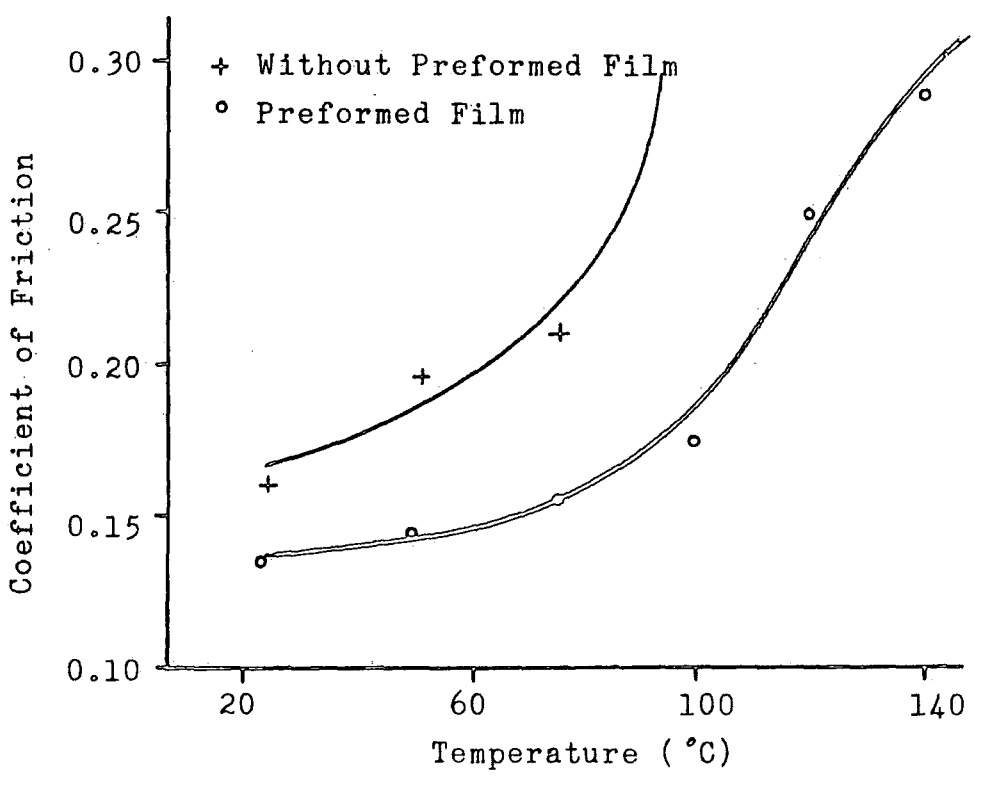


Figure 2.11 Coefficient of Friction v's Temperature

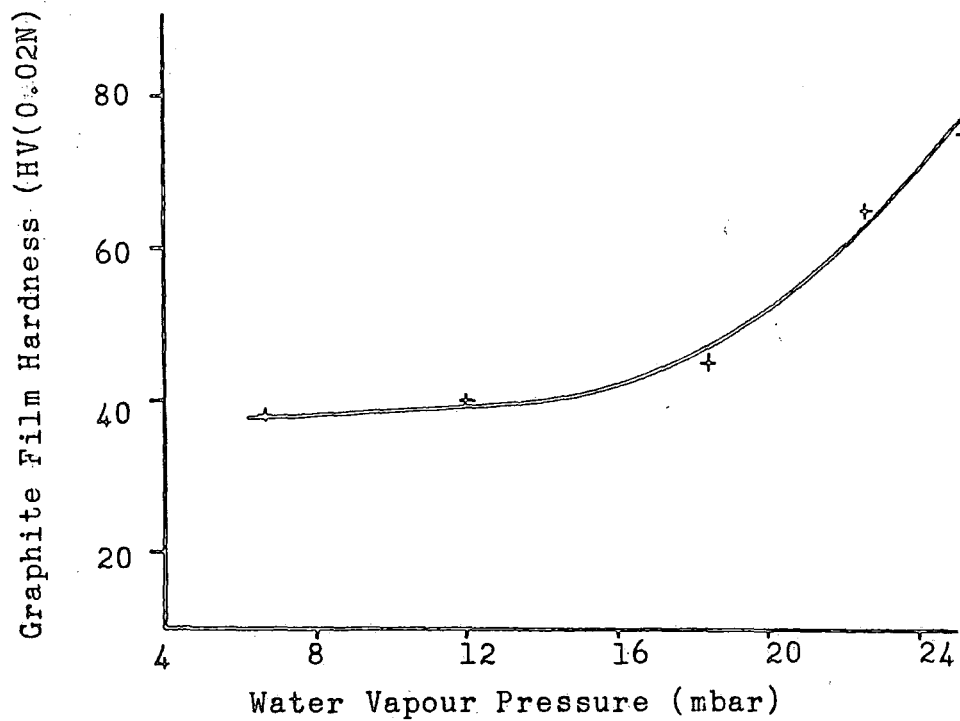


Figure 2.12 Film Hardness v's Vapour Pressure

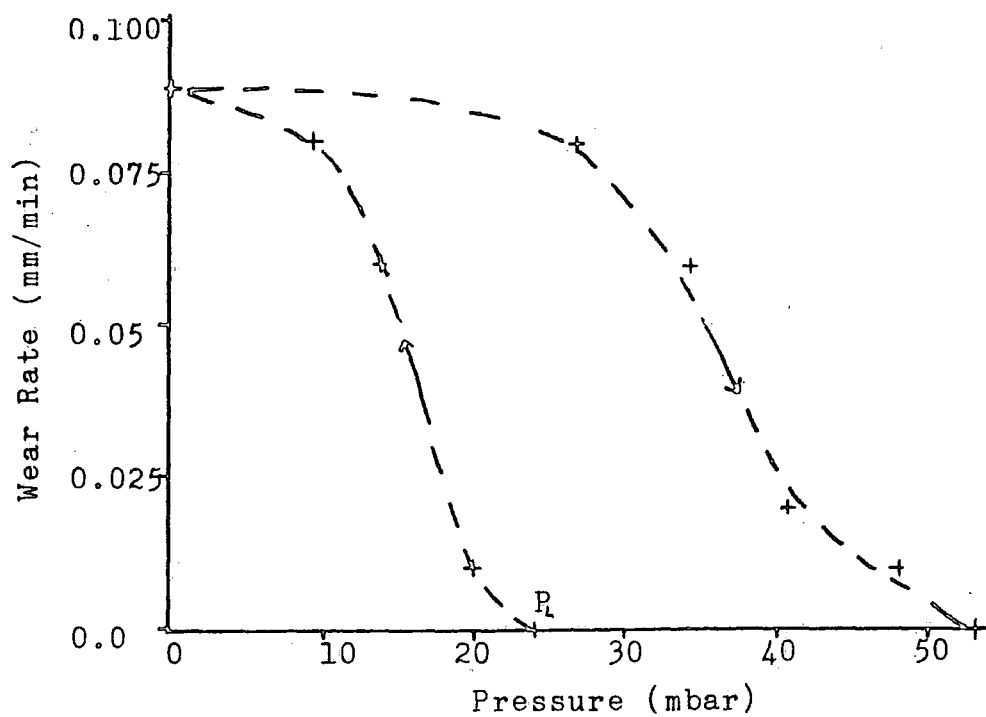


Figure 2.13 Wear in n-Pentane (From Savage 1955)

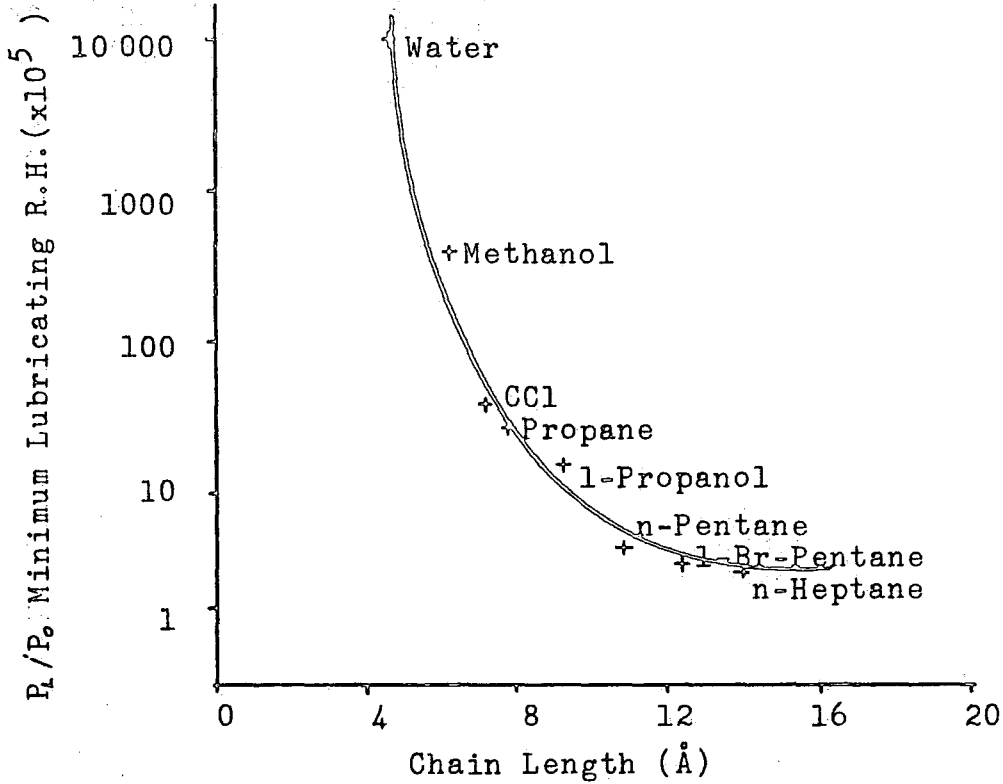


Figure 2.14 Correlation of Molecular Size with Minimum Relative Humidity for Effective Lubrication

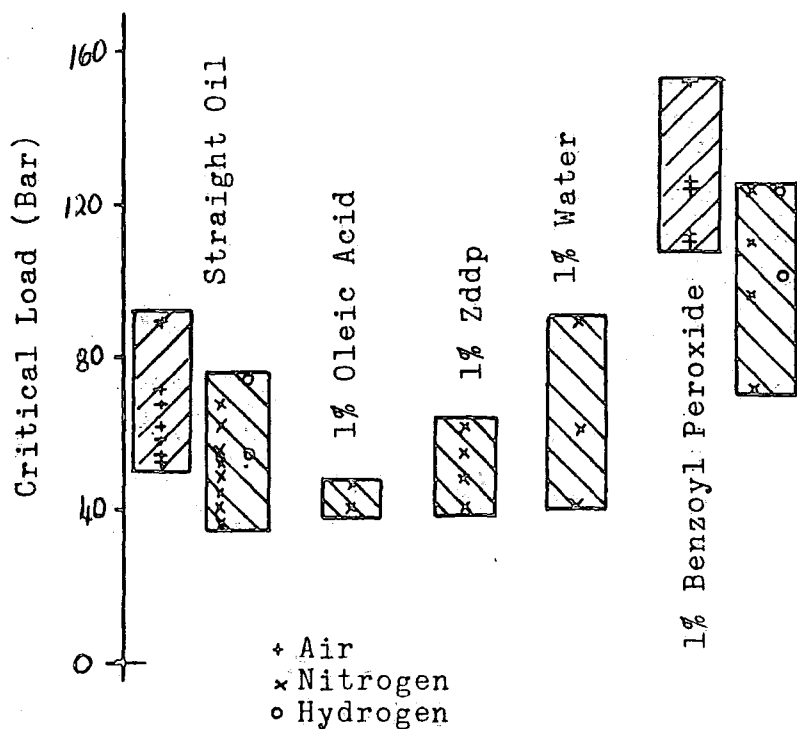


Figure 2.15 Critical Loads for Various Test Conditions

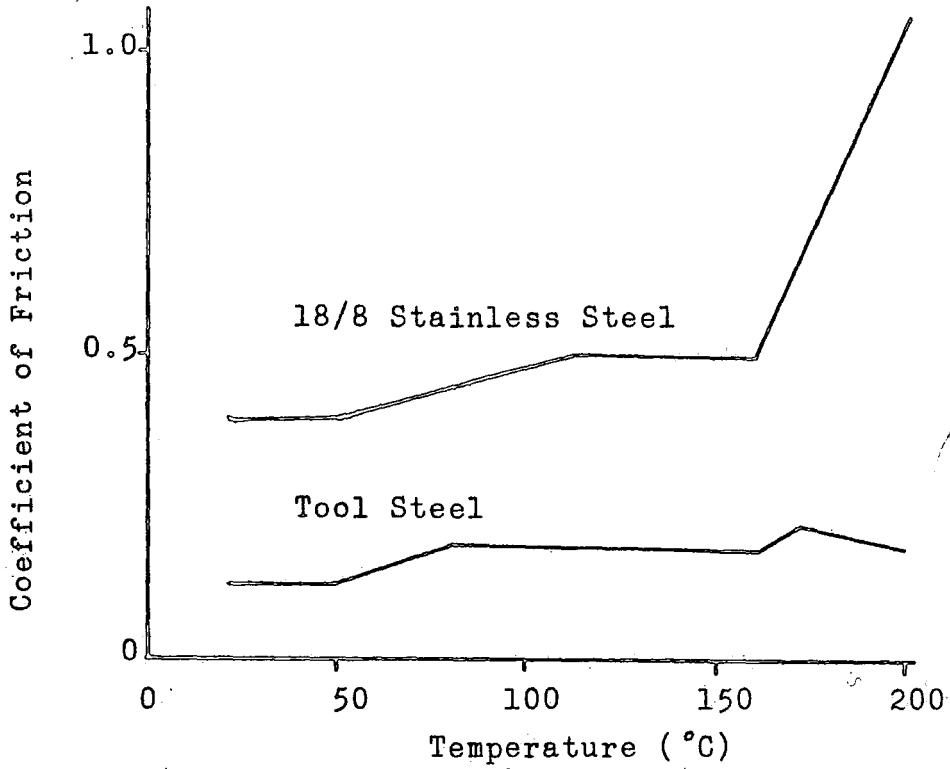


Figure 2.16 Coefficient of Friction to Temperature for a Mineral Oil

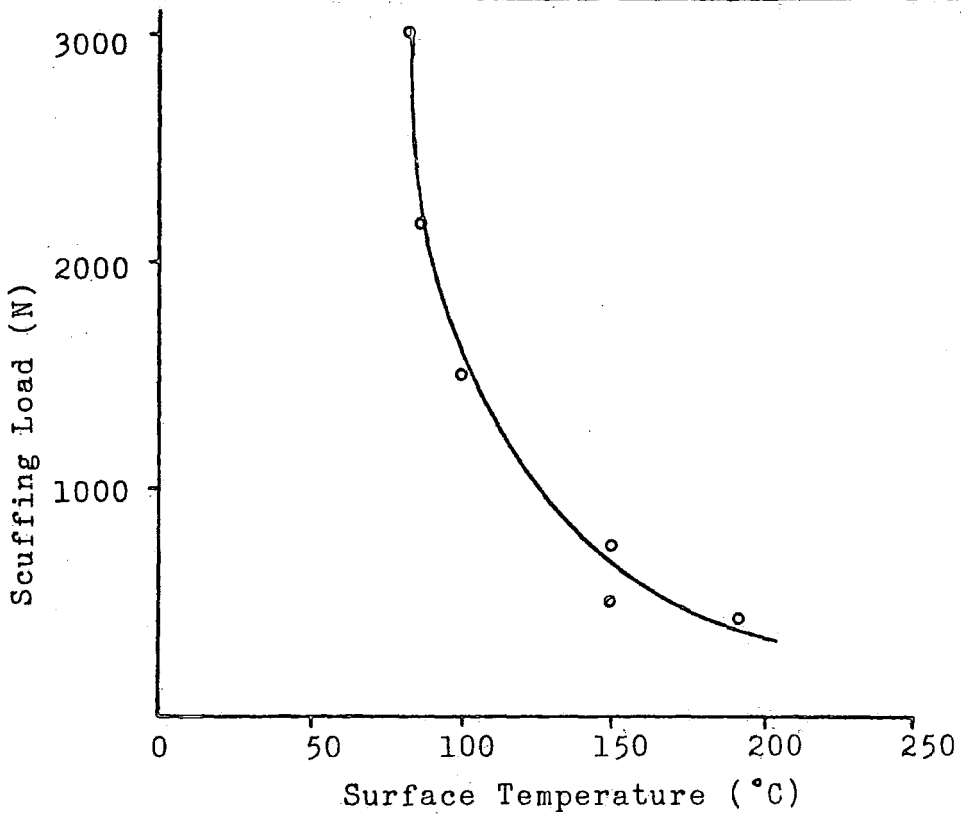


Figure 2.17 Scuffing Load v's Surface Temperature

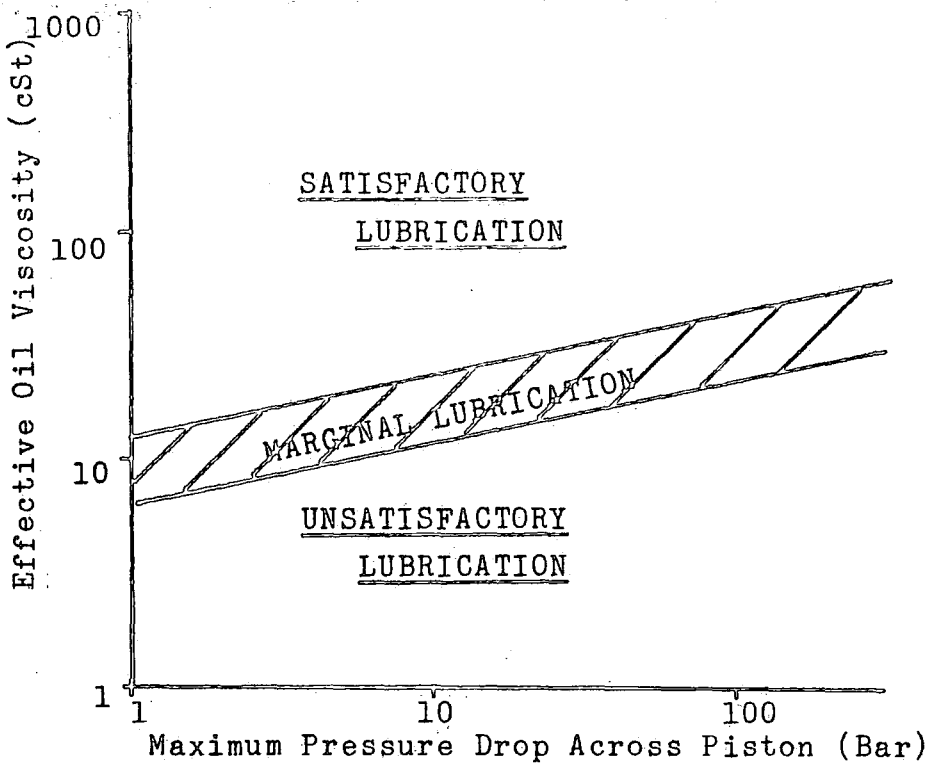


Figure 2.18 Effective Oil Viscosities as a Function of Pressure Drop

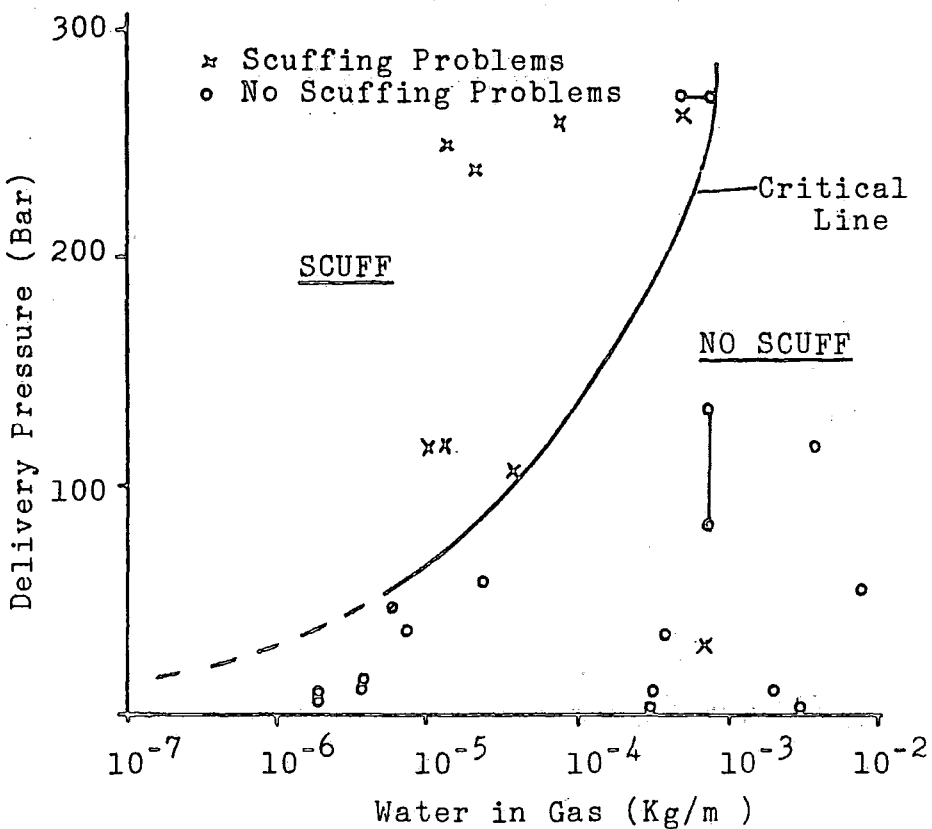


Figure 2.19 Behaviour of Hydrogen Compressors with Cast Iron Piston Rings

CHAPTER 3

EXPERIMENTAL APPARATUS

Two separate experimental rigs are described in this chapter. For the purposes of this thesis they will be referred to as No 1 Friction Apparatus and the Heated Plate Apparatus.

3.1 No 1 Friction Apparatus

3.1.1 General Description

The main function of this equipment was to examine the effects on friction and wear of various gas environments on cast iron rubbing against cast iron in a boundary lubrication regime. Also included in the design philosophy was the possibility of examining the material surfaces by using electron spectroscopy for chemical analysis (E.S.C.A.).

To make the apparatus compatible for use with E.S.C.A. certain design constraints were imposed. The maximum size of specimen that could be examined was 20 x 8 x 4 mm, and this had to be fitted onto a 0.48" diameter probe, of sufficient length to go through an insertion lock and into the X-ray chamber of the spectrometer. The sizes of the environmental chamber and the ball valve were also restricted to allow compatibility with the spectrometer.

A diagram of this apparatus is shown in Figure 3.1.

The actual friction test took place in a controlled environment inside the environmental chamber. The force actuating saddle enabled loads to be applied to the plate (specimen) via two pins whose axis were perpendicular to the plate surface. The ball valve and slide rails allowed the plate to be isolated (between the seal section and the ball valve) and the probe removed, by sliding back the scotch yoke mechanism on the slide rails and undoing the quick-connect coupling. It could then be bolted onto the spectrometer and E.S.C.A. carried out. The scotch yoke mechanism enabled the probe (with attached specimen) to be reciprocated backwards and forwards whilst the two pins rubbed against the plate. The friction generated by this motion was measured by means of strain gauges inside the probe. More detailed descriptions of the above apparatus are contained in the following sections and details of the equipment used are to be found in Appendix C.

3.1.2 The Friction Test

Due to the constraints imposed by the use of E.S.C.A. and the destructive nature of scuffing, a certain amount of thought went into devising a suitable type of friction test. The following points were taken into consideration:-

- i) The specimen had to be of suitable size and shape for examination by E.S.C.A.
- ii) The friction test had to be such that when lubricated any possibility of hydro-dynamic or elasto-hydrodynamic lubrication was excluded.

iii) When scuffing had taken place it was unlikely that the specimen could be re-used, therefore the specimens had to be easy to make in large quantities.

The method chosen for the friction test was to rub the flat end surfaces of two cylindrical pins against a flat specimen (see Figure 3.2) which was reciprocated backwards and forwards at low speed. By applying a high force to the pins and keeping the speed low, boundary lubrication could be ensured.

The two shapes of flat plate specimens decided upon are shown in Figure 3.3. A rectangular one for normal use and a T-shaped one for use with E.S.C.A. This was designed to minimise the amount of unworn surface scanned by the analyser, thereby improving accuracy. Both types of plate could easily be made to a good surface finish.

The plate was held on the end of the probe by drilling a hole 2 mm deep and using a grub screw to prevent it coming loose (Figure 3.3). The pins were held in the pistons also by grub screws which prevented rotation and stopped them from coming loose when the plate was unloaded, which was particularly necessary after scuffing, when the pins tended to adhere to the plate.

It was found to be important to prevent large vertical misalignment of the pins (Figure 3.4), as this tended to twist the probe. A small misalignment was acceptable provided the direction of twist tightened the probe tip onto the probe (see Section 3.1.6 for probe design).

3.1.3 Environmental Chamber (Figure 3.5)

The actual friction tests took place inside a small environmental chamber, consisting of a 6-way cross, a ball valve, a seal section and a quick-connect (disconnect) coupling (see Figure 3.5). The environment inside the chamber was established by pumping the relevant gas into the 6-way cross. The gas flowrate was controlled by the rotameter valve (see Figure 3.10). Oil was pumped or fed by gravity into the chamber and dropped onto the specimen plate. The oil flowrate was controlled by a metering valve, which was resistant to both oil and degreasing agents. Wear debris and excess oil were collected in the catchpot (see Figure 3.7) where they were allowed to flow into a collecting jar positioned below the apparatus. The pressure inside the chamber was measured by a mercury manometer connected to a pressure tapping in the 6-way cross. The glass viewport on top of the chamber was designed to withstand both positive and negative gauge pressure (up to ± 1 bar).

All the connecting bolted flanges were sealed using copper gaskets, with the exception of the glass viewport, which was sealed by rubber 'O' rings. The two branches that took the loading pistons (Figure 3.5) used two rubber 'O' rings spaced 20 mm apart. The brass plates at the end of the branches were to prevent excessive movement of the load pistons.

Inside the seal section, two special steel reinforced rubber seals were used; these seals were the only ones available to suit the probe diameter. As these seals had

to be oriented according to the pressure (ie. positive or vacuum), they had to be changed around when used with E.S.C.A., where a high vacuum seal was required.

The quick-connect coupling enabled the ball valve and seal section to be removed quickly and easily from the chamber, normally for use with E.S.C.A., without the necessity of undoing bolts.

3.1.4 Loading Pistons (Figure 3.6)

Two types of piston were used. Type I which was used for most of the experiments was a plain piston with a hole through the centre for a thermo-couple sensor. The pins were inserted into a hole at the tip and lightly clamped with grub screws.

The other type of piston, shown in Figure 3.6, was designed to heat the pin tip to temperatures in excess of 100°C. To do this a small 25 W heating element was inserted inside a copper conductor, which conducted the heat to the cast iron pin. As it was important to keep the external temperature of the piston low (ie. below 25°C), in order to validate the load calibration (see Section 4.1.1) and to prevent damaging the rubber seals, an internal water jacket cooled the outside of the piston. The water was pumped by a peristaltic pump from a constant temperature reservoir ($\pm 10^\circ\text{C}$), (see Figure 3.6). In order to prevent ice forming around the refrigeration bulb and to prevent corrosion of the inside of the piston, an auto-mobile anti-freeze mixture was used instead of pure water.

As it proved difficult to measure the tip temperatures whilst running the experiment, the heated pistons were calibrated before use (see Section 4.1.5).

3.1.5 Force Actuating Saddle (Figure 3.7)

In order to apply the load perpendicularly onto the specimen, a force actuating saddle was used (Figure 3.7). A pneumatic cylinder and piston were mounted on one side of the saddle while on the other side the adjustable piston could be positioned by turning the screw. It was necessary to adjust the pistons, prior to loading, so that the cylinder was not operating near the end of its stroke, and to put the pins close to the plate so that when loading, both sides were loaded simultaneously. The roller bearings (Figure 3.5) enabled the saddle to adjust its position to balance the load and so compensate for the slight differences in seal performance.

Two sizes of pneumatic cylinder were used: a 42 mm diameter and 100 mm diameter, which were able to deliver forces of up to 500 N and 3000 N respectively, using the laboratory compressed air supply (5 bar max.). The whole system was calibrated by using a pre-calibrated proving ring (see Section 4.1.1), however it was found that the ambient temperature could affect the performance of the piston seals. For this reason tests were carried out when the ambient temperature was between 18°C and 25°C.

The pneumatic circuit diagram associated with the cylinder is also shown in Figure 3.7. The compressed gas supply came from the normal laboratory supply, which had

a maximum pressure of 5 bar. By means of the regulator the pressure of the supply to the cylinder could be adjusted. The two speed control valves ensured that the cylinder did not load or unload too quickly. The pressure in the cylinder was measured by means of a pressure gauge connected to the cylinder "load" supply.

3.1.6 Probe

Certain dimensional restrictions were placed on the probe:-

- i) The outside diameter of the probe had to be 0.480" in order to fit the analyser seals (E.S.C.A.)
- ii) The probe had to be long enough for the plate specimen to be inserted into the X-ray chamber through the ball valve and seal section (see Figure 3.8).

Two probes were built. The first one (shown in Figure 3.9) was made from stainless steel tube and fitted with a short strain gauged section to measure the axial strain on the probe (calibrated for frictional force). The leads for the strain gauges went through the probe to the handle and were connected to the amplifier via an airtight electrical feedthrough, which enabled the probe to be sealed from the outside environment, thus preventing contamination of the inside of the chamber.

The probe tip enabled the plate specimen to be attached by means of two 3 mm diameter grub screws. However it was found that when the pins were heated (ie.

when the heated pistons were used), conduction caused a large temperature rise in the strain gauged section. A special probe tip was therefore made of "tufnel" to insulate the probe from the specimen.

The strain gauged section was calibrated both on and off the rig (see Section 4.1.2). This section was necessarily the weakest part of the probe; however, the maximum axial load before yield was 8 KN, and the maximum buckling load was 4 KN (see Appendix B): both with design criteria (Appendix E).

As the above probe was found unsuitable for use with E.S.C.A. because of its poor surface finish and poor vacuum holding properties, another probe was made of a solid piece of stainless steel rod with a probe tip and a hollow cylindrical handle.

3.1.7 Reciprocating Mechanism

As the apparatus was primarily designed to reproduce boundary lubrication the reciprocating speed had to be low. The mechanism was therefore designed to have an average speed of 20 mm/s and a 20 mm stroke length. From the ICI data given in Appendix A this would correspond to $\pm 0.5^\circ$ T.D.C. for a compressor working at 350 rpm with a stroke of 300 mm (the average valves). A sinusoidal motion was used for simplicity, and this was produced by a scotch yoke mechanism. The above conditions for speed and stroke length correspond to 30 rpm with 10 mm of eccentricity.

A 125 W motor was used to drive the mechanism (see Appendix E for selection criteria). In order to obtain

the low speeds it was necessary to use a reduction gear-box in conjunction with the motor. The final gear ratio was 89:1 giving a speed range of 2-45 rpm. This speed range was chosen because it was expected that speeds lower than 30 rpm would be required most. To prevent the speed from dropping too low when under full load, a shunt wound D.C. motor was chosen. The difference between the no-load and full load speed was less than 10%, but as the motor was twice the necessary size (Appendix E) for the maximum design load, the highest possible speed variation was 5%. In fact, under most applications the speed variation was less than this.

The reciprocating mechanism was designed so that the probe handle could be clamped into a carriage and easily removed when necessary.

3.1.8 Gas Mixing

For many of the friction tests the gas environment was composed of two gas types: either two different gases (Figure 3.10a) or a mixture of water saturated gas and dry gas (Figure 3.10b). The actual mixing took place in a mixing chamber (capacity 750 ml) positioned upstream of the environmental chamber. The flowrates of the two gases into the chamber were controlled by two micrometer valves which gave fine adjustment of the water content (or oxygen content) of the gas. It was found that once the environment had been established with the correct gas flowrate (total gas flow), its composition varied little throughout the test, and in general, no adjustments to the control valves were needed.

3.1.9 Friction Measurement

A schematic diagram of the equipment used to evaluate the frictional force is shown in Figure 3.11. As mentioned previously, the strain in the probe was measured using four strain gauges inside the probe connected to a strain bridge amplifier. The strain was recorded by using the analogue output (+10 v to -10 v) from the strain amplifier, connected to either a X-Y recorder or a micro-computer (via an analogue to digital convertor).

When the micro-computer was used it was possible to record a large number of readings over a period of forty-eight hours before the storage disc needed changing. Also if the friction rose above acceptable safety levels, the test could be terminated immediately, by means of a motor cut-off. The apparatus was also protected by means of computer software and external hardware against power cut-offs and voltage drops.

The circuits used for both the analogue to digital convertor and the motor cut-off are shown in Appendix D, together with a description of their design features. The methods used to evaluate the frictional force, using the X-Y plotter and the A-D convertor, are outlined in the next chapter.

3.2 Heated Plate Apparatus (Figure 3.12)

This apparatus, with the exception of a few modifications, was identical to the apparatus used by Marshall (1983). The friction test, which consisted of a horizontal plate rubbing against a vertically loaded pin (see Figure 3.13), took place inside an environmental chamber. The method of environmental control was identical to the previous apparatus (No 1 Friction Apparatus). The rubbing motion was reciprocating from an electric motor, geared down to give a speed range of 0-45 rpm, with a stroke length of 40 mm.

3.2.1 Plate Heating

The plate was heated using two 25 W heaters (Figure 3.13) positioned underneath the cast iron plate in a P.T.F.E. holder. The plate was bolted onto the moving carriage by means of a clamping plate which was designed to form an oil bath. The clamping plate also contained a thermo-couple pocket for a thermo-couple sensor, so that the plate temperature could be measured by means of a digital thermometer. The plate temperature was controlled by using a variac voltage regulator.

3.2.2 Loading

As in the previous apparatus (No 1 Friction Apparatus), the load was applied by means of a pneumatic cylinder (Figure 3.14), which pushed down onto a cylindrical pin holder. In between the pin holder and the piston was a metal washer which formed a safety device to prevent

damage to the apparatus. If the pin broke (eg. as a result of severe scuffing), the pin holder would drop down, causing the two electrical contacts to complete a circuit turning of the motor, and in addition, all the load would be taken by the washer and not the holder.

3.2.3 Friction Measurement (Figure 3.15)

The friction force was measured by means of four strain gauges mounted on two aluminium strips. The gauges were mounted widthways and lengthways to form a full bridge configuration with temperature compensation. One end of the strip was bolted to a rigid support, and the other, to the cylinder platform. Any frictional forces which may have been caused by the horizontal movement of the platform were reduced by using roller-bearings above and below the platform.

The strain was recorded in an identical fashion to No 1 Friction Apparatus, either by a X-Y plotter or the micro-computer.

3.3 Gas Analysis

In order to ensure the correct environment inside the environmental chamber, gas analysis had to take place. The analysis was tried using a mass spectrometer, but this proved impractical for continuous monitoring, and as only two gas types were present, the use of such a complex system was unnecessary. Therefore, for gas analysis, two types of analyser were used; an oxygen analyser and a dewpoint hygrometer.

The oxygen analyser (Taylor Instruments Ltd) worked by measuring the paramagnetic susceptibility of the sample gas by means of a magneto-dynamic type measuring cell. As oxygen has a far greater paramagnetic susceptibility than other gases, the oxygen content of the gas could be evaluated by measuring the force developed by a strong non-uniform magnetic field on a diamagnetic test body suspended in the sample gas. The operating range of the analyser was 0-100% (volume), but was used in the range of 0 to 30%. Calibration was done by first, roughly calibrating to 21% in air, then zeroing, using pure argon, and then the full range adjusted, by using pure oxygen.

The dewpoint hygrometer (Michell Instruments Ltd) used a thin oxide film sensor which was essentially a water vapour pressure sensitive capacitor, capable of discriminating between very small changes in water content of the gas. Also for use in a hydrogen environment, an intrinsically safe barrier unit (I.S.B.U.) had to be used between the sensor and the hygrometer. Dewpoints from +20 C to -40 C could be measured for a large range of

flowrates. The instrument was pre-calibrated in the factory.

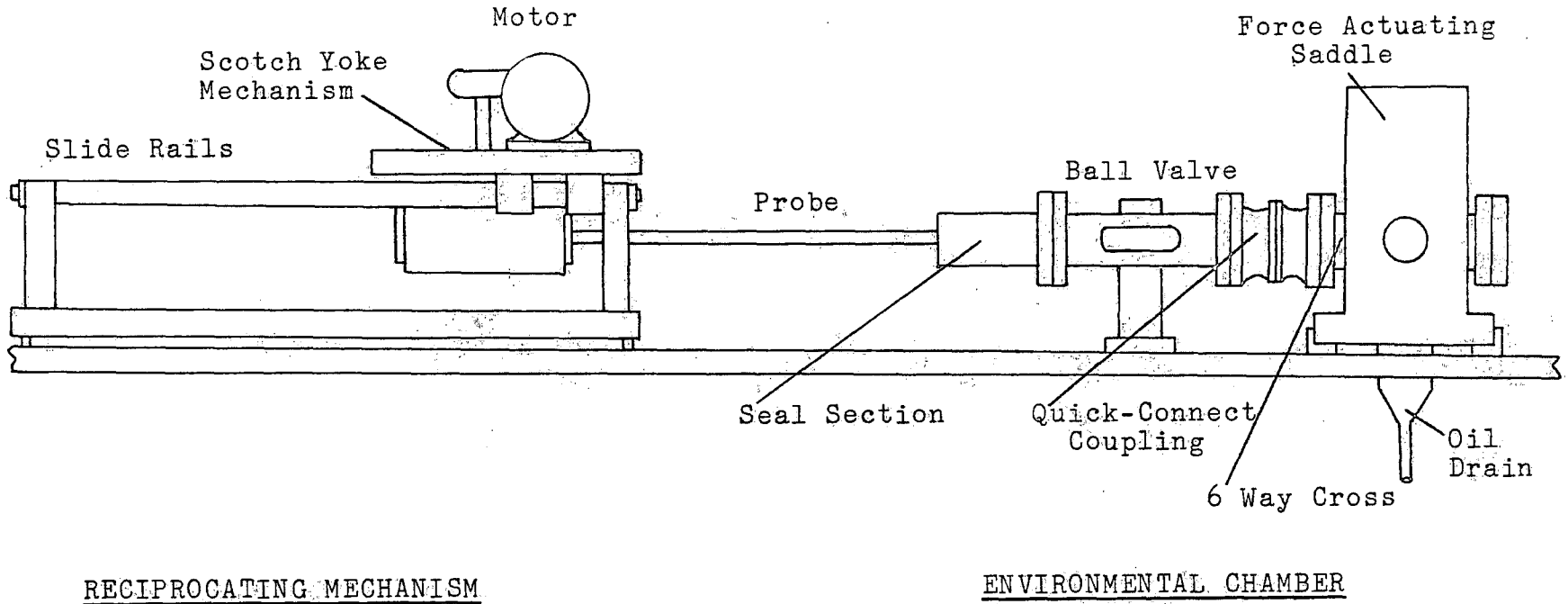


Figure 3.1 No.1 Friction Apparatus (General Assembly)

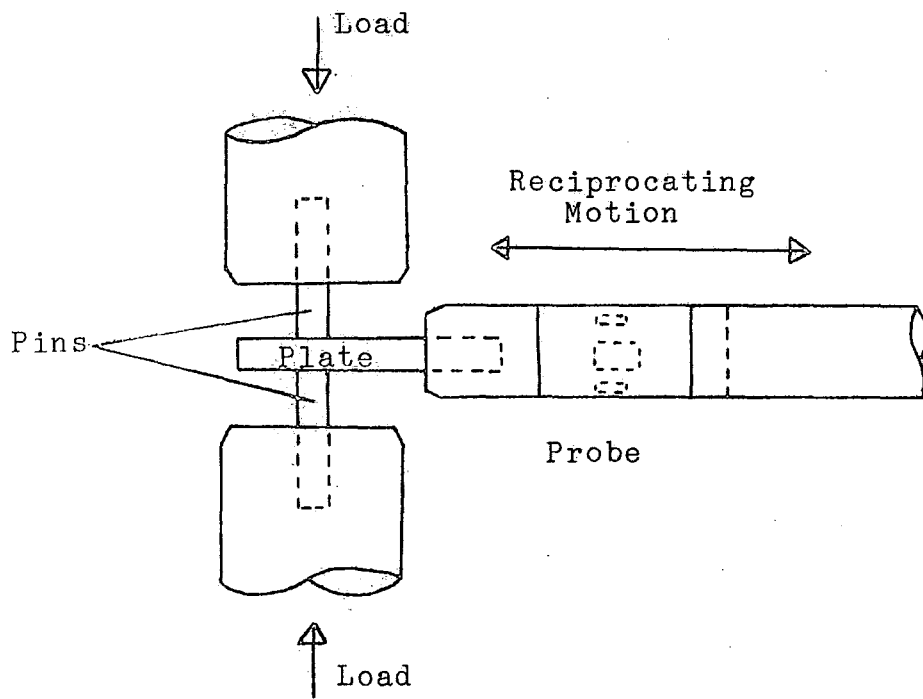


Figure 3.2 The Friction Test

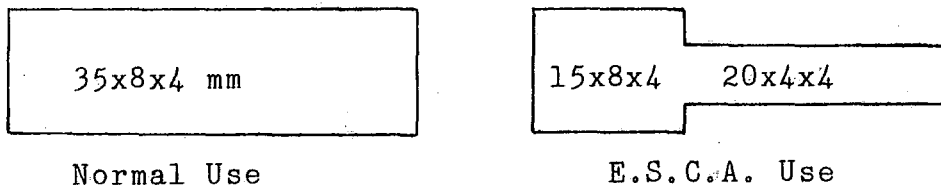


Figure 3.3 Types of Plate Specimen

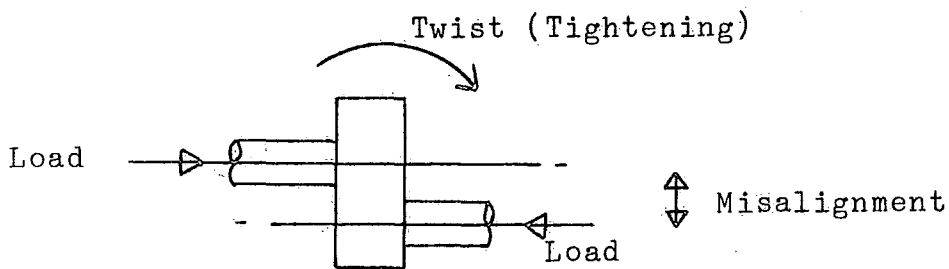


Figure 3.4 Effect of Misalignment

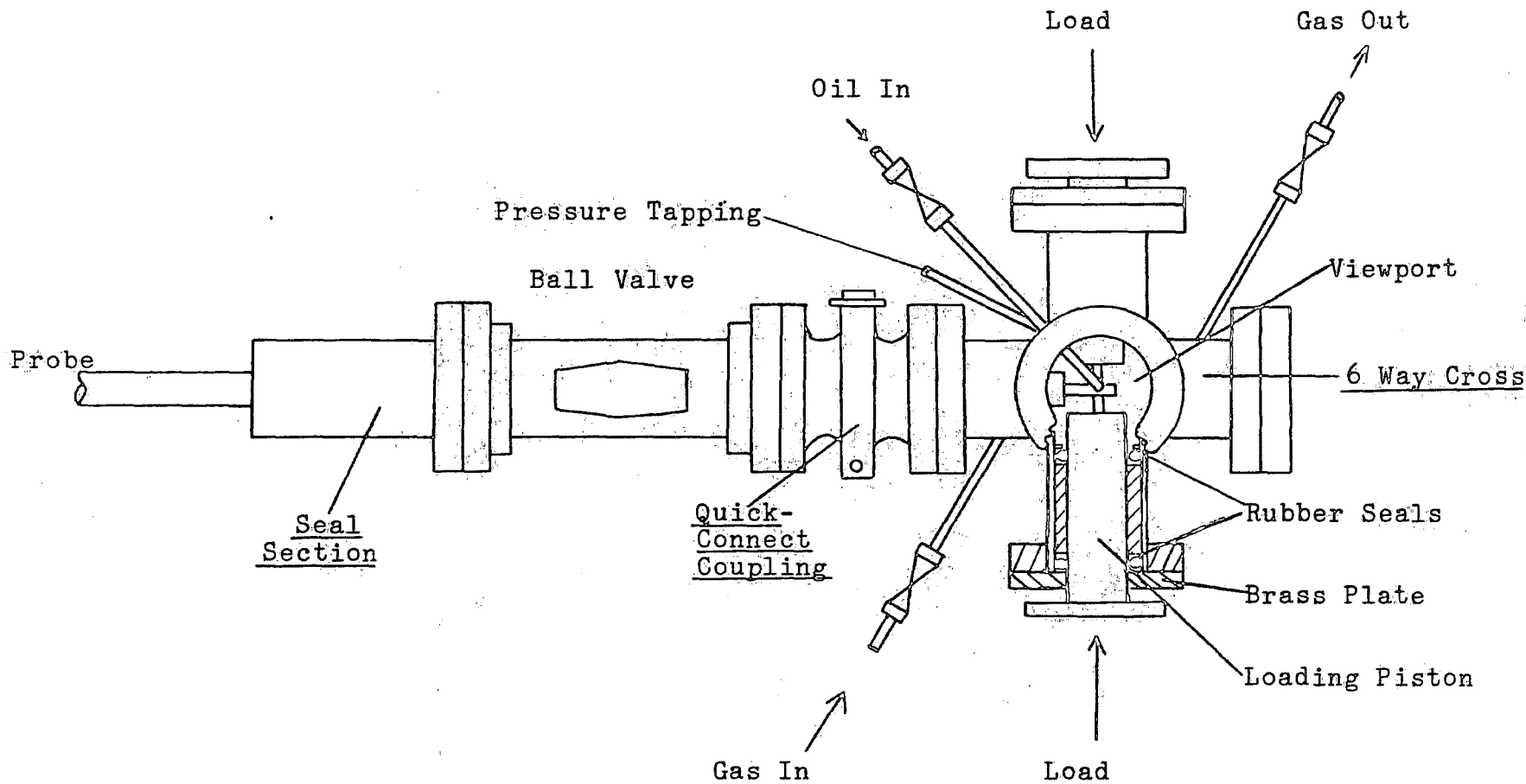


Figure 3.5 Environmental Chamber (Plan View)

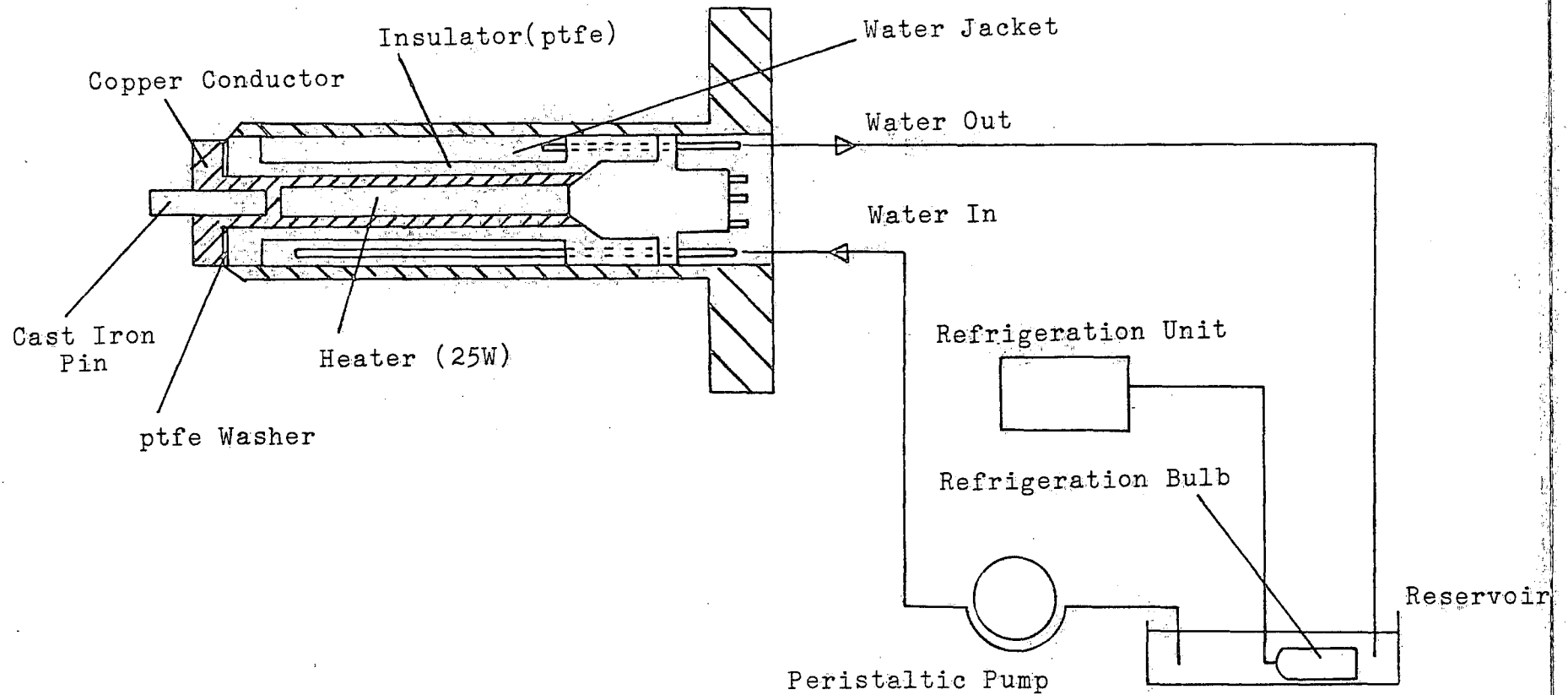


Figure 3.6 Loading Piston ,Heated Pin Type

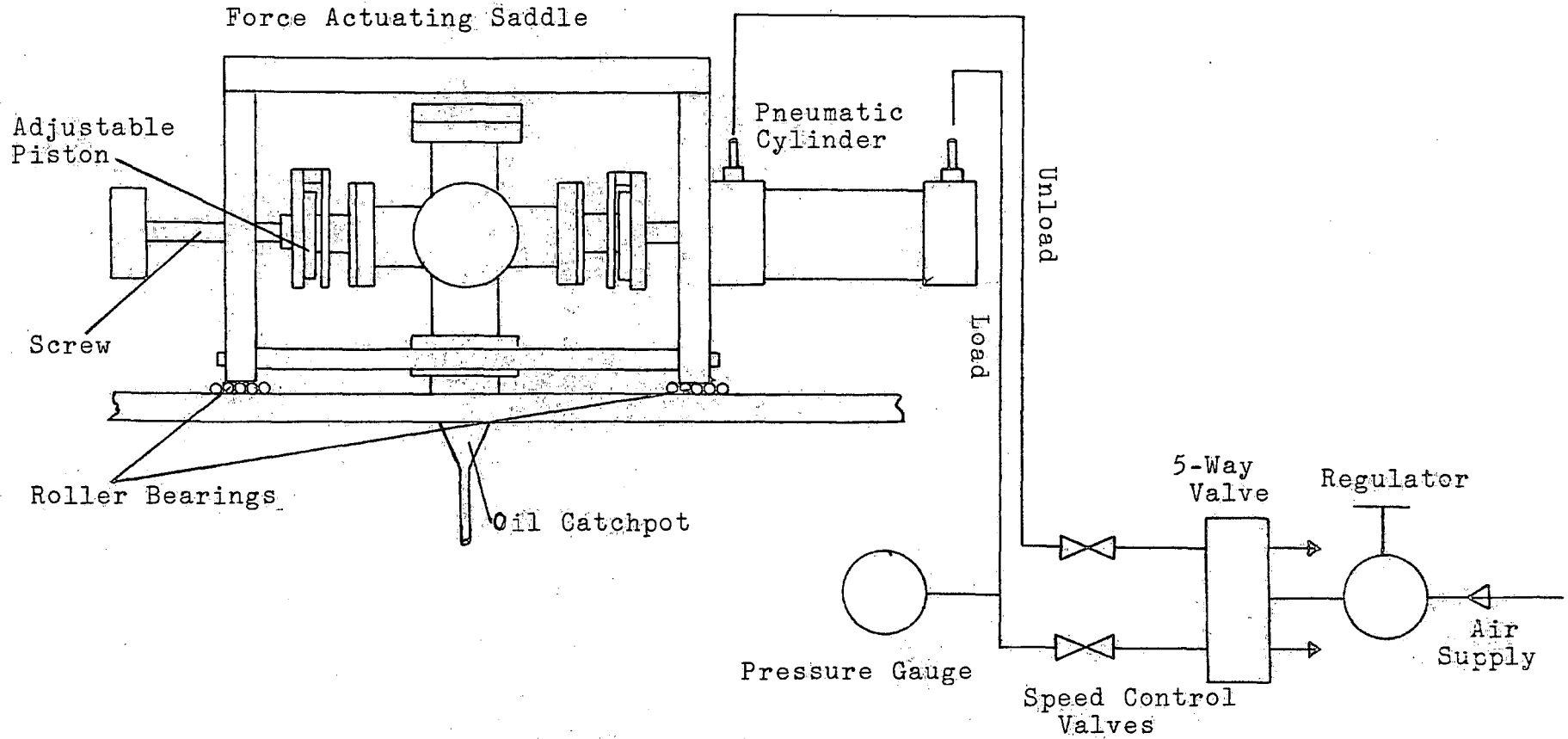


Figure 3.7 Force Actuating Saddle and Pneumatic Circuit Diagram

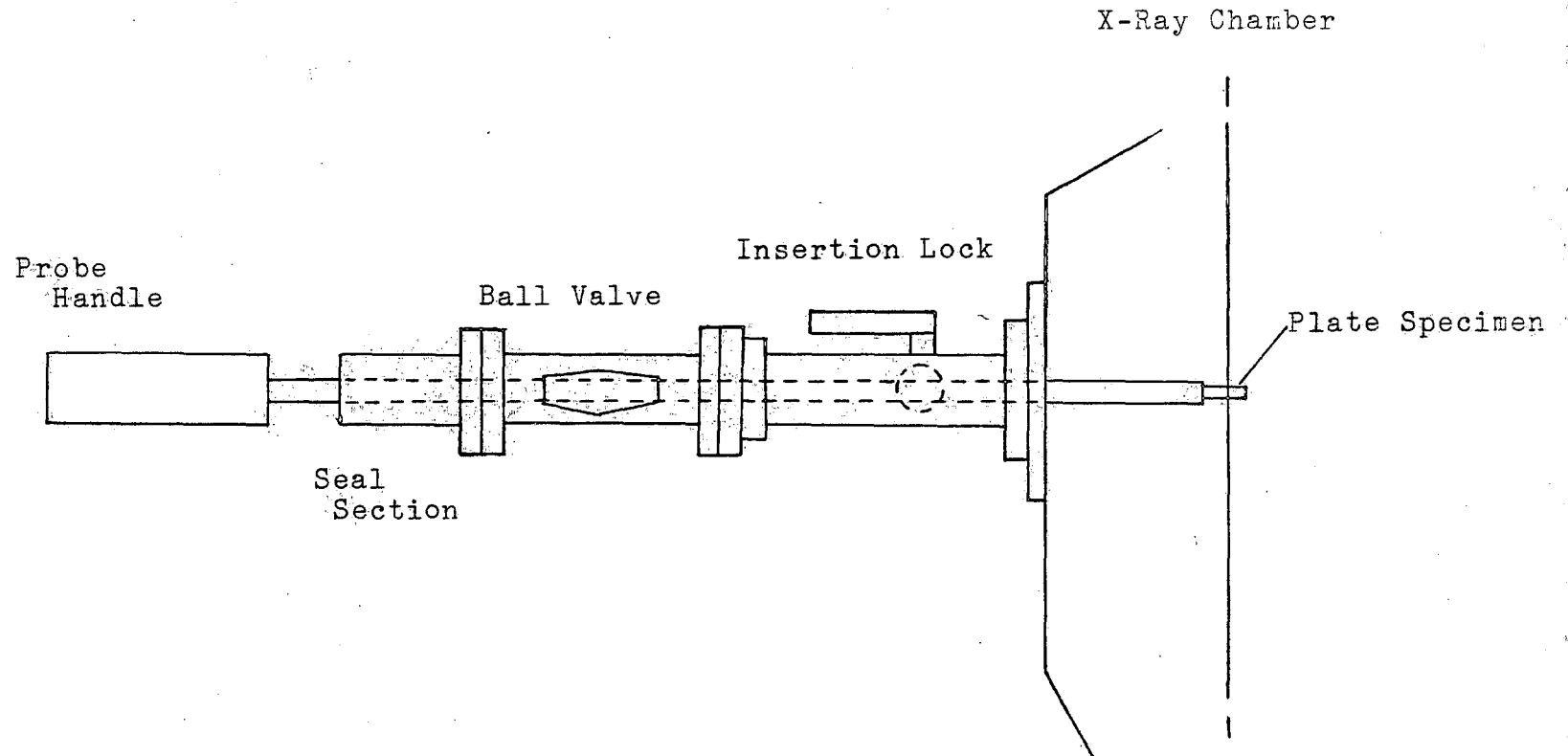


Figure 3.8 Arrangement for Using Electron Spectroscopy for Chemical Analysis

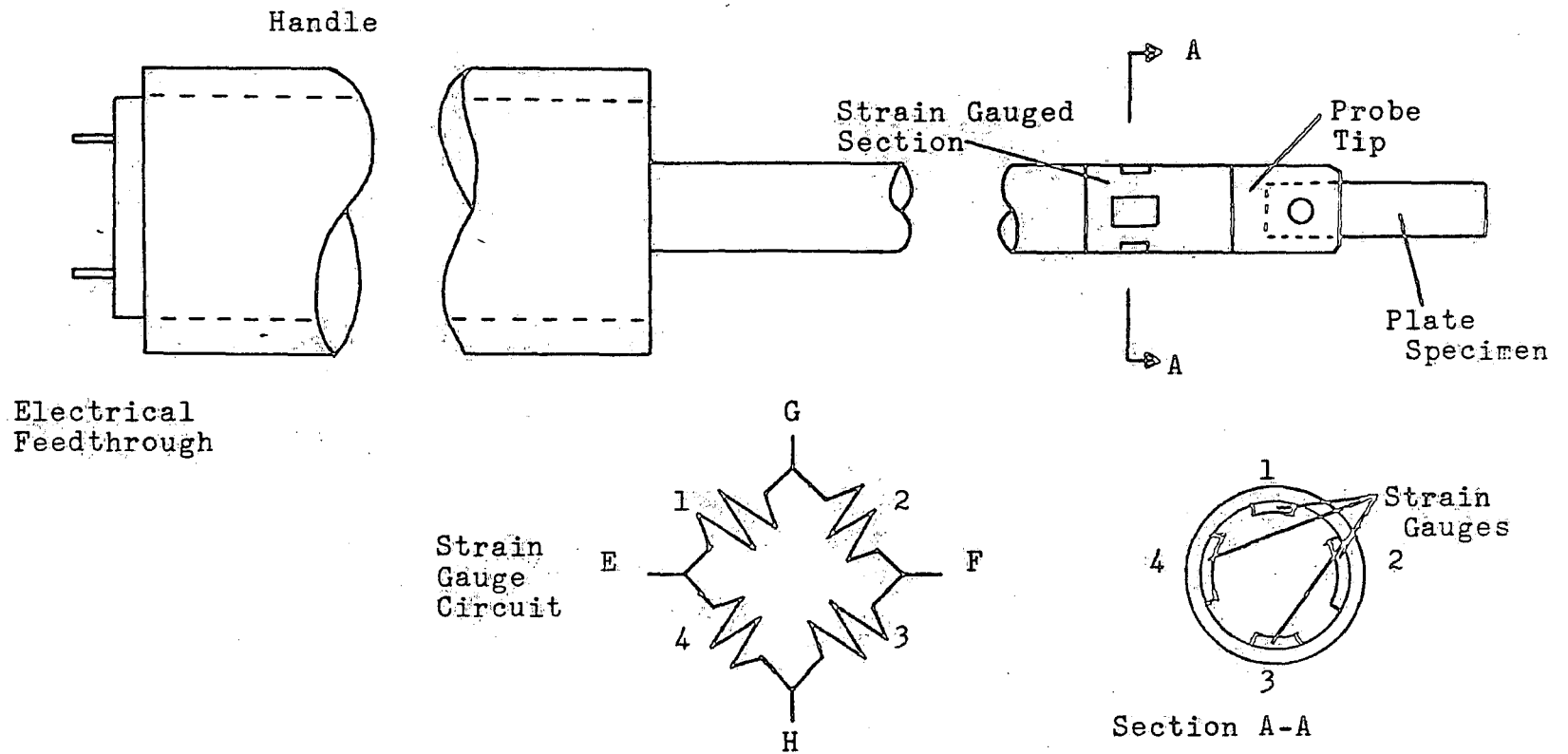


Figure 3.9 Probe

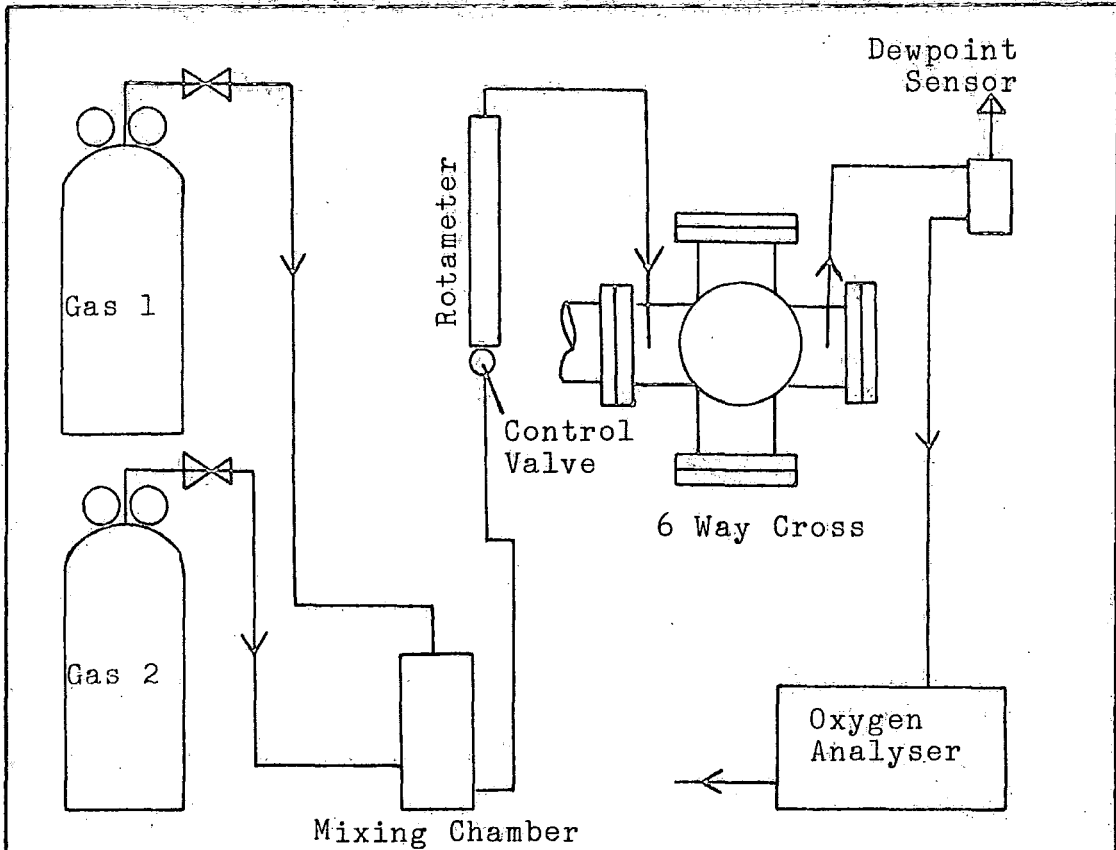


Figure 3.10a Gas Mixing, Two Different Gases

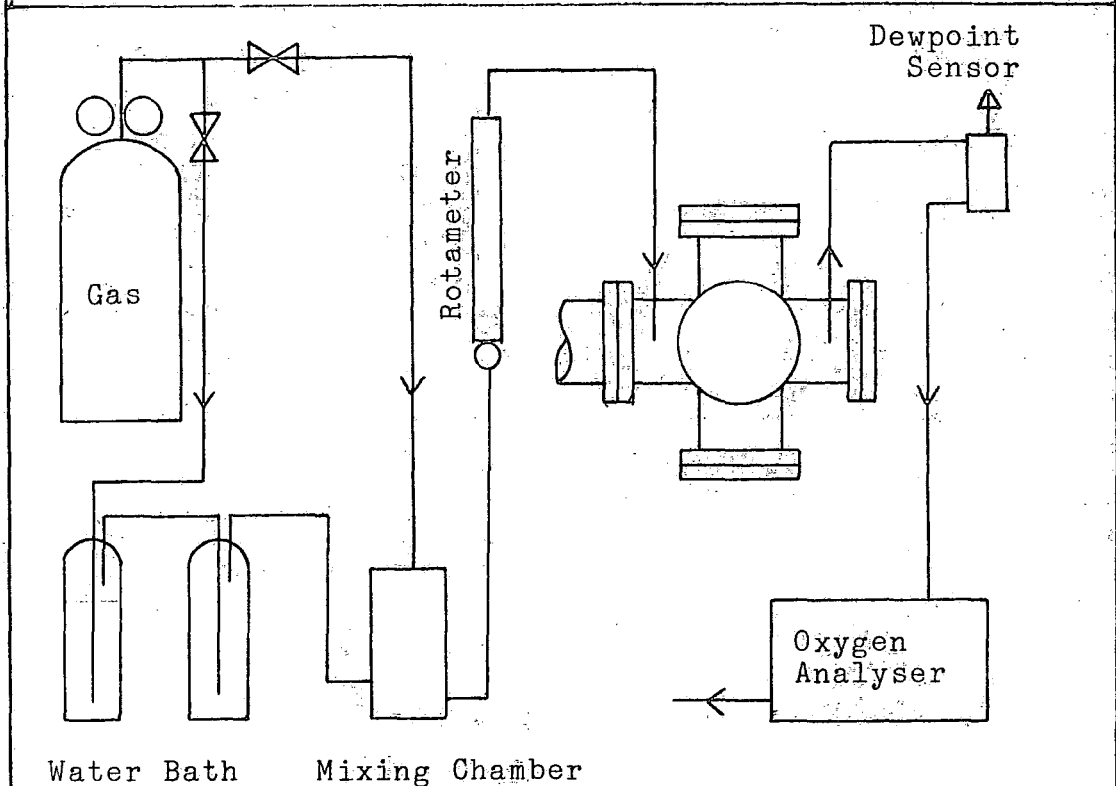


Figure 3.10b Gas Mixing, Wet and Dry Gas

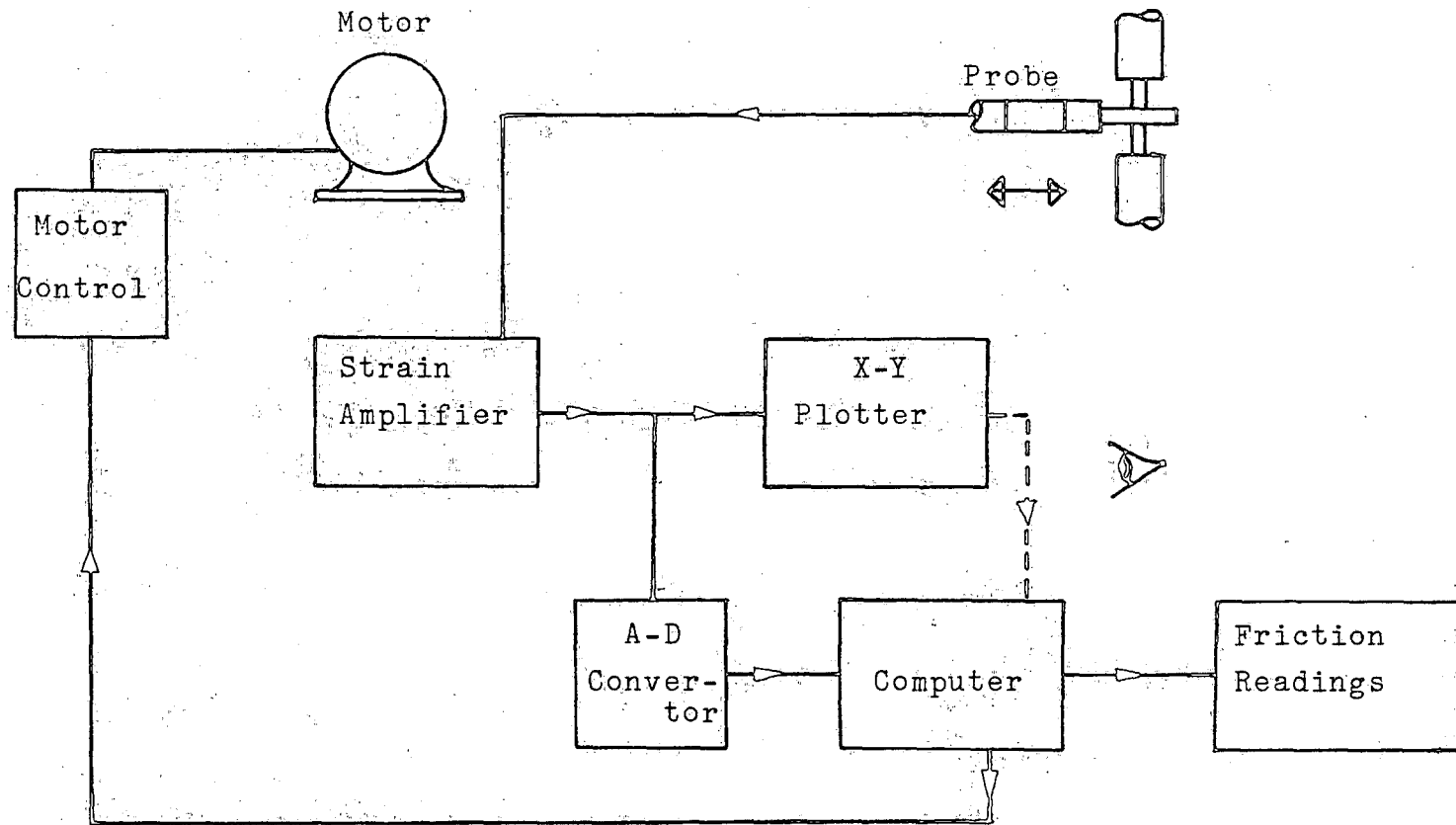


Figure 3.11 Schematic Diagram of Friction Measurement

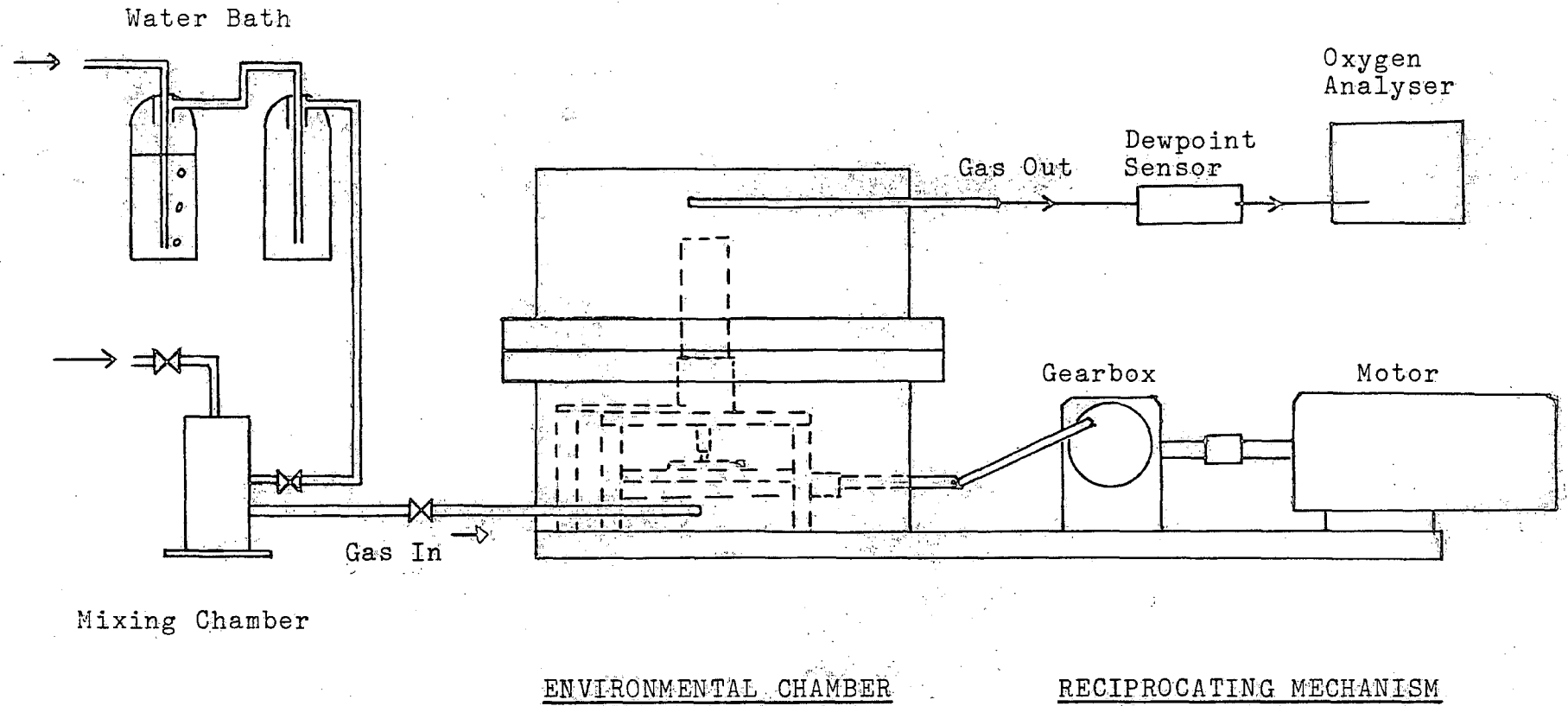


Figure 3.12 Heated Plate Apparatus, General Assembly

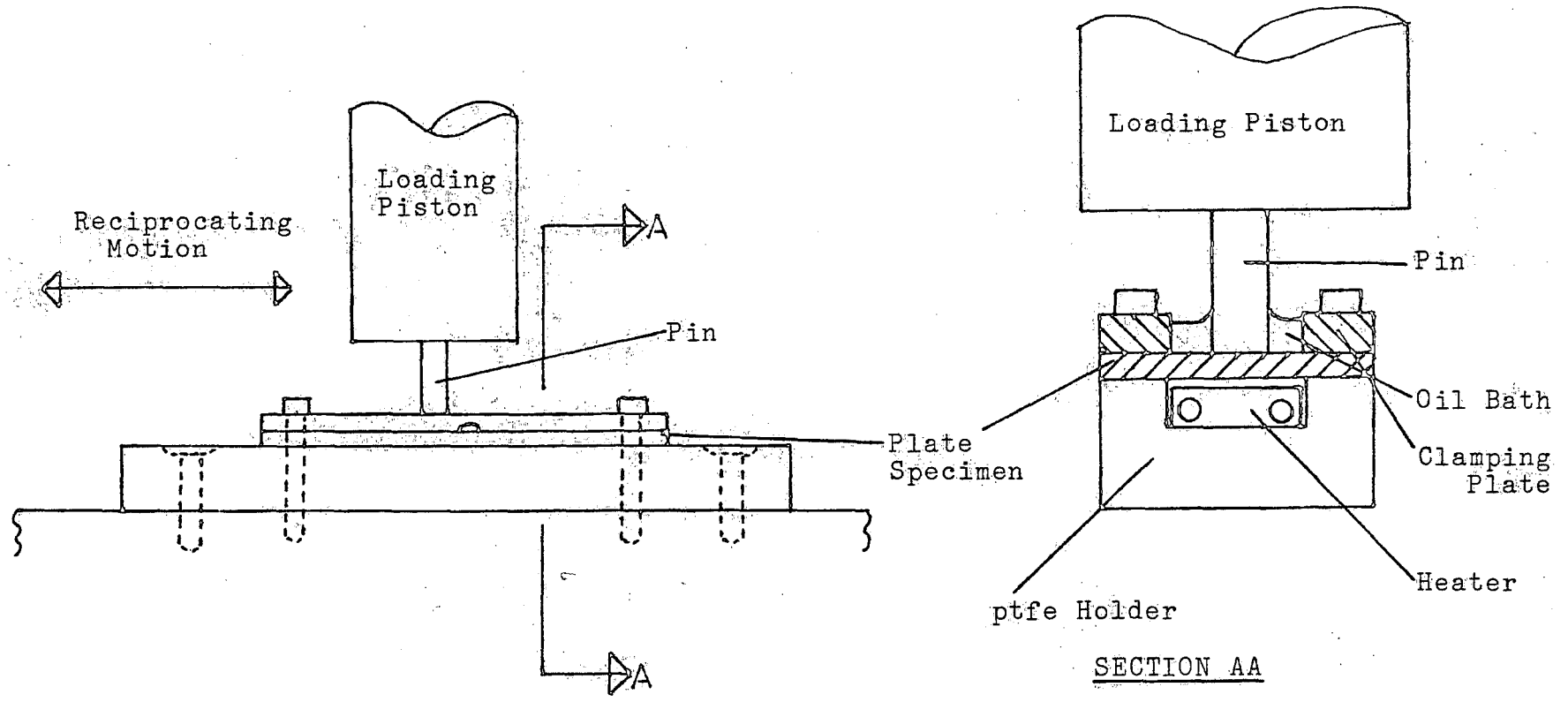


Figure 3.13 Plate Heating Arrangement

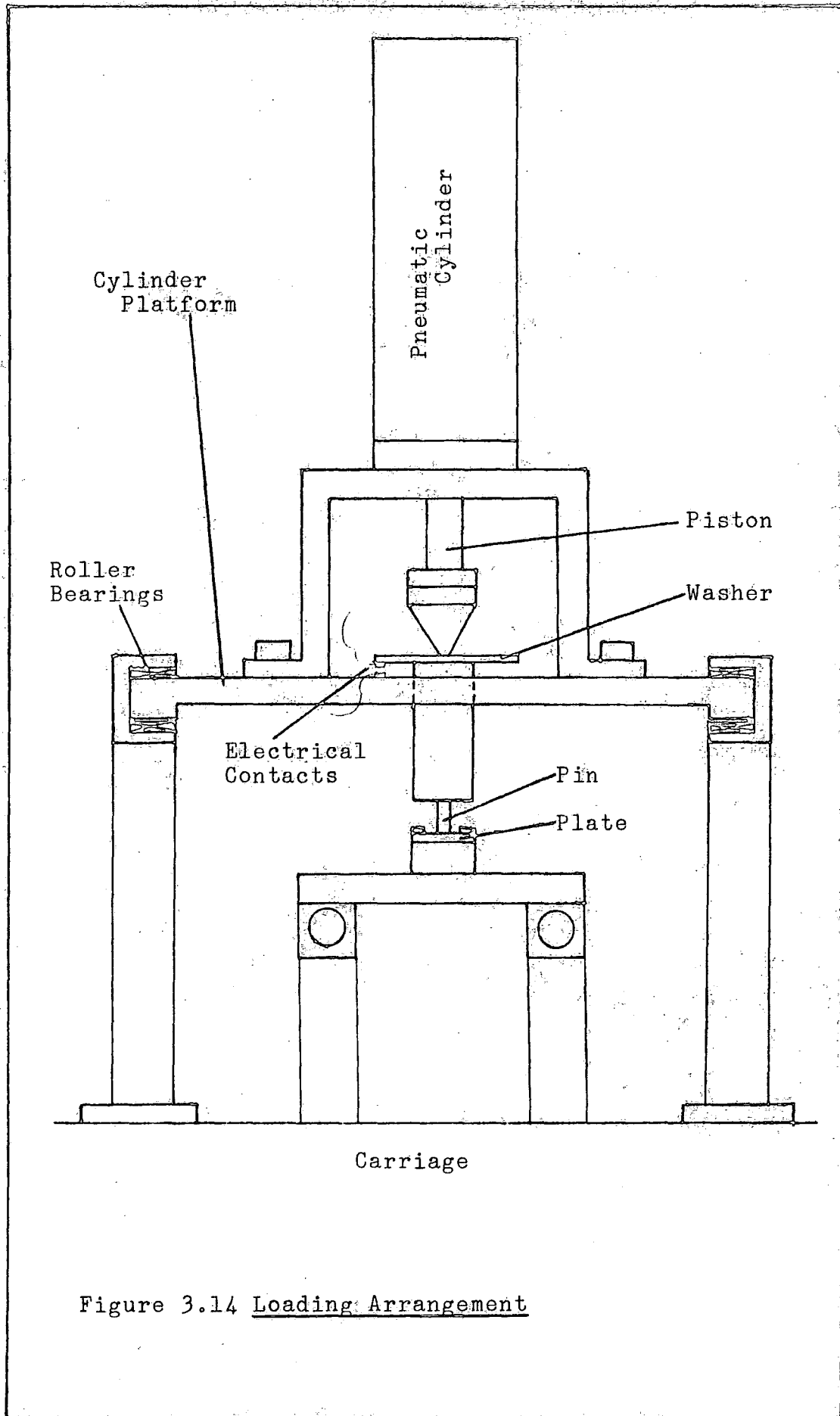


Figure 3.14 Loading Arrangement

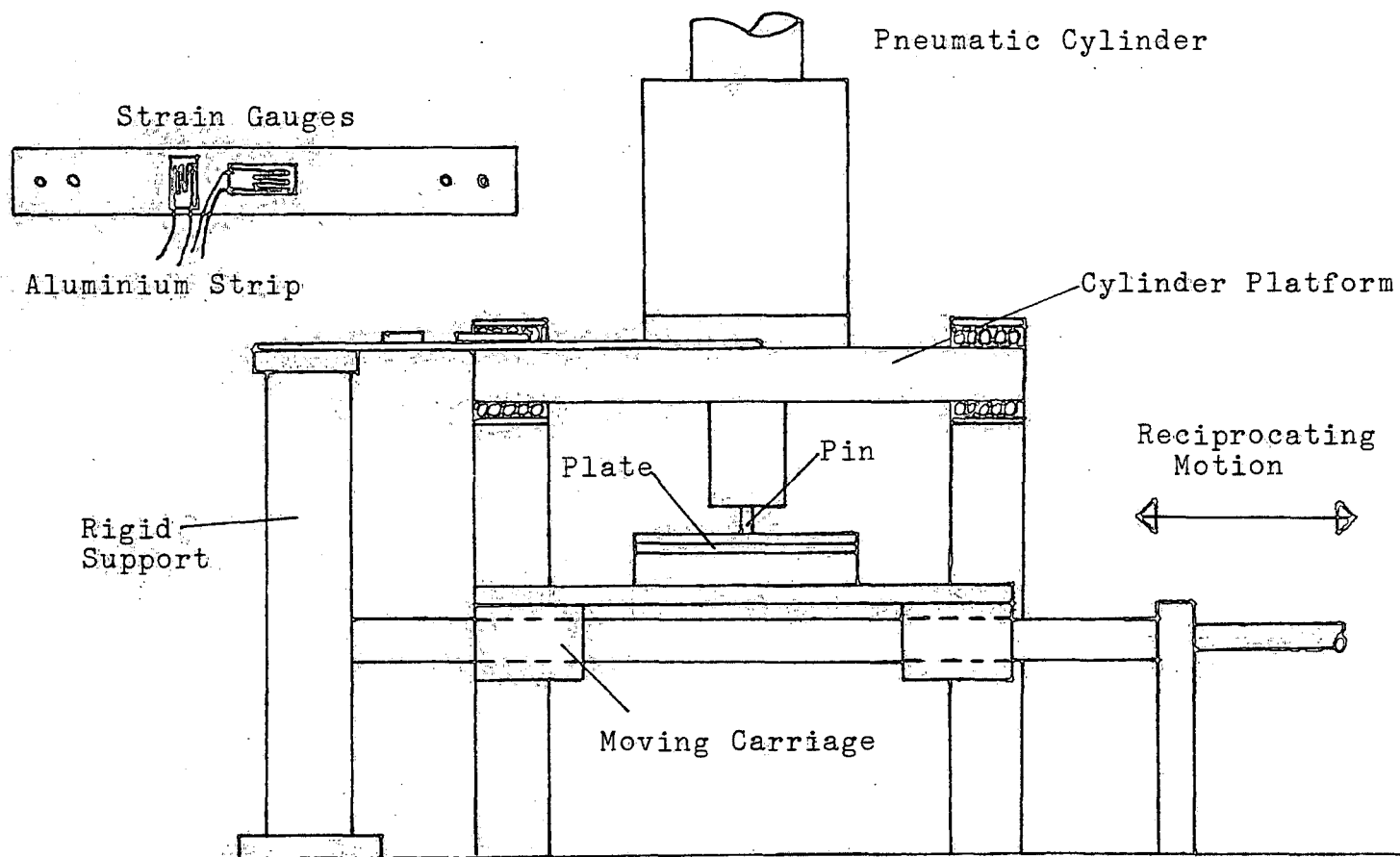


Figure 3.15 Heated Plate Apparatus, Friction Measurement

CHAPTER 4

METHODS AND MATERIALS

In this chapter, calibration methods are outlined, together with experimental procedures and a summary of the experimental programme.

4.1 Calibration of Apparatus

No 1 Friction Apparatus

4.1.1 Pneumatic Cylinder (Load)

For the purpose of calibrating the pneumatic cylinders a proving ring was built, incorporating four strain gauges (Figure 4.1). The proving ring was pre-calibrated on an Instron testing machine. In the case of the 40 mm cylinder it was calibrated up to 500 N and for the 100 mm cylinder up to 3000 N. It was positioned between the force saddle and a loading piston (see Figure 4.1) and the cylinder pressure incremented to give micro-strain readings.

By interpolation, a pressure to force curve could be found from the force-microstrain results obtained from the proving ring calibration. The computer programme that was used to do this is shown in Appendix H.

4.1.2 Probe (Friction Force)

The strain gauged section (transducer) in the probe was calibrated by two methods:-

i) With the transducer off the probe, the section was fitted into a jig and then loaded by the Instron testing machine up to 600 N. (see Figure 4.2a).

ii) With the transducer still on the probe, weights were attached to the probe tip via a pulley. (see Figure 4.2b).

From these, a micro-strain to force curve could be produced, and interpolated to find the friction force. A similar programme to the one used in Appendix H was used for this purpose.

4.1.3 Pin Temperature (Heated Pin Experiments)

For this calibration the pin was heated and the input voltage to the heating coil was measured. The temperature was allowed to settle (for about fifteen minutes) and then the input voltage and pin surface temperature were recorded. Thus a voltage to temperature calibration curve could be produced.

4.1.4 Oxygen Analyser

The oxygen analyser was calibrated prior to each test by first, setting to 21% in air, then zeroing using pure argon, and finally, setting the 100% using pure oxygen.

4.1.5 Dewpoint Hygrometer

This particular piece of apparatus was factory calibrated so could not be checked on a regular basis. The factory calibration and the method used for calculating

vapour flowrates are outlined in Appendix G.

4.1.6 Rotameter Calibration

As the rotameter was factory calibrated only for hydrogen, it had to be calibrated for other gases. This was done by setting a flow through the rotameter and collecting a measured volume of gas under water (Figure 4.5) for a timed period. By this means the rotameter could be used for any gas.

4.1.7 Speed (R.P.M.)

The speed was found by measuring the time taken for a specific number of revolutions and adjusting the motor controller as necessary. However, for some of the later experiments, speed was measured by the computer, although the adjustment was still done manually.

Heated Plate Apparatus

4.1.8 Load Calibration

The method of load calibration for this apparatus was identical to Section 4.1.1 in that the pre-calibrated proving ring was used. In this case the proving ring was placed horizontally onto the carriage (see Figure 4.3) and the pressure incremented.

As before, the computer programme in Appendix H was used to produce a pressure-force curve.

4.1.9 Friction Calibration

Similar to the method used in calibrating the probe (Section 4.1.2), weights were attached to the cylinder platform via a pulley (see Figure 4.3), and thus a micro-strain to force curve could be produced.

4.1.10 Other Calibrations

The other calibrations necessary for this apparatus (eg. rotameter, Oxygen analyser and dewpoint hygrometer) were calibrated as described in previous sections. (as for No 1 Friction Apparatus).

4.2 Specimen Preparation

In order to maintain material homogeneity, the specimen, plates and pins were cut from cast iron bars from the same batch. Sufficient quantities were ordered to enable all the tests to be carried out using the same material. The properties of the cast iron are detailed in Appendix F. The following sections on specimen preparation apply to both sets of apparatus.

4.2.1 Plate Specimens

The plates were cut from the bar in the same direction, ie. the plate length was parallel to the bar axis. This was to ensure the same grain direction. The plates were prepared in batches of fifty and then ground on a surface grinder, keeping the direction of grinding lengthways along the plate (Figure 4.4). Once ground, the surface finish of approximately 10% of the plates was checked.

As a large number of plates were prepared together they had to be stored under a mineral oil to prevent rusting.

4.2.2 Pins

As it would have proved impossible to grind the pins individually, a jig was made to hold them. This was a mild steel block with twenty reamed holes for the pins, which were held in the block by grub screws (Figure 4.5). Using this method, even severely scuffed pins could be reused several times, until ultimately they became too short for further use.

Unlike the plates, the ground pins were rarely kept long before use, but when necessary, a thin film of grease was smeared over the ground surfaces to prevent rusting.

4.2.3 Specimen Cleaning

Prior to each test, both the specimen plate and pin/s were cleaned. They were first wiped clean of any oil or loose particles and ultra-sonically cleaned for ten minutes in a degreaser (acetone), and then allowed to dry in air for thirty minutes. Specimens for all the tests were treated in a similar manner both before and after each test.

Experimental Procedures

4.3 No 1 Friction Apparatus

The procedures for loading and setting the correct environment were the same for all the tests.

4.3.1 Specimen Loading

After cleaning, the masses of the pins and plates were measured using a mass balance, care being taken not to contaminate the rubbing surfaces. The masses were recorded and the pins loaded into the pistons. The plate was inserted into the probe tip and clamped in place.

In order to prevent the plates coming loose from the probe during a test, three methods of attachment were developed. For low load and/or low friction, two indentations, one on each side of the plate, proved sufficient to enable two grub screws to grip the plate. However at higher loads and/or higher friction, it was necessary to put a hole through the plate and to use longer grub screws to hold the plate onto the probe. Finally, as a compromise between the two methods, a hole 2 mm deep was drilled on one side of the plate and one grub screw used to grip it. Thus the plate was both clamped and prevented from detaching itself from the probe tip.

Once the plate and pins were in place, the probe and the loading pistons were inserted into the rig. The probe positioning was then checked, so that the faces of the plate were parallel to the pin faces, and the probe traverse was satisfactory, in that the pins were in contact

with the plate throughout the stroke length. The probe was then clamped into position in the scotch yoke and the force saddle mounted over the pistons. The relevant environment was then set up in the rig and the experiment started.

4.3.2 Setting Up the Environmental Chamber

Before the test could commence the correct environment had to be set up inside the environmental chamber. The flow diagrams for gas mixtures and gas/vapour mixtures are shown in Figure 3.10. When a gas mixture was used (eg. Argon and Air) the apparatus was purged with the correct mixture for at least fifteen minutes before the test was started. In the case of gas/water vapour mixtures the apparatus was first dried by purging with the dry stream gas (Figure 3.10b) until a dewpoint of -10.0°C or lower was recorded. The mixture was then adjusted until the correct mixture was obtained, and as above the apparatus was purged for at least ten minutes before the test started.

The gas flowrate was set using the rotameter, but in the case of gas mixtures, the rotameter had to be calibrated for each mixture. This was done as described previously (Section 4.1.6), by collecting a measured volume under water.

When an inflammable gas, such as hydrogen was used, the apparatus was purged with argon for thirty minutes, to remove any air. The hydrogen was then allowed to flow. On exit from the analysers the hydrogen was burned off. At the end of the test the apparatus was purged once again with argon.

4.3.3 Starting

Before readings could be taken, the influence of the environmental chamber seals (particularly the one between the quick-connect coupling and the 6-way cross) had to be taken into account. This was done by reciprocating the probe at the test speed under no load, and measuring the readings from the strain gauged section. This 'background' reading was subtracted from all the subsequent friction readings.

The pin faces were then positioned to within 0.5 mm of the plate surface by hand. A small positioning load was then applied (approximately 25 N) with the probe reciprocating. Once the pin faces were in contact with the plate the test was considered to have started (ie. time=zero seconds), and reading commenced. The load was then gradually increased until full load was applied. This 'running in' period lasted for approximately thirty seconds depending upon the test load.

4.3.4 Unlubricated Experiments

Early experiments showed that the friction readings stabilised within a thirty minute time period. For this reason thirty minutes was selected as a standard test duration time for unlubricated experiments, although some tests were stopped prematurely, either by the computerised motor cut-off (ie. high friction) or because of excessive wear.

Readings of friction were taken at least every minute, and the oxygen level and/or the dewpoint were closely monitored and kept within experimental limits.

The speed and gas flowrate were also checked periodically.

4.3.5 Lubricated Experiments

For these experiments, there was a wide variation in the amount of oil used and the duration time. For some experiments only one drop of oil on each side of the specimen plate was used, whereas in others a liberal amount of oil was applied to both sides of the plate and oil was supplied continuously throughout the test. The oil flowrate was measured by the rate of fall in level in the oil reservoir. The feed was generally by gravity only. The oil was collected in a collection jar below the apparatus, except when using hydrogen environments, where it was collected in the catchpot (see Figure 3.7) and periodically drained by first changing to an argon environment and then opening the drain valve. The hydrogen environment was then restored once the drain valve had been closed.

As most of the lubricated experiments were carried out for a long period of time, they were mostly computer monitored and carried out in a pure dry gas. The only periodic attention required was the topping up of the oil reservoir and the changing of the storage disc in the computer.

4.3.6 End of the Test

The test was stopped normally for one of three reasons:-

- i) A pre-determined test period

- ii) Excessive wear had taken place
- iii) The friction force reached a set safety limit and was stopped by the computer.

After stopping, the load was taken off the plate and a final 'background' friction reading taken.

In the case of hydrogen environments the apparatus was purged for twenty minutes with argon before the specimens were taken out. The specimens were cleaned and weighed once more. The pins were reground and reused and the plates stored.

4.3.7 E.S.C.A. Experiments

A brief description of electron spectroscopy for chemical analysis (E.S.C.A.) is given in Appendix T.

For experiments involving the use of E.S.C.A., the solid probe (see Section 3.1.6) and a T-shaped specimen were used. Before the friction experiment took place the spectra of the clean, unworn specimen were taken. A friction test was then carried out using the procedure described above for unlubricated experiments. When the experiment was over, the plate specimen was withdrawn into the isolated section (ie. between the seal section and the ball valve, see Figure 3.1), and the ball valve closed. It was necessary to remove any loose wear debris from the plate surface, so the loading pistons were removed and special cleaning pistons inserted. These were loading pistons with foam rubber glued to their ends. The environmental chamber was purged once more with the test gas and the ball valve re-opened, and the plate was

pushed into the 6-way cross to be cleaned by rubbing the surfaces against the foam rubber. The plate was withdrawn once more into the isolated section and the ball valve closed. The motor and scotch yoke mechanism were then slid back on the slide rails (see Figure 3.1) and the quick-connect coupling disconnected. The probe and plate specimen (still inside the isolated section) were then carried to the analyser. The ball valve was bolted onto the insertion lock on the analyser (see Figure 3.8) and the spectra of the worn surface were taken.

4.4 Heated Plate Apparatus

4.4.1 Start of Test

As before, the masses of the pin and plate specimens were measured prior to each test. The plate was bolted to the carriage using the clamping plate and the pin inserted into the pin holder. The metal washer (see Figure 3.14) was put between the pin holder and the load piston and the test load applied. The environmental chamber was then sealed and the correct environment set up. The procedure for setting up the environment was similar to Section 4.3.2, but for most heated plate experiments only pure dry gas was used. Unlike No 1 Friction Apparatus, no 'background' readings were required prior to the commencement of the test.

4.4.2 Single Temperature Experiments

In these experiments, after the correct environment had been set up, the heating coil was turned on and the supply voltage adjusted so that the plate reached the test temperature. The oil was then added in sufficient quantity to fill the oil bath. The motor was then started and readings taken. The plate temperature was kept constant throughout the test by adjusting the supply voltage as necessary. At the end of the set time period (normally three hours), the heating coil was turned off, and the plate allowed to cool whilst still reciprocating under load for fifteen minutes before the motor was turned off.

4.4.3 Incremented Temperature Experiments

As the title implies these tests were not carried out at a single set temperature, but over a range of temperatures normally from ambient (20°C) to 240°C. The environment was set up as before, but the oil put in at ambient temperature. The test was started and the temperature gradually increased in increments, using a stop/start process. The test was run for fifteen minutes at ambient and then stopped for ten minutes whilst the plate temperature was increased to the next temperature setting. This process was repeated until the maximum temperature was achieved. Then as above, the heater was turned off and the plate allowed to cool for fifteen minutes.

4.4.4 End of Test

The test was stopped after the set time period or after the pin had broken. The specimens were cleaned and reweighed, as in the other apparatus.

4.5 Lubricants

4.5.1 No 1 Friction Apparatus

For experiments using No 1 Friction Apparatus, two types of lubricating oil were used: CSB 460, a straight mineral oil, as used in reciprocating compressors, and Shell Risella EL, a light paraffin oil. The properties of these oils are shown in Appendix J.

For most of the experiments the oils were used without any treatment. However, for some tests the oils were out-gassed, by boiling off the dissolved air in a vacuum chamber. For other tests the oils were both out-gassed and scavenged with argon, by bubbling argon through the oil. In this way the dissolved air was replaced by argon, thus the effect of a reactive compound, such as air, in the oil, could be minimised.

4.5.2 Heated Plate Apparatus

In addition to the two oils used above, an EP oil was also used in the heated plate experiments. None of the oils was treated in any way for these experiments.

4.6 Experimental Programme

No 1 Friction Apparatus, Unlubricated Tests

4.6.1 Commissioning Tests

The main purpose of these tests was to commission the experimental apparatus and to evaluate the effect of specimen preparation (eg. cleaning, surface finish).

Table 4.1 No 1 Friction Apparatus,
Commissioning Tests (Unlubricated)

Environment	Speed (mm/s)	Load (N)	Comments
Air	20	100	To study the effect of surface cleaning
Air	10	100	To study the effect of surface finish and hardness
Argon	10	100-200	Stainless Steel Vs UHMWP, for establishment of friction datum
Air & Argon	10	100	Rough humidity tests to establish range (for dewpoint hygrometer)

4.6.2 Effect of Oxygen Content

The effect of oxygen content on friction and wear was examined at different speeds, loads and gas flowrates. A series of tests were carried out, in which the percentage by volume of oxygen content of the gas environment was varied for the conditions of speed, load and gas flowrate, as shown in Table 4.2.

Table 4.2 No 1 Friction Apparatus, Effect of Oxygen Content (unlubricated)

Environment	Speed (mm/s)	Load (N)	Gas Flowrate (ml/s)	Comments
Argon and Air	20	100	20	Tests carried out varying the % (vol) of oxygen present in the environment
Argon and Air	10	100	20	
Argon and Air	10	100	12	
Argon and Air	10	50	20	
Argon and Oxygen	10	100	20	

4.6.3 Effect of Water Content

The effect of humidity on friction was studied at various loads and gas flowrates, while using different host gases. The conditions of load, speed and gas flow-rate are shown in Table 4.3.

In the series of tests marked *, the experimental procedure varied from that described in Section 4.3.4. For these tests, although the humidity was kept constant, the load was gradually increased until scuffing occurred. This was done by putting a small initial load on the plate and running for ten minutes, then stopping the test for two minutes, then restarting the test at a higher load for ten minutes, and stopping it again for two minutes. This cycle was continued until scuffing occurred. A ten minute loading time was chosen from experience, as the previous tests had indicated that failure would either occur within this time period or would not occur at all.

Table 4.3 No 1 Friction Apparatus, Effect of Water Content (Unlubricated)

Environment	Speed (mm/s)	Load (N)	Gas Flowrate (ml/s)	Comments
Hydrogen	10	50	20	Test carried out varying the dewpoint (0°C) of the gas environment
Hydrogen	10	100	20	
Nitrogen	10	75	20	
Nitrogen	10	100	20	
Argon	10	50	20	
Argon	10	50	8.8	
Argon	10	100	20	
Mixed Gas	10	50	20	
Mixed Gas	10	100	20	
Carbon Dioxide	10	100	20	
Air	10	100	20	
Oxygen	10	100	20	
Nitrogen	10	100	0-20	
Nitrogen	10	50	0-20	
Argon*	10	0-200	20	Dewpoint kept constant and load altered until scuff occurred

No 1 Friction Apparatus, Lubricated Tests

4.6.4 CSB 460

Tests at various loads and oil flows in different gas environments were carried out using CSB 460 oil as a lubricant. A summary of the test conditions is shown in Table 4.4.

4.6.5 Shell Risella

As for CSB 460, tests using several experimental variables were carried out. A summary is shown in Table 4.5.

4.6.6 Heated Plate Friction Apparatus

The tests carried out using the heated plate friction apparatus are summarised in Table 4.6.

Table 4.4 No. 1 Friction Apparatus, Lubricated Tests Using CSB 460 Oil

Environment	Speed (mm/s)	Load (N)	Gas Flowrate (ml/s)	Oil Flowrate (ml/hr)	Comments
Air	10	400	0	2	Tests carried out in ambient air with no flow
Argon	10	100-400	20	2	Tests at various loads
Hydrogen	10	100-400	20	2	Tests at various loads
Argon*	10	100-500	20	0	One drop of oil used either side of plate
Argon	10	100	20	2	Heated Pin tests

* In this series of tests only one drop of oil was used on either side of the plate.

Table 4.5: No 1 Friction Apparatus, Lubricated Tests Using Shell Risella Oil

Environment	Speed (mm/s)	Load (N)	Gas Flowrate (ml/s)	Oil Flowrate ml/hr	Comments
Argon	5	400-3000	20	5 ¹	Tests at various loads
Hydrogen	10	100-600	20	5 ¹	Tests at various loads
Argon	10	100-150	20	0 ²	
Air	10	100-150	0	0 ²	Tests in ambient air with no air flow

1) 5ml/hr was the maximum flowrate possible using Shell Risella oil

2) One drop of oil used either side of the plate

Table 4.6 Lubricated Tests Using Heated Plate Friction Apparatus

Environment	Speed (mm/s)	Load (N)	Gas Flow (ml/s)	Oil Type	Temperature °C	Comments
Argon	10	100	100	Risella	20-240	Single temperature tests
Argon	10	100	100	Risella	20-240	Incremented temperature tests
Argon	10	200	100	Risella	20-240	Single temperature tests
Argon	10	200	100	Risella	20-240	Incremented temperature tests
Argon	10	200	100	CSB 460	20-240	Single temperature tests
Argon	10	200	100	CSB 460	20-240	Incremented temperature tests
Argon	10	200	100	EP Oil	20-240	
Argon	10	200	100	EP Oil	20-240	
Air	10	200	0	All	20	Tests in ambient air at ambient temperatures

4.7 Data Recording and Processing

Two methods were used for recording friction data: manually, using an X-Y recorder, and automatically, using an analogue to digital convertor linked to an Apple II computer. Although the recording techniques were different, the processing was identical. Exactly the same methods were used for both sets of apparatus.

4.7.1 X-Y Recorder (Manual)

On the X-Y recorder the X axis was the time scale and the Y axis the strain on the probe. Prior to each test the recorder had to be calibrated. This was done by measuring the Y axis deflection for an input of 1.0 volt (corresponding to 100 μ s). Once the friction test had started the strain was measured by using a ruler to measure the length of the friction plot (see Figure 5.9), and by using the 'background' reading (see Section 4.3.2) and the calibration, the micro-strain could be calculated. The recorder had limitations, in that only thirty-five minute periods could be recorded without adjustment, although by varying the X axis traverse speed, the variation of friction for one cycle could easily be seen.

4.7.2 A-D Convertor (Computer)

The A-D convertor, converted the analogue output from the strain amplifier into an 8 byte binary code, and by this means was capable of being read by the Apple II computer to a sensitivity of 3 μ s. The computer software enabled the strain to be sampled automatically every sixty

seconds. The data was immediately processed and displayed in both graphical and numerical form. In the event of experiments lasting longer than two hundred minutes, data was stored on a floppy disc. At the end of each test the data was retrieved and a 'hard copy' of the results produced.

Further details of the A-D convertor and the computer software are contained in Appendices D and K.

4.7.3 Data Processing

The computer software used for data processing is in Appendix K. The only difference between the two methods of data acquisition was that results from the X-Y recorder were entered manually via the computer keyboard, whereas the results from the A-D convertor were read directly by the computer.

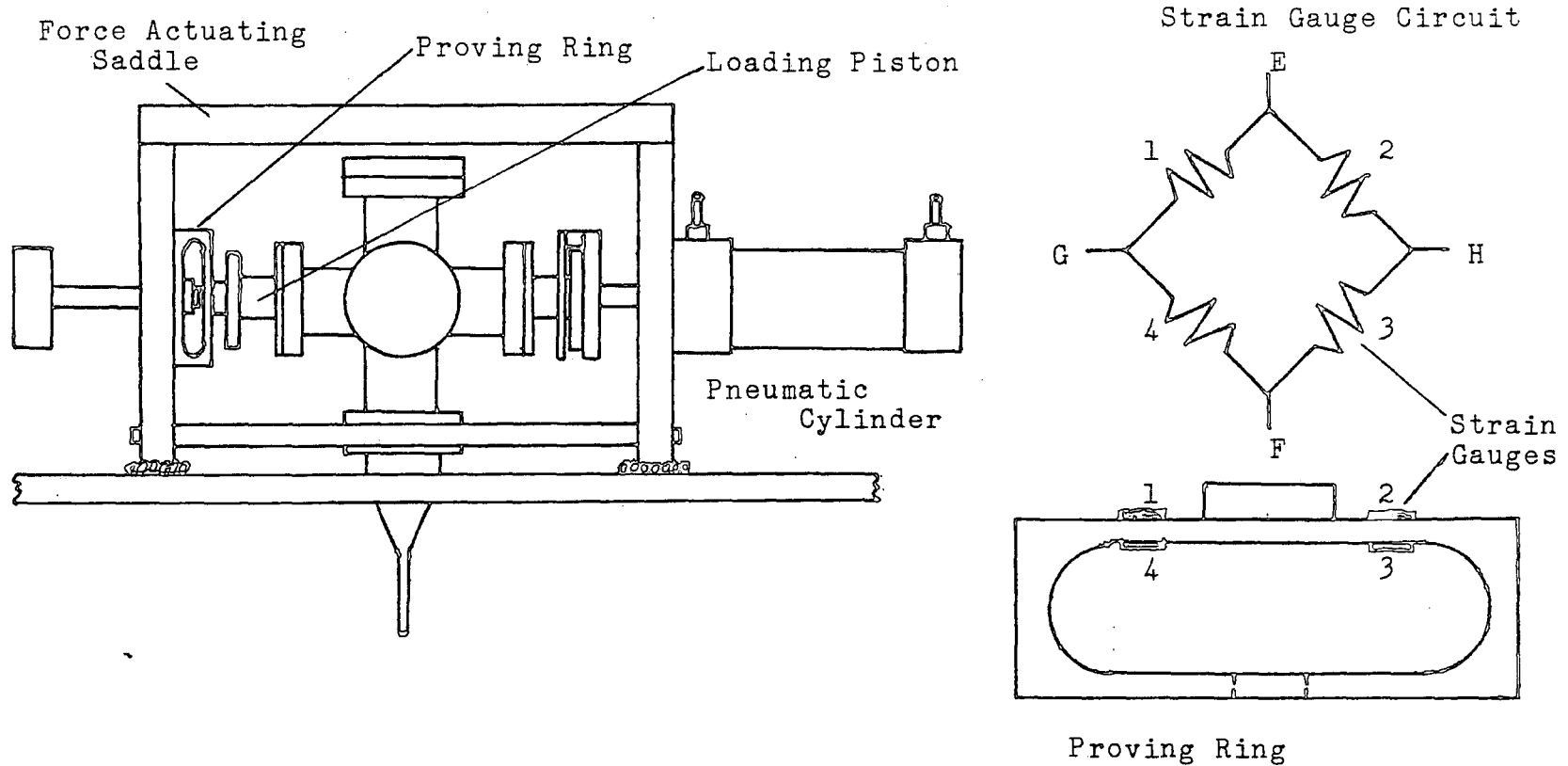
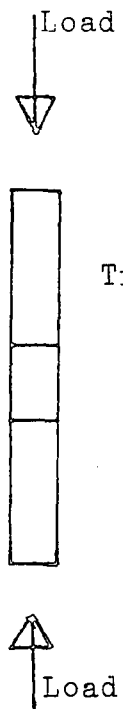


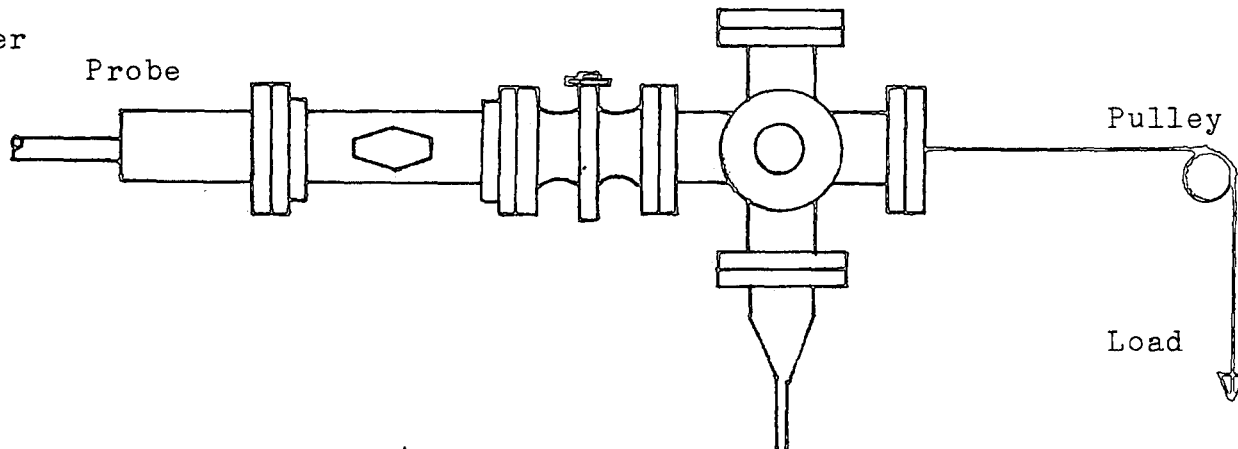
Figure 4.1 Pneumatic Cylinder Calibration (Load)



Transducer

Probe

ENVIRONMENTAL CHAMBER



Pulley

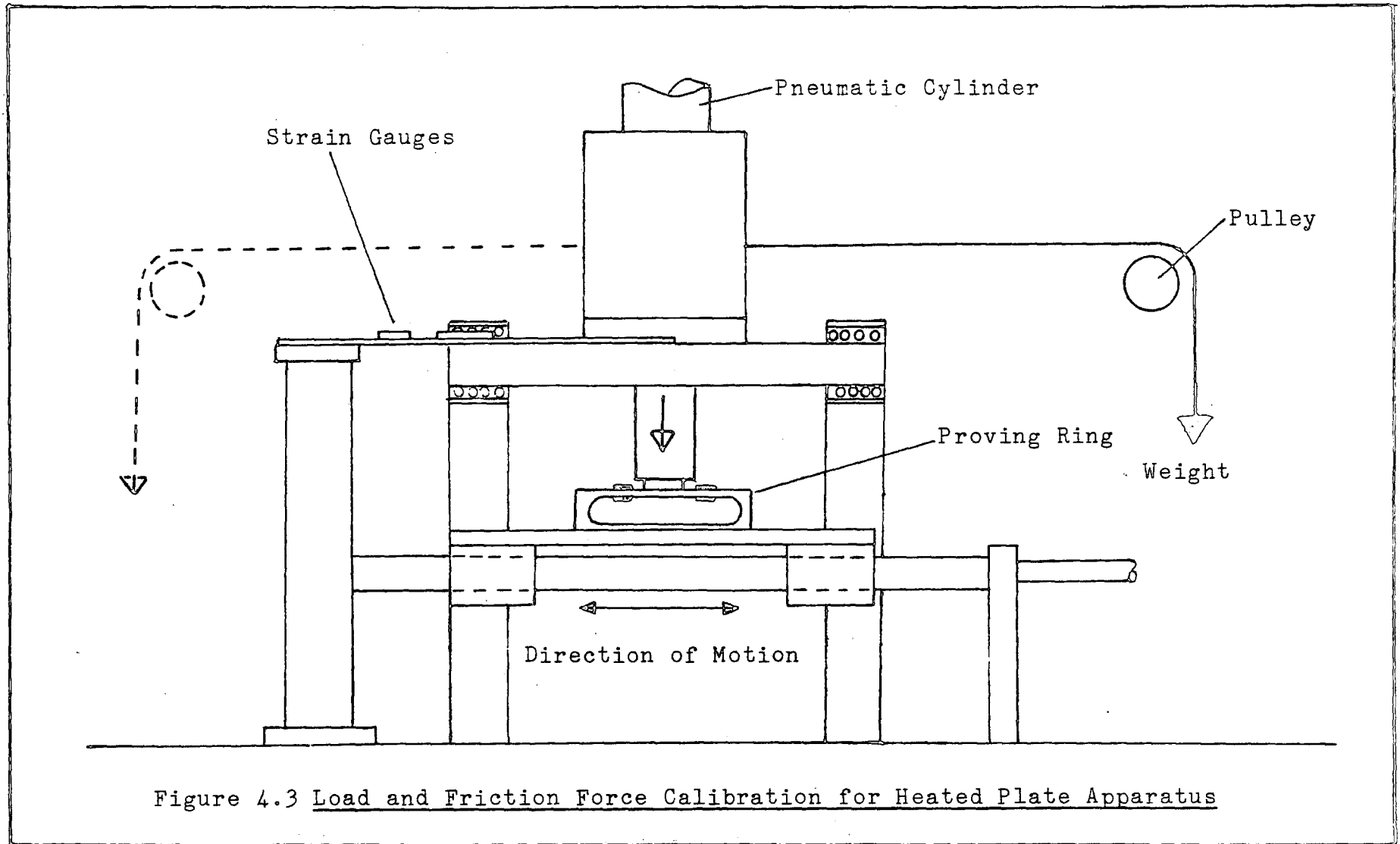
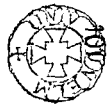
Load

Figure 4.2a

Figure 4.2b In Situ Calibration

Off Probe Calibration

Figure 4.2 Method of Probe Calibration (Friction Force)



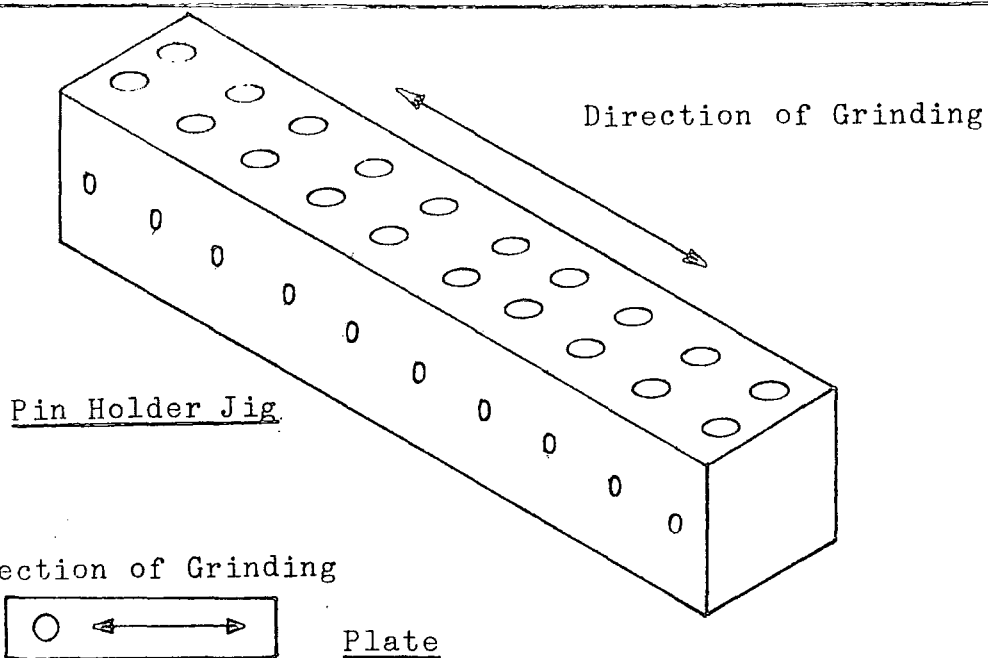


Figure 4.4 Plate and Pin Preparation

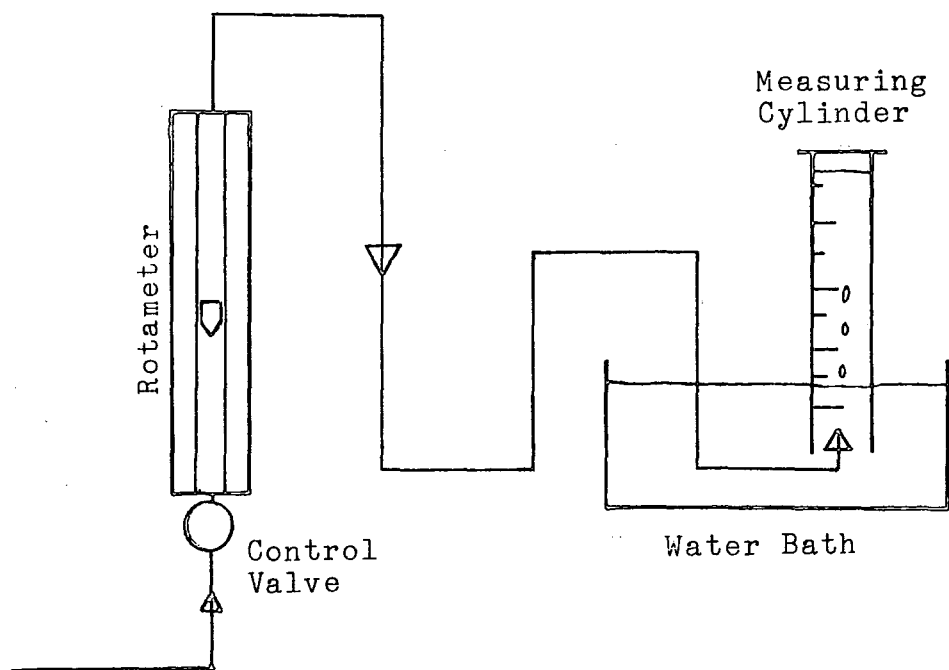


Figure 4.5 Rotameter Calibration

CHAPTER 5

EXPERIMENTAL RESULTS

The first section of this chapter deals with the calibration of various pieces of apparatus for both No 1 Friction Apparatus and the Heated Plate Apparatus.

The next sections can be divided into two parts, referring to unlubricated and lubricated tests. The use of the term 'lubricated' is not intended to imply fluid film lubrication, but merely that the test was carried out in the presence of a lubricant. In the above two sections only cast iron plates and pins were used. The final section refers to a series of tests carried out using mild steel plates and pins so that comparisons could be made between the behaviour of mild steel and cast iron contacts.

The tables of results relevant to this chapter are shown in Appendices L, M and N.

5.1 Calibration Results

No 1 Friction Apparatus

5.1.1 Friction Probe

The calibration results shown in Figure 5.1 indicate that the strain gauged section has been consistent throughout the test period. The curve shown is a result of averaging the tension and compression results.

When the tension and compression results were

compared there was found to be very little difference between the two sets of results. The strain for a given load in tension (see Figure 4.2) was similar in value (but opposite in direction) to the strain for the same load in compression. For this reason, and the fact that the friction calculation and computer software were made much simpler, the results were averaged and a single curve produced.

5.1.2 Proving Ring

As it was not possible to calibrate the pneumatic cylinders on both rigs using known loads, a pre-calibrated proving ring was used (see Section 4.1.1). The calibration curves for the proving ring are shown in Figure 5.2. The four curves show a variation in the calibration with time. The later results differ from the first calibration by as much as 33%. However, when used for cylinder calibrations, the most recent proving ring calibration was used and in the worst case this would have given a 10% error in Pressure - Load values.

The variation in the calibration curves with time was possibly caused by a gradual hardening of the strain gauge adhesive. Thus in later calibrations the strain gauges followed the movement of the proving ring more closely as the flexibility of the adhesive decreased.

5.1.3 Piston Calibrations

Two sets of load pistons and two pneumatic cylinders were used during the experimental period. Early experi-

ments used the 40 mm diameter pneumatic cylinder and No 1 load pistons and later experiments used both the 40 mm diameter and 8 mm diameter cylinders and No 2 pistons. The diameters of No 2 load pistons were 0.025 mm greater than No 1 load pistons. This was to give better sealing after the type of seal in the 6-way cross (see Section 3.1.3) had been changed.

For the No 1 pistons the results of four calibrations are shown in Figure 5.4; the maximum variation was 0.75 bar at 400 N and 0.1 bar at 100 N. However the calibrations were done after major alterations to the piston seals (eg. new seals or spacers) and some variation was to be expected. The results of the calibrations for No 2 pistons are shown in Figures 5.5 and 5.6; the three calibrations for low loads show a very good correlation. For both sets of pistons an initial pressure of 0.3 bar was needed to overcome the seal resistance.

5.1.4 Stainless Steel Vs UHMWP Friction Test

Since a good deal was known about the friction and wear of ultra high molecular weight polythene (UHMWP) sliding on stainless steel (Hughes 1979), a calibration test of two UHMWP pins and a stainless steel plate was carried out.

The test consisted of a twenty minute period in an air environment at 100 N load followed by forty minutes in an argon environment where the load was gradually increased from 100 N to 200 N. At 200 N the UHMWP pins started to deform so the test was stopped.

Throughout the test the coefficient of friction remained at 0.03, independent of load or environment, which compared favourably with previous workers.

Heated Plate Apparatus

5.1.5 Friction Calibration

The calibration curve for the friction measurement strain gauges (see Section 3.2.3) is shown in Figure 5.7. The calibration is a definite curve and as in the case of the friction probe (Section 5.1.1) is a result of averaging the tension and compression results.

5.1.6 Load Calibration

The load calibration is shown in Figure 5.8 This calibration used the proving ring, as in Section 5.1.3. The calibration proved to be a straight line.

For both the friction and load calibrations the two sets of readings done at different times, were so similar that only one calibration curve was required for each.

Unlubricated Experiments

No 1 Friction Apparatus

The unlubricated experiments are divided into three sections: the first deals with introductory experiments to examine the possible effects of specimen preparation. In the other two sections the effects of controlling the oxygen content or water content of the environment are investigated. In all cases tests were carried out at ambient temperature (20°C) using freshly prepared plates and pins. Of necessity, to control the environment there was a gas flow through the apparatus for all the experiments. Most of the tests referred to were carried out for a thirty minute time period.

5.2 Introductory Experiments

5.2.1 Friction Measurement and Wear Rates

Two typical unlubricated friction traces are shown in Figure 5.9. The first shows a non scuff trace where there is no surface damage; in the second trace severe scuffing is taking place. The frictional force is determined by the amplitude of the friction trace (a). The value of the coefficient of friction used in the relevant table or graph depended upon the friction - time curve. In most tests, particularly the scuffed tests, the maximum recorded coefficient of friction was used, but in some cases the initial friction values were high (see Figure 5.10) and in these cases the later steady state

values were used (μ_a). Another point to bear in mind was that for some of the scuffed tests the experiment had to be stopped prematurely, either because the friction became too high (ie. exceeded safety limits) or the wear was so severe that the probe began to foul the load pistons (see Figure 5.11).

Turning now to wear rates, where zero wear is recorded it means that no measurable wear had occurred. In most of these cases the surface had been discoloured, indicating that some small amount of wear had occurred.

5.2.2 Effect of Cleaning

Two similar plate specimens were used. One was simply wiped clean using a dry cloth and the other was wiped clean and then degreased in an ultra sonic cleaner for ten minutes, using acetone (see Section 4.2.3).

A thirty minute test at 100 N load, 20 mm/s, in air was carried out and it was found that the more thoroughly cleaned specimen gave the highest coefficient of friction (0.58 cf 0.47).

However, after considering experimental error and comparing the results with other tests in air (see Section 5.2.3), the two results do not differ significantly enough to cause concern about the effect of slight variations in specimen cleaning.

All the specimens used throughout this project, with the exception of the above, were ultra sonically cleaned in acetone.

5.2.3 Effect of Surface Finish and Hardness

The surface finish and hardness of a sample size of approximately 10% of the plates were checked. The surface finish varied between 0.09 and 0.40 microns R_a , in the direction of motion and range of hardness (Vickers hardness test) was 186.6 to 284 MN/m^2 , (HV (40)). Similarly the surface finish of approximately 5% of the pin specimens was checked and found to vary between 0.3 and 0.7 microns R_a in the direction of grinding (see Section 4.2.2).

Eight plate specimens were chosen at random plus two deliberately roughened plates. A thirty minute friction test was carried out on all of them, at 100 N load, 10 mm/s sliding speed in ambient air and no gas flowrate. The results are tabulated in Table 1 Appendix M, and Figures 5.12 to 5.15 show the scatter of the results. The wide scatter of the hardness (Figures 5.12 and 5.13) and the surface finish results (Figures 5.14 and 5.15) suggest that within the test ranges, hardness and surface finish had little or no effect on friction. Even beyond that range (ie. the deliberately roughened samples) surface finish had no definite effect. The values of surface finish plotted are a summation of the plate R_a value and the pin R_a value similar to the method used when evaluating the effect of fluid film thickness in hydrodynamic lubrication.

5.2.4 Surface Temperature Measurement

In an attempt to measure the temperature rise due to the friction test, thermo-couple sensors were put into

the pins using two different methods.

1) A small diameter hole was drilled in the pin to within 1 mm of the surface. The sensor was then coated in a heat sink compound and inserted into the hole. The heat sink compound was a high conductivity paste used to allow the sensor to quickly reach the pin temperature.

2) A small diameter hole was drilled all the way through the pin and the sensor was araldited or soldered to be close to the surface. The pin was ground down until the sensor actually formed part of the pin face.

Table 5.1 Results of Surface Temperature Measurement

Method	Load (N)	Speed (mm/s)	Environment	Temperature Rise (°C)
1	100	20	Argon	1.75
1	100	20	Air	2.0
1	100	20	Argon	2.5
2) Solder	100	15	Argon	1.0
2) Araldite	100	15	Argon	1.0

As can be seen from Table 5.1 the temperature rise above ambient was very small even when the thermo-couple formed part of the pin surface.

5.3 Effect of Oxygen Content

The oxygen content of the environment was varied by controlling either a gas mixture of compressed ambient air and argon or industrial oxygen and argon (see Appendix P for gas properties). Most of these tests were carried out without the benefit of a dewpoint hygrometer to measure the water content of the test environment, but tests carried out using wet and dry bulb thermometers indicated water vapour pressures of between 7.05 mbar and 12.2 mbar for the test period. Estimates of the partial pressures corresponding to the oxygen content (ie. air content) of the environment are shown in Table 5 in Appendix M.

Five series of tests were carried out to study the effect of sliding speed, gas flowrate and load as well as to compare tests done in argon/air mixtures with those in argon/oxygen mixtures.

5.3.1 Effect of Speed (Figures 5.16 and 5.17)

The graphs of friction against oxygen flowrate for the two speeds of 20 mm/s and 10 mm/s show similar behaviour with a gradual decrease in the coefficient of friction as oxygen content increases. The higher speed curve however shows higher coefficients of friction for similar oxygen contents.

Similarly, the wear rate (Figure 5.17) is highest at 20 mm/s, for oxygen contents above 150 mg/min, but lower wear rates were recorded at low oxygen contents.

5.3.2 Effect of Total Gas Flowrate (Figures 5.18 and 5.19)

Lowering the gas flowrate gave lower values of friction for similar oxygen flowrates and similarly, lower wear rates were also found.

5.3.3 Effect of Load (Figures 5.20 and 5.21)

The frictional results (Figure 5.20) appear to follow the same curve, with a tendency for the lower load (50 N) results to have had slightly lower coefficients of friction for similar oxygen flowrates.

On the other hand the 50 N load produced higher wear rates at low oxygen flows but reached zero at a lower flowrate than the 100 N load results.

5.3.4 Comparison of Air and Oxygen (Figures 5.22 and 5.23)

When oxygen was used rather than air, the levels of friction became higher at high oxygen flowrates (0.8 cf 0.6) but similar at low oxygen flowrates.

Similarly, wear rates for oxygen were higher at high oxygen flowrates and at low flowrates the wear rate was similar to air.

5.4 Effect of Water Content

This section is divided into two parts. In the first, the effect of the water content of inert or reducing environments is considered and in the second, the effect of water content of oxidising environments. Information on gas properties can be found in Appendix P. As before, fresh specimens were used for each test, which was normally of thirty minutes duration. The total gas flowrate (volumetric) was kept at 20 ml/s for each test unless stated otherwise.

Inert and Reducing Gases

5.4.1 Hydrogen

Six graphs of coefficient of friction against time are shown in Figure 5.24, for 100 N load tests. The first three (left hand side) show low coefficients of friction. In these three cases no scuffing occurred. The other three graphs show high friction and in all these cases scuffing occurred. The transition from no scuff to scuff behaviour was very sharp. A decrease in water vapour pressure from 17.94 mbar to 16.72 mbar brought about severe scuffing. Similar behaviour was found for a 50 N load, but the transition pressures were lower (approximately 12 mbar, Figure 5.25). The wear rate also echoed this with a dramatic drop from high wear to a negligible wear (Figure 5.26).

In the interests of safety, the high scuff tests in hydrogen were stopped before thirty minutes had elapsed.

5.4.2 Nitrogen (Figures 5.27 and 5.28)

A similar observation to the tests in hydrogen occurred in nitrogen. There was a transition from high friction (scuff) to low friction (non scuff). The transition pressure for nitrogen however was slightly higher at 100 N load (ie. 21 mbar) than hydrogen. As above, when the load was lowered a lower transition pressure was observed eg. 18 mbar for 75 N.

Two other tests were carried out in nitrogen in which the gas flowrate was altered. It was found that for 100 N, at 21 mbar vapour pressure and 50 N load at 16 mbar vapour pressure, that despite lowering the total gas flowrate from 20 ml/s to 4 ml/s (hence lowering the water flowrate) no scuffing occurred. Thus scuffing seems independent of total vapour flow but more related to the vapour pressure.

5.4.3 Argon

Argon showed identical behaviour with the previous two gases with transition pressures similar to nitrogen (Figures 5.29 and 5.30).

The effect of water vapour pressure on scuff load is shown in Figure 5.31. In these tests, the environment was set up with a specific vapour pressure and the load gradually increased until scuffing occurred. The time spent at each load was fifteen minutes, but as each load increment corresponded to 15 N the indicated scuff load (Table 19 Appendix M) is only approximate. Also included are two points evaluated from Figure 5.29

corresponding to the 50 N and 100 N scuff vapour pressures.

The results showed that higher loads required higher vapour pressures in order to prevent scuffing. The increase appears to be gradual without any sudden transitions.

As a comparison, a series of tests were carried out at a lower gas flowrate (8.8 ml/s) for 50 N loads. This series was used to compare results plotted using water flowrates with results plotted using vapour pressures. As can be seen from Figures 5.32 and 5.33 the transition occurred at similar vapour pressures but completely different water flow rates. This is further emphasised in the wear results, Figures 5.34 and 5.35.

Oxidising Gases

Included within this section are results from tests in carbon dioxide and a mixed gas (N_2 , CO_2 , CO) which, whilst not necessarily oxidising, have been included for convenience.

5.4.4 Mixed Gas (83% N_2 , 12% CO_2 , 5% CO)

The mixed gas behaved in a similar fashion to the inert and reducing gases in having a sharp transition pressure from high to low friction (Figure 5.36). The 50 N transition was 10 mbar and the 100 N transition was 15 mbar. The 100 N wear results were much more difficult to plot with wild variations in wear from 20 mg/m to 60 mg/m in the scuff range (Figure 5.37).

5.4.5 Carbon Dioxide (Figures 5.38 and 5.39)

The carbon dioxide went from a scuff to no scuff condition at around 10 mbar. However between 6.2 and 10 mbar there was a tendency for scuffing to occur on one side of the plate only (see Table 16 Appendix M for results). As a result of this the friction was approximately half the value of the two sided scuff (ie. results less than 6.2 mbar). The wear results (Figure 5.39) suggest that the transition is gradual from high wear to low wear.

The phenomena of one sided scuff had been noticed in several of the previous tests, particularly in tests carried out at vapour pressures near the transition pressure. In most of the previous cases the other side also started to scuff after a short time. The carbon dioxide was unusual in that six tests were done in which one sided scuff only occurred, and these occurred over a relatively wide range of partial pressures.

The distilled water used in the water bath (Chapter 3) changed from a pH 7 to pH 5 after a few minutes of carbon dioxide bubbling indicating a change from a neutral to an acidic solution.

5.4.6 Air (Figures 5.40 and 5.41)

Unlike all the previous gases, air showed a gradual change from severe to mild levels for both friction (Figure 5.40) and wear (Figure 5.41). Another difference was that the plates showed a gradual decrease in scuff severity as the partial pressure increased, unlike the scuff and no scuff conditions of the previous tests. In

air there was no apparent scuffing above 11 mbar.

5.4.7 Oxygen (Figures 5.42 and 5.43)

The friction results for oxygen (Figure 5.42) show very little change in the coefficient of friction over the full range of partial pressures, ie. from 1.2 to 0.9. In the dry state (low partial pressure) the coefficient of friction is very low compared with the other gases but at higher partial pressures the coefficient is quite high at 0.9.

The wear was also comparatively low at low partial pressures. In fact, the scuff severity was much lower than any of the previous tests with scuff occurring only over about 50% of apparent contact area. But unlike previous tests at high partial pressures some scuffing occurred, although this was more like individual scratch marks (ie. scoring) than severe surface damage.

5.5 E.S.C.A. Tests

A number of tests using E.S.C.A. were carried out to compare the surface composition of the cast iron plates before and after a friction test. The friction test was carried out at a 50 N load, at 10 mm/s in a dry argon environment ($P_{H_2O} < 0.8$ mbar). Severe scuffing occurred in all these tests and a large proportion of the exposed plate surface (T-shape) was severely worn ($\approx 80\%$).

The results of the spectroscopic analysis are shown in Figures 5.44 to 5.47; in all cases the spectra of the surface prior to the test is shown at the top.

5.5.1 Wide Scan (Figure 5.44)

The worn specimen showed an increase in the carbon peak but still contained a significant proportion of oxygen.

5.5.2 Iron (Figure 5.45)

The worn specimen still showed iron oxide with no signs of exposed iron.

5.5.3 Oxygen (Figure 5.46)

A slight change in the oxygen peak but no significant difference.

5.5.4 Carbon (Figure 5.47)

The unidentified peak (a) at 294 eV had disappeared but otherwise no change.

5.5.5 Other Tests

The differences in the unworn and worn spectra above, were similar to those recorded between two different unworn specimens, and the unidentified peak on the carbon spectra was not present on any other spectrum.

Lubricated Experiments

5.6 No 1 Friction Apparatus

As for the unlubricated experiments each test was carried out using freshly prepared plates and pins. The gas temperatures were ambient at all times. The properties of the oils used are in Appendix J. In all cases the gases used were as dry as conditions would allow ($P_{H_2O} < 0.8$ mbar).

5.6.1 CSB 460

When tests were carried out with a definite oil flow (Table 5.2) the friction was low and the wear rate small, and independent of the environment. In the only case where scuff occurred, it occurred after a long time (thirty-four hours), and a possible cause of the scuffing was a lubrication failure.

Table 5.2 Lubricated Tests, Oil Flow 2.0 ml/hr

Air

Load (N)	Speed (mm/s)	Duration (mins)	μ_{max}	Wear Rate (mg/m)
400	10	309	0.08	0.013
400	10	364	0.14	0.0

Argon

Load (N)	Speed (mm/s)	Duration (mins)	μ_{max}	Wear Rate (mg/m)
100	10	42	0.1	0
200	10	2096	0.560*	0.074
400	10	309	0.08	0.013
400	10	364	0.14	0.0
400	10	5760	0.1	-

* Scuff

Table 5.2 (cont'd)

Hydrogen

Load (N)	Speed (mm/s)	Duration (mins)	μ_{max}	Wear Rate (mg/m)
100	10	225	0.09	0.0
400	10	360	0.11	0.004

When only one drop of oil was put on either side of the plate and the test carried out, the test duration (time until scuffing occurred) varied depending upon the load (Table 5.3). As the load got higher the test duration decreased, eg. the 300 N load test scuffed in 337 minutes compared with 186 minutes for 400 N load. For the 100 and 200 N load cases, scuffing did not occur despite running for long periods without further lubrication.

Table 5.3 0.5 ml Oil, Argon Environment

Load (N)	Speed (mm/s)	Oil Flow (ml/hr)	Duration (mins)	μ_{max}	Wear Rate (mg/m)
100	10	0.3	100	0.2	0.0
100	10	0.09	330	0.12	0.0
100	10	0.015	1905	0.10	0.001
200	10	0.085	360	0.10	0.009
300	10	0.09	337	0.674*	0.54
400	10	0.16	186	0.585*	0.97
500	10	0.30	100	0.2	0.0

* Scuffed

The oil flows are calculated for 0.5 ml of oil (0.25 ml either side) applied to the plate. The flow is

probably the minimum flowrate required to prevent scuffing for the 300 and 400 N load cases.

5.6.2 Shell Risella

The results of tests using Shell Risella oil are shown in Table 5.4. Despite using the maximum possible load (3000 N) and a low speed (5 mm/s) scuffing did not occur even when the oil used had been outgassed and scavenged with argon.

Table 5.4 Lubricated Tests Using Shell Risella,
Oil Flow 5 ml/hr

Argon

Load (N)	Speed (mm/s)	Duration (mins)	μ	Wear Rate (mg/m)
400	5	360	0.23	0.007
1000	5	300	0.23	0.056
1000*	5	192	0.18	0.016
2000*	5	520	0.2	0.009
3000*	5	190	0.2	0.016

Hydrogen

Load (N)	Speed (mm/s)	Duration (mins)	μ	Wear Rate (mg/m)
100*	10	225	0.09	-
400*	10	360	0.22	0.08
600*	10	230	0.22	0.007
600*	10	360	0.22	0.08

* Outgassed and scavenged oil was used in these tests.

If the oil was reduced to a minimum by simply dipping the specimen in oil and allowing any excess to drain off, a long time was still required to produce

scuffing (Table 5.5).

Table 5.5 Lubricated Tests Using Shell Risella,
No Oil Flow

Argon

Load (N)	Speed (mm/s)	Duration (mins)	μ	Wear Rate (mg/m)
100	10	35	0.1	0
120	10	35	0.2	0
150	10	100	0.2	0
100	10	420	0.69*	-

* Scuff

Air

Load (N)	Speed (mm/s)	Duration (mins)	μ	Wear Rate (mg/m)
100	10	35	0.23	0
120	10	40	0.18	0
150	10	90	0.20	0

The coefficient of friction for the Risella tests was approximately 0.2 (independent of environment) compared with 0.1 for the CSB 460 tests.

5.6.3 Heated Pin Experiments

The results of the heated pin experiment are shown in Figure 5.48. For pin temperatures of 100°C, a coefficient of friction of about 0.3 was recorded; when the heat was turned off the friction dropped to a coefficient of around 0.15. After the heater was turned on again (to a temperature of 120°C) the coefficient rose to 0.4. Thus

the effect of temperature was to raise the coefficient of friction. It was decided on the basis of these experimental results to design and build the heated plate apparatus.

The oil used in this experiment was CSB 460 at a flowrate of 2 ml/hr, the load was 100 N with a speed of 10 mm/s.

5.7 Heated Plate Friction Apparatus

In all these tests a freshly prepared plate and pin specimens were used. The gas environment was dry argon, giving a water vapour pressure of approximately 2.0 mbar. The properties of the three oils used are summarised in Appendix J. Two types of friction test were used: single temperature experiments and incremented temperature experiments. The experimental procedures used are described in Sections 4.4.2 and 4.4.3 respectively.

For these tests a broken pin was a common occurrence after scuffing. The force required to break a pin was approximately 400 N so in all cases where the pin was broken the maximum friction force was recorded as 400 N. It must be noted however that if the pin had not broken the maximum friction force may have been higher. Another deceptive feature of these results was the wear rates. For many of the tests, low friction and wear was recorded for a long time, until very suddenly, scuffing occurred and friction and wear rose dramatically (normally within thirty seconds). The increased friction often broke the pin. Thus the time used in calculating the wear rate includes a long period in which little or no wear took place and the calculated wear rate bears no resemblance to the instantaneous wear rate at the time of breakage.

Tables of results for this section are contained in Appendix N.

5.7.1 Shell Risella (Figures 5.49 and 5.50)

The non incremented tests showed a dramatic increase in friction after a certain temperature was reached: 150°C for a 200 N load and 180°C for a 100 N load. In Figure 5.49 the maximum coefficient of friction for 100 N is shown as 4.0 and for 200 N as 2.0. It must be noted that these points correspond to the pin shear force, and as stated above, may not correspond to the maximum coefficient of friction that may have been achieved had the pin not sheared. When a single plate and gradual temperature increments were used no dramatic rise in friction was recorded and the friction remained low throughout the whole test.

In all the cases where the pin broke, breakage occurred within twelve minutes of starting the test.

5.7.2 CSB 460 (Figures 5.51 and 5.52)

With these tests pin breakage (ie. scuffing) occurred at 160, 200 and 240°C, but only at 240°C did the pin break after only a short time (4½ minutes). For this reason, and the fact that the 180°C and the 220°C tests did not scuff, the transition temperature is shown at 240°C. As in the Risella tests, the single plate incremented test did not scuff but the friction at 240°C was higher than the Risella.

5.7.3 EP Oil (Figures 5.53 and 5.54)

For the EP oil the transition temperature was 180°C but the non scuff friction was much lower than either the

Risella or CSB 460 oil. As above, the incremented test did not scuff and the friction remained low despite temperatures well above the transition temperature of the one plate, one temperature tests.

5.7.4 Tests in Air

Three tests were carried out at ambient temperature in air, for each of the three oils. The results are shown in Table 5.6.

Table 5.6 Lubricated Tests in Air
Heated Plate Friction Apparatus

Load = 200 N, Speed = 10 mm/s

Oil	μ	Wear Rate	Temperature Rise
Risella	0.08	0.01	7.7
CSB 460	0.043	0	7.0
EP Oil	0.08	0	6.6

The temperature rise shown was the rise in the plate temperature after three hours of continuous running. As can be seen from Table 5.6 the highest temperature was recorded with Risella oil. Risella was also the only test in which a measurable amount of wear was recorded.

5.8 Mild Steel

Various tests were carried out with mild steel plates and pins, in order to compare them with similar tests carried out using cast iron. The results of these tests are summarised in Table 5.7. From these results it can be seen that in the presence of oil, mild steel behaved favourably, giving low friction and relatively low wear. However, when compared with the performance of cast iron (see later), although the coefficients of friction were similar, the mild steel showed far higher wear rates and was more prone to scuffing than cast iron, although the presence of oil prevented high wear.

When no oil was present both friction and wear were high, even in a good oxidising environment such as wet oxygen (oxygen saturated with water vapour at ambient temperature). When compared with cast iron, in a water saturated argon environment, the mild steel scuffed at 25 N, whereas the cast iron plate and pins scuffed at 150 N.

Table 5.7 Mild Steel Tests

Lubricated

Oil Flow = 9.6 ml/hr (Shell Risella),
Water Vapour Flow less than 0.1 mg/min

Environment	Load (N)	Speed (mm/s)	μ	Wear Rate (mg/m)
Argon	500-1500	5	0.33	0.104
Argon	1000-2000	5	0.15	0.018
Argon	1000-2500	5	0.15	0.017

Table 5.7 (cont'd)

Unlubricated

Environment	Load (N)	Speed (mm/s)	μ	Wear Rate (mg/m)	Vapour Pressure (mbar)
Argon	100	10	1.47	29.23	20.95
Argon	50	10	5.64	16.4	23.96
Argon	25	10	2.2	4.25	21.86
Air	25-50	10	2.6	20.86	-
Oxygen	50	10	2.0	5.63	22.66
Argon*	25-150	10	0.6	2.83	22.10

* Cast Iron Test

The coefficient of friction (μ) shown for the unlubricated tests relates to the coefficient when the test was stopped. Had the test been allowed to continue friction would very likely have gone much higher.

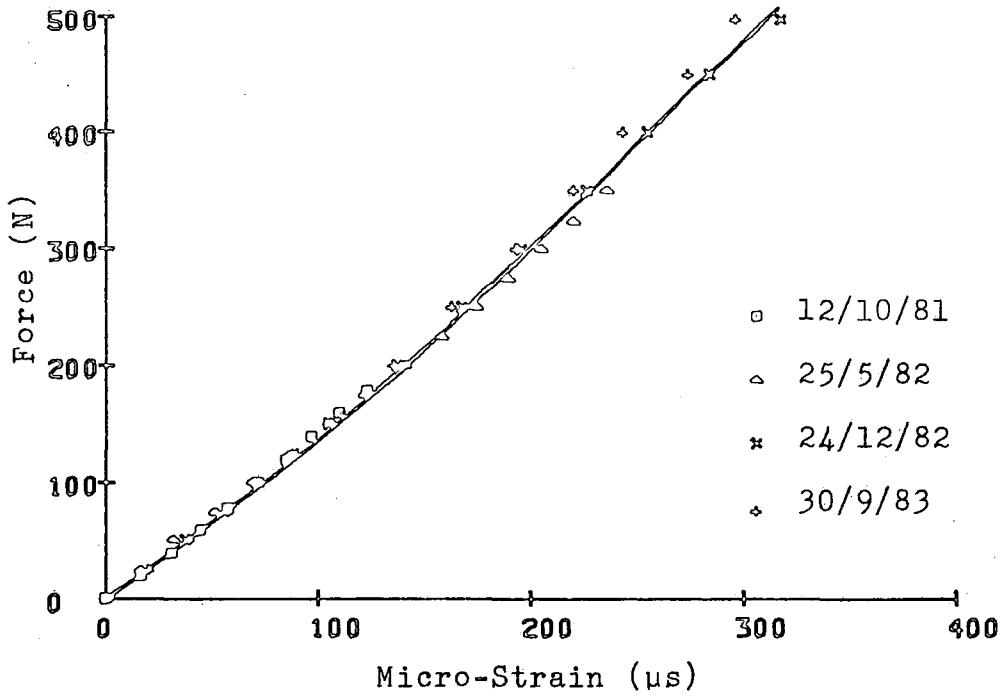


Fig 5.1 Friction Probe Calibration

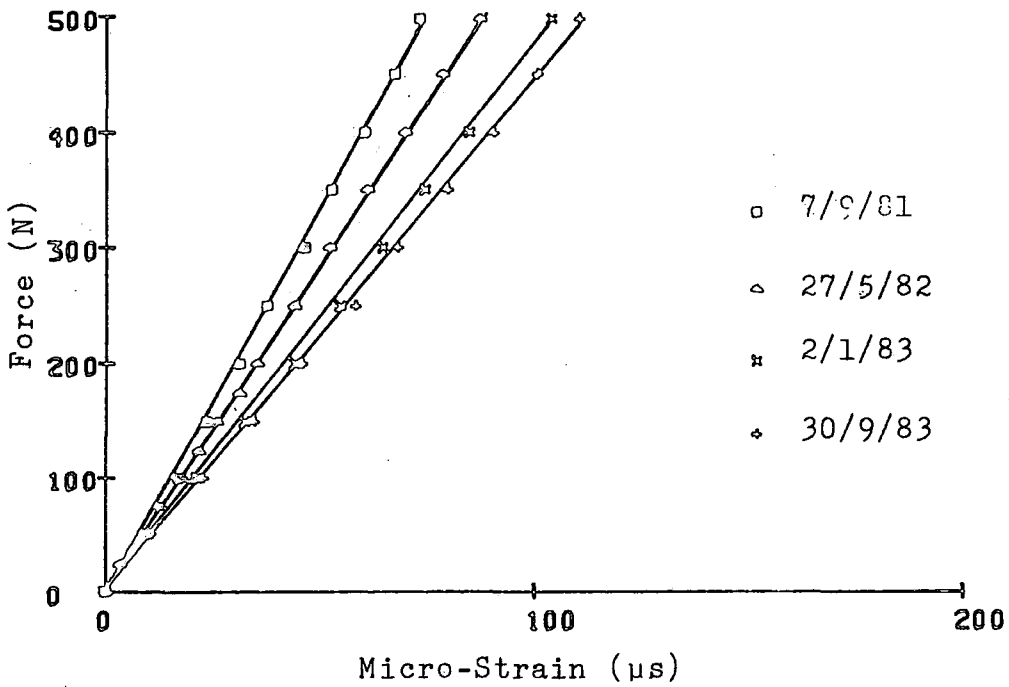


Fig 5.2 Proving Ring Calibrations

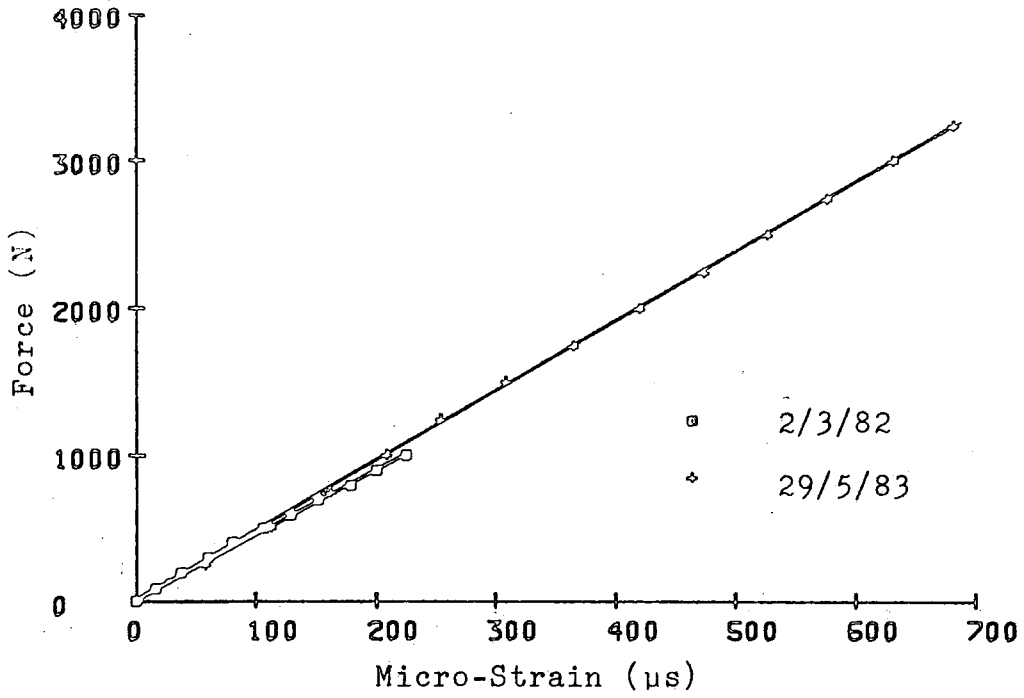


Fig 5.3 Proving Ring Calibrations (High Load)

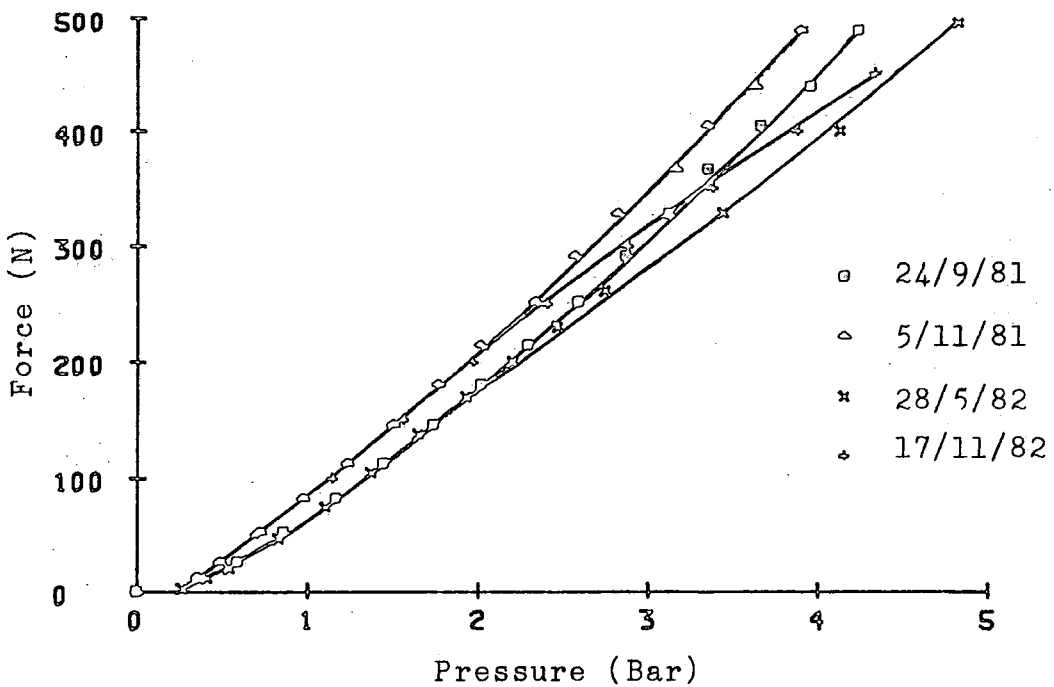


Fig 5.4 Piston Calibrations (No.1 Pistons)

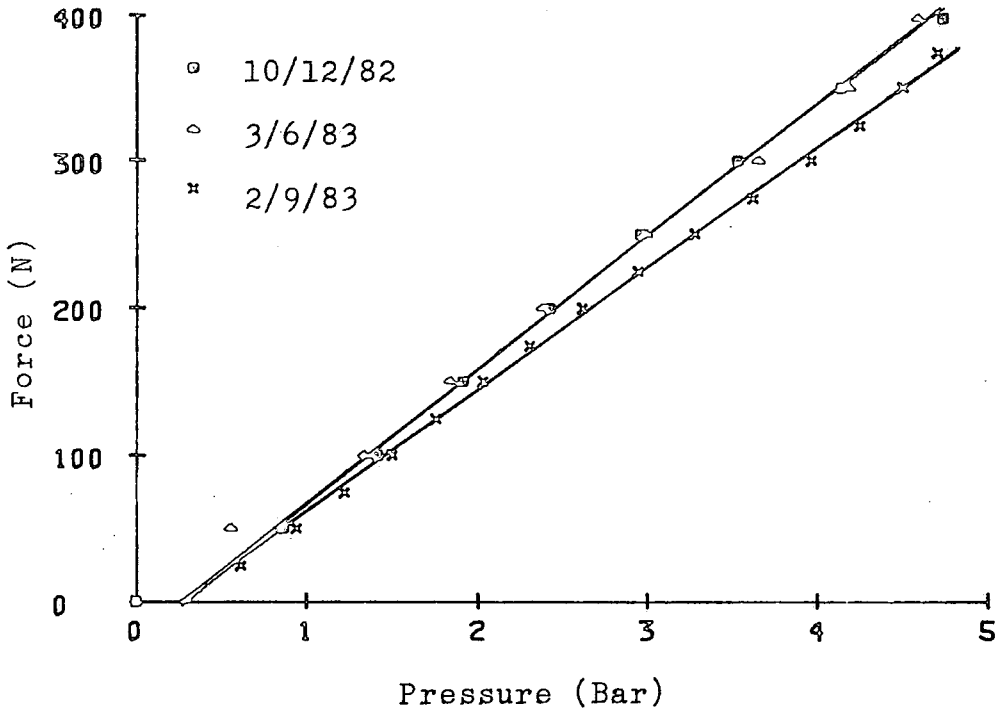


Fig 5.5 Pistons Calibrations (No.2 Pistons)

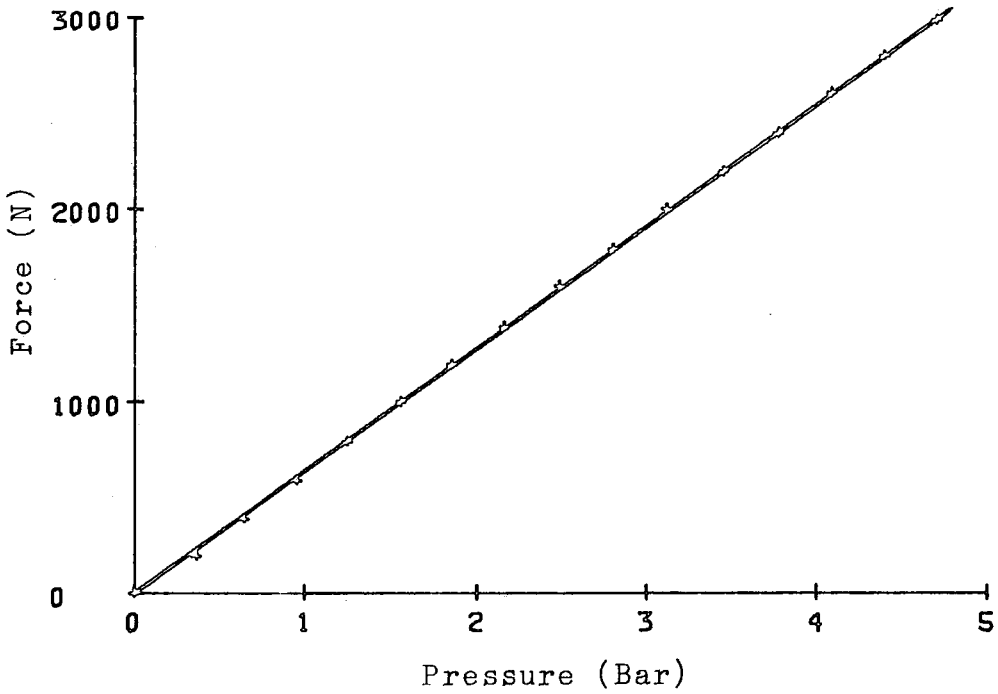


Fig 5.6 Piston Calibration, No 2 Pistons at High Load

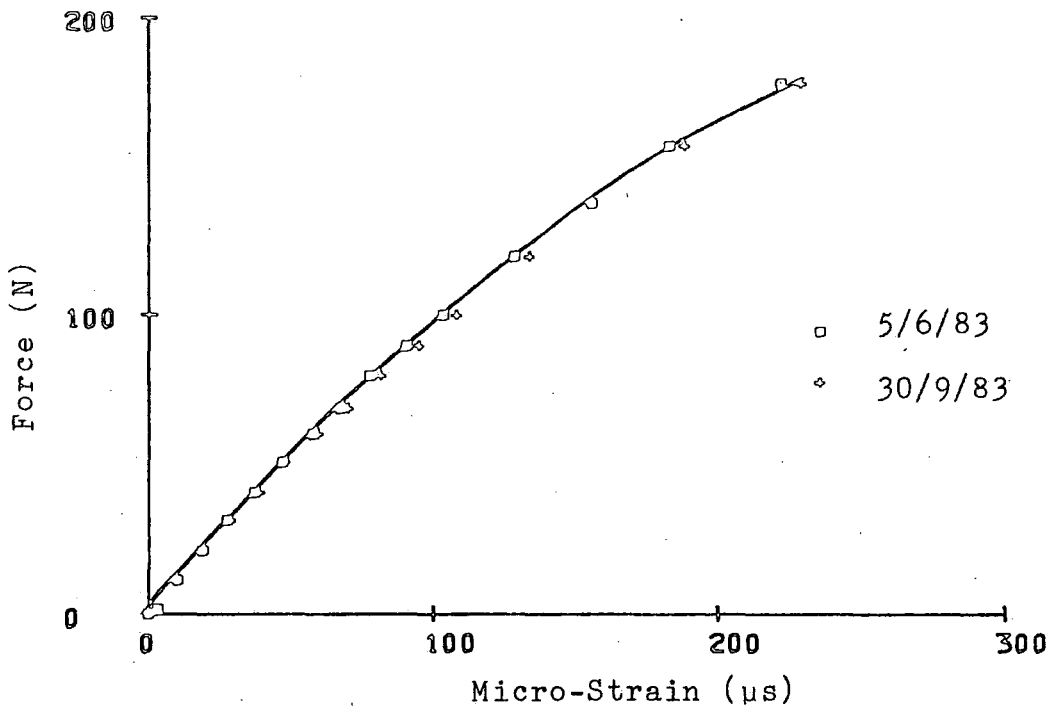


Fig 5.7 Friction Force Calibration (Heated Rig)

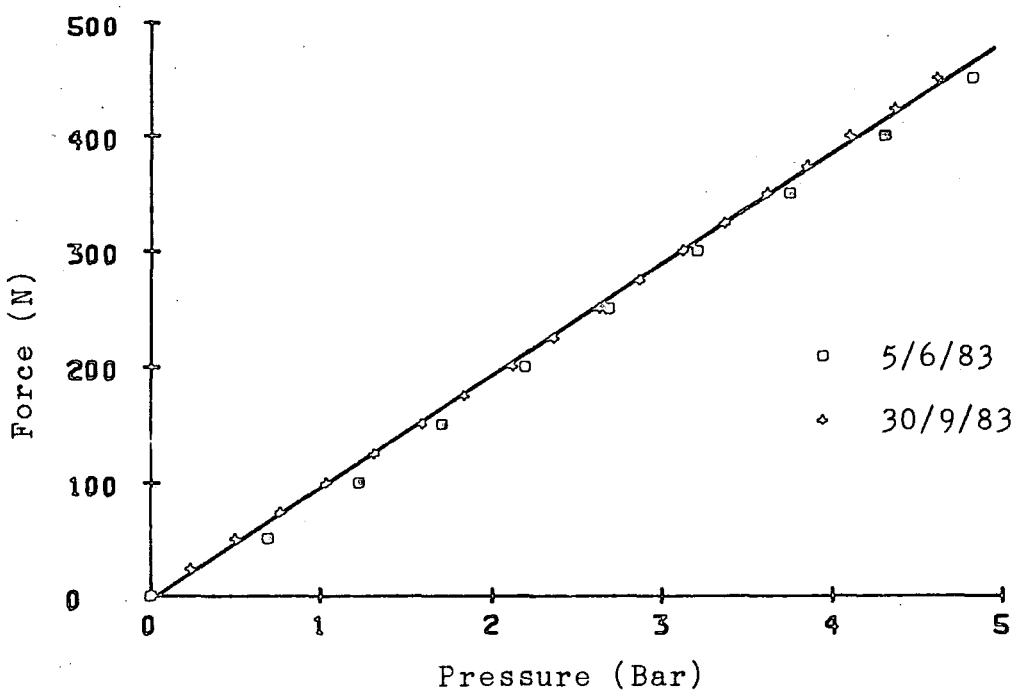


Fig 5.8 Load Calibration (Heated Rig)

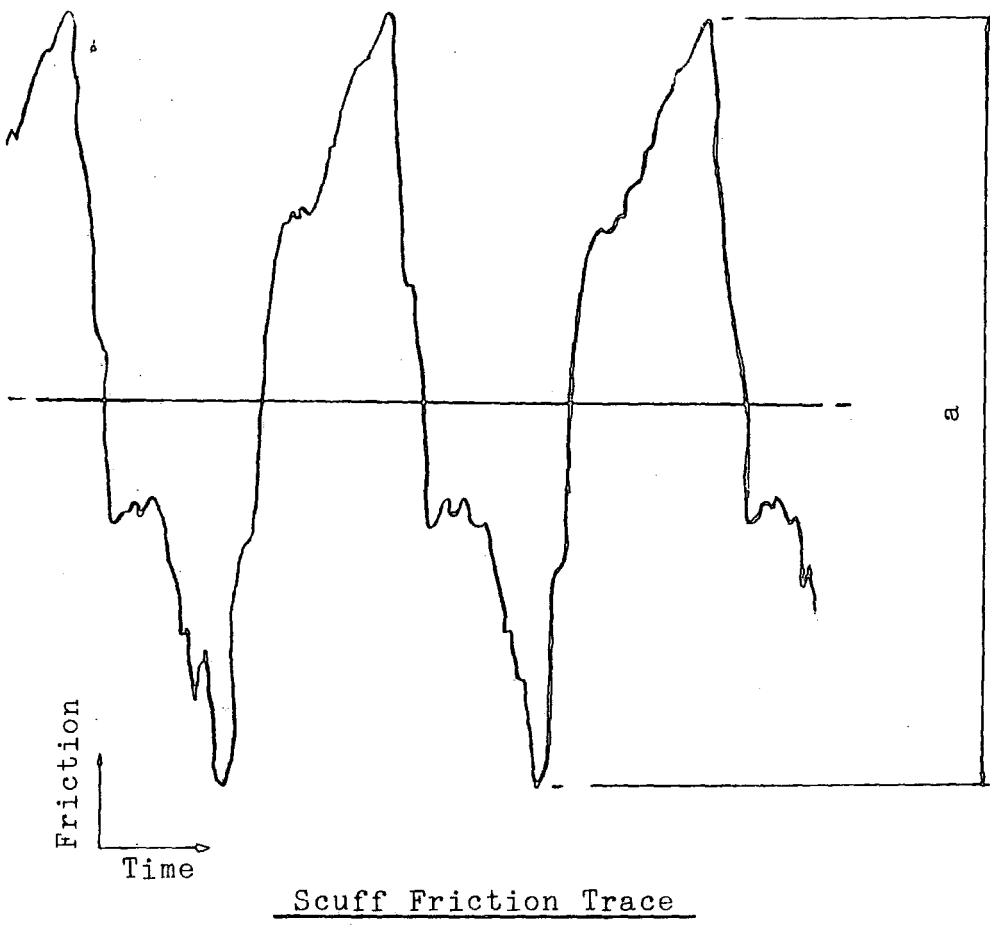
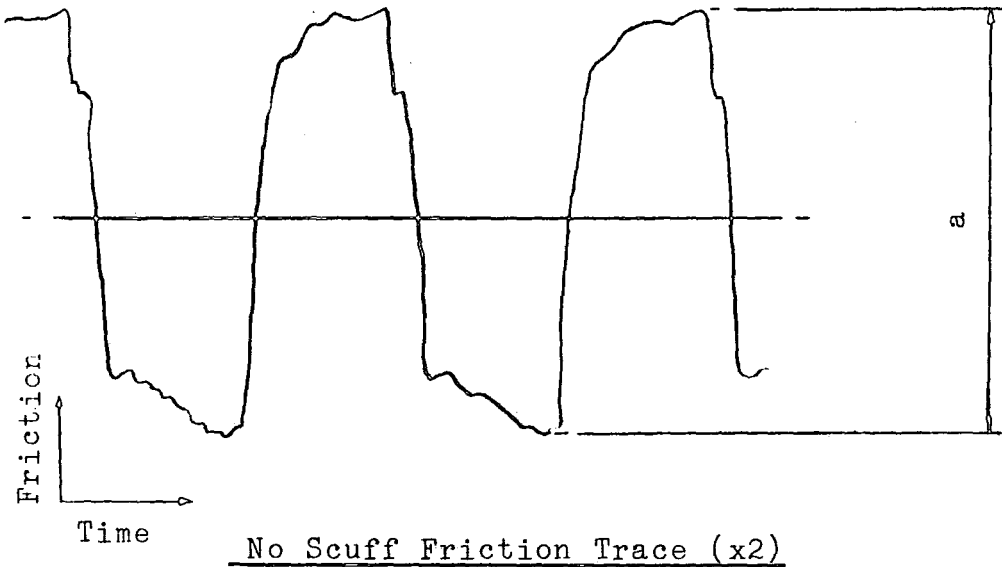


Figure 5.9 Scuff and No Scuff Friction Trace for Cast Iron

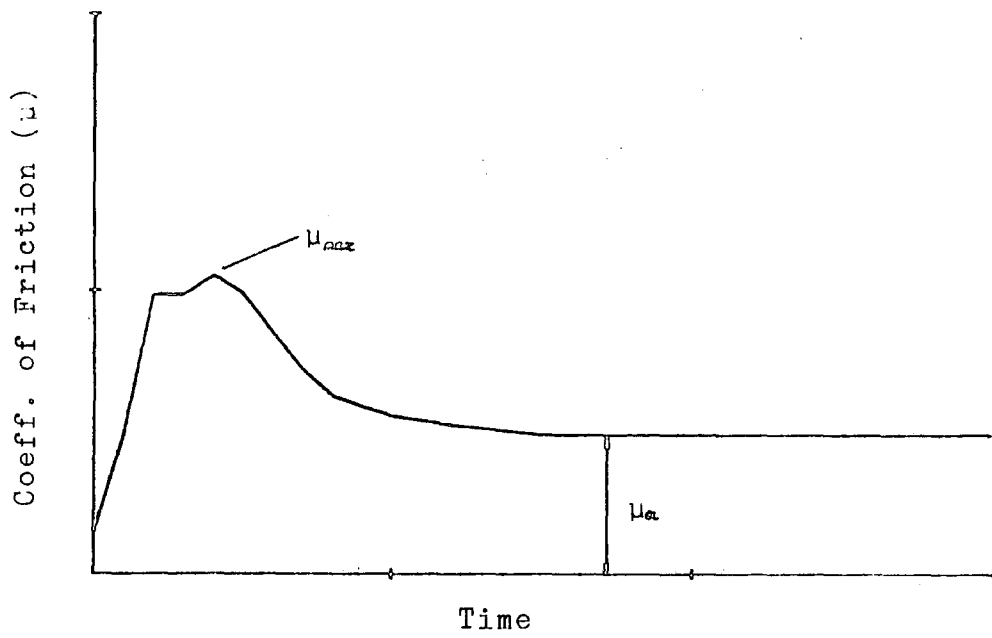


Figure 5.10 Coefficient of Friction to Time Curve

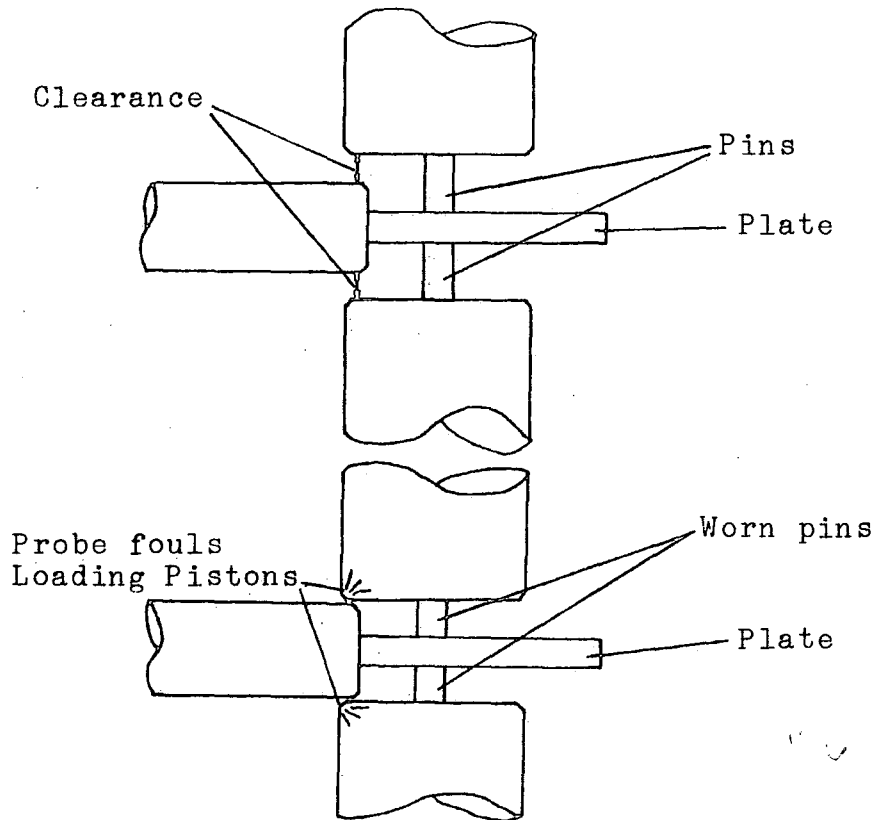


Figure 5.11 Effect of Pin Wear on Probe-Piston Clearance

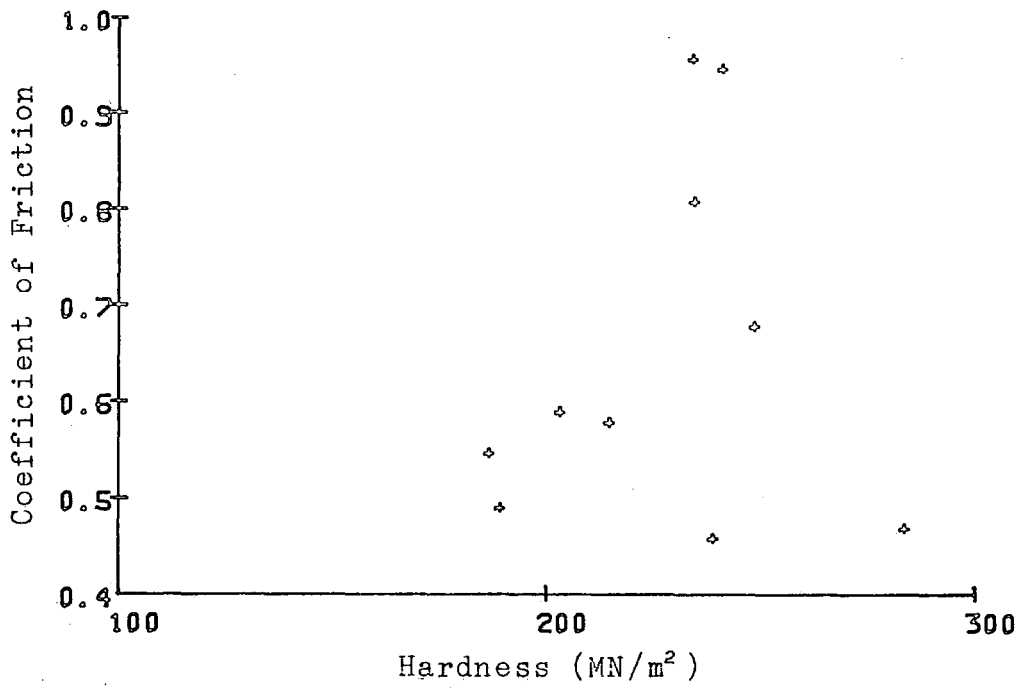


Fig.5.12 Effect of Hardness on Coefficient of Friction

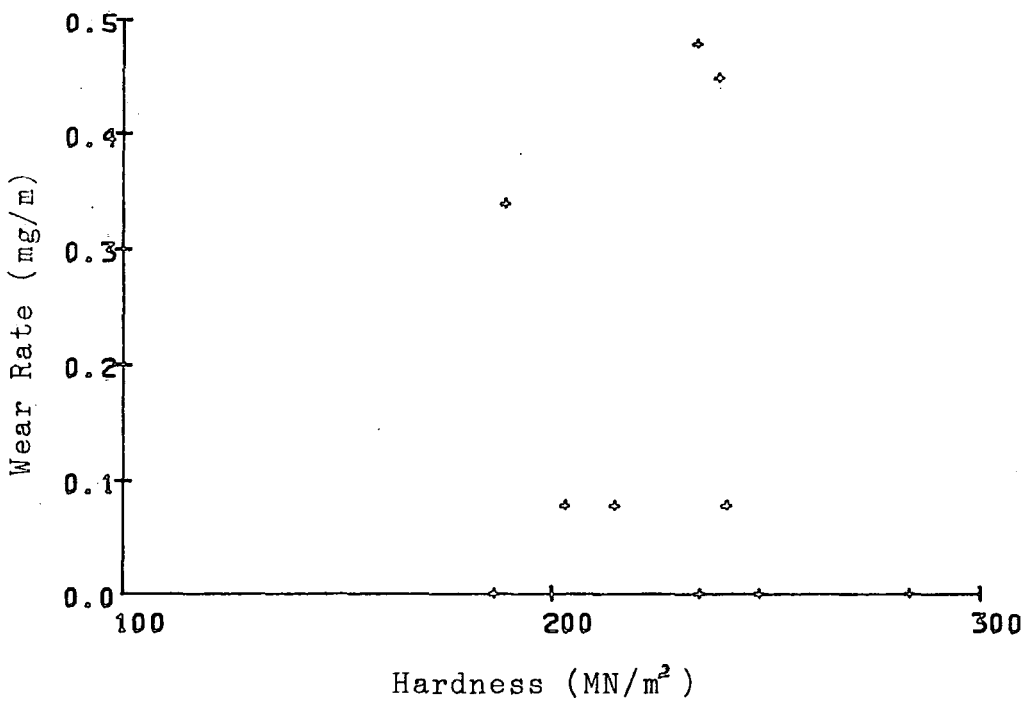


Fig.5.13 Effect of Hardness on Wear Rate

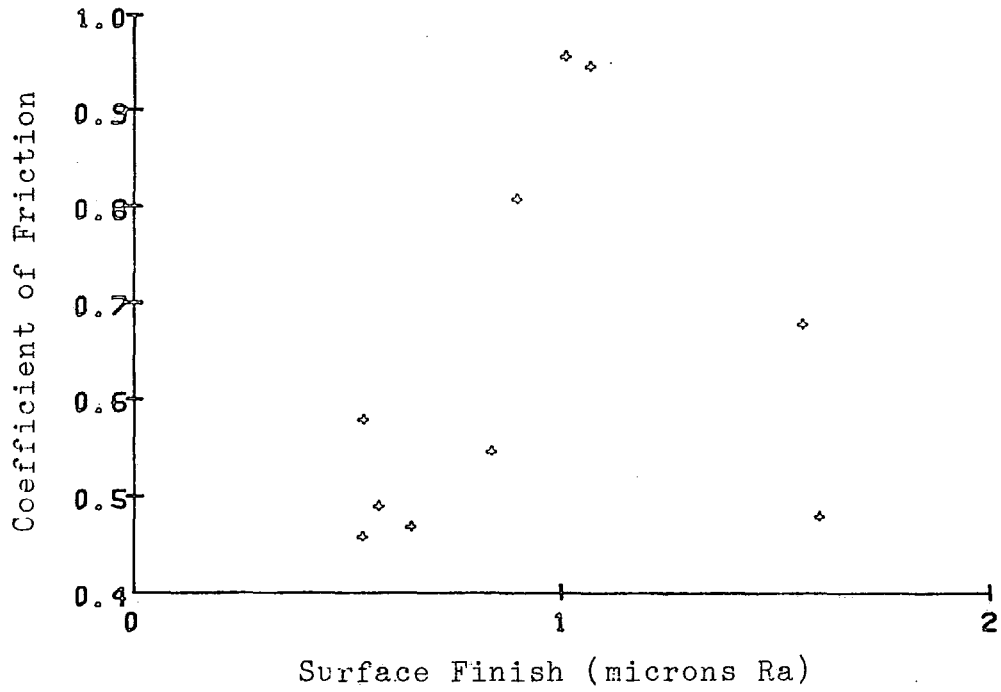


Fig 5.14 Effect of Surface Finish on Coefficient of Friction

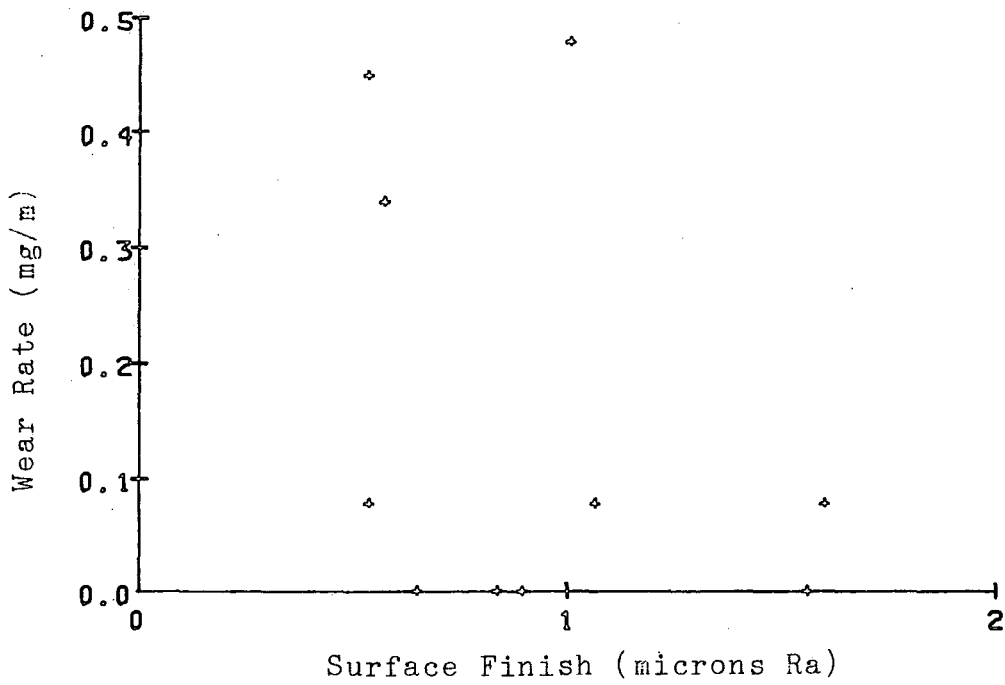


Fig 5.15 Effect of Surface Finish on Wear Rate

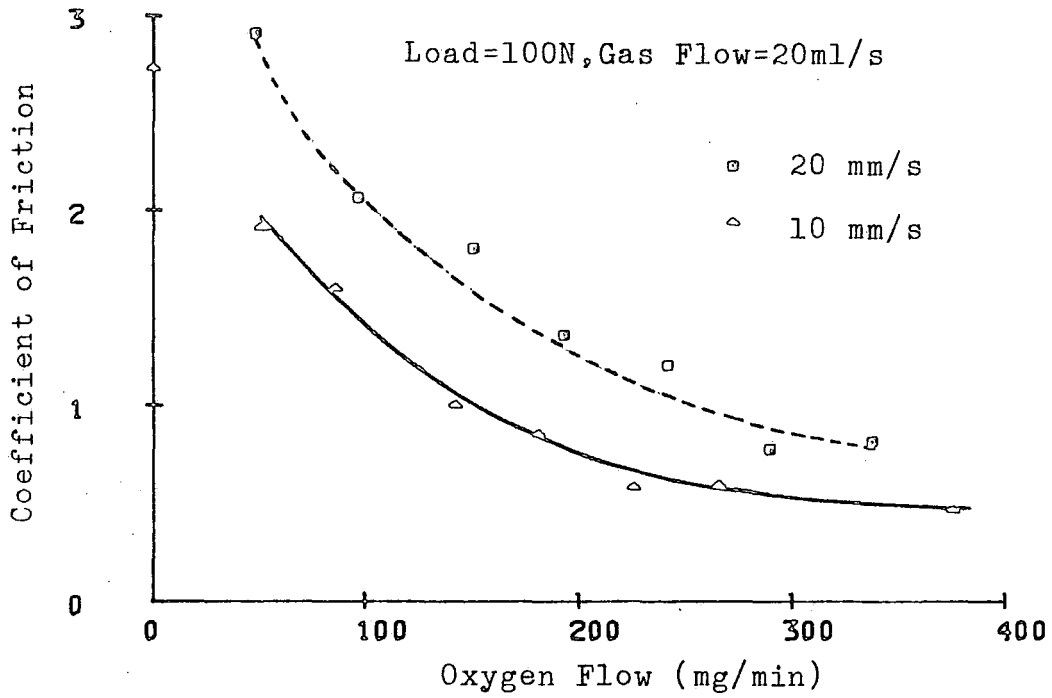


Fig.5.16 Effect of Speed on Friction

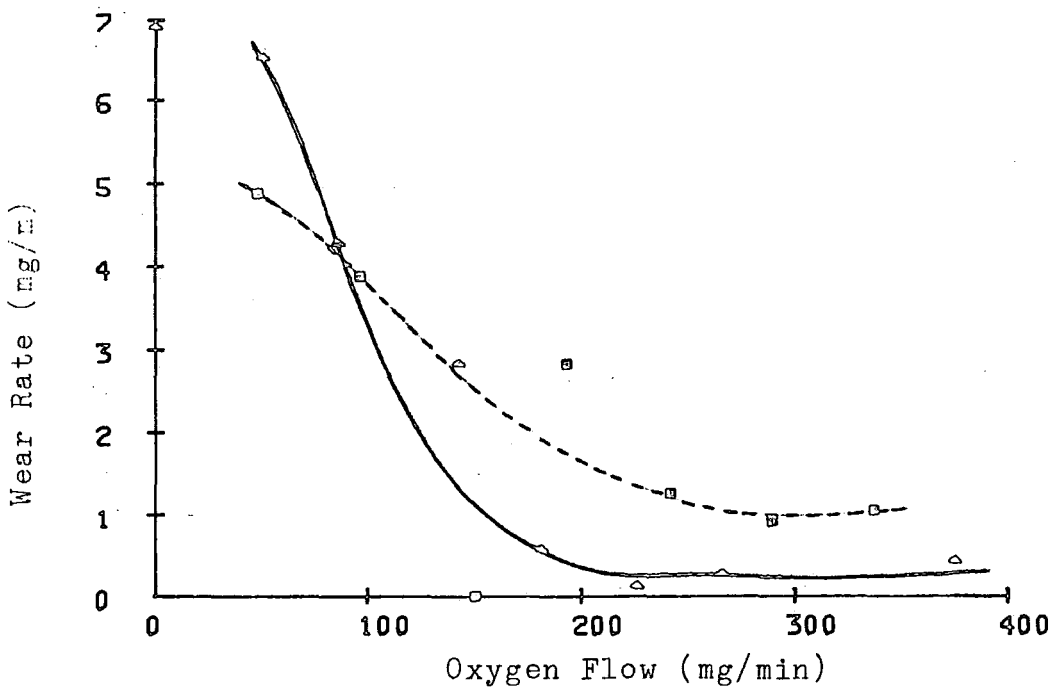


Fig.5.17 Effect of Speed on Wear Rate

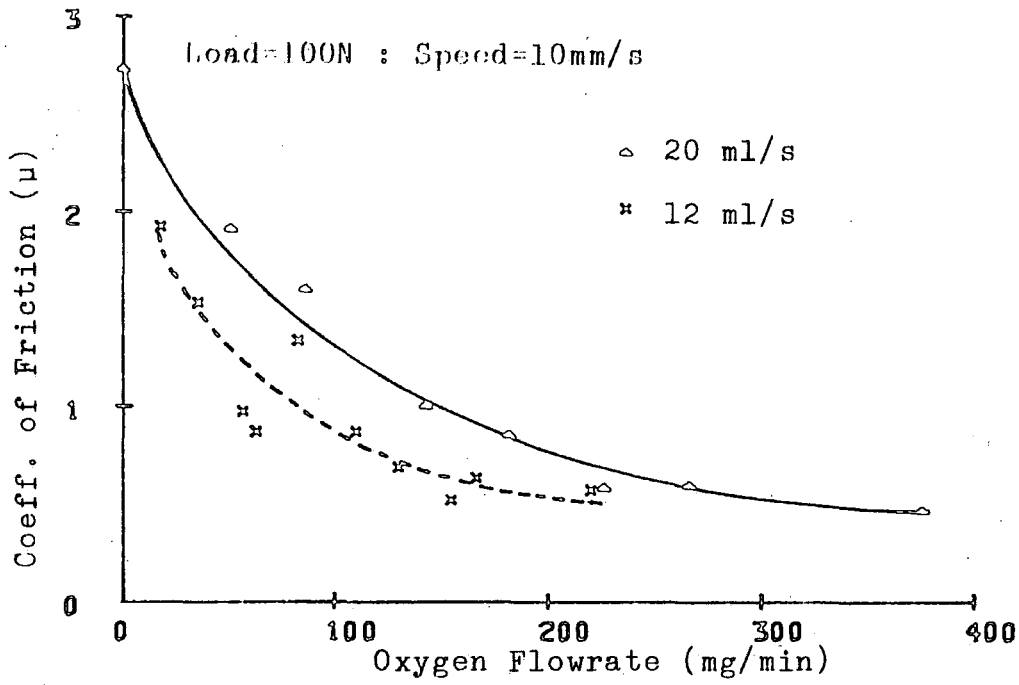


Figure 5.18 Effect of Gas Flowrate on Friction

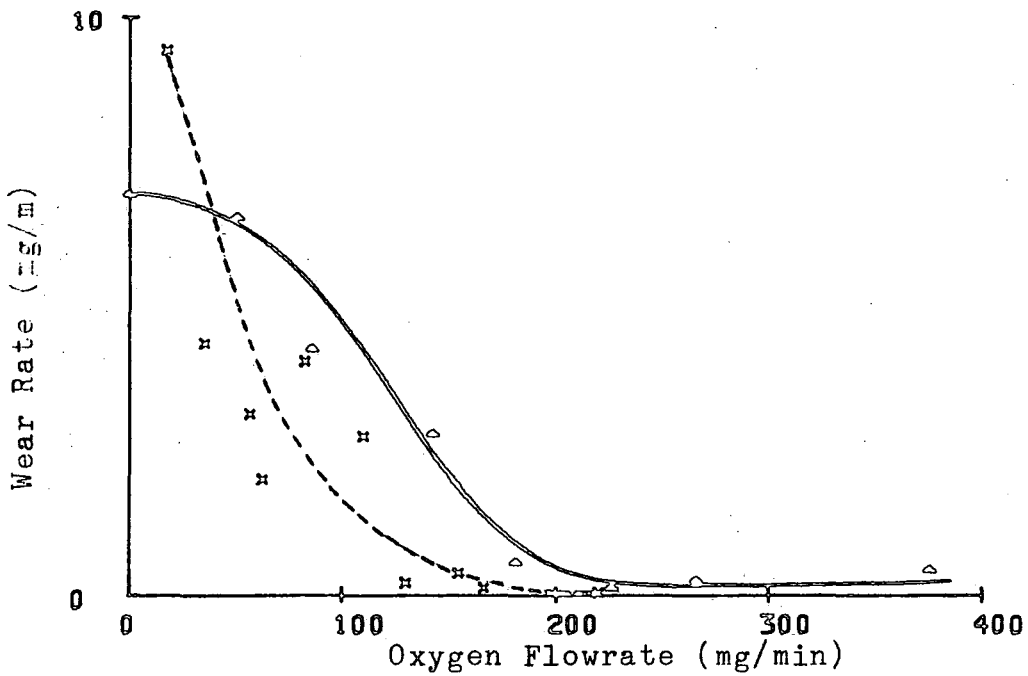


Figure 5.19 Effect of Gas Flowrate on Wear Rate

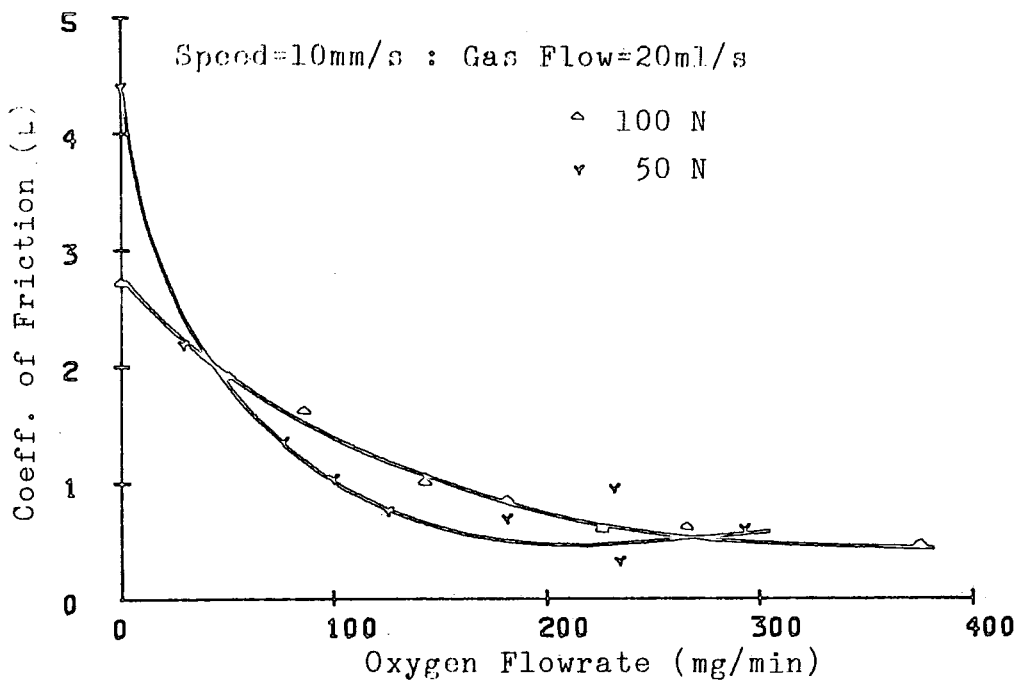


Figure 5.20 Effect of Load on Coefficient of Friction

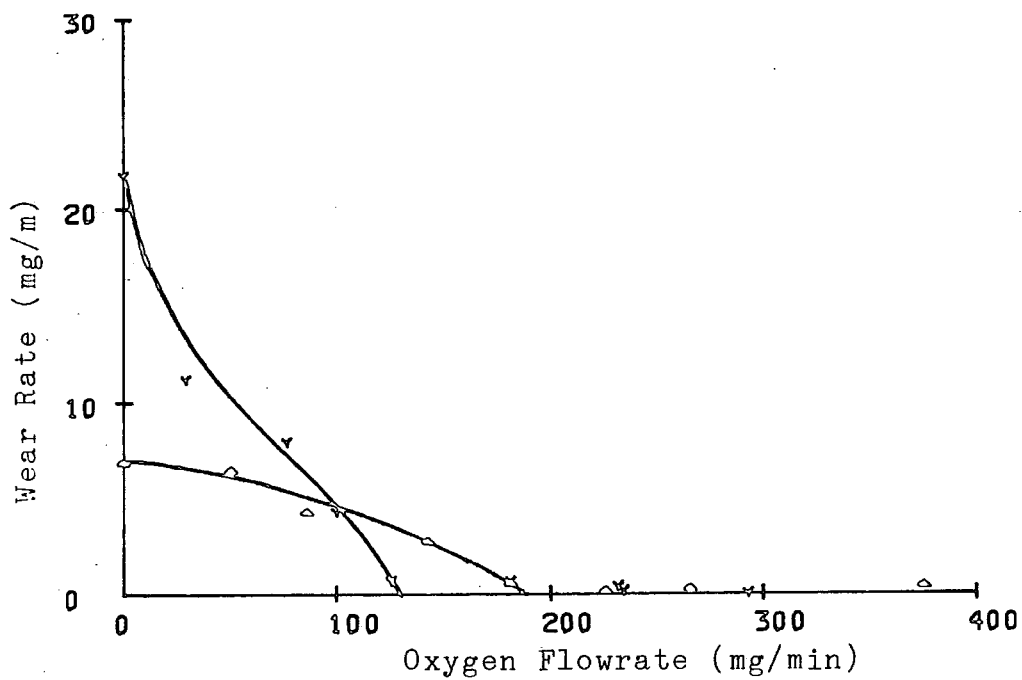


Figure 5.21 Effect of Load on Wear Rate

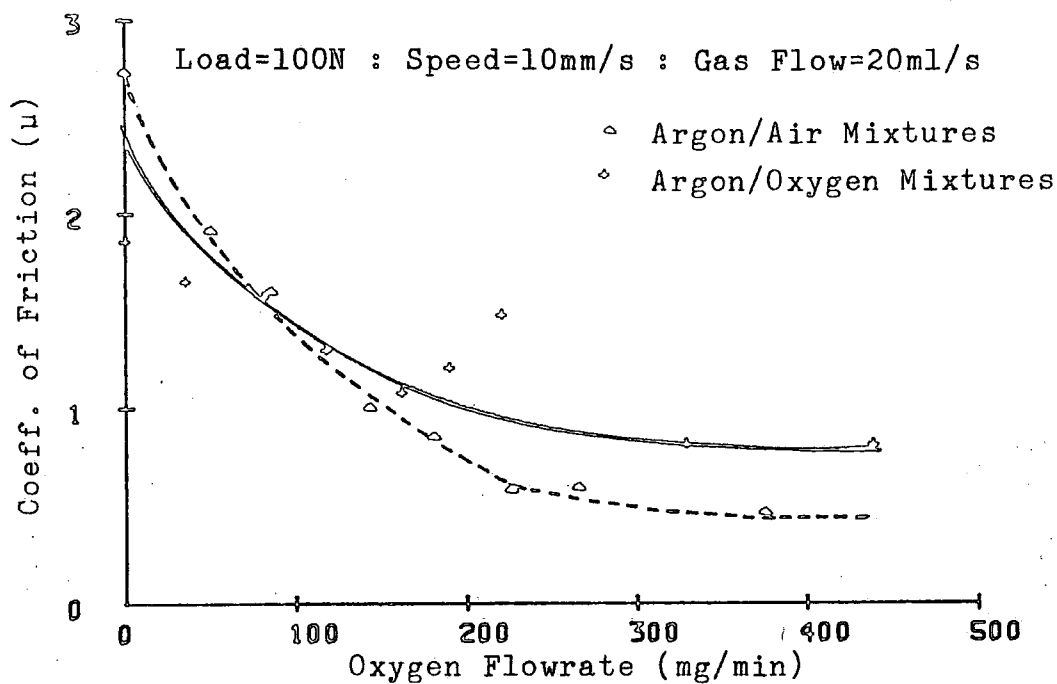


Figure 5.22 Comparison of Air & Oxygen (Friction)

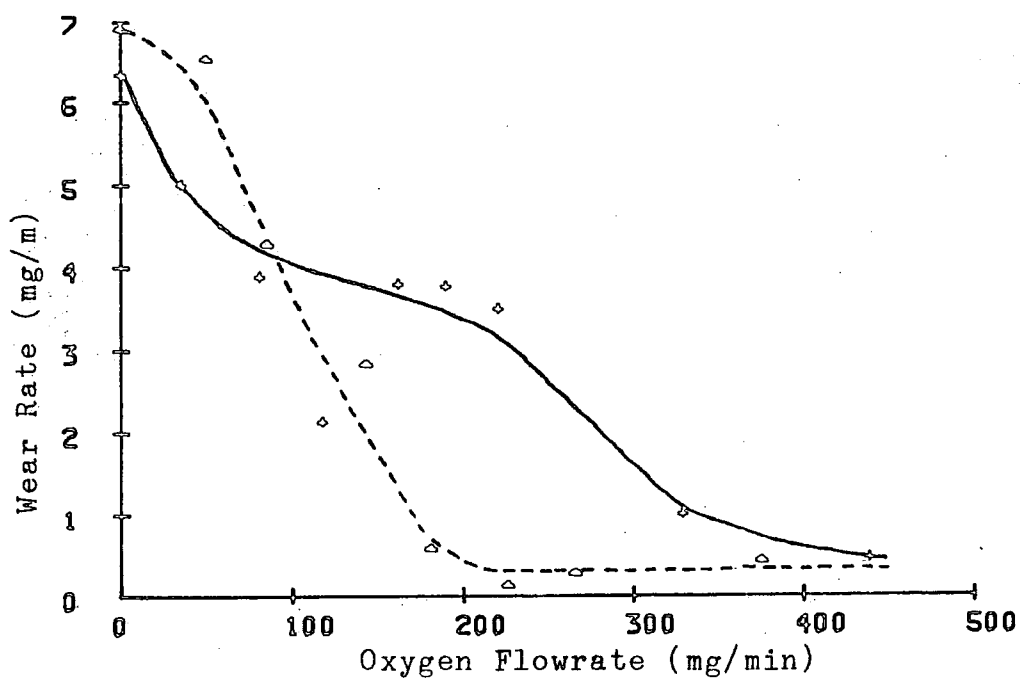
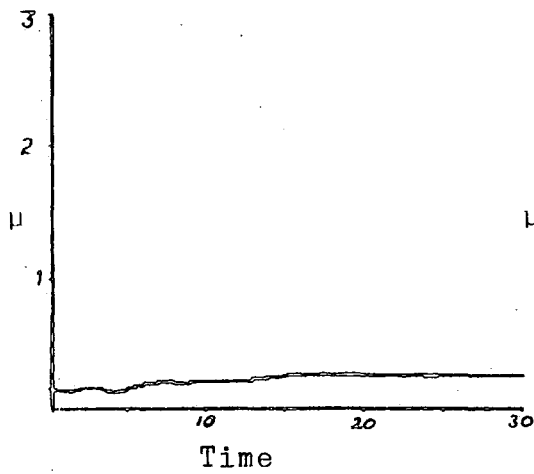
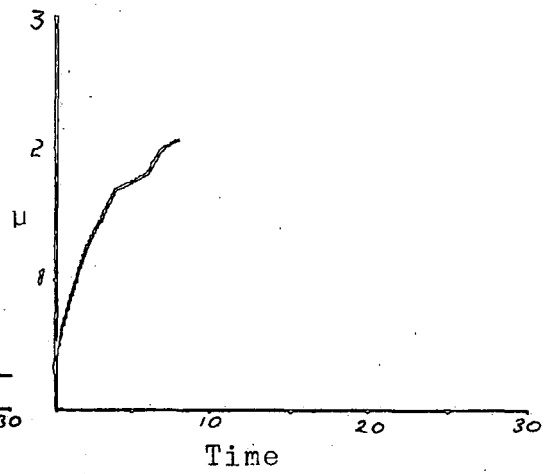


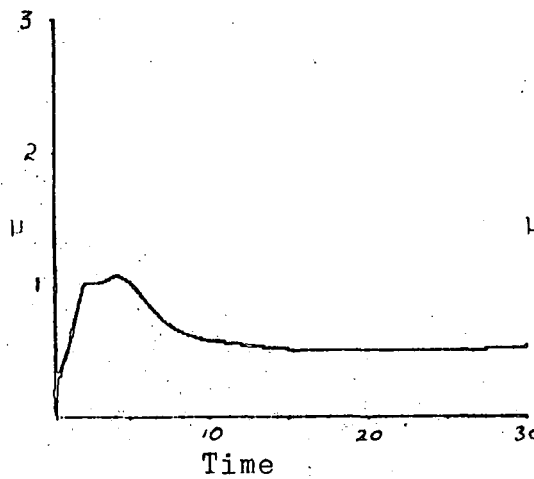
Figure 5.23 Comparison of Air & Oxygen (Wear Rate)



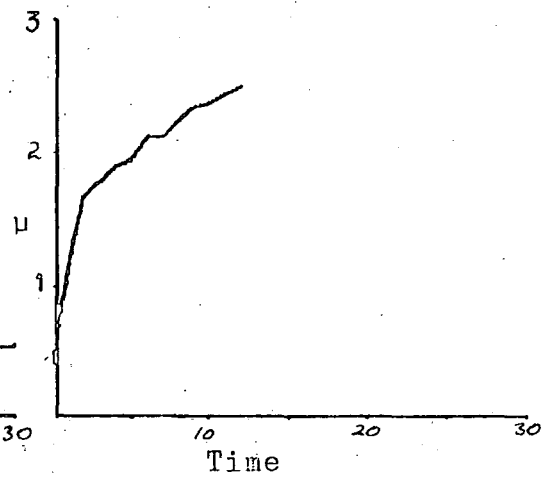
$P_{H_2O} = 23.82$ mbar



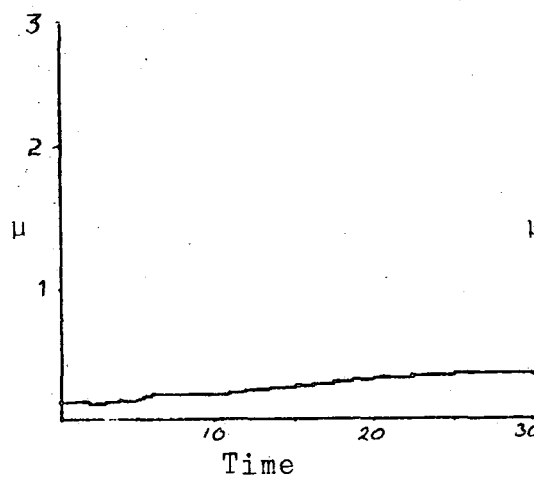
$P_{H_2O} = 16.72$ mbar



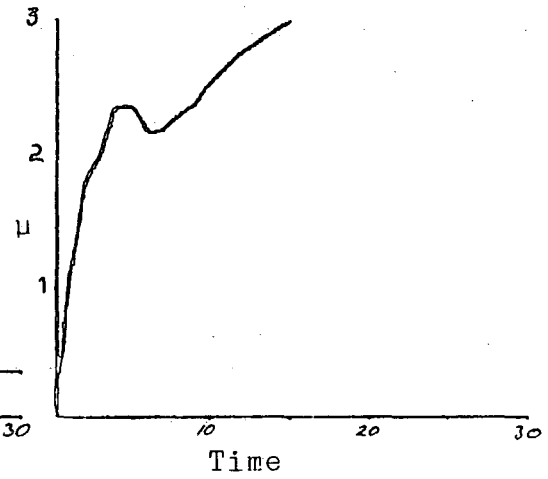
$P_{H_2O} = 19.86$ mbar



$P_{H_2O} = 13.03$ mbar



$P_{H_2O} = 17.94$ mbar



$P_{H_2O} = 9.28$ mbar

Figure 5.24 Friction to Time Curves for Hydrogen

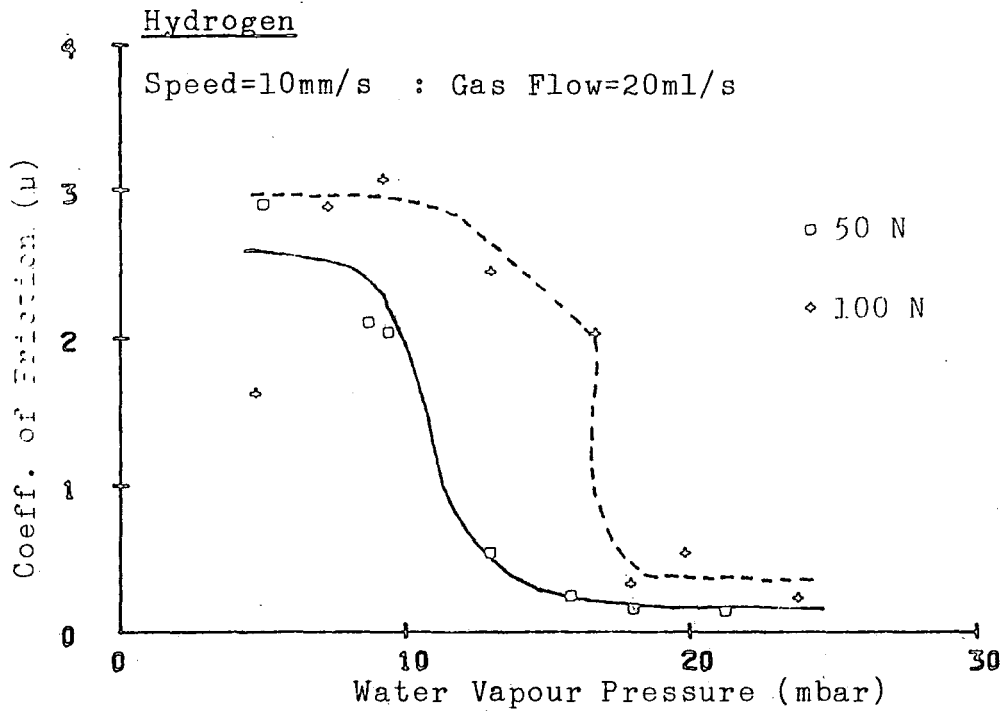


Figure 5.25 Friction to Water Vapour Pressure (Hydrogen)

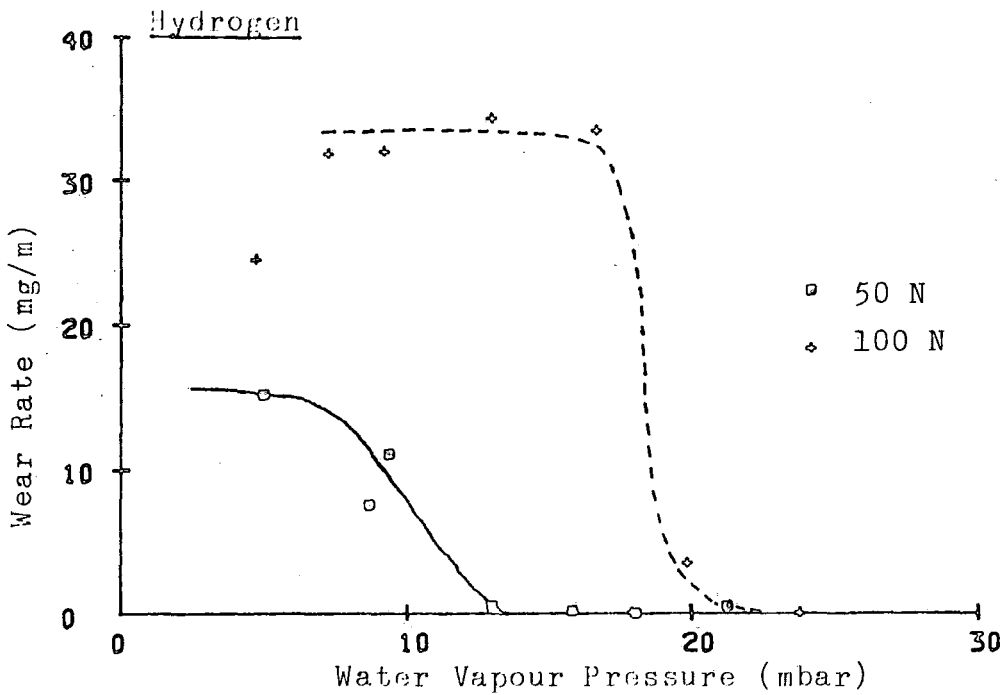


Figure 5.26 Wear Rate to Water Vapour Pressure (Hydrogen)

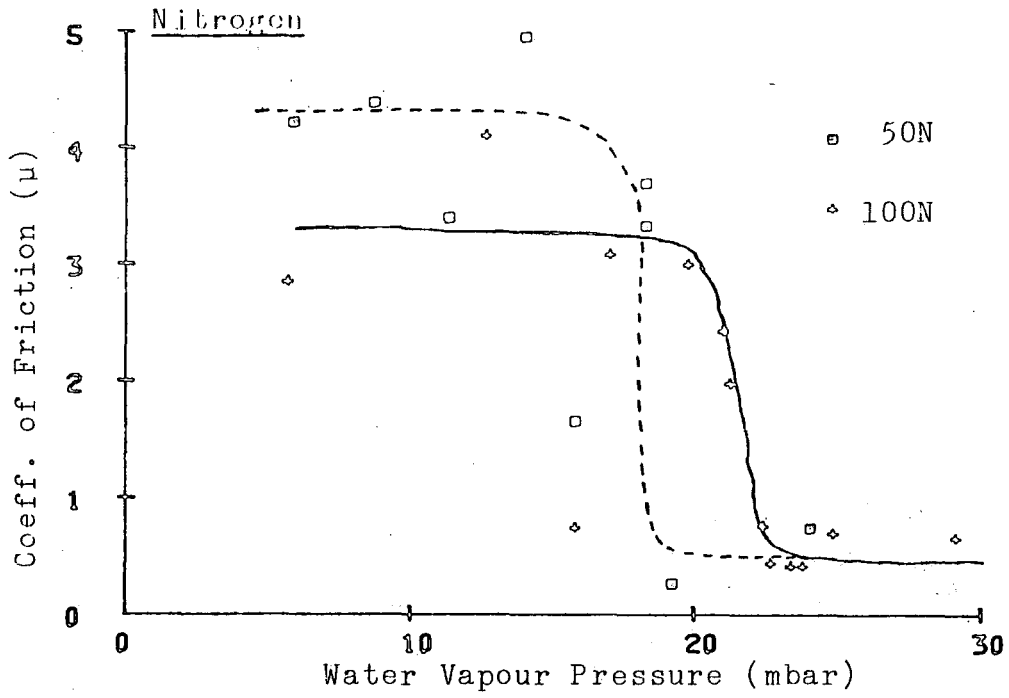


Figure 5.27 Friction to Water Vapour Pressure (Nitrogen)

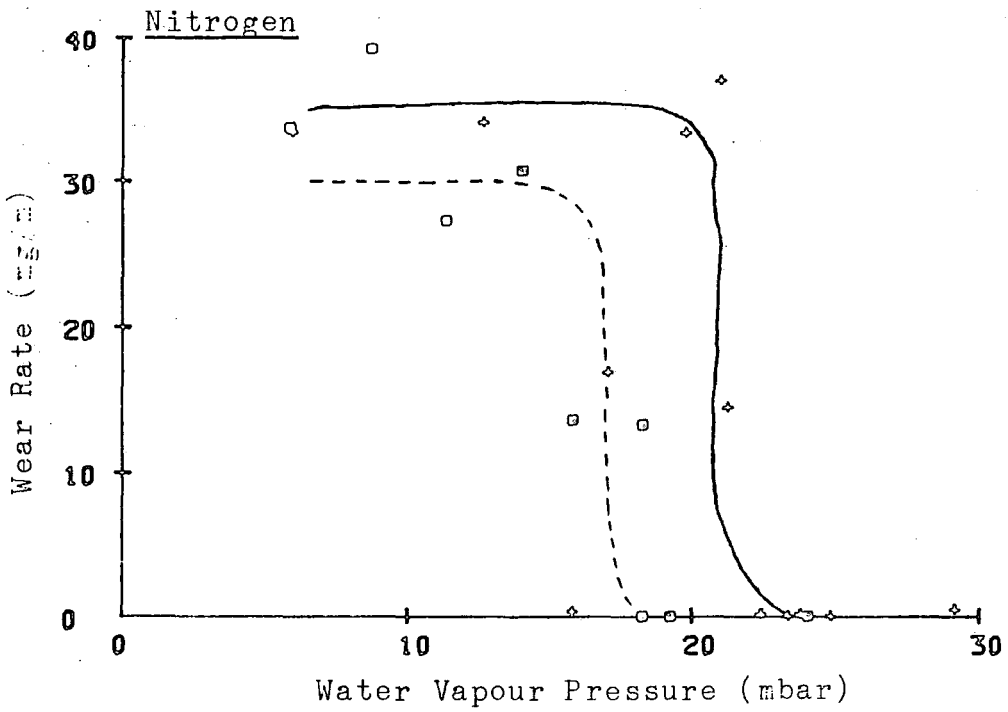


Figure 5.28 Wear Rate to Water Vapour Pressure (Nitrogen)

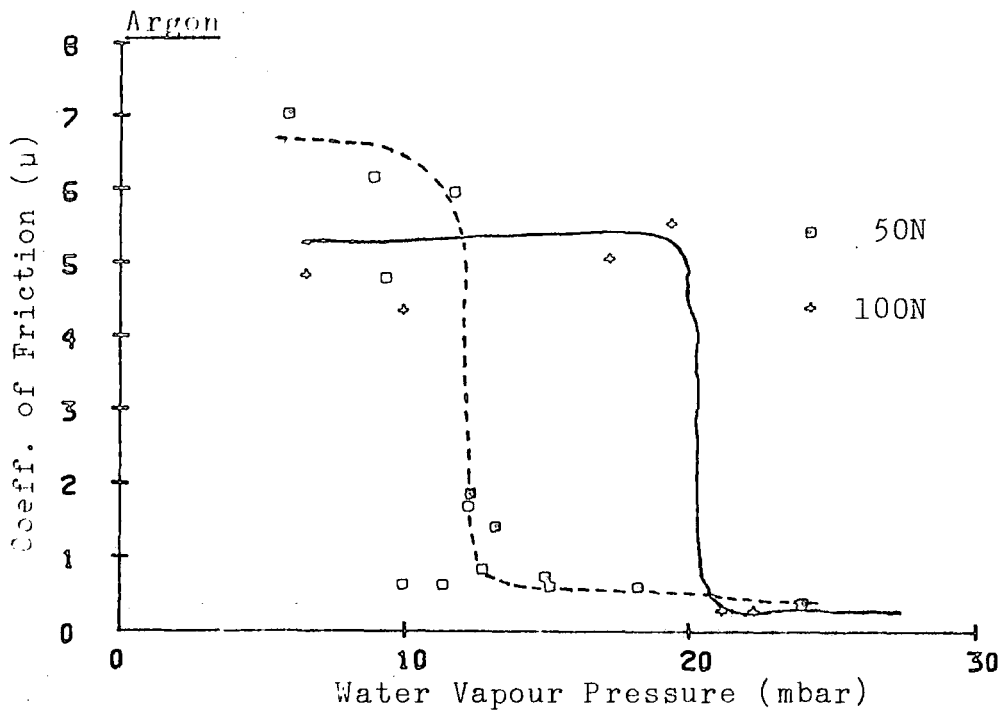


Figure 5.29 Friction to Water Vapour Pressure (Argon)

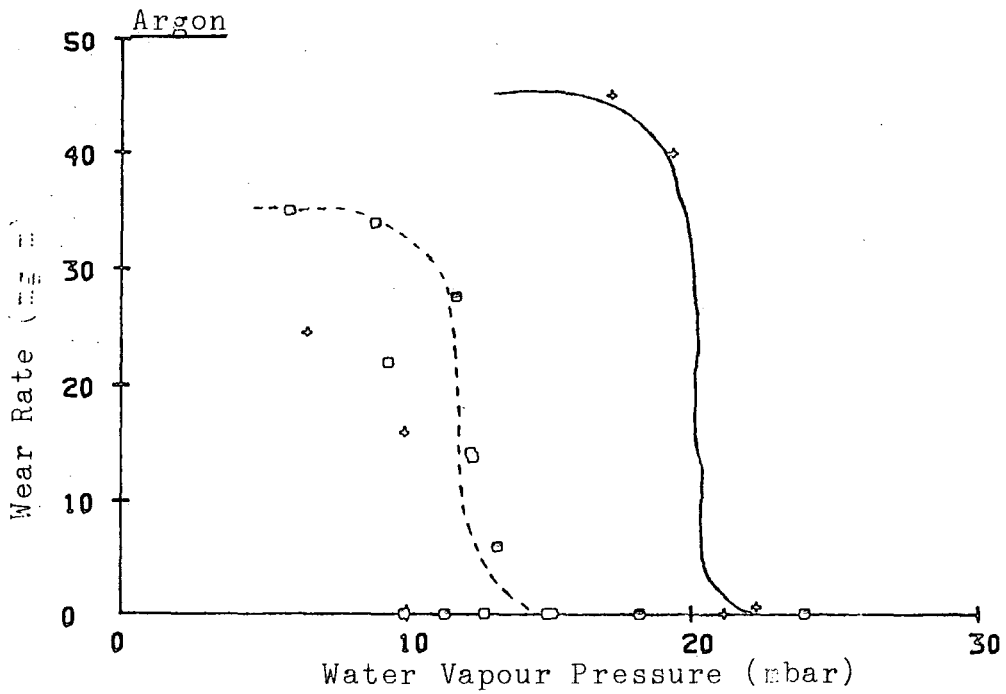


Figure 5.30 Wear Rate to Water Vapour Pressure (Argon)

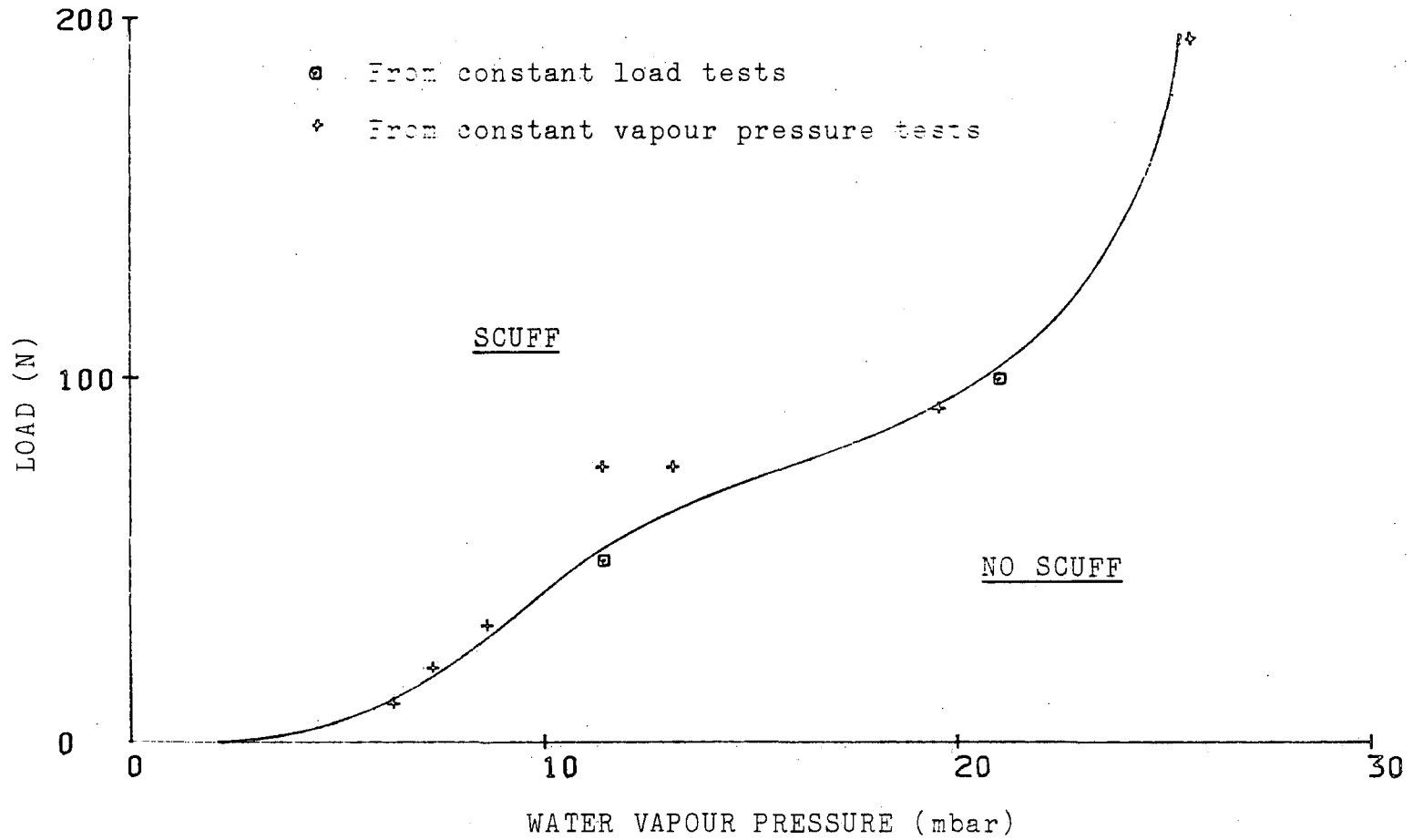


Figure 5.31 Scuff Load to Vapour Pressure (Argon)

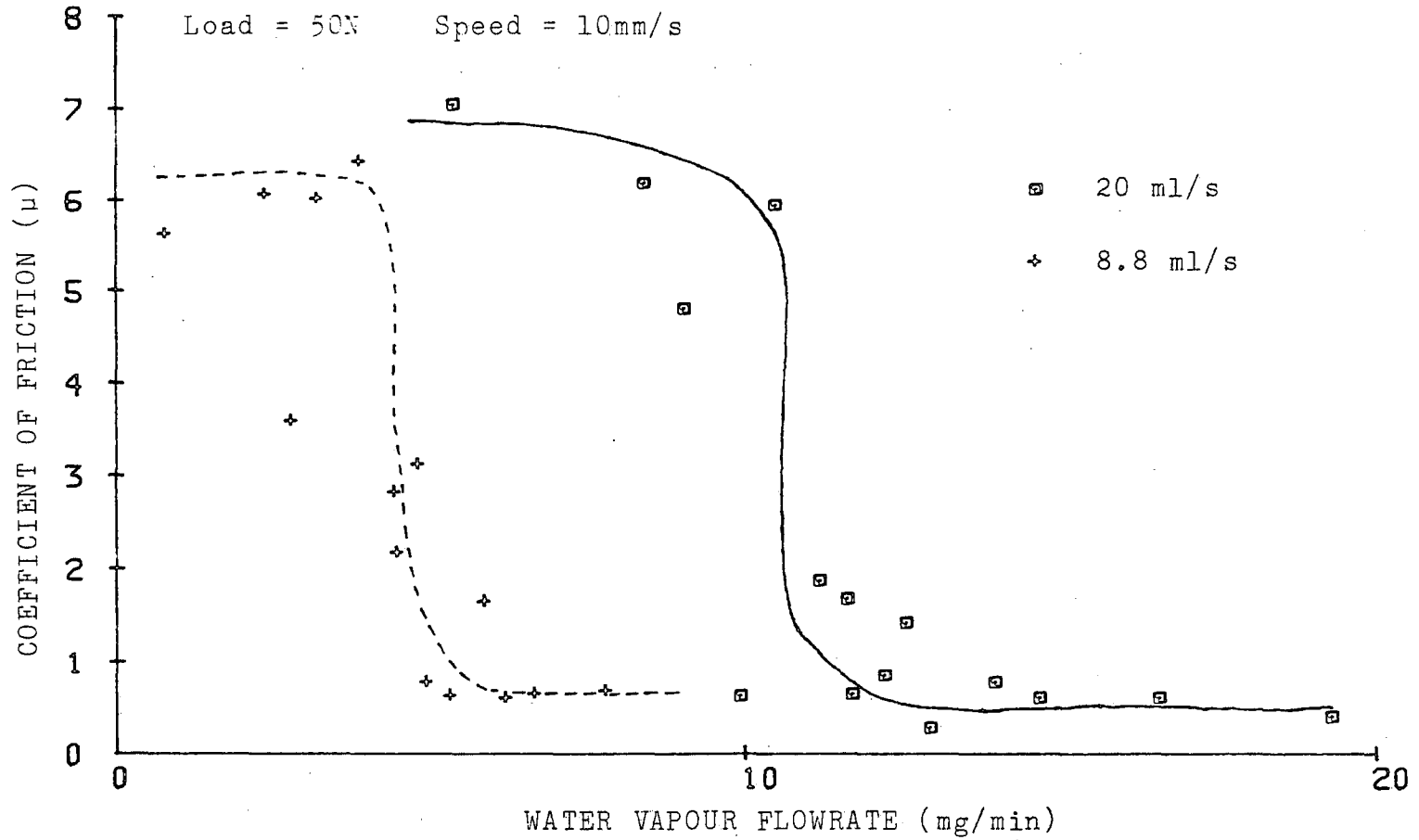


Figure 5.32 Effect of Water Vapour Flowrate on Coefficient of Friction

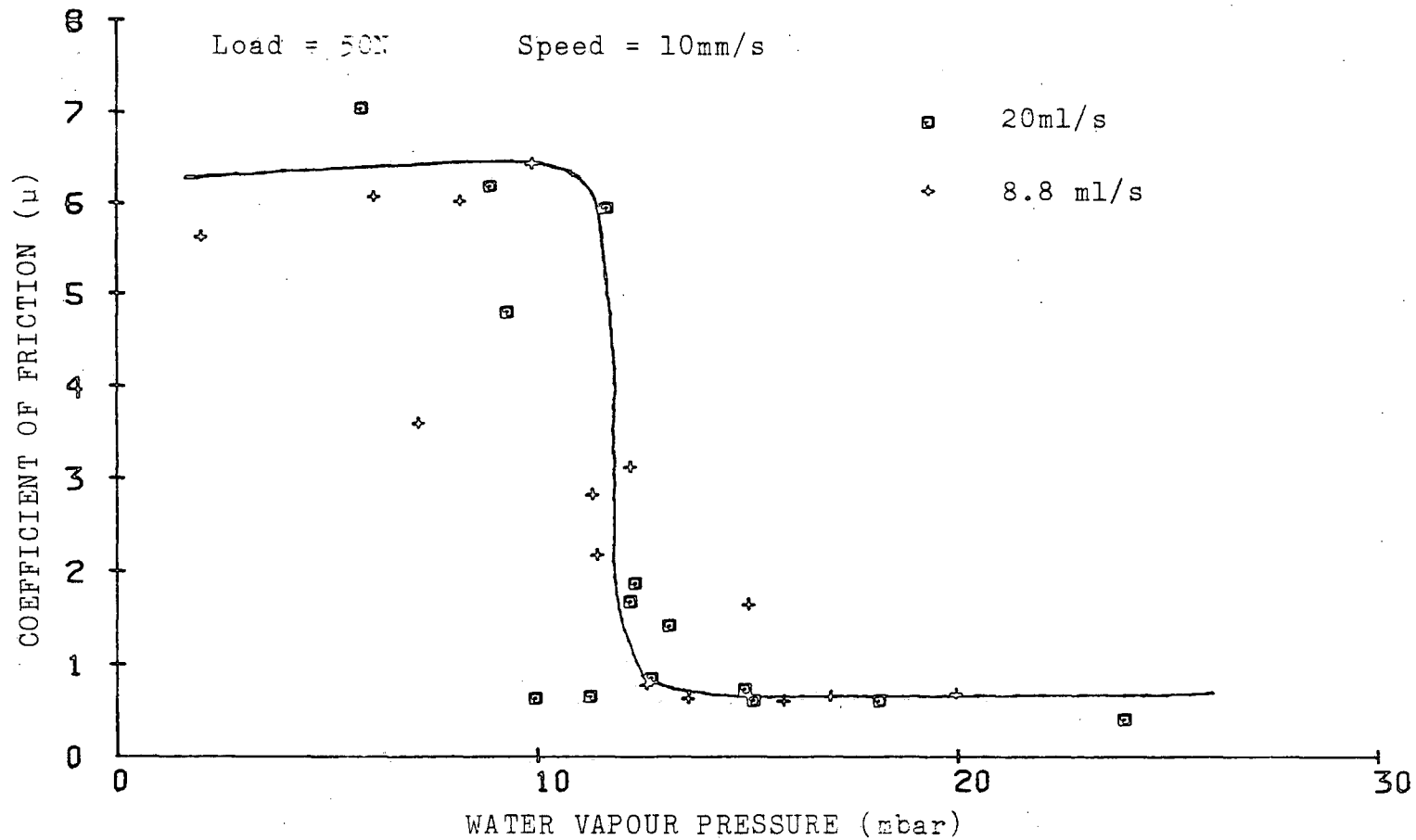


Figure 5.33 Effect of Water Vapour pressure on Coefficient of Friction

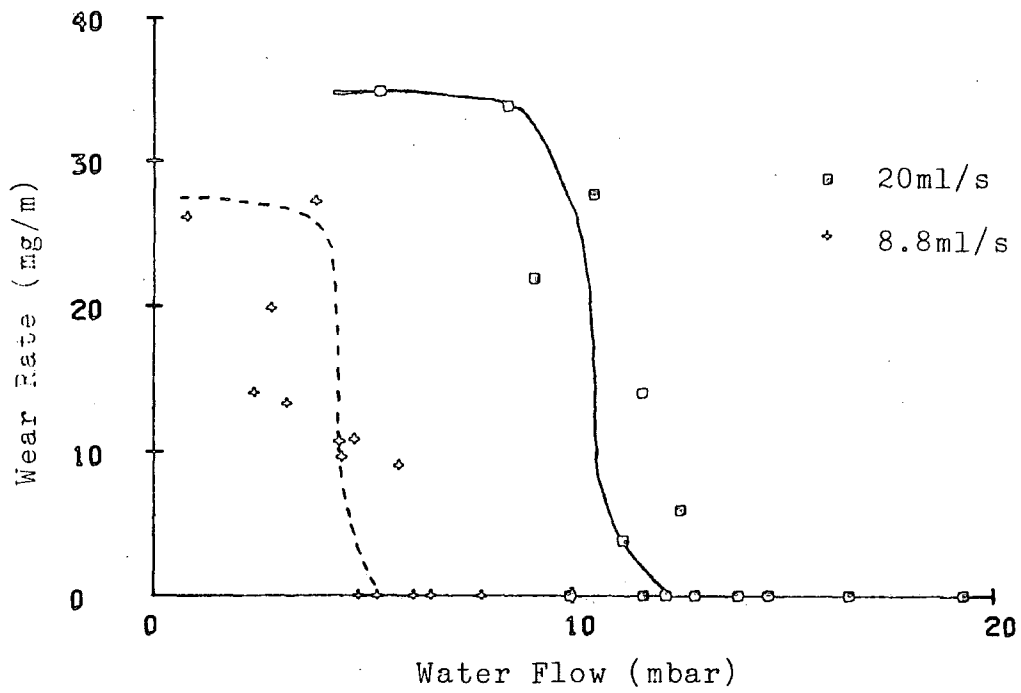


Figure 5.34 Effect of Water Flow on Wear Rate

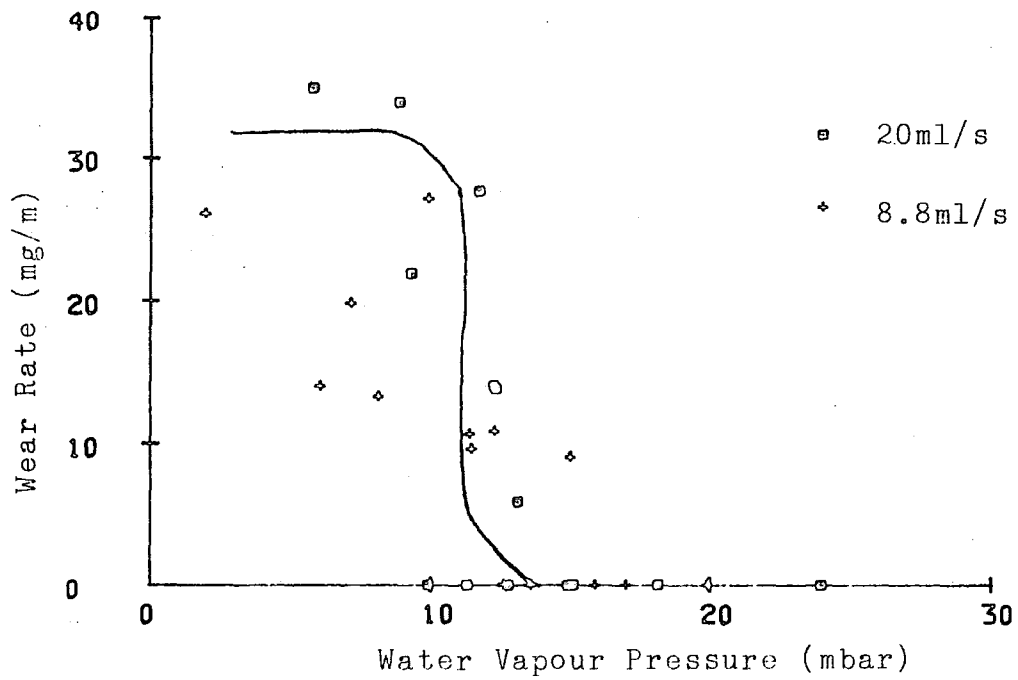


Figure 5.35 Effect of Water Vapour Pressure on Wear Rate

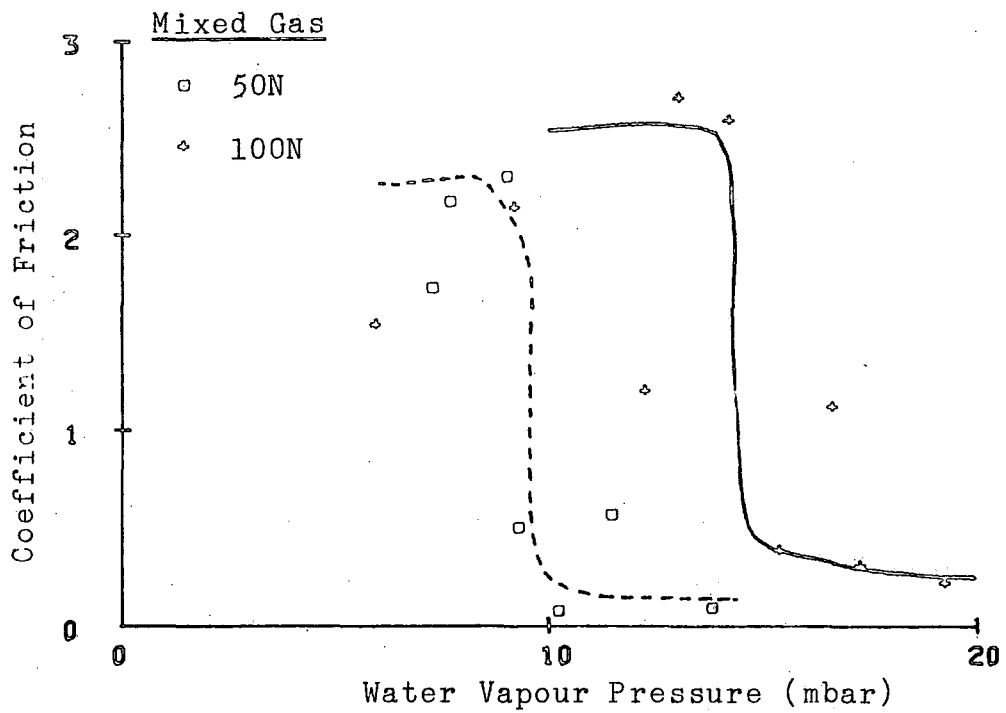


Figure 5.36 Friction to Water Vapour Pressure (Mixed Gas)

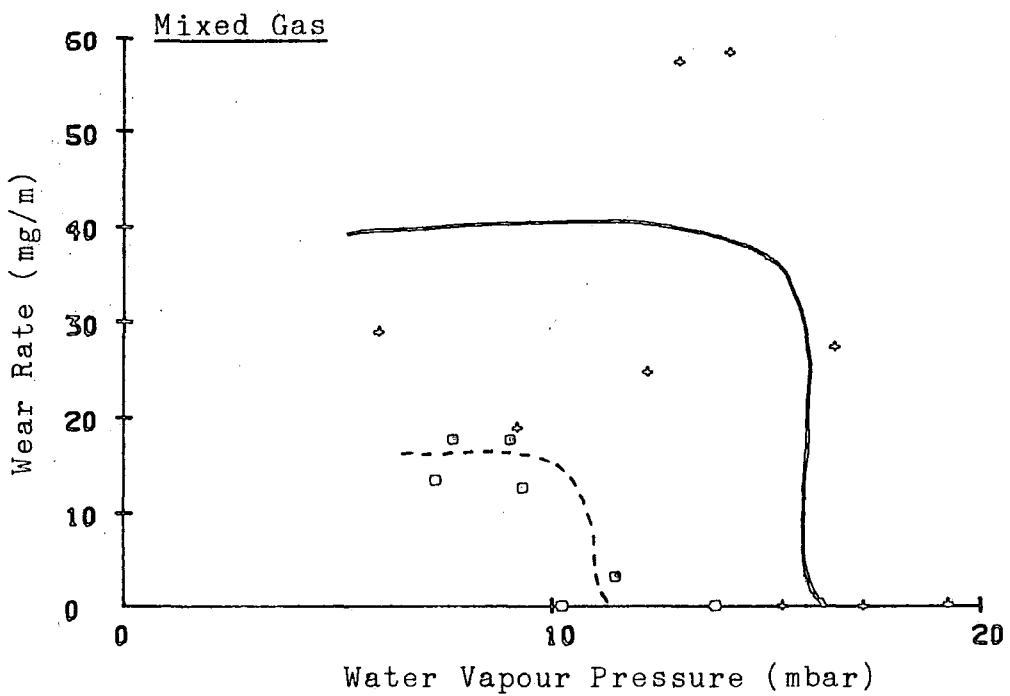


Figure 5.37 Wear Rate to Water Vapour Pressure (Mixed Gas)

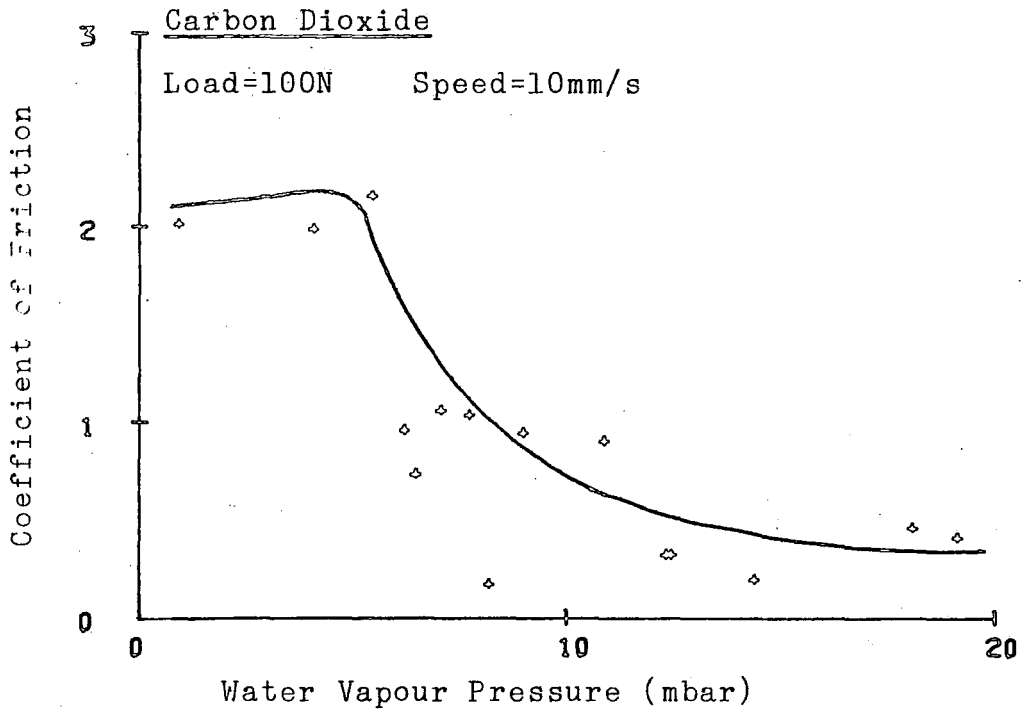


Figure 5.38 Friction-Water Vapour Pressure (CO₂)

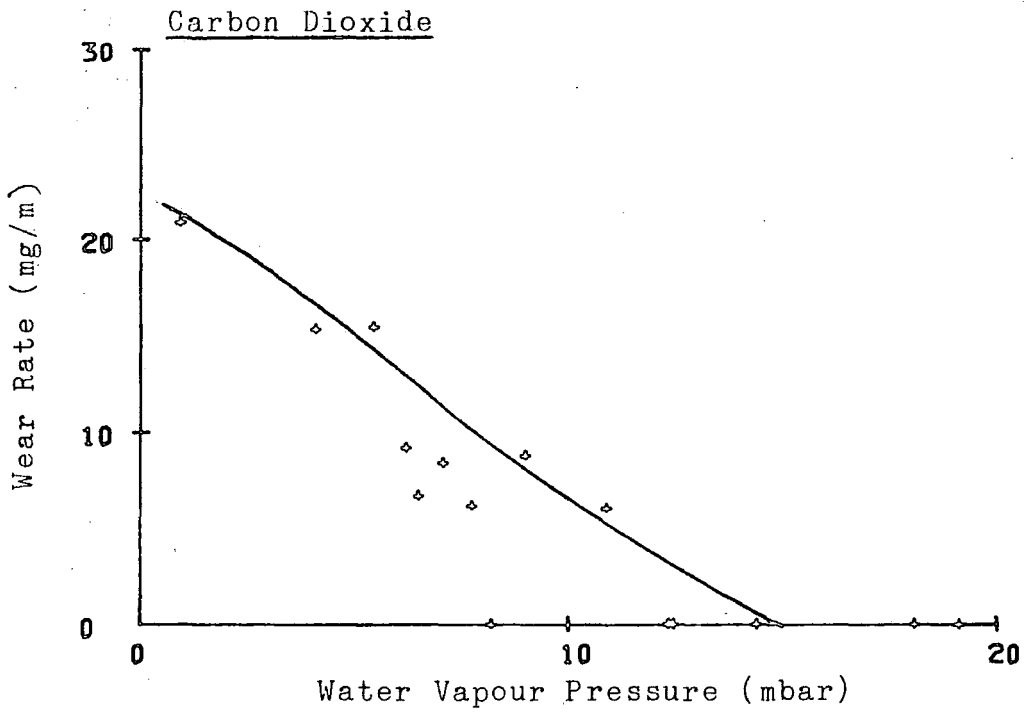


Figure 5.39 Wear Rate-Water Vapour Pressure (CO₂)

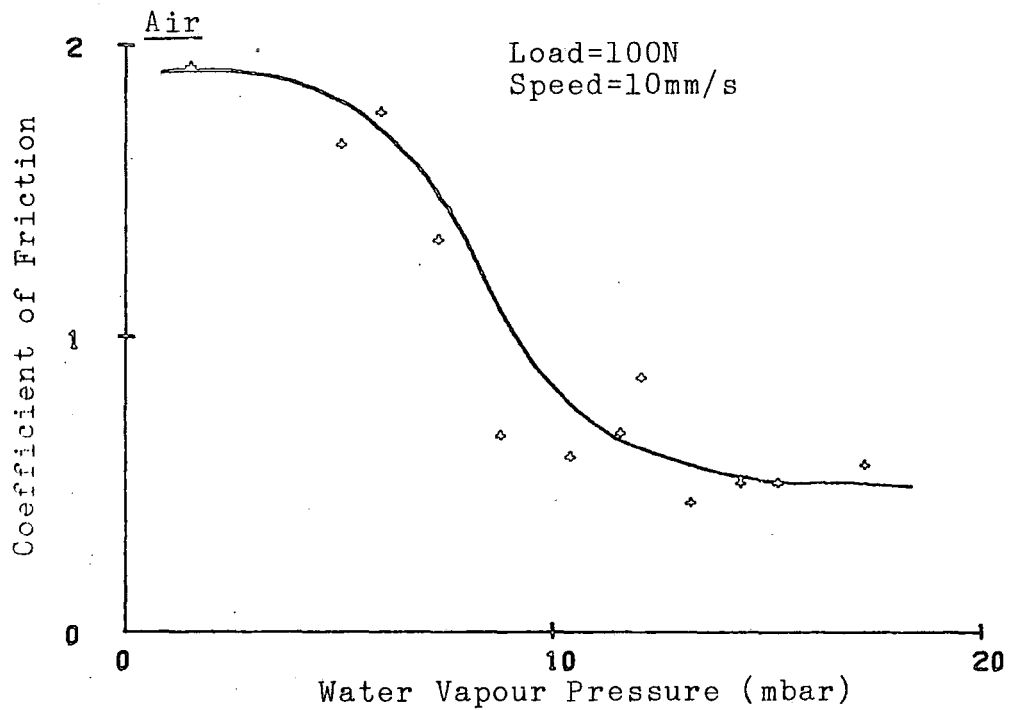


Figure 5.40 Friction-Water Vapour Pressure (Air)

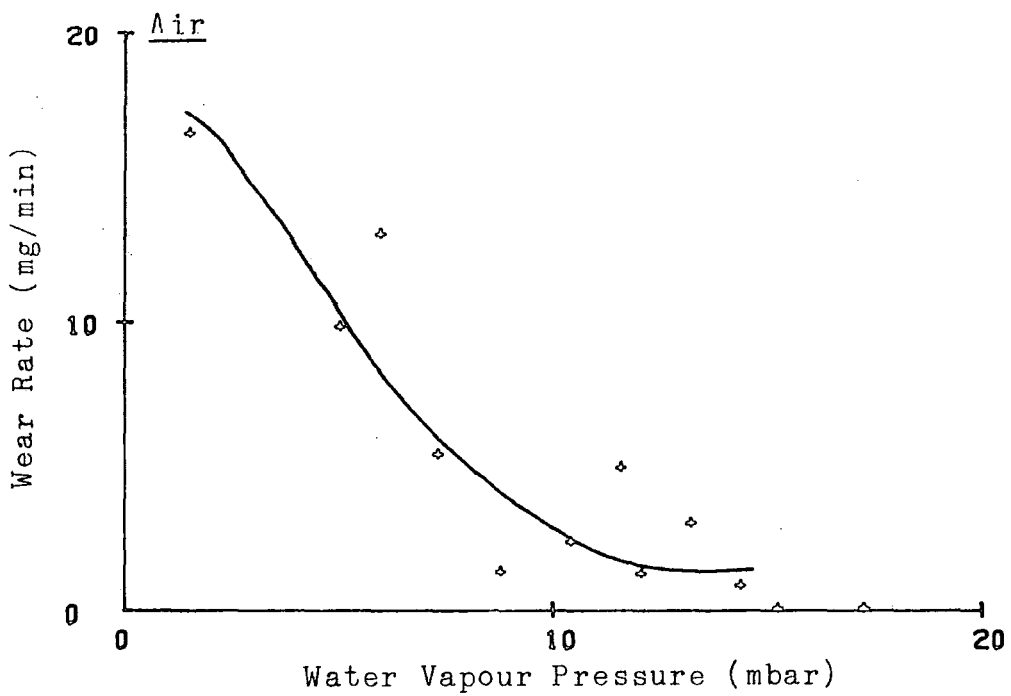


Figure 5.41 Wear Rate-Water Vapour Pressure (Air)

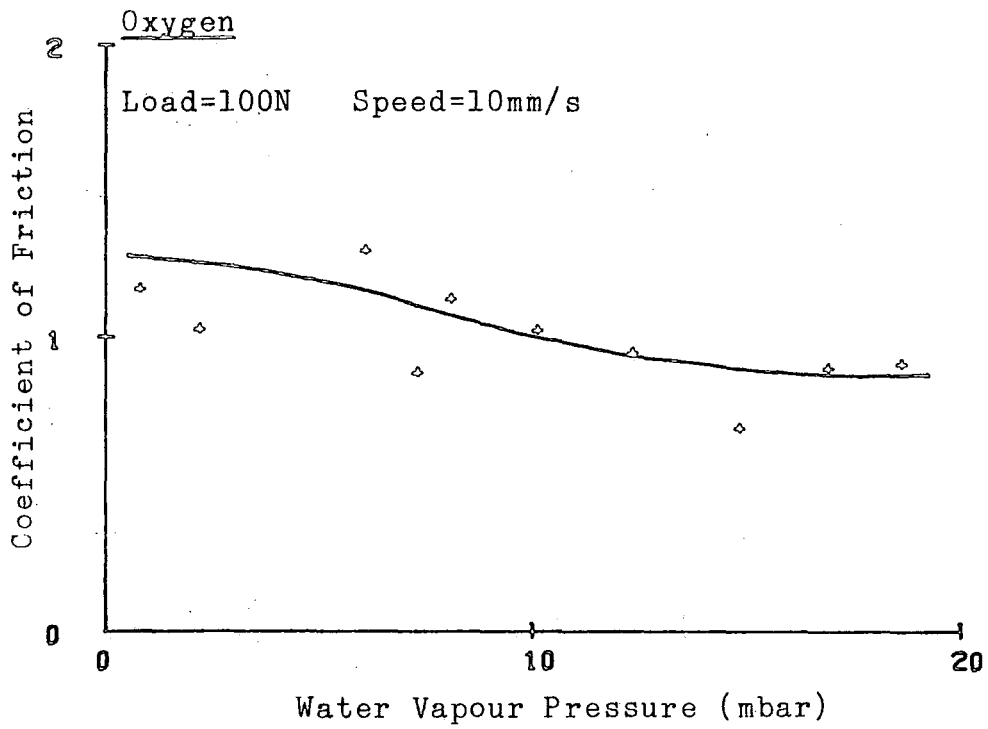


Figure 5.42 Friction-Water Pressure (Oxygen)

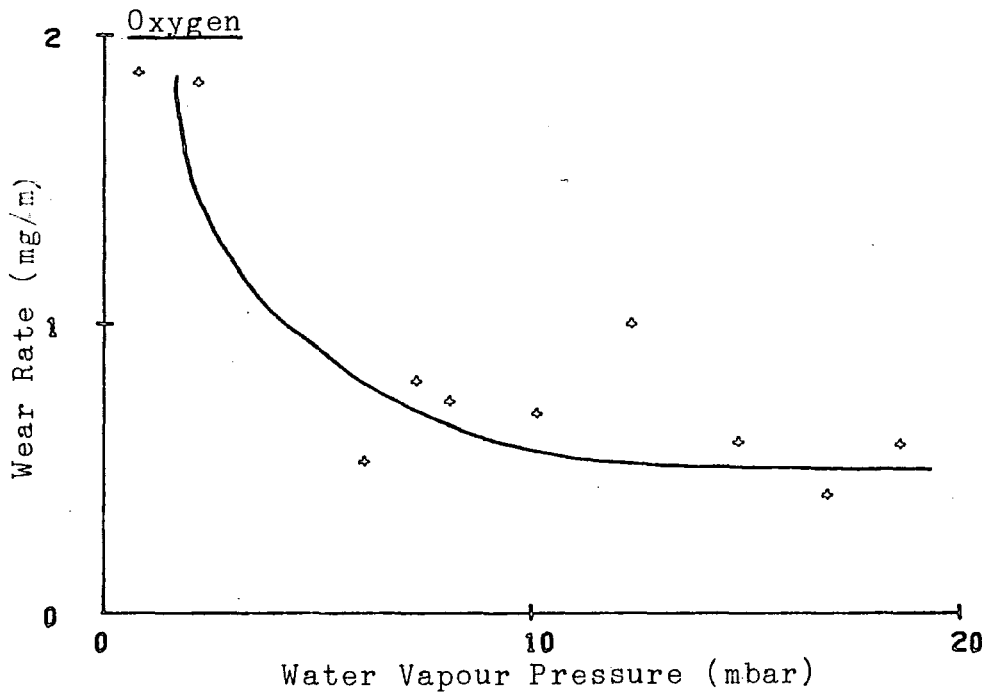


Figure 5.43 Wear Rate-Water Vapour Pressure (Oxygen)

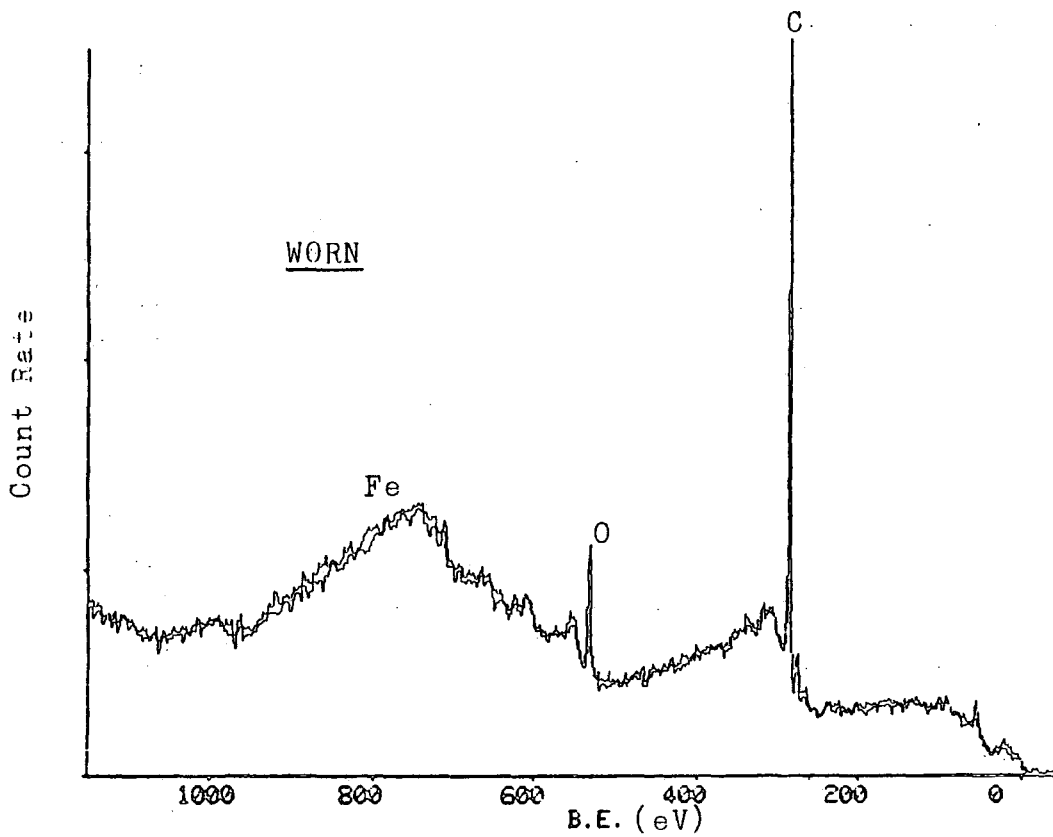
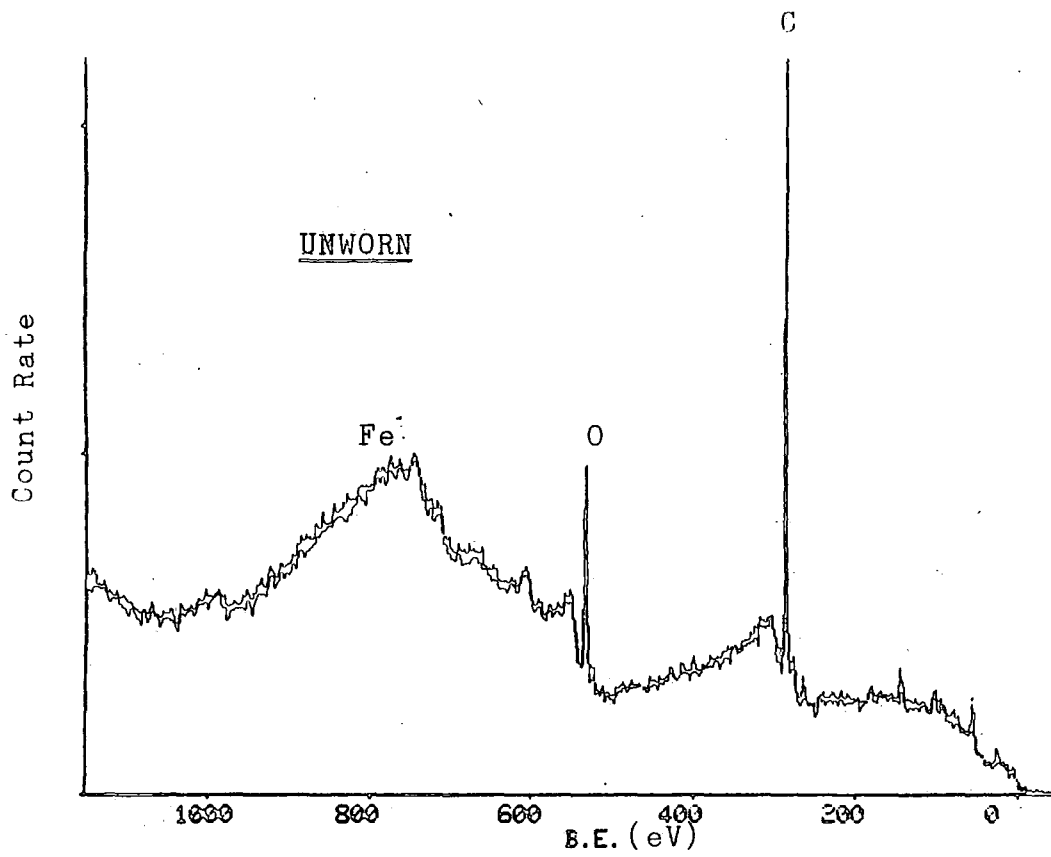


Figure 5.44 Wide Scan Spectra of Worn and Unworn Plate

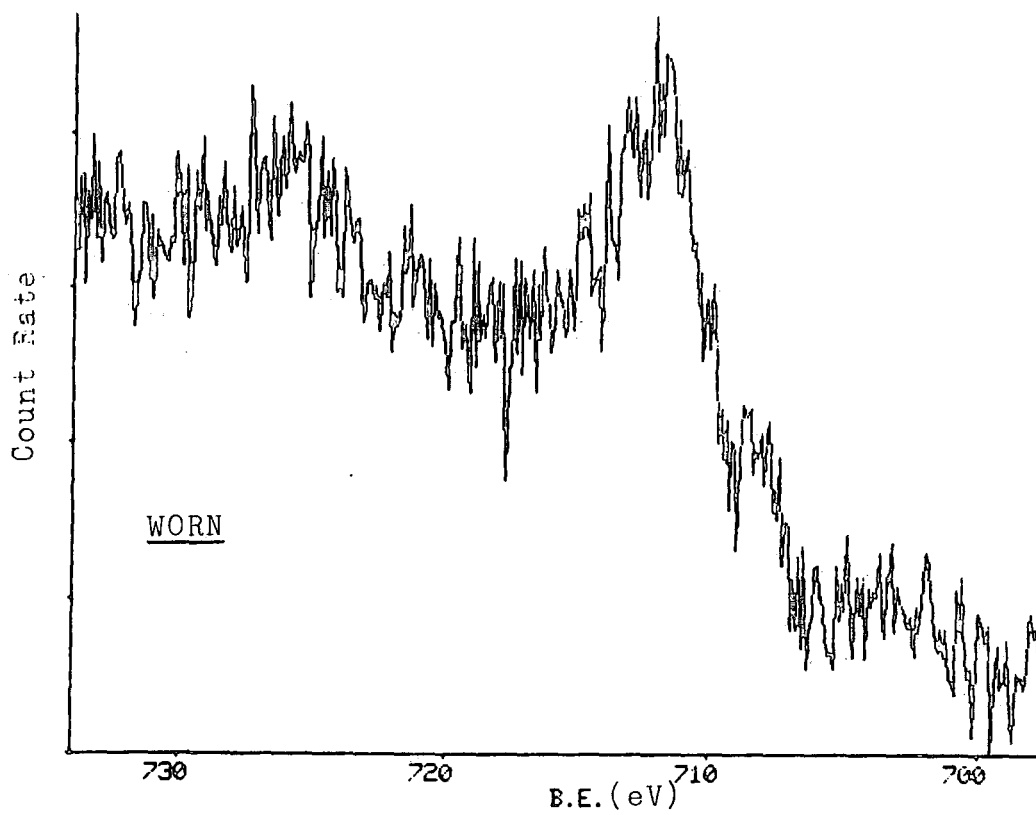
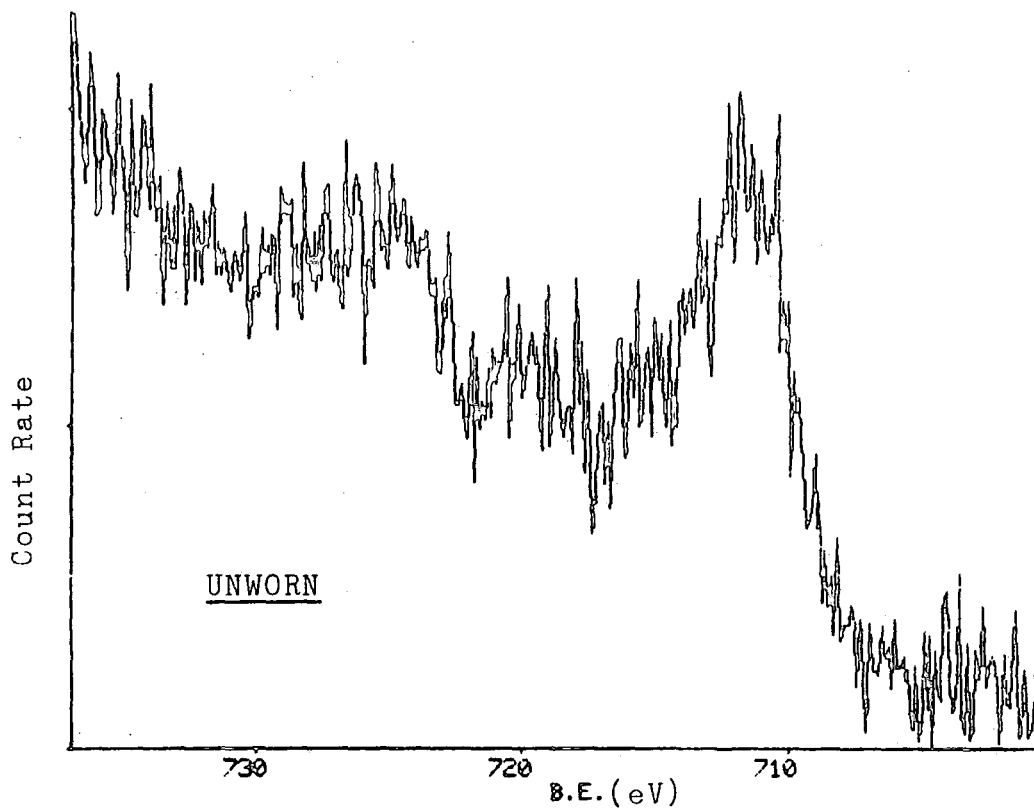


Figure 5.45 Iron Spectra of Unworn and Worn Plate Specimen

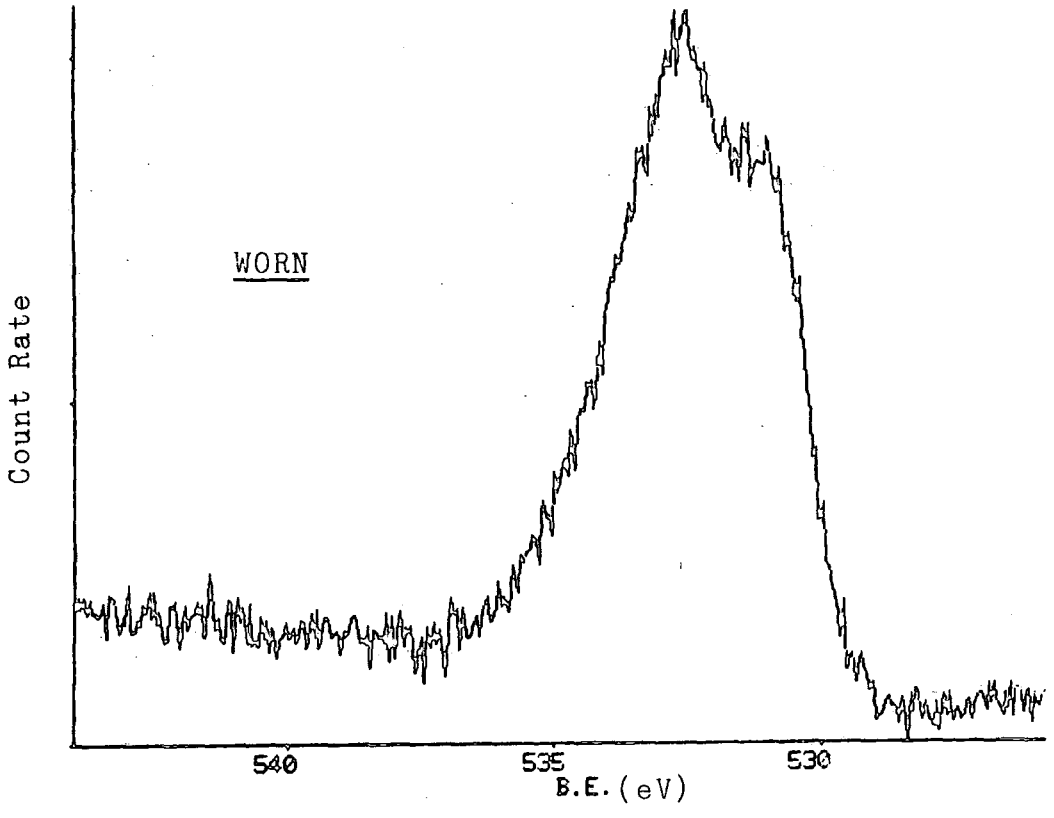
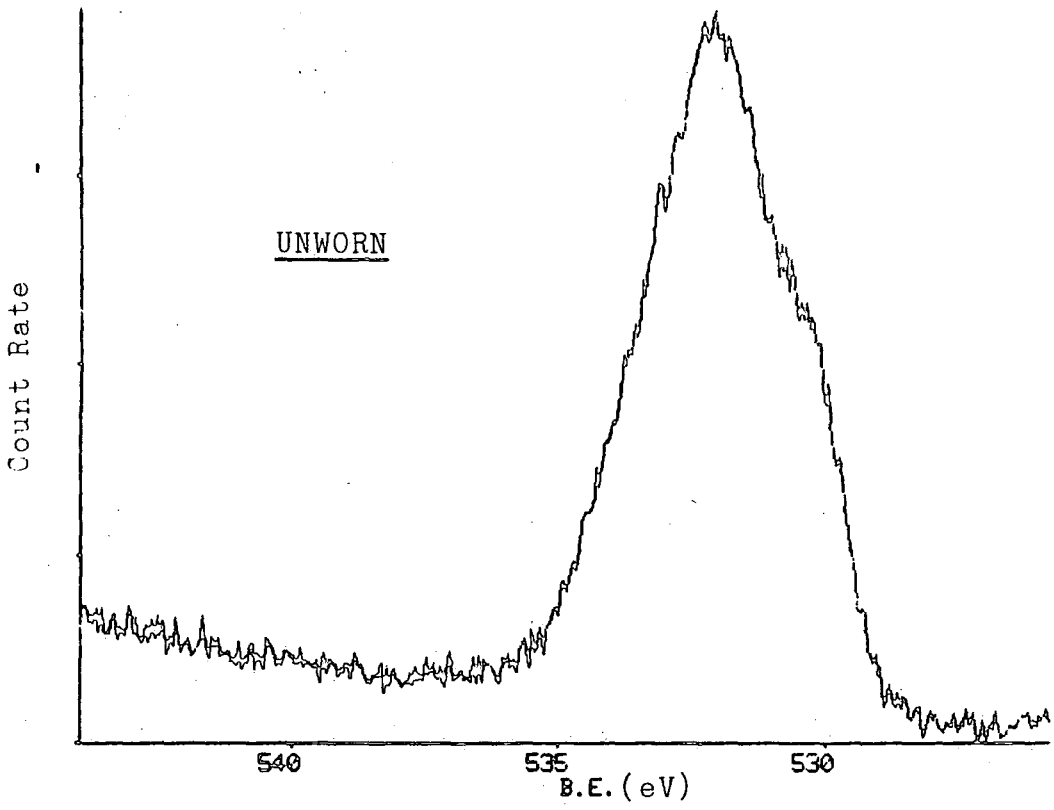


Figure 5.46 Oxygen Spectra of Unworn and Worn Plate Specimen

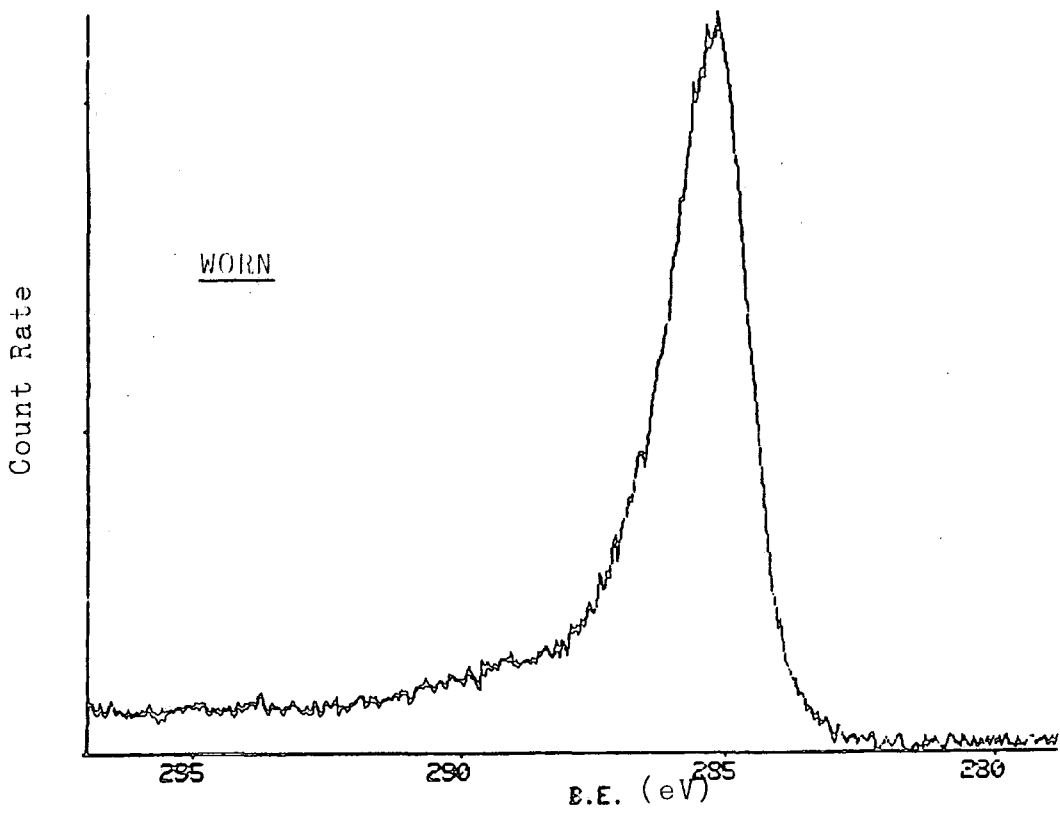
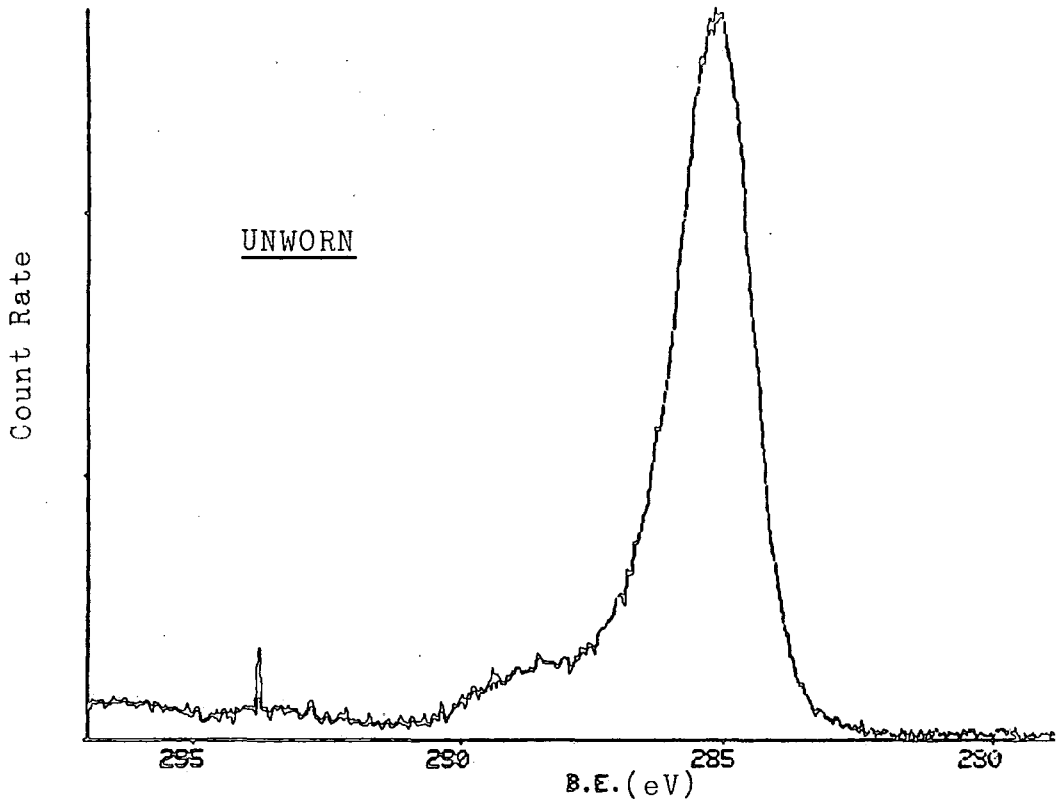


Figure 5.47 Carbon Spectra of Unworn and Worn Plate Specimen

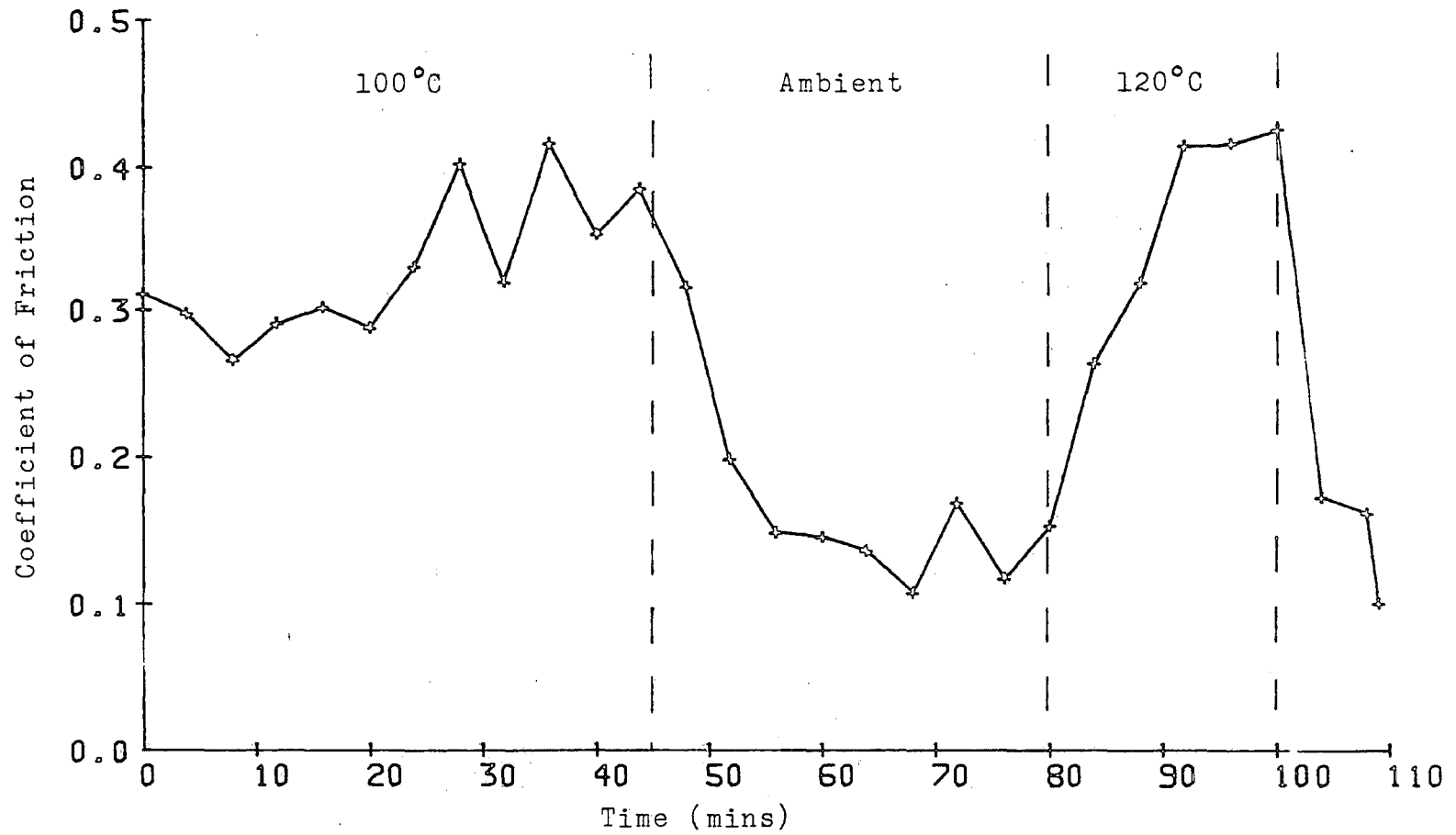


Figure 5.48 Heated Pin Experiment (Lubricated)

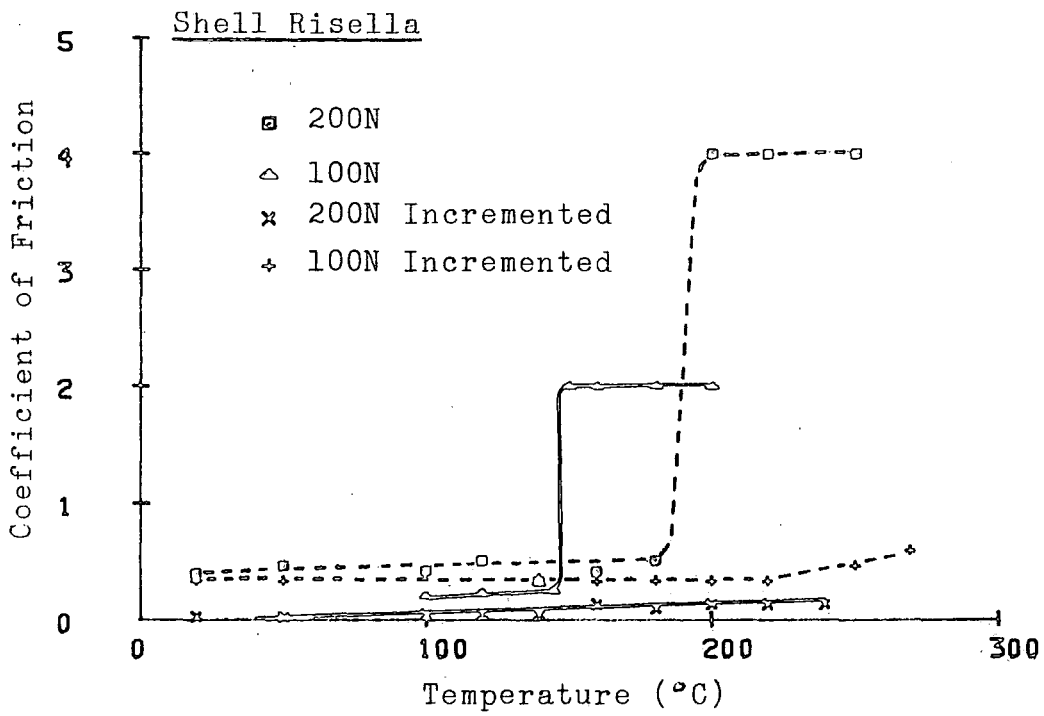


Figure 5.49 Coefficient of Friction - Temperature (Risella)

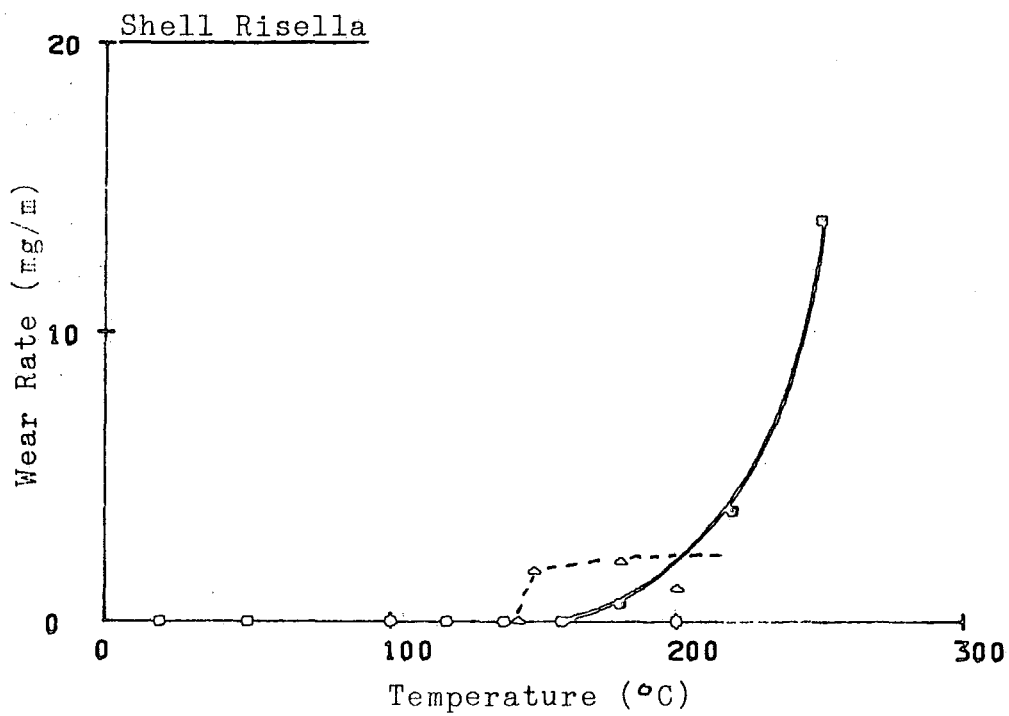


Figure 5.50 Wear Rate -Temperature (Risella)

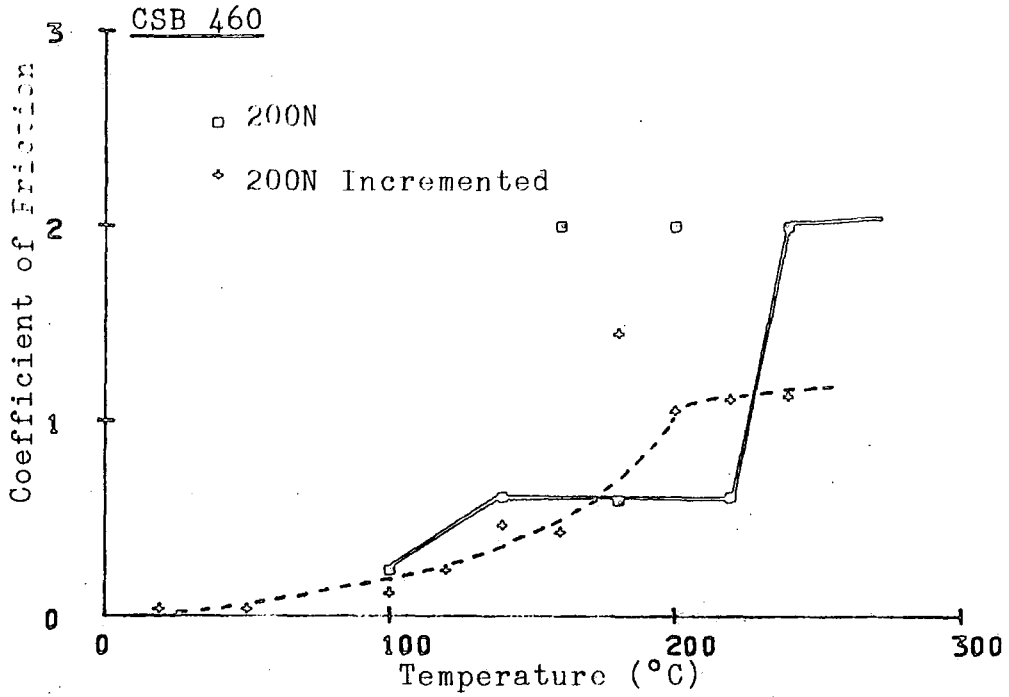


Figure 5.51 Coefficient of Friction - Temperature (CSB 460)

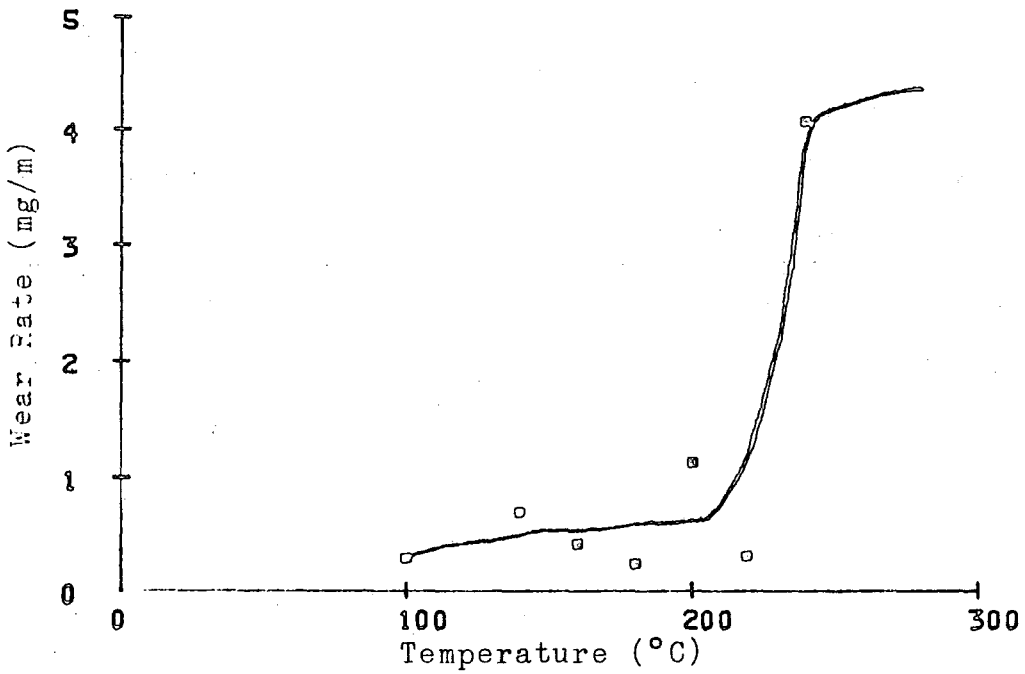


Figure 5.52 Wear Rate - Temperature (CSB 460)

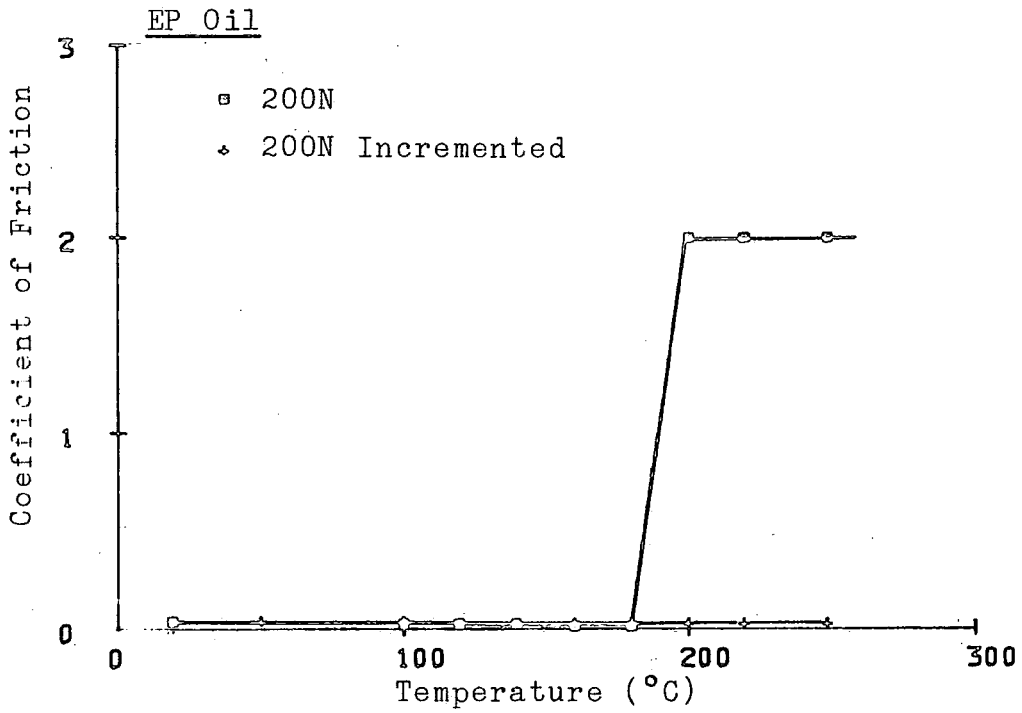


Figure 5.53 Coefficient of Friction - Temperature (EP Oil)

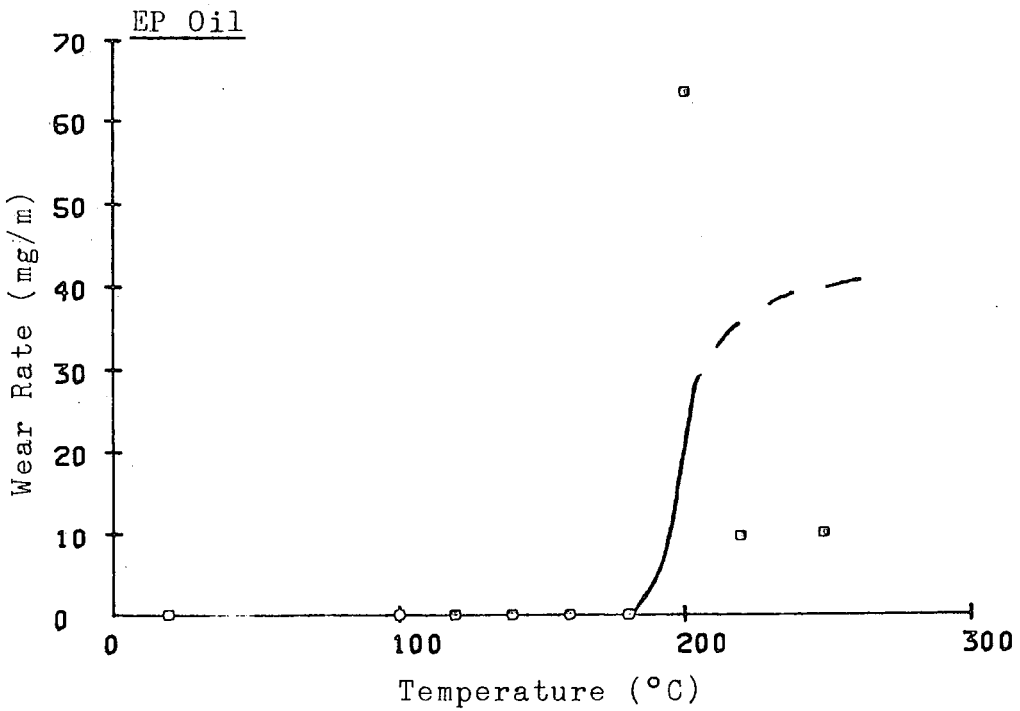


Figure 5.54 Wear Rate-Temperature (EP Oil)

CHAPTER 6

DISCUSSION

6.1 Errors of Measurement

6.1.1 Oxygen Analyser

The oxygen analyser was accurate to $\pm 0.1\%$. As well as measuring the oxygen content it was useful in monitoring the purity of non-oxidising gases, since the use of a mass spectrometer was found to be impractical. However, because of its low accuracy, a zero reading on the analyser could correspond to 0.1% (or 1000 vpm), thus a substantial amount of oxygen (eg. from air) could go undetected in the gas stream. A long period of purging could be expected to reduce this oxygen level but no accurate figures could be obtained to express it.

6.1.2 Dewpoint Hygrometer

The accuracy of the dewpoint hygrometer was approximately $\pm 0.2^\circ\text{C}$ and together with fluctuations which occurred throughout the tests, the actual dewpoint probably varied between $\pm 0.4^\circ\text{C}$ of the recorded average value. In terms of water vapour pressure this value corresponded to approximate variations of ± 0.5 mbar for a dewpoint of 20°C , and to ± 0.2 mbar for a dewpoint of 0°C .

The lowest recorded dewpoint was -35°C (200 vpm) but this was recorded after several hours of purging with dry gas and using metal gas lines. The normal 'dry'

level used in lubricated and unlubricated tests was approximately -25°C (600 vpm). For the heated plate or heated pin tests a low dewpoint was difficult to obtain; this was possibly due to the heating of the lubricant and hence the production of vapour. As the dewpoint was raised for outgassed oil (ie. a low water content) the rise was probably due to the oil vapour as well as any water vapour present in the oil.

6.1.3 Gas Purity

From the above it can be seen that the apparatus rarely operated with less than 600 vpm of water together with a possibility of a further undetected 1000 vpm of oxygen. This was despite using very pure gases with impurities of less than 20 vpm (see Appendix P). Even long periods of purging could not remove all the water vapour. This would seem to indicate that atmospheric water was getting into the apparatus as any residual water in the apparatus would be removed by prolonged purging. The possible cause of the high water content was the hygroscopic nature of the plastics in the gas lines. Replacing the plastic tubing with metal tubing decreased the water content, but not all the plastics could be replaced (eg. the mixing vessel and the rotameter). There was also a possibility of atmospheric air getting into the apparatus via the probe seals as the probe was reciprocated backwards and forwards, although the positive pressure in the environmental chamber should have kept this to a minimum.

For most experiments where water vapour of lubricants were deliberately introduced the gas impurities would have had little affect. However, for tests carried out in order to use E.S.C.A., the oxygen and water vapour present would have likely to have had a detrimental effect on the results (see later).

6.1.4 Measurement of Friction

The calibrations of the friction probe showed very good agreement between the first and last results despite two years of operation. This was also found for the friction measurement strain gauges on the heated plate apparatus. The major inaccuracies in reading the frictional forces came from using the analogue to digital (A-D) convertor. The A-D convertor worked by returning a number between 0 and 256 depending on the output voltage from the strain amplifier (see Chapters 3 and 4) where 123 corresponds to zero volts and 3 and 243 to -10 v and +10 v respectively (ie 12 units = 1 volt). The normal setting for the strain amplifiers was 100 $\mu\text{s}/\text{v}$ thus corresponding to an accuracy of $\pm 4 \mu\text{s}$ on the computed reading, which was $\pm 6 \text{ N}$ and $\pm 4 \text{ N}$ for No 1 Friction apparatus and the heated plate apparatus respectively. Although the accuracy of the strain amplifier could be increased to 10 $\mu\text{s}/\text{v}$ this was impractical in cases where the maximum friction level was likely to be high eg. if the strain rose above 100 μs (10 volts) this would be off the range of the A-D convertor (± 10 volts). Also the motor 'cut out' load was often set to a high value

(600 N) and could only offer protection if the A-D convertor was operating in a range capable of measuring the cut out load (ie. 100 $\mu\text{s/v}$).

In cases of low friction the most sensitive results were obtained from the X-Y plotter which could amplify the strain output to give a sensitivity of $\pm 0.5 \mu\text{s}$. Thus these results were used in preference to the computed results particularly in the 50 and 100 N load cases where the coefficient of friction was below 1.0. The resolution of these results was typically better than $\pm 0.5 \text{ N}$ for both sets of apparatus. However as the friction became higher (greater than 100 N) the X-Y recorder became less sensitive to use as it became necessary to lower the amplification and the computed results were used instead.

6.1.5 Load Measurement

The load calibrations on the proving ring (Figure 5.2) showed a large variation with time. A difference of 40 μs (45%) was recorded at 500 N and 2.2 μs (25%) at 50 N. However the results used for piston calibrations always corresponded to the most up to date calibration of the proving ring. Therefore the piston calibrations were unlikely to be more than 5% out at 50 N and 10% at 500 N. In some cases the variation would be smaller as the piston calibration was carried out within twenty-four hours of the proving ring calibration.

On No 1 friction apparatus, No 1 loading pistons showed a large variation between calibrations of up to 20% at 500 N and 10% at 50 N. Although it must be stressed

that these large variations were probably due to seal or spacer changes. Indeed for No 2 loading pistons (where no changes took place) the variation was down to 2%. The heated plate apparatus had an even smaller variation of 0.5%.

6.1.6 Coefficient of Friction

When the possible errors in both the friction and load measurements are taken into account the error in the coefficient of friction for No 1 friction apparatus is approximately $\pm 6\%$ at 50 and 100 N loads with a larger error of $\pm 10\%$ at higher loads (500+N). For the heated plate apparatus the errors are smaller, approximately $\pm 1\%$ at 200 N load (at which the majority of the tests were carried out).

6.1.7 Temperature Measurement (Heated Plate Apparatus)

The digital thermometers used had an error of $\pm 1^\circ\text{C}$ and as the temperature could only be maintained to $\pm 2^\circ\text{C}$ of the test temperature the actual plate temperature was likely to have varied between $\pm 3^\circ\text{C}$ of the test temperature.

6.2 Effect of Surface Finish and Hardness

The coefficient of friction for the hardness and surface tests varied between 0.95 and 0.45 with peak readings at the mid-range hardness (240 MN/m^2) and the mid-range surface finish (1.1 microns R_a). However the most likely cause of this large variation in friction was the variation in atmospheric humidity. Most of the tests on specimens of varying surface finish and hardness (see Section 5.2.3) were carried out on different days and the atmospheric humidity was not recorded. Fortunately for the weeks in which these tests took place a university energy survey was being carried out, which included the measurement of atmospheric humidity (using wet and dry bulb thermometers) for the engineering laboratories. From the results of this survey it was found that the water vapour pressure varied between 7.05 and 12.2 mbar for the test period. The coefficients of friction for a similar range of vapour pressures are shown to be between 1.5 and 0.6 (see Figure 5.40). Thus considering the range of water vapour pressure for the test period, the coefficients of friction could be expected to show a large variation. Indeed, from these results and those shown in Figures 5.40 and 5.41 (vapour pressure to μ and wear rate for air) the atmospheric humidity is a very important consideration when conducting friction or wear tests with cast iron.

The tendency of the mid-range hardness and surface finish to show the highest friction and wear is thought to be purely coincidental.

6.3 Effect of Oxygen Content

From Campbell and Summit (1936), as the thickness of a boundary film increases the coefficient of friction decreases (see Figure 2.5). An estimate of film thickness may be found from formulae derived by Quinn (1969), if we assume that the surface film produced is an oxide (Fe_2O_3).

The oxidation process may be linearly or parabolically dependent upon time:

$$\rho_{af} = A_n e^{-Q_n/R\theta_c} \times t \quad (\text{linear}) \quad 6.1$$

$$\rho_{af} = A_p^{\frac{1}{2}} e^{-Q_p/2R\theta_c} \times t^{\frac{1}{2}} \quad (\text{parabolic}) \quad 6.2$$

If the coefficient of friction (μ) is dependent upon the film thickness then μ would remain constant for a constant film thickness. The film thickness will remain constant provided that the rate of film removal (ie. wear rate) does not exceed the rate of film formation.

$$\text{ie. } w = \rho_{af} \text{ for constant } \mu \quad 6.3$$

Note: wear rate w is in Kg/s

The real area of contact (a) is dependent on the applied load (L) and the hardness of the material (p_m).

$$a = \frac{L}{p_m} \quad (\text{Bowden and Tabor 1974})$$

so 6.3 becomes

$$w = \frac{L}{p_m} \rho_{af} \quad 6.4$$

and 6.1 and 6.2 become

$$\frac{L}{p_m} \rho_{af} = A_n e^{-Q_n/R\theta_c} \times t \quad 6.5$$

$$\frac{L}{P_m} \rho f = A \rho^{\frac{1}{2}} e^{-Q_p/2R\theta_c} \times t^{\frac{1}{2}} \quad 6.6$$

From the above equations, the likely effect of speed, load and gas flowrate can be evaluated. If the speed is increased for a reciprocating system, t (the average time between passes) becomes smaller.

$$\text{ie. } t = \frac{\text{stroke length}}{u} \quad 6.7$$

and the thickness ($f \times t$) is reduced (all other factors being constant) and so μ would increase. Similarly, increasing the load, L , would also reduce the thickness and so increase μ . With regards to gas flowrate, sufficient oxidising gas must be provided in order that oxidation can take place. In the case of Fe_2O_3 oxygen forms 30% (by mass) of the oxide, therefore

$$m_g \geq 0.3 w$$

Although this is a simplistic analysis of the oxidation chemistry, it is likely that the oxidising gas flowrate must be above a certain level, proportional to the wear rate, in order to keep the film thickness constant.

$$\text{ie. } m_g = Kw$$

$$\text{or } \frac{m_g}{K} = \frac{L}{P_m} \rho f \quad (\text{for constant film thickness}) \quad 6.8$$

Thus the effect of reducing the flowrate of the oxidising gas would be to reduce the film thickness and so increase the coefficient of friction, μ .

To summarise the above hypothesis, it can be said that for a given flowrate of oxidising gas, increasing the

speed or load will increase the coefficient of friction. Increasing the total gas flowrate (but keeping the oxidising gas flowrate the same) should have no effect on friction, neither should changing the gas from air to oxygen, if oxygen is accepted as the main reactive constituent of air.

Note: It is important to differentiate between the oxidising gas flowrate and the total gas flowrate. The total gas flowrate is the flowrate of all the gas passing. The oxidising gas flowrate is the flowrate of the oxidising portion of the total gas flowrate (eg. oxygen only).

Some of the experimental results in Section 5.3 support the hypothesis, but some do not behave as might be predicted. In all the tests the coefficient of friction decreased as the oxidising gas flowrate (ie. oxygen flowrate) increased and an increase in speed increased the coefficient of friction for similar oxygen flowrates. However increasing the load gave little or no increase in the coefficient of friction and similar oxygen flowrates gave higher coefficients of friction for higher total gas flows (Figure 5.18). When air and oxygen are compared, agreement was found at low oxygen flowrates, but at high oxygen flows the argon/oxygen mixture gave higher coefficients of friction (0.8 cf 0.6), the difference being greater than the predicted experimental error (6%, see Section 6.1.6).

If a 'rough and ready' analysis is done, it can be shown that an oxygen flowrate of 0.1 mg/min is sufficient

to produce an oxide film of 100 Å (see Appendix Q), four times greater than the oxide film on a steel surface after polishing (Samuel 1956) and a comparatively thick film by boundary lubrication standards. If one looks closer at the oxygen and air comparisons (Figures 5.22 and 5.23) for a friction and wear mechanism based on oxide films, similar oxygen flows should give similar coefficients of friction, but as stated above, different coefficients of friction were found. The explanation may be in the nature of the gases used, eg. nitrogen (from air) is normally considered to be inert but nitrides can be formed although the temperatures may have been too low. However the most likely cause of the deviation from the oxide theory is the water content of the ambient air used in the air/argon mixtures. The water vapour pressure of the ambient air was known to vary between 7.05 and 12.2 mbar. This vapour is likely to have had a beneficial effect in reducing friction for the argon/air mixtures. The effect of water vapour pressure on friction in air is shown in Figure 5.40.

For the comparison purposes the water vapour pressures for the air/argon mixtures at 100 N load, 10 mm/s were estimated using an ambient air humidity of 33% R.H., the average for the test period. The results are shown in Table 3, Appendix M, and a plot of water vapour pressure to coefficient of friction is shown in Figure 6.1 together with the results of humidity tests in air only and in argon only. It can be seen from Figure 6.1 that the argon/air mixtures gave lower coefficients of friction than the air only tests for sim-

ilar water vapour pressures despite having lower concentrations of oxygen. In fact, it was only when the oxygen concentration got below 2.7% (by volume) that the argon/air mixtures gave higher coefficients of friction (the two points on the argon/air curve with the lowest water vapour pressures).

From the above discussion it is apparent that the water vapour pressure plays a much more important role in the unlubricated rubbing of cast iron against cast iron than the oxygen concentration or the oxygen flowrate. As water vapour pressure increased with increasing oxygen content (ie. air content), this could explain the reduction in friction with increasing oxygen flowrate, since the oxygen flowrate was adjusted by keeping the total gas flow constant and increasing the percentage by volume of air in the gas. However, the effect of the oxide film cannot be dismissed completely because in argon/oxygen mixtures, only dry gases were used but the friction was still reduced as the oxygen content increased.

6.4 Effect of Water Content

The effect of water vapour pressure on friction was very much dependent upon the nature of the gas environment. In inert and reducing gases (eg. argon, nitrogen and hydrogen) there was a definite transition from high friction to low friction (see Figure 6.2). The transition pressure was similar (within experimental errors) for argon and nitrogen (≈ 21 mbar at 100 N load) but lower for the lighter and more reducing hydrogen (18 mbar). The maximum value of coefficient of friction recorded for the above three gases went in ascending order of molecular weights. Hydrogen was the lowest at $\mu = 3.0$, followed by nitrogen with $\mu = 3.6$ and finally argon at $\mu = 5.5$. The sample of three gases was probably too small however, to predict the values for other inert or reducing gases by molecular weights.

When the gas was oxidising or a mixture containing an oxidising gas (eg. oxygen or carbon dioxide) the transition from high to low friction was less dramatic. The maximum coefficients of friction were much lower than the three inert and reducing gases. As above, oxygen and carbon dioxide (ie the single gas types) showed a similar relationship in that the heavier carbon dioxide had a higher maximum coefficient of friction than oxygen. The two gas mixtures, air (21% oxygen, 79% nitrogen) and mixed gas (83% nitrogen, 12% carbon dioxide, 5% carbon monoxide), gave results which lay between the results of their major constituents. At low vapour pressures air gave higher coefficients of friction and

higher wear rates (Figures 5.41 and 5.43) than oxygen but lower than nitrogen. With higher vapour pressures air gave lower coefficients of friction than oxygen. These were similar to the results of 'wet nitrogen' but at lower vapour pressures. The mixed gas compared in a similar manner to nitrogen and carbon dioxide, the effect of carbon monoxide being unknown. From Figure 6.1, when the behaviour of argon/air mixtures are compared with air and argon, the results are different from the above in that the argon/air mixtures gave lower coefficients of friction than air or argon for most of the vapour range.

6.4.1 The Detrimental Effect of Oxygen

One interesting aspect of the comparisons shown in Figure 6.2 is that at high water vapour pressures (12+ mbar) oxygen gave higher coefficients of friction than other gases (0.9 cf 0.6). In a similar manner, the wear rates were higher for oxygen than for air (≈ 0.5 mg/m cf ≈ 0.2 mg/m) at high vapour pressures. It appears therefore that a high concentration of oxygen (in this case 100%) is not helpful in reducing friction at high water vapour pressures. A possible cause of this effect is that the high concentration of oxygen forms iron oxides which interfere with the setting up of a continuous graphite film. Such an effect was found by Lancaster (1962) when he found that a surface film of cuprous oxide prevented the transfer of graphite from an electographic brush to a copper disk. Another insight into the detrimental effect of oxygen can be found in the previous section

(6.3) where it was mentioned that when the oxygen content was reduced by the presence of argon, air/argon mixtures gave lower friction and wear values for corresponding vapour pressures than pure air.

It must be pointed out however that at low vapour pressures (less than 5 mbar) oxygen gave low coefficients of friction and low wear rates compared with other gases.

6.4.2 Water Flow Vs Vapour Pressure

From the experimental results outlined in Section 5.4.3 it appears that it is not important to exceed a certain water vapour flowrate to prevent scuffing, but a certain water vapour pressure (or relative humidity). If the water vapour was acting as a reactive medium in order to produce surface films then a similar analysis to to the one done in Section 6.3 would apply, and increasing the vapour flow should decrease the friction. However, the evidence suggests that the vapour was acting as a lubricant, and in common with the actions of other lubricants, only a small quantity is required. It is possible that a small water vapour flowrate (at the correct vapour pressure) is necessary, but none of these experiments were able to prove this.

These results give further confirmation that in the unlubricated rubbing of cast iron against cast iron it is the production of a graphite film that is important in successful low friction rubbing and the production of a chemical reaction type film is not necessary.

6.4.3 Effect of Load on Transition Vapour Pressure

The vapour pressure at which the transition from high friction to low friction takes place in inert or reducing gases is dependent upon load (Figure 5.31).

The transition pressure gets higher with increased load.

Lancaster and Pritchard (1981) concluded that the load, speed and ambient temperature are only important in that they influence the attainment of a critical contact temperature at which transition takes place. The suggested mechanism of vapour lubrication of graphite is that vapour is physically adsorbed in to basal planes (see Section 2.5), and the adsorption depends on a certain critical concentration of vapour (Cannon 1964). Lancaster and Pritchard (1981) suggested that the critical concentration is dependent upon the ratio of P_L/P_0 where P_L is the vapour pressure for effective lubrication and P_0 the saturation pressure of the vapour at the critical contact temperature. Thus Lancaster and Pritchard, in common with Savage and Scheaffer (1956), suggest that the ratio P_L/P_0 depends only upon the type of vapour, and a single value is valid for all the conditions of load, speed and ambient temperature, for that particular vapour.

An analysis was done of the load to vapour pressure results plotted in Figure 5.31, in which the relevant contact temperatures were calculated using Archard (1958) (see Appendix R). Then the saturation pressures for the contact temperatures were found and the ratios of P_L/P_0 (or P_L/P_s for water vapour) evaluated (see Table 19).

The results are plotted in Figure 6.3 where it can be seen

that unlike Lancaster and Pritchard the transition ratio P_L/P_0 varies considerably with load and is roughly proportional to $1/\sqrt{\text{Load}}$.

If we make the assumption that

$$\frac{P_L}{P_S} = K \times \frac{1}{\sqrt{\text{Load}}} \quad 6.9$$

then by using the results in Table 19, K can be given a value of 0.171 (evaluated by finding the average value for the results in Table 19) and equation 6.9 becomes

$$\frac{P_L}{P_S} = 0.171 \frac{1}{\sqrt{L}} \quad 6.10$$

Values of K for other gases can also be evaluated using the transition water vapour pressures for nitrogen, $K = 0.205$, for hydrogen, $K = 0.178$ and for mixed gas, $K = 0.149$. However, because only two values of transition vapour pressure were used these values can only be approximate.

There are however, some major differences between this work and that of Lancaster and Pritchard. The speeds used in this work were much lower (10 mm/s cf 30 to 3000 mm/s) and the motion was reciprocating, ie. speed varied between 0 and 15.2 mm/s whereas Lancaster and Pritchard used continuous speeds. The overriding evidence from these tests however is that the ratio P_L/P_0 is dependent upon $1/\sqrt{\text{Load}}$ and does not remain constant over a range of loads.

The dependence of the transition from high to low friction on a critical contact temperature may go some

way towards explaining the phenomenon of one sided scuff. One side of the plate may be at a slightly higher ambient temperature than the other. More likely though a slight surface deformation on one side acts to raise the friction high enough to increase the contact temperature above the critical one and hence scuffing (and high friction) commences.

6.5 E.S.C.A.

The E.S.C.A. results given in Section 5.5 show very little difference between an unworn specimen and a severely scuffed specimen. The iron oxide present could be identified as Fe_2O_3 (see Figure T.2, Appendix T) and was present for both worn and unworn spectra.

As previously discussed (Section 6.1.3) even in pure dry gases there was a possibility of large amounts of impurities being present. Up to 1000 vpm of oxygen could go undetected in the gas stream which would be capable of producing an oxide film 890 Å thick in one second (see Appendix Q). Water vapour was also present in the gas stream (up to 600 vpm) and this would also react to produce a surface film. The surface films produced, although sufficient to completely cover the plate surface, did not prevent scuffing as in dry argon the coefficient of friction rose to approximately 5.5.

There were some problems in using E.S.C.A. which may have prevented the production of a spectrum of the 'true' surface. Once scuffing had taken place a large amount of loose wear debris was left on the plate surface, which was likely to include iron oxide and graphite. This proved difficult to remove and not all the debris could be removed with certainty. Although this debris may have played an important role in the scuffing process (eg. abrasive wear) it may have also included particles from the original unworn surface. Another problem lay in the use of the spectrometer itself. There was no provision, optically or otherwise, for predicting the exact section of

the specimen being sampled and some spectra may have included unworn parts of the specimen. Steps were taken to avoid this, by using T-shaped plates (see Section 3.1.2) and taking spectra of different parts of the plate (by moving the probe further in or out of the chamber). Finally it must be pointed out that it was possible that atmospheric air leaked into the isolated section (see Section 4.3.7) via the seals or the ball valve and so contaminated the plate surface.

From the high coefficients of friction recorded one might have expected metal-metal contact (as opposed to oxide-oxide) and a great deal of pure iron showing on the spectra after the oxide film had been completely worn away. However this was not the case; oxide showed in all the spectra. Unfortunately E.S.C.A. could not be used to determine the origin of the oxide, as to whether it was caused by impurities in the gas stream, leaks in the system or wear debris. E.S.C.A. is perhaps best used in detecting chemical reactions that have only one possible cause eg. sulphide films produced by EP additives.

To some extent E.S.C.A. is not a useful tool in the study of tribology. Loose wear particles must be removed in case they damage the ultra-high vacuum pumps. Specimens that have been lubricated must be thoroughly cleaned and degreased before entry into the X-ray chamber, and so in many cases, removing the surface film which was the object of study. Also E.S.C.A. is only done on the material surface and reactions with the atmosphere or other contaminants can easily obscure the surface under study.

6.6 Lubricated Tests

6.6.1 No 1 Friction Apparatus

At ambient temperatures scuffing only occurred when the lubricant supply failed and even then at low loads there was a considerable time delay between the stopping of the lubricant supply and failure, eg. thirty hours at 100 N for CSB 460 and seven hours at 100 N for Risella. In all cases the coefficient of friction was low, although not as low as those recorded by N.C.T. at Risley (1971-3) (ie. 0.2-0.1 cf 0.06-0.03) although with the high speeds used at Risley hydro-dynamic lubrication was a definite possibility.

Another aspect of the lubricated tests was that for most cases where there was an oil flow a wear rate was recorded, but in cases where there was no oil flow (see Table 5.5) no wear rate was recorded. The most likely explanation of this comes from the appearance of the used oil. In all cases when used with cast iron the oil became black, indicating that some wear products (possibly graphite and iron oxide) had been washed away by the oil. So whilst the oil was washing away the surface films it became necessary to renew them, hence a wear rate was recorded. This washing away of the surface films could also be the cause of the much higher friction recorded by the heated pin tests (≈ 0.3 for 100°C at 100 N) compared with the heated plate test (≈ 0.1 for 100°C at 200 N) where no oil flow was taking place. If the film was washed away before it could become fully

established it would not offer as much protection and temperature had a definite affect on scuffing (see later).

The most important findings of these tests were that, despite loads which were equivalent to a 2400 bar compressor (see Appendix S) and gas environments too dry to support unlubricated rubbing, when oil was definitely present on the plate surface no scuffing occurred and this applied for both the Risella and CSB 460 oils.

6.6.2 Heated Plate Apparatus

Unlike the previous experiments carried out in the No 1 friction rig, scuffing did occur in the heated plate rig when lubricant was present on the plate, but the temperature at which the transition occurred depended upon the type of oil. Unfortunately, as in the previous tests, some specimens appeared to scuff due to oil starvation rather than any type of film breakdown. In cases where the test lasted for more than fifteen minutes before failing and where subsequent hotter tests with the same oil did not give failure, failure was assumed to be due to starvation, unless there were definite signs of lubricant present on the plate surface. This starvation was likely to have come about for one of two reasons. First, the high temperatures would cause a high ratio of evaporation of the oil, and the gas flow would remove the oil vapour leading to the eventual removal of all the oil. Second, the two piece oil bath (see Figure 3.12) had a tendency to leak when the oil viscosity was lowered (ie. due to high temperatures) although it was attempted to

stop this by wrapping ptfе tape around the oil bath.

If the contact temperature is calculated (Archard 1958) for 100 N and 200 N loads, the difference between the two (34°C) is similar to the difference between the two transition temperatures for Risella oil (150°C for 200 N and 180°C for 100N), thus indicating that transition takes place at the same total temperature (ie. the sum of the surface temperature and the contact temperature) similar to Bailey and Cameron (1973). With the two other oils, it was surprising that the EP oil failed at lower temperatures than the mineral oil, CSB 460, despite its extreme pressure additives (180°C cf 240°C). The results of the EP oil did not agree with the results found by Marshall (1983) who gave a transition temperature of around 200°C. Some guesswork however had to be employed in estimating the loads used by Marshall (as the applied load was not documented) and the gas flow-rate (which may have had a cooling effect) was also unknown.

The total transition temperatures of the oils used (ie. the sum of the contact temperature and the transition surface temperature) were for Risella oil, 280°C, for CSB 460. 360°C and for the EP oil 320°C. Thus on No 1 friction apparatus even loads of 3000 N were insufficient to give a total temperature exceeding the transition temperature of Shell Risella (3000 N gave a total temperature of 166°C), although the oil flow would have played an important part in reducing the temperature.

One of the most significant aspects of these tests is the way in which the subsequent failure depends upon the method used to reach the required temperature. If the temperature is incremented in steps whilst sliding is taking place, the transition temperatures are less obvious. In fact, in the case of the Risella and EP oil these are non-existent (see Figures 5.49 and 5.53). This method can also enable the transition temperature to be exceeded without scuff taking place. One explanation of this phenomenon is that a surface film is formed at low temperatures (possibly graphite) and once formed is not destroyed at higher temperatures and carries on protecting the surface. However the film cannot be formed above a certain temperature, possibly due to other surface interactions taking place. Sugishita and Fujiyoshi (1981) found a similar phenomenon in that seizure occurred at lower temperatures when a graphite film had not been preformed than when it was preformed (see Section 2.4 and Figure 2.11).

The failures recorded on cooling (see Table 1 and 3, Appendix N) may have been due to thermal distortions (caused by rapid cooling), increasing the friction, and hence the contact temperature. No cooling failures were recorded when slow cooling was used and most tests cooled down to ambient temperature without mishap.

6.7 Reciprocating Gas Compressors

It is perhaps worth looking at the effect of the previous discussion on the lubrication of reciprocating gas compressors.

If the nature of the gas environment being compressed is such that unlubricated rubbing may take place without scuff occurring (eg. high water content), then it is unlikely that piston ring failure will occur. Using the results plotted in Figure 6.3 a similar graph for compressor discharge pressures is shown in Figure 6.4 (for argon). The pressures were calculated by dividing the load by the apparent surface area of the pin and from Appendix S this pressure would be equivalent to the discharge pressure. As argon was proved to require the highest water vapour pressures to prevent scuff (see Figure 6.2), operating within the non scuff region shown by Figure 6.4 should prove satisfactory for other gases. Unfortunately because only ambient temperatures were used (20°C), higher water vapour pressures than 21 mbar could not be obtained and the graph only reached a discharge pressure of 160 bar. The prevention of scuffing could be expected at higher pressures provided higher water vapour pressures are obtained eg. by higher gas temperatures. The graph could be extrapolated by using the formula shown in equation 6.11:

$$\frac{P_L}{P_S} = K \frac{1}{\sqrt{P_1}} \quad 6.11$$

By using the values of load and minimum lubricating ratio (P_L / P_S) shown in Table 19, Appendix M, K can be

given a value of 0.15 (ie. the average of the results).

Equation 6.11 becomes:

$$\frac{P_L}{P_S} = 0.15 \frac{1}{\sqrt{P_1}} \quad 6.12$$

where P_1 is in bar.

As an example of this formula at work, a 1000 bar compressor would require a minimum lubricating ratio of 0.0047 and from the calculated contact temperature for such a pressure a water vapour pressure of 0.76 bar would be required. Considering that most compressors operate at a temperature of approximately 120°C this water vapour pressure would give a relative humidity of 38% which would not be acceptable because of its affect on gas purity.

However, if other vapours are used, lower minimum lubricating ratios could be expected. Savage (1955) found that the minimum lubricating ratio for n-Heptane was 7000 times smaller than that of water (Table 2.4). The use of other vapours would also mean that the vapour content of the gas would be reduced and so the gas would be more likely to be within acceptable levels of purity.

For many compressors, because of the level of gas purity required, adding vapours would not be feasible. In these cases lubricated rubbing is the only solution. From the experiments carried out in this project, three factors emerge as important in the lubricated rubbing of cast iron against cast iron in inert or reducing atmospheres. They are the oil transition temperature, oil starvation and the formation of surface films.

As discussed in Section 6.2.2 scuffing is likely to occur if the lubricant transition temperature is exceeded. The important factor however, is not the surface temperature, but the total temperature ie. the sum of the contact temperature and the surface temperature. For the oils used, the total transition temperatures were , for Risella 280°C, CSB 460 360°C and EP oil 320°C. So in compressor lubrication it is important that the sum of the cylinder wall temperature and the ring contact temperature does not exceed the lubricant transition temperature. If the oil with the lowest transition temperature is used as a guide then any compressor with a discharge pressure over 160 bar (equivalent to 200 N) would be in danger if its cylinder wall temperature was to exceed 150°C. Considering that many compressors operate with gas discharge temperatures of around 120°C, this does not leave a large margin for error.

If for any reason there is a lubricant supply failure in the compressor, the high gas flowrates are likely to remove the surface oil at the stroke extremities very quickly and metal to metal contact and hence scuffing is likely to occur. The time in which this takes place would be very short. In the heated plate apparatus the transition time from low friction to severe scuffing was under twenty seconds, which for 15 rpm was only five cycles. If such a transition was to occur in the same number of cycles for a compressor operating at 300 rpm then only one second would be required. Once scuffing is initiated the contact temperature would rise and

depending upon the gas environment (which would determine the maximum value of μ) the total temperature may rise above the oil transition temperature. If the oil transition temperature is exceeded it is unlikely that scuffing could be stopped, even if the oil supply is resumed. The effect of the friction coefficient on the contact temperature is perhaps one of the reasons why inert or reducing gas compressors are more prone to scuffing than oxidising gas compressors. For the air the maximum coefficient of friction recorded was 1.93 compared with 7.05 for argon. As the contact temperature is directly proportional to the coefficient of friction (Archard 1958) a temperature rise three and a half times greater would be recorded for an argon environment than an air environment. Hence in an argon environment a temperature above the oil transition temperature is more likely to be achieved for momentary lubricant supply failures.

In the heated plate experiments it was also found that the lubricant transition temperatures could be safely exceeded if the surface temperature was increased gradually as the apparatus was running. This stresses the importance of a gradual running in process for a compressor. If the graphite film is allowed to develop at low temperatures it will go on protecting the surfaces even at temperatures above oil transition temperature. Therefore for all compressor start ups it would be recommended to gradually increase the gas discharge temperature and pressure over a long time period.

If oxidising additives are used in the lubricant

(eg. benzoyl peroxide) they may serve to protect the surface for a period of unlubricated rubbing, but would be unlikely to completely stop wear and the friction coefficient would be similar for unlubricated rubbing in a dry oxygen environment ($\mu = 1.2$). The presence of such a reactive additive would also be likely to contaminate the process gas. From the results of this project, if a certain level of impurities in the process gas are acceptable, more protection can be offered from water vapour (or organic vapours) than any free oxygen which may be liberated from a solution of oil and benzoyl peroxide.

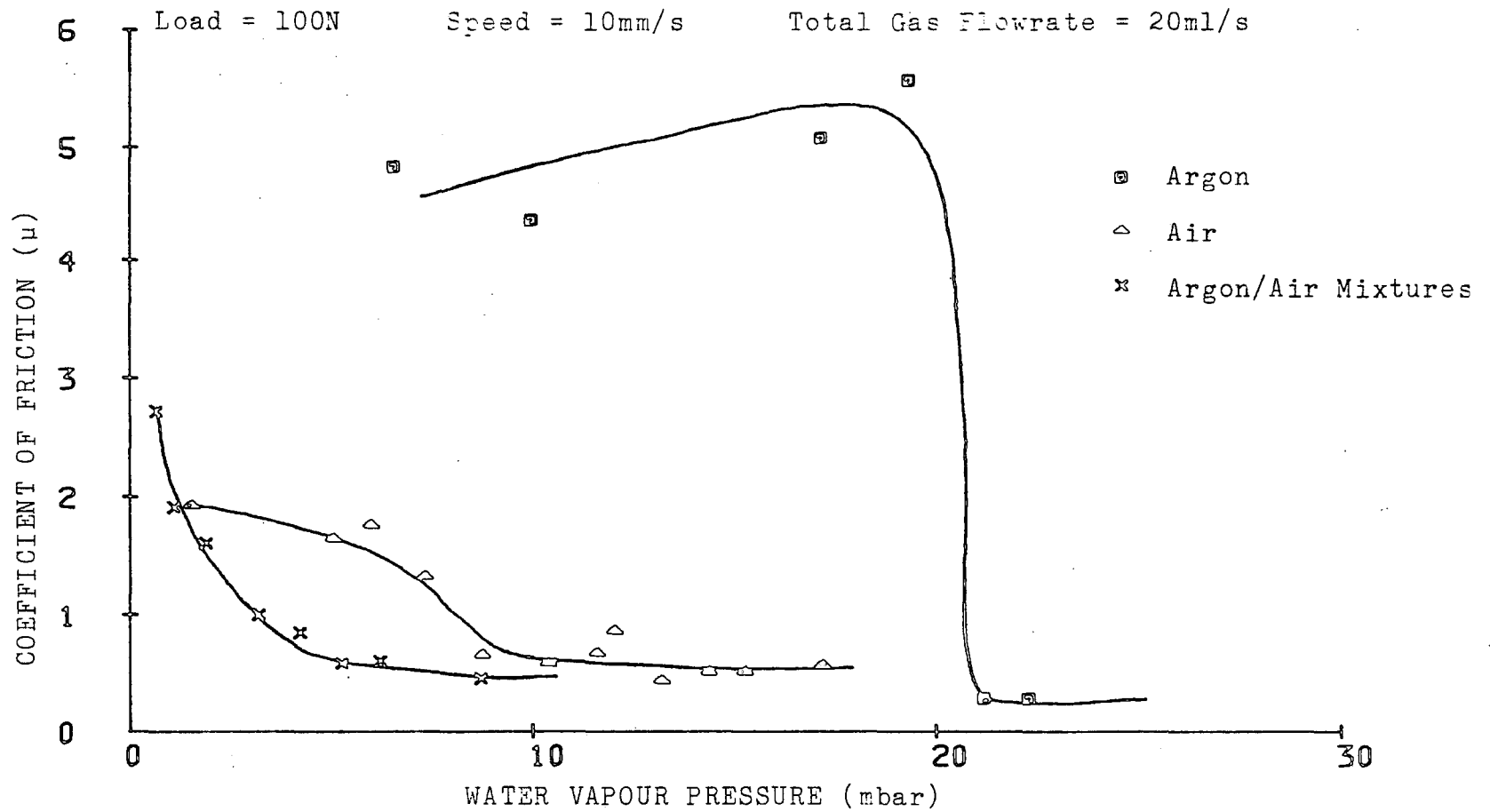


Figure 6.1 Comparison of Air, Argon and Argon/Air Mixtures

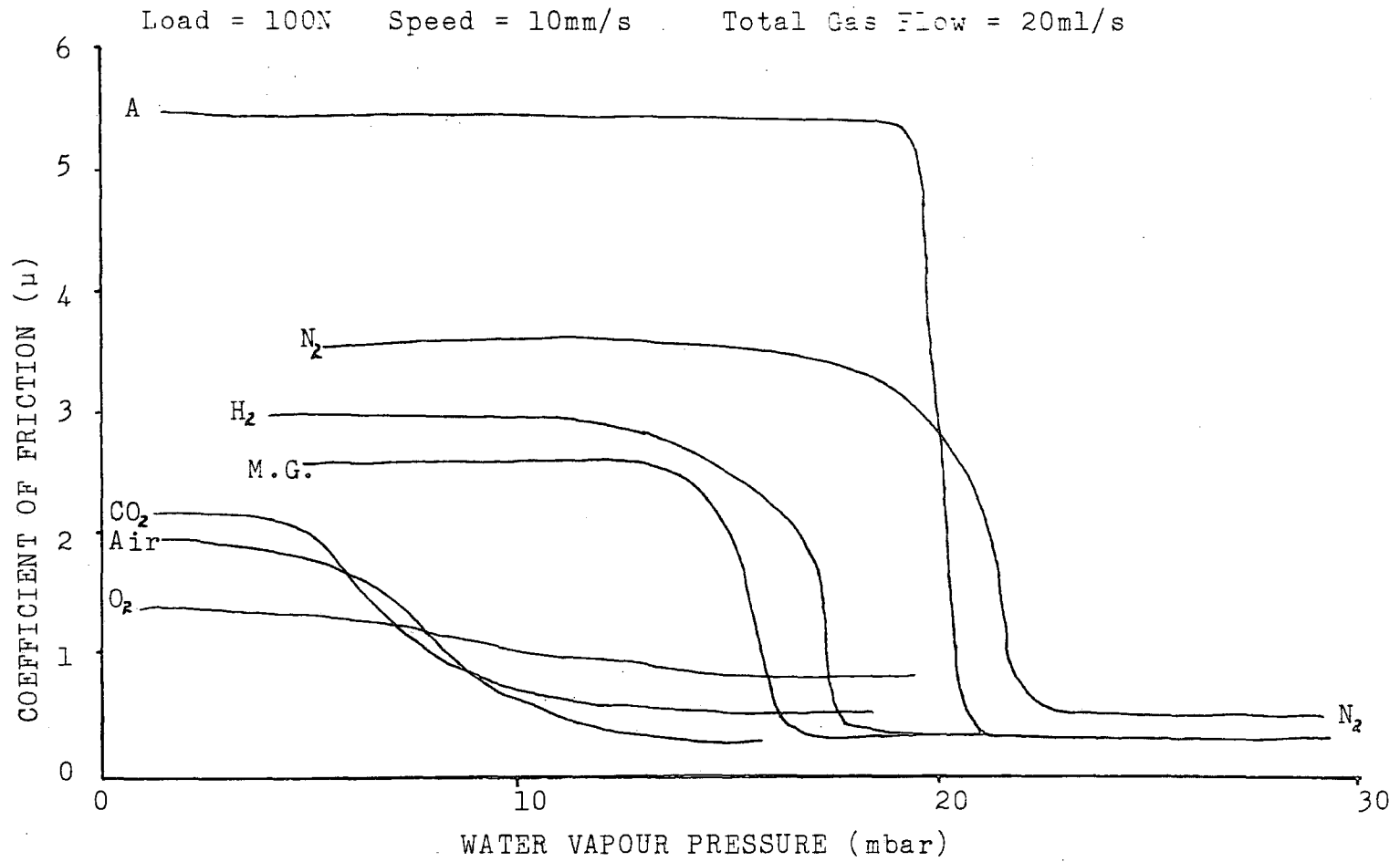


Figure 6.2 Water Vapour Pressure to Coefficient of Friction for Different Gases

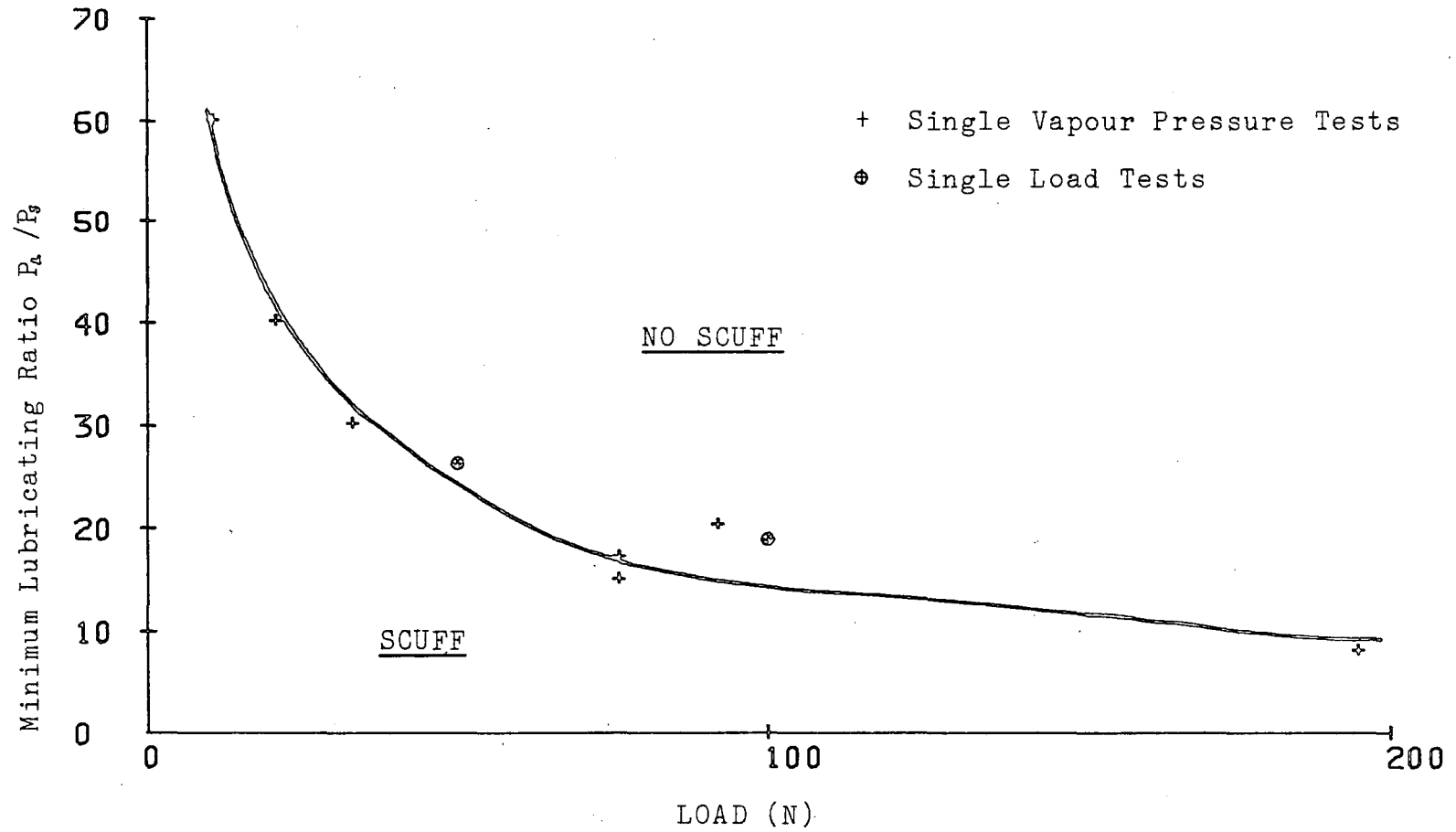


figure 6.3 Minimum Lubricating Ratio to Load

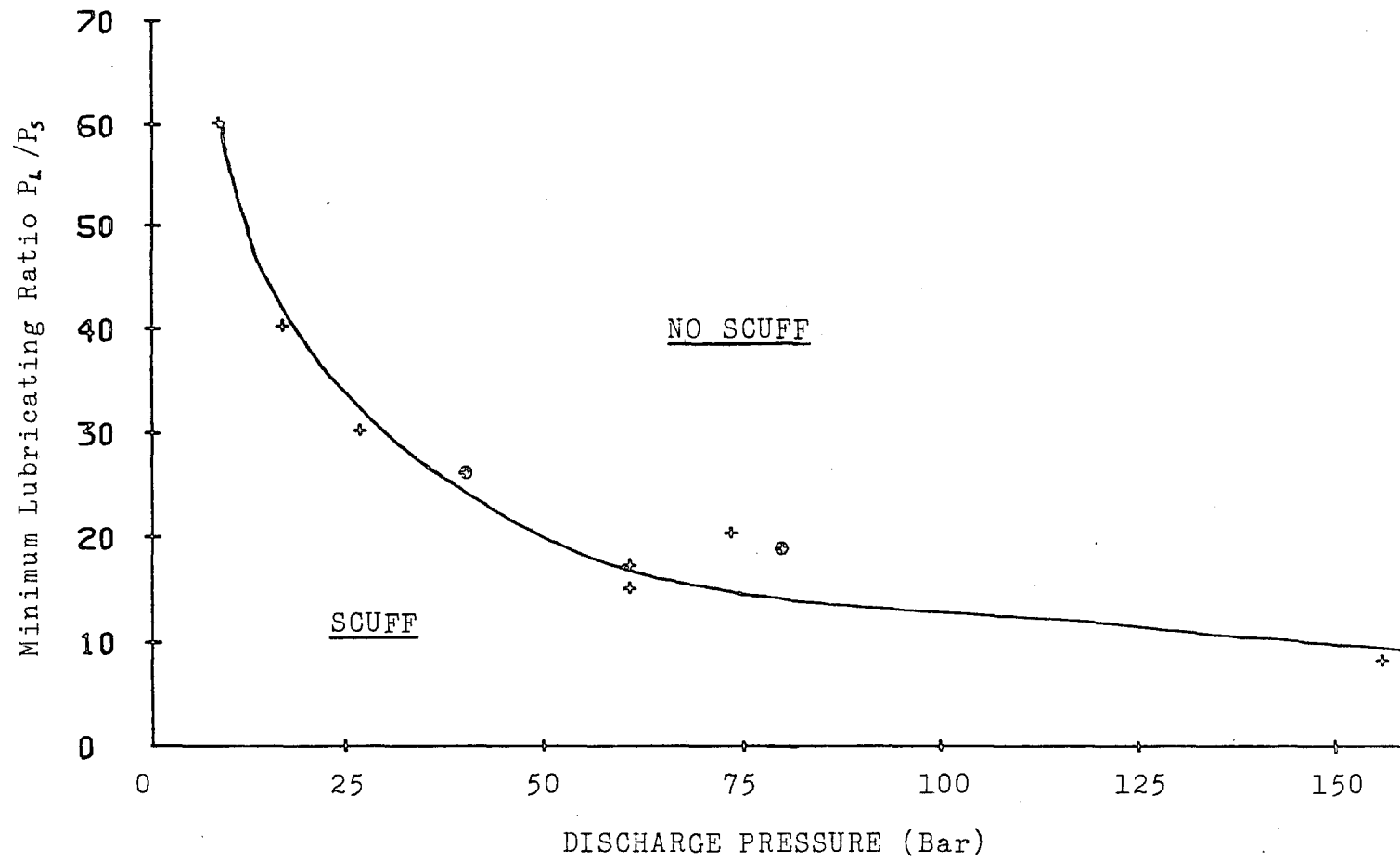


Figure 6.4 Minimum Lubricating Ratio to Discharge Pressure

CHAPTER 7

CONCLUSIONS AND SUGGESTIONS FOR FURTHER WORK

7.1 Conclusions

7.1.1 Unlubricated

The coefficient of friction and wear rate recorded for cast iron sliding on cast iron was found to be dependent on the environment in which sliding took place. The partial pressure of water vapour in the environment was also found to be very important while the water vapour flowrate was of little consequence.

In dry gas environments (ie low partial pressure of water vapour) the coefficient of friction and the wear rate were found to be at their highest. In inert and reducing gas environments they were very high and their maximum values were in ascending order of molecular weight. The maximum coefficients of friction for argon, nitrogen and hydrogen were 5.5, 3.6 and 3.0 respectively, and the wear rates were 45, 37 and 34 mg/m respectively, for 100 N loads at 10 mm/s sliding speed. For oxidising gases the coefficients of friction were much lower, but also varied in order of molecular weight. The coefficients of friction and wear rates for carbon dioxide, air and oxygen were 2.02 and 21.02 mg/m, 1.93 and 16.47 mg/m and 1.17 and 1.87 mg/m, for 100 N loads at 10 mm/s sliding speed.

As the partial pressure of water vapour was increased there was a transition from high friction and wear to low friction and wear ($\mu \approx 0.6$ and wear rate ≈ 0). For oxidising gases this transition was gradual over a

wide range of partial pressures, but for inert and reducing gases the transition was sudden and required only a small change in the partial pressure of water vapour to take place.

For inert and reducing gases the water vapour at which the transition took place was found to be load dependent and by using the formula

$$\frac{P_L}{P_S} = \frac{K}{\sqrt{L}}$$

the minimum partial pressure of water vapour for low friction (P_L) for a specific load (L) could be calculated (where P_S is the saturation vapour pressure for the total surface temperature; total surface temperature = contact temperature + surface temperature). The experimental results gave the values of K for argon, nitrogen and hydrogen as 0.171, 0.205 and 0.178 respectively.

7.1.2 Lubricated *

In order to prevent scuff occurring in inert gas environments for cast iron sliding on cast iron in the presence of an oil lubricant three factors were found to be important. They were the total surface temperature of the sliding surfaces (contact temperature plus the surface temperature), avoiding oil starvation and the preforming of surface films by a 'running in' procedure.

Lubricants were found to have a total transition temperature at which they became ineffective at preventing scuff. This transition temperature varied, depending

upon the oil used: for CSB 460 (a mineral oil) it was 360°C, for Shell Risella oil (a paraffin oil) it was 280°C and for an EP oil (to SAE 80) it was 340°C. Oil flow however could play an important part in keeping the temperature low, as it was found that high loads could be achieved without scuffing with an oil flow of 5 ml/hr.

One of the main causes of scuffing was found to be oil starvation (normally because the oil was removed in some way) and care had to be taken to avoid this.

It was also found that the transition temperatures could be safely exceeded if a surface film (probably graphite) was allowed to form by a procedure of gradually incrementing the specimen surface temperature, whilst running.

* The use of the term lubricated is not intended to imply hydro-dynamic or elasto-hydrodynamic lubrication but merely that sliding is taking place in the presence of a lubricant.

7.1.3 Reciprocating Gas Compressors (Recommendations)

By far the best means of preventing piston ring scuffing in a reciprocating gas compressor is to add sufficient water vapour (or possibly organic vapours (Savage and Schaeffer 1956)) to the gas being compressed, to allow unlubricated low friction rubbing of cast iron against cast iron to occur. In order to determine the amount of water vapour required to prevent scuff a modified version of the equation shown in Section 7.1.1

can be used:

$$\frac{P_L}{P_S} = \frac{0.15}{\sqrt{P}}$$

where P is the gas discharge pressure (in bars). However, if organic vapours are used then smaller values of P_L/P_S could possibly be used.

If it is not possible to add vapour to the gas being handled then care must be taken to prevent oil starvation (even for a short period) and not to exceed the oil transition temperature. As a rough guide any compressor with a discharge pressure of over 160 bar could be in danger if its cylinder wall temperature was to exceed 150°C.

The 'running in' procedure of a compressor is also important, as this allows a surface film to be formed which can enable the oil transition temperature to be exceeded. A running in procedure in which the cylinder wall temperature and the discharge pressure are increased gradually over a long period of time is preferable.

7.2 Suggestions for Further Work

7.2.1 Unlubricated

The equation shown in Section 7.1.1, ie:

$$\frac{P_L}{P_S} = \frac{K}{\sqrt{L}}$$

was determined for a limited number of gases and for few load conditions. Further verification of this equation is required, particularly in finding values of K, and extending the load range beyond 200 N. Also as a test of the temperature dependence of P_S , higher surface temperatures should be used.

The above equation is only relevant for water vapour, but Savage and Schaeffer (1956) found that other vapours were effective in the vapour lubrication of graphite. It would be useful therefore, if this work could be extended to other vapours to study their effect on cast iron sliding and to see if similar equations can be evolved.

In addition to cast iron, several other materials are used in reciprocating gas compressors for piston rings and/or cylinder liners such as nitrided steel, lead-bronze and ptfe. The study of the unlubricated sliding of these materials in different gases and the effect of vapours on their performance would be beneficial to the further understanding of compressor lubrication. Another material that would be worthy of further investigation is cast iron itself, as for this work, only one grade was used and several more types are available.

The effect of cast iron metallurgy on vapour lubrication in non oxidising gases should be studied to make sure the correct types of cast iron are used for compressor rings and liners.

7.2.2 Lubricated

From the results of the heated plate experiments it is obvious that every oil has a separate transition temperature, above which it offers very little protection against scuff. It is important that the transition temperatures for the oils commonly used in the reciprocating compressors are found so that safe operating parameters (eg. pressure and temperatures) can be established.

7.2.3 Reciprocating Gas Compressors

Despite concern regarding piston ring failures in gas compressors there was little information available on ring life for different compressors. In fact, Table 1.1 was the only information readily available. It would be very useful therefore if a survey of reciprocating compressors is carried out, particularly relating to such information as ring/liner usage, pressures, temperatures, lubricating oils and the composition of the gases handled. It is also important to establish whether ring life depends on the length of time of operation under full load or upon the number of stop/start cycles a compressor goes through. There is also no comparison available for the ring usage of different ring/liner materials. In fact, in many cases, the choice of materials seems to be

purely arbitrary. It is important that the correct materials are used for the type of gas being handled and this point should be borne in mind when designing new compressors. Unless more work is done to find out some of the information outlined above it will be very difficult to establish whether any of the solutions previously suggested (eg. the addition of water vapour to the gas) are successful in reducing ring life. In fact, without reliable figures on ring usage and failures it will be impossible to decide whether a solution is economically feasible or not.

Other information of use is a measure of the fluid film thickness for piston rings in a reciprocating compressor. It is probable that some of the research into film thicknesses for piston rings in I.C. engines could be easily adapted for reciprocating gas compressors and may be able to tell us for how much of its stroke a compressor operates under boundary conditions.

APPENDIX A

COMPRESSOR DATA

Speed (R.P.M.)	Stroke (mm)	Bore (mm)	Delivery Pressure (Bar)	Gas
330	254	80	261	CO
388	203	38	255	H ₂
416	241	54	255	H ₂
240	229	51	361	CO ₂
384	267	108	150	N ₂
420	267	108	290	N ₂
235	400	220	107	Air
296	380	85	104	Air
300	350	90	266	N ₂
300	350	163	266	H ₂
465	220	58	261	N ₂
250	381	146	361	Syngas
250	500	107	339	Syngas
400	216	82	270	H ₂
300	140	165	273	H ₂ , NH ₃
180	150	135	306	H ₂ , N ₂ , NH ₃
170	400	45	1962	C ₂ H ₆
120	203	51	1314	C ₂ H ₆
240	254	90	245	C ₂ H ₄
230	450	190	260	NH ₃
120	610	171	260	NH ₃
125	610	432	55	NH ₃
160	457	381	55	NH ₃
230	450	380	55	NH ₃
333	381	203	275	NH ₃
405	280	356	4.5	N ₂
375	254	305	4.6	Air
420	305	83	44.8	C ₂ H ₆
420	279	121	72.4	C ₂ H ₄
580	407	305	14.6	C ₂ H ₄
330	356	171	278	H ₂
120	460	280	260	H ₂ , N ₂
300	305	305	10.3	H ₂ , N ₂
330	356	105	265	CO
150	280	108	150	N ₂
370	330	368	11	Air
115	279	32	360	CO ₂
170	160	135	250	NH ₃ , H ₂ , N ₂
329	356	584	9	Air
300	343	139	231	CO ₂
300	395	276	331	Syngas
300	395	276	325	N ₂
333	381	171	325	Syngas
740	159	159	53	H ₂ , CH ₄
294	400	210	270	H ₂ , CH ₄

Appendix A (cont'd)

Compressor Data

Speed (R.P.M.)	Stroke (mm)	Bore (mm)	Delivery Pressure (Bar)	Gas
214	381	184	290	H ₂ , CO
290	229	107	360	NH ₃
300	305	146	41	Air
970	127	127	8	Air
428	254	578	14	H ₂ , C ₂ H ₄
428	254	440	19	NH ₃
428	254	229	64	H ₂ , C ₂ H ₄ , C ₃ H ₆
593	203	117	240	H ₂
333	305	229	28	Air
250	381	146	17	Air
735	159	260	8	Air
375	254	241	69	H ₂ , CH ₄
295	292	267	32	CO ₂
450	305	457	9	N ₂
590	203	368	8	N ₂
428	254	234	45	H ₂ C
428	254	184	63	H C
326	381	216	1140	CO ₂
415	203	203	10	NH ₃
330	381	267	50	H ₂
420	260	190	59	H ₂ , CH ₄
360	203	102	55	CO ₂

Appendix B

Calculation of Maximum Permissible Load on Probe

The highest load anticipated on the probe was 2000N, which corresponded to a coefficient of friction of 1.0 at a load of 1000N (ie. on both sides of the specimen plate).

Failure by Yielding

Thinnest section of the probe was the strain gauged section, therefore yield calculations were based on dimensions of this section.

$$\begin{aligned}\text{Cross Sectional Area} &= 36 \times 10^{-6} \text{ m}^2 \\ \text{Yield Stress for Steel} &= 240 \times 10^6 \text{ N/m}^2\end{aligned}$$

$$\begin{aligned}\text{Yield Force} &= \text{Yield Stress} \times \text{Cross Sectional Area (A)} \\ &= 36 \times 10^{-6} \times 240 \times 10^6 \text{ N} \\ &= 8640 \text{ N}\end{aligned}$$

Well above maximum friction force.

Failure by Buckling

The worst possible case is one end clamped and one end pinned giving an Euler buckling load (F_B):

$$F_B = \frac{20.25 EI}{l^2}$$

$$\begin{aligned}\text{For this case } E &= 0.20 \times 10^{12} \text{ N/m}^2 \\ I &= 598 \times 10^{-12} \text{ m}^4 \\ l &= 15 \times 10^{-6} \text{ m for strain gauged section} \\ l &= 0.5 \text{ m for probe}\end{aligned}$$

For Strain Gauged Section:

$$F_B = \frac{20.25 \times 0.20 \times 10^{12} \times 598 \times 10^{-12}}{(15 \times 10^{-6})^2}$$

$$= 10.76 \text{ MN}$$

PTO.

Appendix B (cont'd)

For Probe:

$$F_0 = \frac{20.25 \times 0.20 \times 10^{12} \times 598 \times 10^{-12}}{(0.5)}$$
$$= 9.69 \text{ KN}$$

Both well within design limits.

Maximum Strain

$$E = \frac{\sigma}{\epsilon} \Rightarrow \epsilon = \frac{\sigma}{E}$$

$$\sigma = \frac{F_m}{A} = \frac{2000}{36 \times 10^6} = 5.55 \times 10 \text{ N/m}^2$$

therefore

$$\epsilon = \frac{5.55 \times 10^7}{2.0 \times 10^{11}} = 2.78 \times 10^{-4} \text{ m}$$
$$= 278 \text{ micro-strain.}$$

Appendix C

Details of Experimental Apparatus

No. 1 Friction Apparatus

Force Saddle

Air Cylinders

Bore 42mm Stroke 25mm

Bore 100mm Stroke 25mm

Maximum Working Pressures 10 bar

Maximum Loads at 5 bar.

42mm cylinder = 500N
100mm cylinder = 3000N

Probe

Strain Gauges

Type: Tokyo Sokki Kenkyuzo FLE-1-11

Gauge Length = 1mm Gauge Resistance = $120 \pm 0.3 \Omega$

Gauge Factor = 2.01

Heated Loading Pistons

Peristaltic Pump: Watson Marlow MHRE 72L

Anti-Freeze: Smiths 'Bluecol'

Reciprocating Mechanism

Motor

Type: Parvalux SD11 MM Shunt Wound D.C.

Power: 125W Speed: 4000rpm

Gearbox: 89:1

Appendix C (cont'd)

Controller

Parvalux Thyristor D.C. Controller

Supply: 240V 50 Hz

Speed Range: 25:1

Instrumentation

Strain Bridge Amplifier: Peekel 581 DNH

Dewpoint Hygrometer: Michell Instruments Series 2000, range
- 40°C to + 20°C

Oxygen Analyser: Taylor Instruments Analytics

Servmex OA.570 range 0% to 100%

X-Y Plotter Bryans 26000 A3

Micro-Computer: Apple II

Heated Plate Apparatus

Air Cylinder

Bore 42mm Stroke 25mm

Strain Gauges

Type: Tokyo Sokki Kenkyuzo

Gauge Length = 3mm Gauge Resistance = $120 \pm 0.3 \Omega$

Gauge Factor = 2.1

Motor

Normand Electrical Co Ltd

Power = 95W

Motor Controller: Tecquipment Type 83

Range: 1 - 45 rpm

Appendix C (cont'd)

Strain Amplifier

Peekel 581 DNH

All other apparatus as No. 1 Friction Apparatus.

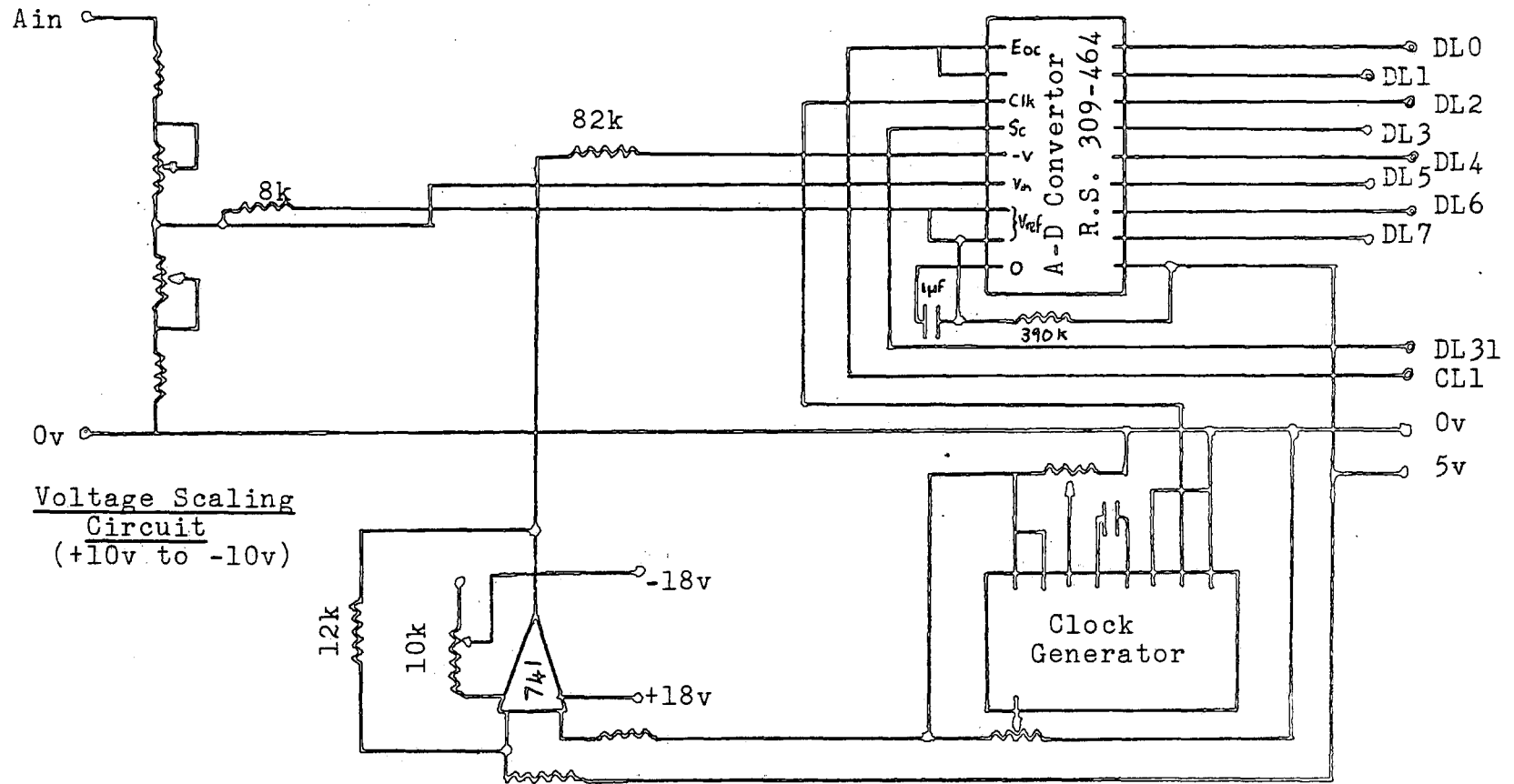


Figure D.1 Circuit Diagram of Analogue to Digital (A-D) Converter

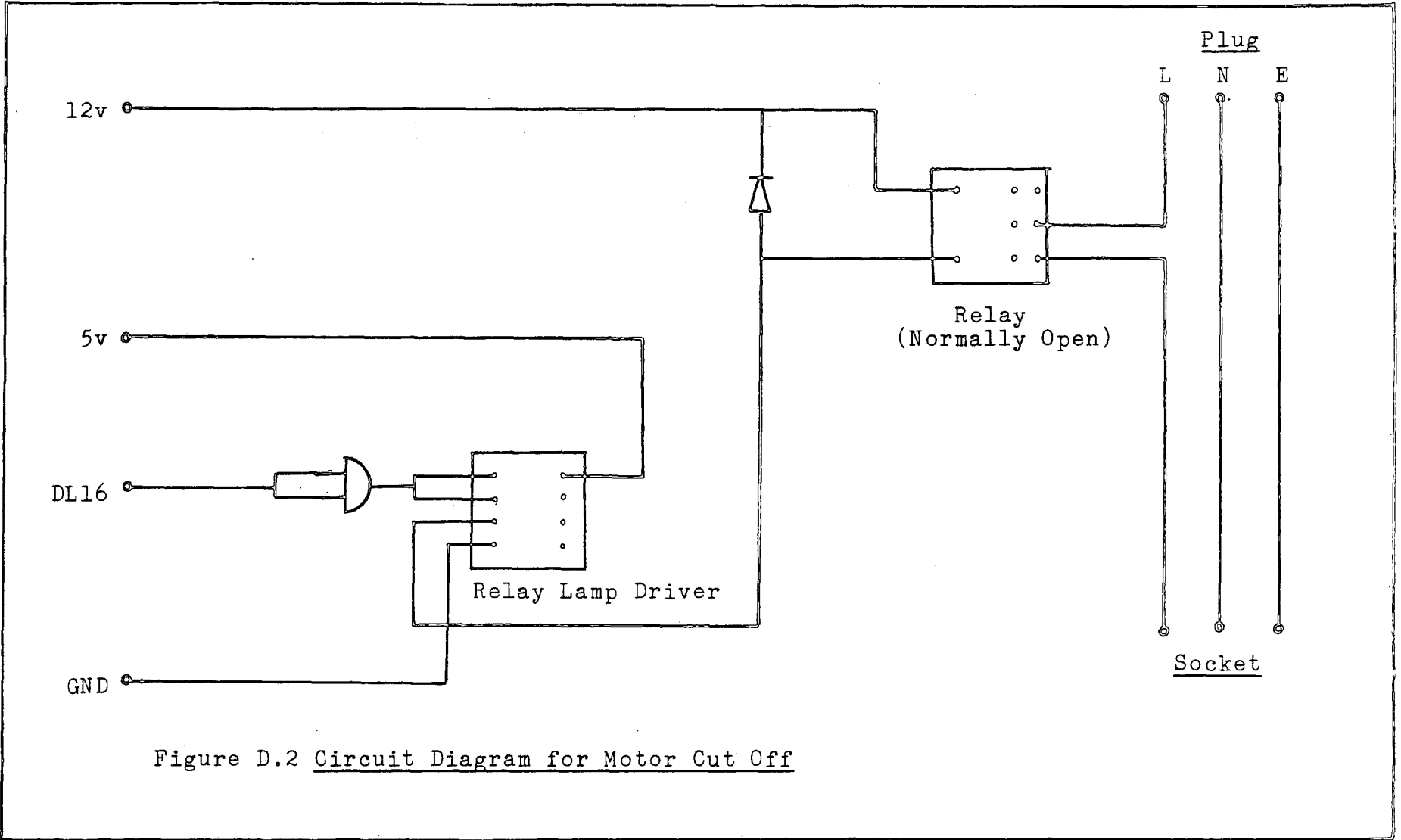


Figure D.2 Circuit Diagram for Motor Cut Off

APPENDIX E

Reciprocating Mechanism, Motor Selection

Design Criteria (Motor)

- i) The motor had to be able to operate when maximum design load had been applied and scuffing had taken place. Maximum design load was 1000N and scuffing was considered to be taking place with a coefficient of friction of 1.0
- ii) Must be able to operate at various speeds around 30rpm.
- iii) The load-speed characteristics had to be such, that the motor speed would vary only by a small amount as the friction load increased
- iv) Had to be as small as possible

If we take into account i) and ii) the minimum motor power can be evaluated:

If $\mu = 1.0$ the force on the probe, with a 1000N load will be 2000N (ie. both sides at $\mu = 1.0$)

The eccentric is 10mm off centre, therefore torque is:

$$\begin{aligned}\text{Torque} &= 2000 \times 10^{-2} \text{ Nm} \\ &= 20 \text{ Nm}\end{aligned}$$

Power = Torque x Angular Velocity

$$= 20 \times \frac{30 \times \pi}{60} = 62.8 \text{ W}$$

Note: Angular Velocity used is for 30rpm.

By using a safety factor of 2 the motor power required was 125 W ($\frac{1}{6}$ H.P).

For details of motor see Appendix C.

APPENDIX F

Properties of Cast Iron Specimens

Specification

B.S. 1452 Grade 14/17

Chemical Analysis

Carbon	3.30%
Silicon	2.40%
Manganese	0.69%
Phosphorus	0.05%
Sulphur	0.05%
Chromium	0.06%
Tin	0.09%

Source: Eurocast Bar Ltd, Sutton Coalfield

Physical Properties

Vickers Hardness (HV (40)) = $2300 \times 10 \text{ N/m}^2$

Tensile Strength = $2.43 \times 10 \text{ N/m}^2$

Surface Finish = 0.20 microns Ra \pm 0.1

APPENDIX G

Calculation of Water Vapour Flowrate

If we assume that water vapour behaves as perfect gas,

Then:

$$m_{H_2O} = \frac{P_{H_2O} V_T}{R_{H_2O} T_K} \quad G1$$

$$R = 0.4619 \text{ KJ/Kg}^\circ\text{K}$$

Dewpoint

Definition:- The temperature to which, if a sample of wet gas is cooled at constant pressure, it becomes saturated.

Therefore:

$$P_{H_2O} = P_{D.P} \quad G2$$

and G1 becomes

$$m_{H_2O} = \frac{P_{D.P} V_T}{R_{H_2O} T_K} \quad G3$$

Results of Tables 11 and 13 were calculated using this formula.

Dewpoint Hygrometer, Factory Calibration

Calibration Gas Dewpoint	-40	-30	-20	-10	0	10	20
Instrument Readout	-38	-28	-22	-12	-2	9	20

APPENDIX H

Piston Calibration Programme

This programme reads in calibration data for the piston and the proving ring, and by means of best-fit curves produces a force-pressure table.

Curve-fitting Routine is a basic version of NAG Library Routine EOIACF (Numerical Algorithms Group 1978).

```

5 REM *****
10 REM I.MURRAY DURHAM UNIV
20 REM 12/11/92
30 REM PISTON CALIBRATION PROGRAMME
35 REM *****
40 DIM P(50),MP(50),F(50),MF(50)
50 DIM X(50),Y(50),B(5),C(5),D(5)
60 DIM A(100),AA(5),AH(100),RX(100),R%(100)
70 D$ = "": REM CTRL D
80 REM ** READ IN PRESSURE RESULTS
90 REM * X=PRESSURE Y=MICRO-STRAIN
95 F$ = "PISTON DATA"
100 PRINT D$;"OPEN";F$
110 PRINT D$;"READ";F$
120 INPUT N:NP = N
130 FOR I = 1 TO N
140 INPUT P(I),MP(I)
150 X(I) = P(I):Y(I) = MP(I)
160 NEXT I
165 PRINT D$;"CLOSE";F$
170 GOSUB 5000: REM CURVE FIT
180 FOR I = 1 TO 5:B(I) = A(I): NEXT I
185 FOR I = 1 TO 5:R(I) = 0: NEXT I
190 REM ** READ IN FORCE DATA
200 REM * X=MICRO-STRAIN Y=FORCE
201 F2$ = "FORCE DATA"
210 PRINT D$;"OPEN";F2$
220 PRINT D$;"READ";F2$
230 INPUT N:NF = N
240 FOR I = 1 TO N
250 INPUT MF(I),F(I)
260 X(I) = MF(I):Y(I) = F(I)
270 NEXT I
280 PRINT D$;"CLOSE";F2$
290 GOSUB 5000
300 FOR I = 1 TO 5:C(I) = A(I): NEXT I
310 FOR I = 1 TO 5:R(I) = 0: NEXT I
320 MX = MP(NP)
330 IF MF(NF) < MP(NP) THEN MX = MF(NF)
335 REM ** TO WORK OUT PRESSURE-FORCE
340 N = 36:XI = 0
350 FOR I = 1 TO N
360 P(I) = XI
370 GOSUB 2000
380 Y(I) = YI
385 PRINT XI,YI
390 XI = XI + 2
400 NEXT I
410 FOR I = 1 TO N
420 XI = Y(I)

```

```

430 IF XI > MX THEN 500
440 GOSUB 3000
450 F(I) = YI
470 NEXT I
500 N = I - 1
510 FOR I = 1 TO N
520 X(I) = P(I):Y(I) = F(I)
530 NEXT I
540 GOSUB 5000
550 REM ** TO WORK OUT FORCES
551 REM FOR FORCE -PRESSURE TABLE
560 FOR I = 1 TO 5:B(I) = A(I): NEXT I
570 FT = 25
571 PRINT 0$;"PR#1"
572 PRINT TAB( 1)"LOAD"; TAB( 15)"PRESSURE"
573 PRINT TAB( 1)" (N)"; TAB( 15)" PSI "
574 PRINT "-----"
580 FOR I = 1 TO N
590 IF F(I) > FT THEN 610
600 NEXT I
610 PH = P(I):PL = P(I - 1)
611 IF FT = INT (F(I)) THEN PH = P(I + 1)
620 XI = -(PH + PL) / 2
630 GOSUB 2000
640 IF FT * 10 = INT (YI * 10) THEN 704
650 IF YI > FT THEN PH = XI
660 IF YI < FT THEN PL = XI
670 GOTO 620
704 PRINT TAB( 1)FT; TAB( 16)XI
705 FT = FT + 25
710 IF FT < 500 THEN 580
715 PRINT 0$;"PR#0"
720 STOP
1999 REM *****
2000 REM ** TO GET PRESS-MICROSTRAIN
2001 REM *****
2005 YI = 0
2010 FOR J = 1 TO 5:YI = YI + B(J) * (XI ^ (J - 1)): NEXT
J
2020 RETURN
2999 REM *****
3000 REM ** TO GET FORCES
3001 REM *****
3010 YI = 0
3020 FOR J = 1 TO 5:YI = YI + C(J) * (XI ^ (J - 1)): NEXT
J
3030 RETURN

```

```

5000 REM I.MURRAY DURHAM UNIV.
5001 REM *****
5010 TEXT
5020 REM 26/8/82
5030 REM CURVE FITTING ROUTINE
5040 REM %% READ IN DATA POINTS
5080 M1 = 5
5100 REM %% OUT OF BOUNDS PARAMTERS
5110 IF M1 > N THEN GOTO 6380
5120 IF M1 > 100 THEN GOTO 6380
5130 FOR I = 2 TO N: IF X(I) < X(I - 1) THEN GOTO 6380
      : NEXT I
5140 M2 = M1 + 1
5150 M = M1 - 1
5160 PR = 0.0
5170 R%(1) = 1.0
5180 R%(M2) = N
5190 D = (N - 1) / M1
5200 H = D
5210 FOR I = 2 TO M1
5220 R%(I) = INT (H + 0.5) + 1
5230 H = H + D
5240 NEXT I
5250 H = - 1.0
5260 FOR I = 1 TO M2
5270 RI = R%(I)
5280 RX(I) = X(RI)
5290 A(I) = Y(RI)
5300 RH(I) = - H
5310 H = - H
5320 NEXT I
5330 FOR J = 1 TO M1
5340 I1 = M2
5350 A1 = A(I1)
5360 R1 = RH(I1)
5370 I = M2
5380 I = I - 1
5390 J1 = I - J + 1
5400 DENOM = RX(I1) - RX(J1)
5410 AI = A(I)
5420 HI = RH(I)
5430 A(I1) = (A1 - AI) / DENOM
5440 RH(I1) = (R1 - HI) / DENOM
5450 I1 = I
5460 A1 = AI
5470 R1 = HI
5480 IF (I - J) > 0 THEN GOTO 5380
5490 NEXT J
5500 H = - A(M2) / RH(M2)

```

```

5510 FOR I = 1 TO M2
5520 A(I) = A(I) + R%(I) * H
5530 NEXT I
5540 J = M1
5550 J = J - 1
5560 XJ = R%(J)
5570 I = J
5580 AI = A(I)
5590 J = J + 1
5600 FOR I1 = J TO M1
5610 A1 = A(I1)
5620 A(I) = AI - XJ * A1
5630 AI = A1
5640 I = I1
5650 NEXT I1
5660 J = J - 1
5670 IF (J - 1) > 0 THEN GOTO 5550
5680 HM = ABS (H)
5690 IF HM > PR THEN GOTO 5720
5700 A(M2) = - HM
5710 GOTO 6210
5720 A(M2) = HM
5730 IM = R%(1)
5740 HX = H
5750 J = 1
5760 RJ = R%(J)
5770 FOR I = 1 TO N
5780 IF I = RJ THEN GOTO 5920
5790 XI = X(I)
5800 HN = A(M1)
5810 K = M1
5820 K = K - 1
5830 HN = HN * XI + A(K)
5840 IF (K - 1) > 0 THEN GOTO 5820
5850 HN = HN - Y(I)
5860 AB = ABS (HN)
5870 IF AB < HM THEN GOTO 5950
5880 HM = AB
5890 HX = HN
5900 IM = I
5910 GOTO 5950
5920 IF J > M2 THEN GOTO 5950
5930 J = J + 1
5940 RJ = R%(J)
5950 NEXT I
5960 PRINT IM, R%(1)
5970 IF IM = R%(1) THEN 6290
5980 FOR I = 1 TO M2
5990 IF IM < R%(I) THEN GOTO 6020
6000 NEXT I

```

```

6010 I = M2
6020 I2 = INT ( I * 0.5 )
6030 I2 = I - 2 * I2
6040 XN = H
6050 IF I2 = 0 THEN XN = - H
6060 IF HX * XN < 0.0 GOTO 6090
6070 R%(I) = IM
6080 GOTO 5250
6090 IF IM > R%(1) THEN 6180
6100 J1 = M2
6110 J = M2
6120 J = J - 1
6130 R%(J1) = R%(J)
6140 J1 = J
6150 IF ( J - 1 ) > 0 THEN 6120
6160 R%(1) = IM
6170 GOTO 5250
6180 IF IM < R%(M2) THEN 6260
6190 J = 1
6200 FOR J1 = 2 TO M2
6210 R%(J) = R%(J1)
6220 J = J1
6230 NEXT J1
6240 R%(M2) = IM
6250 GOTO 5250
6260 R%(I - 1) = IM
6280 GOTO 5250
6290 FOR I = 1 TO M1:AR(I) = R(I): NEXT I
6300 FOR I = 1 TO N
6310 Y(I) = 0
6320 FOR J = 1 TO M1
6330 Y(I) = Y(I) + A(J) * (X(I) ^ (J - 1))
6340 NEXT J
6350 PRINT TAB( 1)I; TAB( 5);X(I); TAB( 15);Y(I)
6360 NEXT I
6370 GOTO 6400
6380 PRINT "FAIL"
6390 STOP
6400 RETURN

```

APPENDIX J

Properties of Lubricating Oils

Shell Risella EL

Viscosity at 40 C 9.0 cSt min
 11.0 cSt max

CSB 460

Viscosity at 40 C 414.0 cSt min
 506.0 cSt max

E.P. Oil (SAE 80)

Viscosity at 0 C 3257 cSt min
 21716 cSt max

APPENDIX K

Data Reading Programme

Function

The function of this programme was to read in automatically, friction readings from the probe, via an A-D convertor and then to process and store the data in the form of friction forces. Also contained within the programme was the necessary software to detect high (unsafe) friction forces and so terminate the friction test.

The following data was entered manually before the test commenced:-

- 1) Mass of plate specimen in grammes
- 2) Mass of pins (both) in grammes
- 3) Atmospheric Pressure in mm Hg
- 4) Vessel Pressure in mm Hg
- 5) Applied Load (N)
- 6) Speed (R.P.M.)
- 7) Ambient Temperature ($^{\circ}\text{C}$)
- 8) Total gas flowrate (Lt/min)
- 9) Dewpoint ($^{\circ}\text{C}$)

From this data, the water vapour flowrate and the coefficient of friction could be calculated. When the test was running the coefficient of friction and graph of coefficient to time was displayed on the V.D.U. On completion of the test, the final mass of the plate and pins were entered, together with any alterations to previous data. Data was stored by means of a hard copy (from the printer) and on a floppy disc.

APPENDIX K

Data Reading Programme

```
10 REM *****
20 REM
30 REM 1.MURRAY DATA READING PROG
40 REM 29/10/82
50 REM REAL TIME VERSION
60 REM THIS VERSION 9/2/83
70 REM THIS VERSION 22/3/83
80 REM THIS VERSION 12/4/83
90 REM *****
100 DIM A(6),B(5),C(300),UA$(11),VA(11),AA$(2)
110 DIM FF(200),FC(200),X%(200),Y%(200),XT(200)
120 FOR I = 1 TO 6: READ A(I): NEXT I
130 ZC = 1:ZF = 1:F1 = 65:F2 = 65
140 D$ = ""
150 PRINT "FILE SUFFIX PLEASE": INPUT AA$(2)
160 ONERR GOTO 30000
170 TM = 0:ZE = 123:ZI = 1:B3 = 0:IT = 1
180 FOR I = 1 TO 5: READ B(I): NEXT I
190 FOR I = 1 TO 11: READ UA$(I): NEXT I
200 REM DATA FOR A ARRAY (UAP PRESS)
210 DATA 6.10749613,0.503067786,0.0188481743
220 DATA 4.17340154E-04,5.65893427E-06,3.76574447E-08
230 REM DATA FOR B ARRAY (FORCE)
240 DATA -3.921247,1.306629,4.5572458E-4
250 DATA 2.7211500E-6,-4.59017648E-9
260 REM DATA FOR READ VALUES
270 DATA MASS OF PLATE,MASS OF PINS,ATMOS PRESSURE (MM HG)
280 DATA VESSEL PRESSURE,LOAD (N),SPEED(RPM)
290 DATA TEMPERATURE (C),FLOWRATE (LT/MIN),DEWPOINT (C)
300 DATA MASS OF PLATE(FINAL),MASS OF PINS(FINAL)
310 PRINT "DATE...": INPUT DT$
320 PRINT "DESCRIPTION...": INPUT DS$
330 D110 = - 16384 + 5 * 256
340 POKE D110 + 18,255
350 POKE D110 + 16,255
360 POKE D110 + 3,0: POKE D110 + 11,0
370 POKE D110 + 27,128
380 REM *** INPUT OTHER DATA ***
390 FOR I = 1 TO 9: PRINT UA$(I);" ": INPUT VA(I): NEXT I
400 GOSUB 2000: GOSUB 20000
410 G$ = CHR$(7): PRINT G$
420 CH = 11
430 REM *** BACK GROUND ROUTINE ***
440 PRINT "INPUT A LETTER WHEN READY": GET AN$
450 POKE D110 + 19,1: FOR I = 1 TO 200: NEXT I
460 N = 300: GOSUB 4000: GOSUB 8000
470 B3 = AC: PRINT "B3=";B3
480 REM *** START OF SAMPLING ROUTINE ***
```

```

480 REM *** START OF SAMPLING ROUTINE ***
490 GOSUB 8000
500 POKE 0110 + 19,1
510 GOTO 50000
520 PRINT G$;G$;G$
530 N = 300: GOSUB 4000
540 XT(IT) = TM
550 GOSUB 8000
560 GOSUB 10000
570 FOR I = 1 TO 8000: NEXT I
580 IT = IT + 1: TM = TM + 1
590 IF IT = 200 THEN 25000
600 IF TT = 123 THEN 620
610 RETURN
620 IF TC = 123 THEN 640
630 RETURN
640 TEXT
650 POKE 0110 + 19,0
660 PRINT "INPUT A LETTER TO RESTART MOTOR";: INPUT AN$
670 POKE 0110 + 19,1
680 PRINT "FINAL DATA"
690 PRINT VA$(10);" ";: INPUT VA(10)
700 PRINT VA$(11);" ";: INPUT VA(11)
710 REM *** DATA CHECK ***
720 FOR I = 1 TO 11
730 PRINT I;" ";VA$(I);" ";VA(I)
740 NEXT I
750 PRINT "ARE THESE OK": INPUT AN$
760 IF AN$ = "Y" THEN 850
770 PRINT "INCORRECT VALUE": INPUT J
780 PRINT VA$(J);" ";: INPUT VA(J)
790 IF J = 3 OR 4 THEN GOSUB 2000
800 IF J = 5 THEN GOSUB 12000
810 IF J > 5 THEN GOSUB 2000
820 GOTO 710
830 GOSUB 12000
840 REM RESULTS LISTING
850 HOME
860 D$ = "": REM CTRL D
870 PRINT D$;"PR#1"
880 PRINT DT$
890 PRINT DS$
900 UF = INT(UF * 970):UF = UF / 1000
910 PRINT "VAPOUR FLOWRATE=" ;UF;" MG/MIN"
920 PRINT TAB( 1)"TIME"; TAB( 10)"FORCE"; TAB( 20)"COEFF"
930 PRINT TAB( 1)"(MINS)"; TAB( 11)"(N)"; TAB( 20)"FRICTION"
"
940 FOR I = 1 TO (IT - 1) STEP 21
950 FF(I) = INT(FF(I) * 970):FF(I) = FF(I) / 1000
960 FC(I) = INT(FC(I) * 970):FC(I) = FC(I) / 1000
970 PRINT TAB( 3)XT(I); TAB( 10)FF(I); TAB( 20)FC(I)
980 NEXT I
990 PRINT TAB( 3)XT(IT - 1); TAB( 10)FF(IT - 1); TAB( 20)FC
(IT - 1)
1000 DU = IT - 1
1010 REM WEAR RATES
1020 WP = VA(1) - VA(10):WI = VA(2) - VA(11)
1030 DI = VA(6) * 40E - 3 * (DU - 1)
1040 WR = (WP + WI) * 950 / DI
1050 NR = INT(WR * 950):NR = NR / 1000
1060 PRINT "WEAR RATE=" ;NR;"MG/M

```

```

1060 PRINT "WEAR RATE= ";WR;"MG/M
1070 POKE - 12524,0: REM INVERSE
1080 POKE - 12525,64: REM HIGH RES P2
1090 PRINT "": REM CTRL 0
1100 PRINT 0$;"PR#0"
1110 REM ** TO STORE DATA
1120 PRINT "NAME OF DATA FILE ": INPUT A$
1130 PRINT "HAVE YOU INSERTED THE DATA DISC IN DRIVE 2": INPUT
AN$
1140 IF AN$ < > "Y" THEN 1120
1150 PRINT 0$;"OPEN";A$;"02"
1160 PRINT 0$;"WRITE";A$
1170 PRINT 0T$: REM DATE
1180 PRINT 0S$: REM DESCRIPTION
1190 PRINT 0F$: REM VAPOUR FLOW
1200 FOR I = 1 TO 11
1210 PRINT 0A$(I)
1220 PRINT 0A(I)
1230 NEXT I
1240 PRINT 0U
1250 FOR I = 1 TO 0U
1260 PRINT 0X(I)
1270 PRINT 0F(I)
1280 PRINT 0C(I)
1290 NEXT I
1300 PRINT 0$;"CLOSE";A$
1310 STOP

2000 REM *****
2010 REM *** VAPOUR FLOWRATE SUBROUTINE
2020 REM *****
2030 REM ** PSAT
2040 PS = 0
2050 FOR I = 1 TO 6:PS = PS + A(I) * (UA(9) ^ (I - 1)): NEXT
I
2060 REM ** FLOWRATE
2070 PT = (UA(3) + UA(4)) / 750:PP = UA(3) / 750
2080 U1 = PS / ((PT * 950) - PS)
2090 H = UA(8) * 1E - 3
2100 TK = UA(7) + 273
2110 UF = ((2.1649E2 * PP * H * U1) / TK)
2120 UF = UF * 1E6
2130 RETURN

4000 REM *****
4010 REM *** SAMPLING ROUTINE ***
4020 REM *****
4030 FOR I = 1 TO N
4040 POKE 0110 + 20,I: POKE 0110 + 21,0
4050 WAIT 0110 + 13,1,254
4060 C(I) = PEEK (0110 + 1)
4070 NEXT I
4080 RETURN

```

```

6000 REM *****
6001 REM AXIS PLOTTING & TIC MARKS ***
6002 REM *****
6010 HGR2 : HCOLOR= 3
6020 HPLOT 9,0 TO 9,180 TO 270,180
6030 FOR I = 1 TO 30
6040 IY = 182
6050 IF I - 1 = 10 THEN IY = 185
6060 IF I - 1 = 20 THEN IY = 185
6070 HPLOT (I * 9),180 TO (I * 9),IY
6080 NEXT I
6090 HPLOT 8,90 TO 10,90
6130 HPLOT 140,191 TO 140,185
6140 HPLOT 137,185 TO 143,185
6150 HPLOT 147,191 TO 147,185
6160 HPLOT 151,191 TO 151,185 TO 154,189 TO 157,185 TO 157,1
91
6170 HPLOT 164,191 TO 161,191 TO 161,185 TO 164,185
6180 HPLOT 161,188 TO 164,188
6190 HPLOT 10,180
6200 RETURN

```

```

8000 REM *****
8010 REM *** ROUTINE TO EVALUATE FRICTION COEFFS ***
8020 REM *****
8030 REM ** TO SORT +VE & -VE VALUES
8040 J = 0:K = 0:TT = 0:TC = 0:ZE = 0
8050 REM ** ZERO
8060 FOR I = 1 TO N:ZE = ZE + C(I): NEXT I
8070 ZE = ZE / N
8080 ML = C(1):MX = C(2)
8085 REM ** 1ST APPROX
8090 FOR I = 1 TO N
8100 IF C(I) < ML THEN ML = C(I)
8110 IF C(I) > MX THEN MX = C(I)
8120 IF INT (C(I) * 110) = INT (ZE * 110) THEN 8170
8130 IF C(I) > ZE THEN 8160
8140 TC = TC + C(I):J = J + 1
8150 GOTO 8170
8160 TT = TT + C(I):K = K + 1
8170 NEXT I
8180 IF J = 0 THEN 8200
8190 TC = TC / J: GOTO 8210
8200 TC = ZE
8210 IF K = 0 THEN 8230
8220 TT = TT / K: GOTO 8260
8230 TT = ZE
8240 IF TT = TC THEN 840
8245 REM ** FINAL VALUES
8260 ZH = INT (TT + 0.5):ZL = INT (TC)
8270 IF B3 = 0 THEN 8420
8280 TT = 0:TC = 0:J = 0:K = 0
8290 FOR I = 1 TO N
8300 IF C(I) > = ZH THEN 8350

```

```

8310 IF C(I) < = ZL THEN 8330
8320 GOTO 8360
8330 TC = TC + C(I):J = J + 1
8340 GOTO 8360
8350 TT = TT + C(I):K = K + 1
8360 NEXT I
8370 IF K = 0 THEN 8390
8380 TT = TT / K
8390 IF J = 0 THEN 8420
8400 TC = TC / J
8415 REM ** TO EVALUATE FRICTION FORCE
8420 AC = ABS (TT - TC)
8425 IF B3 = 0 THEN RETURN
8430 IF AC < B3 THEN 640
8440 AN = MX - ML
8450 REM EVAL FORCE
8460 MI = (AC - B3) / 4
8470 MI = 100 * MI / CM: REM TO MICRO-STRAIN
8480 FF(IT) = 0
8490 FOR I = 1 TO 5:FF(IT) = FF(IT) + B(I) * (MI ^ (I - 1)):
NEXT I
8500 FC(IT) = FF(IT) / UA(5): REM FRICTION COEFF
8510 IF ZF > ZC THEN 8530
8520 IF FC(IT) > 3.0 THEN GOSUB 15000
8525 REM ** MOTOR CONTROL
8530 IF FF(IT) > 250 THEN POKE D110 + 19,0
8540 IF B3 = 0 THEN 8700
8550 IF DU > 1 THEN 8700
8560 UTAB (10)
8590 PRINT "COEFF OF FRICTION= ";FC(IT)
8600 PRINT "AT ";XT(IT);" MINS"
8670 POKE - 16304,0
8680 POKE - 16299,0
8690 POKE - 16297,0
8700 RETURN

```

```

10000 REM *****
10010 REM *** PLOTTING ROUTINE ***
10020 REM *****
10030 X%(IT) = INT ((IT - 1) * 9 / ZI) + 9
10040 Y%(IT) = INT (FC(IT) * (60 / ZF))
10050 IF Y%(IT) < 0 THEN Y%(IT) = 0
10060 Y%(IT) = 180 - Y%(IT)
10070 IF Y%(IT) < 0 THEN Y%(IT) = 0
10080 H PLOT TO X%(IT),Y%(IT)
10090 IF IT = ZI * 30 THEN 10120
10100 FOR I = 1 TO 1000: NEXT I
10110 RETURN
10120 REM ** X AXIS ALTERATION
10130 ZI = ZI + 1
10140 GOSUB 6000
10150 FOR I = 1 TO IT
10160 X%(I) = INT ((I - 1) * 9 / ZI) + 9
10170 H PLOT TO X%(I),Y%(I)
10180 NEXT I
10190 RETURN

```

```

12000 REM *** REDO RESULTS ***
12010 DU = IT
12020 GOSUB 6000
12030 FOR IT = 1 TO DU: GOSUB 10000: NEXT IT
12040 IT = DU
12050 RETURN

```

```

15000 REM *****
15010 REM *** TO ALTER Y-AXIS ***
15020 REM *****
15030 ZF = ZF + 1
15040 GOSUB 6000
15050 FOR KI = 1 TO IT - 1
15060 Y%(KI) = INT (FC(KI) * (60 / ZF))
15070 IF Y%(KI) < 0 THEN Y%(KI) = 0
15080 Y%(KI) = 180 - Y%(KI)
15090 IF Y%(KI) < 0 THEN Y%(KI) = 0
15100 HPL0T TO X%(KI),Y%(KI)
15110 NEXT KI
15120 RETURN

```

```

20000 REM *****
20010 REM *** CHECK FOR POWER SUPPLY ON/OFF ***
20020 REM *****
20030 N = 10: GOSUB 4000
20040 NORMAL
20050 IF C(5) < > 0 THEN RETURN
20060 HOME : FLASH : UTAB (10)
20070 PRINT "TRY SWITCHING ON POWER SUPPLY": GOTO 20030

```

```

25000 REM *****
25010 REM *** TO STORE DATA ON DISC ***
25020 REM *****
25025 D$ = "": REM CTRL D
25030 AA$(1) = CHR$(F1)
25050 PRINT D$;"OPEN";AA$(1);AA$(2)
25060 PRINT D$;"WRITE";AA$(1);AA$(2)
25070 FOR I = 1 TO IT
25080 PRINT XT(I): REM TIME
25090 PRINT FF(I): REM FRICTION FORCE
25100 PRINT FC(I): REM FRICTION COEFF
25110 NEXT I
25120 PRINT D$;"CLOSE";AA$(1);AA$(2)
25130 F1 = F1 + 1: IT = 1: ZI = 1
25140 IF F1 > 90 THEN 25170
25150 GOSUB 6000
25160 GOTO 600
25170 F1 = 65: F2 = F2 + 1
25180 GOTO 25150

```

```

30000 POKE 0110 + 19,0
30010 TEXT
30020 PRINT PEEK (222): REM ERROR CODE
30030 PRINT "PRESS ANY KEY": GET AN#
30040 GOTO 660

```

```

50000 REM TIME OF DAY PROG
50010 HOME : TEXT
50020 PRINT "BLOAD TIME.OBJ0"
50040 HOME : UTAB 5
50060 HR = 0:MN = 0:SC = 0
50080 IF SC > 59 GOTO 50060
50090 IF MN > 59 GOTO 50060
50100 IF HR > 23 GOTO 50060
50110 POKE 6,SC
50120 POKE 7,MN
50130 POKE 8,HR
50140 INPUT "HIT ANY KEY TO START ";A$
50150 CALL 36864
50160 HOME
50170 UTAB 1
50180 HR = PEEK (8)
50190 MN = PEEK (7)
50200 SC = PEEK (6)
50210 PRINT "TIME ";HR;": ";MN;": ";SC;
50220 PRINT " "
50230 FOR I = 1 TO 150: NEXT I
50235 IF SC = 1 THEN GOSUB 520
50236 TEXT
50240 GOTO 50170
50280 PRINT "RESET OR POWER DOWN."

```

APPENDIX I

Calibration Results

Table 1 Probe

12/10/81		Load N	25/05/82	24/12/82	30/09/83
Load	μs		μs	μs	μs
0	0	0	0	0	0
20	16.94	25	16.5	-	20.5
40	31.25	50	32.8	38.17	39.75
60	44.81	75	52.0	-	57.75
80	58.38	100	69.5	72.8	72.0
100	71.56	125	87.8	-	90.5
120	84.75	150	105.8	104.8	107.0
140	97.44	200	140.3	137.0	136.0
160	110.19	250	174.3	167.8	163.25
180	122.56	300	205.8	196.2	193.0
		350	236.5	226.8	221.0
		400	-	255.0	242.5
		450	-	283.8	273.25
		500	-	317.0	296.0

Table 2 Proving Ring

Load N	7/09/81 μs	27/05/82 μs	2/01/83 μs	30/09/83 μs
0	0	0	0	0
50	10.5	8.8	9.9	11.0
100	17.5	17.6	21.25	23.0
150	23.5	26.2	32.6	35.0
200	31.0	35.2	43.9	46.0
250	38.0	44.1	54.4	58.0
300	46.5	52.4	64.9	68.0
350	53.0	61.2	74.9	80.0
400	60.5	69.9	85.0	91.0
450	67.5	78.5	-	101.0
500	73.5	87.6	104.5	111.0

Table 3 Proving Ring

2/03/82	
Load N	µs
0	0
100	18.0
200	39.5
300	60.5
400	82.0
500	107.0
600	131.0
700	153.0
800	179.5
900	201.5
1000	225.0

29/05/83	
Load N	µs
0	0
250	59.5
500	113.25
750	163.3
1000	209.8
1250	255.8
1500	309.8
1750	365.5
2000	420.0
2250	473.8
2500	526.8
2750	576.8
3000	629.3
3250	680.8

Table 4 No 1 Pistons

24/09/81	
P Bar	Load N
0	0
0.60	27.6
0.86	53.7
1.16	82.9
1.45	113.8
1.74	146.3
2.03	182.1
2.30	216.3
2.59	253.7
2.88	292.7
3.13	328.5
3.35	367.5
3.67	406.5
3.97	440.7
4.25	489.43

5/11/81	
P Bar	Load N
0	0
0.36	15.1
0.49	27.6
0.73	53.7
0.97	82.9
1.25	113.8
1.51	146.3
1.77	182.1
2.03	216.3
2.34	253.7
2.58	293.7
2.82	328.5
3.17	367.5
3.36	406.5
3.90	440.7

28/05/82	
P Bar	Load N
0	0
0.28	2.5
0.41	11.2
0.55	21.6
0.83	46.4
1.10	75.1
1.38	106.0
1.65	138.1
1.93	170.1
2.21	201.5
2.48	231.8
2.76	260.9
3.45	329.5
4.14	401.3
4.83	496.4

17/11/82	
P Bar	Load N
0	0
0.72	50.0
1.16	100.0
1.57	150.0
1.98	200.0
2.42	250.0
2.87	300.0
3.40	350.0
3.90	400.0
4.34	450.0

P - Pressure

Table 5 No 2 Pistons

10/12/82		3/06/83		2/09/83	
Pressure Bar	Load N	Pressure Bar	Load N	Pressure Bar	Load N
0	0	0	0	0	0
0.87	50	0.56	50	0.63	25
1.42	100	1.35	100	0.95	50
1.93	150	1.84	150	1.23	75
2.43	200	2.38	200	1.50	100
2.97	250	2.99	250	1.76	125
3.54	300	3.65	300	2.04	150
4.14	350	4.19	350	2.32	175
4.73	400	4.59	400	2.63	200
				2.95	225
				3.29	250
				3.63	275
				3.96	300
				4.24	325
				4.49	350
				4.70	375

Table 6 No 2 Pistons (High Load)

Pressure Bar	Load N
0	0
0.37	200
0.66	400
0.97	600
1.25	800
1.56	1000
1.86	1200
2.17	1400
2.49	1600
2.81	1800
3.13	2000
3.46	2200
3.79	2400
4.10	2600
4.41	2800
4.71	3000

Table 7 Heated Plate Apparatus (Friction)

Load N	5/06/83 μ s	30/09/83 μ s
0	0.6	0.3
1.96	3.6	3.3
11.77	10.8	10.6
21.58	19.5	19.4
31.39	28.5	28.5
41.20	38.1	38.2
51.02	47.7	47.7
60.82	57.9	58.0
68.67	68.1	68.2
80.44	78.6	78.8
90.25	91.2	91.4
100.06	104.1	104.4
119.68	128.4	128.8
137.64	155.4	156.0
156.96	182.7	183.4
178.54	221.7	223.0

Table 8 Heated Plate Rig (Load)

Load N	5/06/83 Pressure Bar	30/09/83 Pressure Bar
0	0	0
25	-	0.24
50	0.69	0.50
75	-	0.77
100	1.23	1.04
125	-	1.32
150	1.72	1.59
175	-	1.85
200	2.20	2.12
225	-	2.38
250	2.70	2.63
275	-	2.88
300	3.22	3.13
325	-	3.37
350	3.76	3.62
375	-	3.86
400	4.31	4.11
425	-	4.37
450	4.83	4.63

APPENDIX M

Table 1 Effect of Surface Finish and Hardness

Hardness Vickers HV(40)	Surface Finish			μ_{max}	μ_{min}	Wear- Rate Total
	Plate microns Ra	Pin microns Ra	Total microns Ra			
239.4	0.09	0.453	0.543	0.46	0.30	0.45
214.7	0.09	0.453	0.543	0.58	0.40	0.08
189.3	0.125	0.453	0.578	0.49	0.31	0.34
186.6	0.147	0.695	0.842	0.55	0.25	0
284.0	0.20	0.453	0.654	0.47	0.42	0
234.8	0.204	0.695	0.899	0.81	0.76	0
234.0	0.313	0.695	1.008	0.96	0.30	0.48
241.4	0.37	0.695	1.065	0.95	0.51	0.08
248.6	0.868*	0.695	1.563	0.68	0.37	0
203.3	0.913*	0.695	1.608	0.59	0.48	0.08

* Deliberately Roughened

Effect of Oxygen Content

Table 2 Argon/Air Mixture, Load = 100 N, Speed = 20 mm/s
Total Gas Flow = 20 ml/s

Oxygen Content (% vol)	Oxygen Flow (mg/min)	μ	Wear Rate (mg/m)
2.5	48.3	2.92	4.9
5.0	96.6	2.07	3.9
7.8	150.6	1.81	-
10.0	193.1	1.37	2.82
12.5	241.4	1.22	1.30
15.0	289.7	0.78	0.92
17.5	337.9	0.83	1.08

Table 3 Argon/Air Mixture, Load = 100 N, Speed = 10 mm/s,
Total Gas Flow = 20 ml/s

Oxygen Content (% vol)	Oxygen Flow (mg/min)	μ	Wear Rate (mg/m)	Vapour Pressure (mbar)
0.0	0.0	2.73	6.91	0.70
2.7	51.0	1.92	6.54	1.13
4.6	86.6	1.61	4.30	1.92
7.8	143.5	1.01	2.83	3.26
10.2	182.1	0.86	0.60	4.24
12.8	226.6	0.59	0.15	5.32
15.0	266.6	0.61	0.30	6.32
21.0	375.8	0.47	0.45	8.77

Table 4 Argon/Air Mixture, Load= 100 N, Speed = 10 mm/s,
Total Gas Flow = 12 ml/s

Oxygen Content (% vol)	Oxygen Flow (mg/min)	μ	Wear Rate (mg/m)
0.2	17.9	1.93	9.41
3.3	35.8	1.54	4.39
5.6	62.6	0.88	2.06
5.5	57.2	0.98	3.17
7.6	83.1	1.34	4.07
10.1	109.9	0.88	2.78
12.5	130.5	0.69	0.25
14.75	154.7	0.52	0.43
17.3	166.3	0.64	0.13
21.0	220.8	0.58	0.08

Table 5 Argon/Oxygen Mixture, Load = 100 N, Speed = 10 mm/s
Total Gas Flow = 20 ml/s

Oxygen Content (% vol)	Oxygen Flow (mg/min)	μ	Wear Rate (mg/m)
0.0	0.0	1.87	6.36
2.4	35.8	1.66	5.01
5.6	82.2	1.58	3.89
7.8	118.9	1.30	2.14
11.4	162.4	1.09	3.79
13.1	190.4	1.22	3.78
14.8	221.7	1.49	3.50
22.1	330.8	0.82	1.0
30.1	438.8	0.83	0.48

Table 6 Argon/Air Mixture, Load = 50 N, Speed = 10 mm/s,
Total Gas Flow = 20 ml/s

Oxygen Content (% vol)	Oxygen Flow (mg/min)	μ	Wear Rate (mg/m)	Vapour Pressure (mbar)
0	0	4.4	21.80	1.62
2.21	30.0	2.18	11.27	1.75
5.73	77.2	1.36	8.05	2.67
6.84	100.3	1.03	4.30	3.00
9.01	125.75	0.75	0.68	4.47
12.6	181.48	0.68	0.72	5.42
15.7	232.93	0.95	0.40	5.56
17.75	234.35	0.32	0.24	8.09
21.0	292.95	0.60	0.11	10.22

Effect of Water Content

Table 7 Environment = Hydrogen, Load = 50 N, Speed = 10 mm/s
Total Gas Flow = 20 ml/s

Dewpoint (°C)	Vapour Pressure (mbar)	μ	Wear Rate (mg/m)
-2.20	5.07	2.91	15.33
5.00	8.72	2.11	7.70
6.10	9.42	2.05	11.10
10.90	13.03	0.55	0.65
13.85	15.82	0.24	0.22
15.84	17.99	0.16	0.17
18.46	21.24	0.15	0.62

Table 8 Environment = Hydrogen, Load = 100 N. Speed =
10 mm/s, Total Gas Flow = 20 ml/s

Dewpoint (°C)	Vapour Pressure (mbar)	μ	Wear Rate (mg/m)
-2.72	4.76	1.63	24.6
2.5	7.31	2.88	31.79
5.9	9.28	3.07	32.03
10.9	13.03	2.46	34.24
14.7	16.72	2.04	33.35
15.8	17.98	0.34	0.03
17.4	19.86	0.54	3.48
20.3	23.82	0.24	0.0

Table 9 Environment Nitrogen, Load = 75 N, Speed = 10 mm/s

Dewpoint (°C)	Vapour Pressure (mbar)	μ	Wear Rate (mg/m)
-0.5	5.88	4.22	33.64
5.0	8.72	4.41	39.3
8.8	11.32	3.40	27.38
12.1	14.11	4.96	30.84
13.9	15.87	1.66	13.69
15.0	17.04	3.70	13.42
16.1	18.29	3.34	-
16.9	19.24	0.27	0.0
20.5	24.11	0.74	0.04

Table 10 Environment = Nitrogen, Load = 100 N,
Speed = 10 mm/s

Dewpoint (°C)	Vapour Pressure (mbar)	μ	Wear Rate (mg/m)
-0.85	5.73	2.85	25.6
-0.25	6.00	1.93	33.3
10.0	12.27	1.99	21.2
10.5	12.69	4.13	34.11
13.9	15.87	0.76	0.5
15.0	17.04	3.1	16.97
17.3	19.74	3.0	33.29
18.3	21.02	2.45	37.05
18.5	21.29	1.98	14.51
19.3	22.38	0.77	0.26
20.0	23.38	0.423	0.0
20.3	23.82	0.42	0.2
21.0	24.86	0.711	0.0
23.9	29.18	0.66	0.55

Table 11 Environment = Argon, Load = 50 N, Speed = 10 mm/s

Dewpoint (°C)	Vapour Pressure (mbar)	Water Flow (mg/min)	μ	Wear Rate (mg/m)	Total Gas Flow (ml/s)
-0.5	5.88	5.39	7.05	35.0	20.66
5.3	8.90	8.43	6.20	34.0	21.37
5.93	9.30	9.05	4.82	22.1	21.96
6.90	9.95	9.96	0.63	0.03	22.59
8.8	11.32	11.72	0.65	0.0	23.36
9.3	11.71	10.51	5.97	27.8	20.24
10.0	12.27	11.64	1.69	14.2	21.40
10.1	12.35	11.22	1.88	13.86	20.49
10.6	12.77	12.23	0.85	0.02	21.61
11.1	13.21	12.59	1.44	6.04	21.49
11.5	13.56	12.94	0.28	0.03	21.52
13.0	14.97	13.98	0.73	0.0	21.07
13.2	15.17	14.68	0.62	0.05	21.83
16.0	18.17	16.59	0.62	0.08	20.60
20.4	23.96	19.31	0.41	0.08	18.18

Table 12 Environment = Argon, Load = 100 N, Speed = 10 mm/s

Dewpoint (°C)	Vapour Pressure (mbar)	μ	Wear Rate (mg/m)
1.0	6.57	4.84	24.75
6.9	9.95	4.37	16.01
15.11	17.17	5.09	45.03
17.0	19.37	5.57	40.07
18.44	21.21	0.30	0.0
19.25	22.31	0.30	0.77

Table 13 Environment = Argon, Load = 50 N, Speed = 10 mm/s

Dewpoint (°C)	Vapour Pressure (mbar)	Water Flow (mg/min)	μ	Wear Rate (mg/m)	Total Gas Flow (ml/s)
-12.8	2.02	0.79	5.64	26.2	8.8
0.1	6.15	2.40	2.10	14.09	8.8
2.27	7.19	2.81	3.62	19.84	8.8
4.1	8.19	3.19	2.03	13.45	8.8
6.88	9.93	3.87	6.46	27.24	8.8
8.86	11.37	4.44	2.83	10.83	8.8
9.0	11.47	4.47	2.18	9.71	8.8
10.0	12.27	4.79	3.14	10.9	8.8
10.43	12.63	4.93	0.78	0.1	8.8
11.6	13.65	5.33	0.63	0.06	8.8
13.09	15.06	5.88	1.67	9.28	8.8
13.96	15.94	6.22	0.62	0.09	8.8
15.0	17.04	6.65	0.67	0.106	8.8
17.5	19.99	7.80	0.68	0.04	8.8

Table 14 Environment = Mixed Gas, Load = 50 N,
Speed = 10 mm/s

Dewpoint (°C)	Vapour Pressure (mbar)	μ	Wear Rate (mg/m)
2.4	7.26	1.73	13.43
3.2	7.68	2.18	17.77
5.5	9.03	2.3	17.80
6.0	9.35	0.51	12.80
7.35	10.26	0.08	0.03
9.0	11.47	0.58	3.32
11.8	13.83	0.1	0.113

Table 15 Environment = Mixed Gas, Load = 100 N, Speed = 10 mm/s

Dewpoint (°C)	Vapour Pressure (mbar)	μ	Wear Rate (mg/m)
-0.45	5.91	1.55	29.12
5.8	9.22	2.15	19.08
10.0	12.27	1.22	24.89
10.85	12.99	2.72	57.44
12.2	14.20	2.6	58.43
13.43	15.40	0.4	0.0
14.6	16.61	1.14	27.47
15.225	17.29	0.32	0.07
16.93	19.28	0.23	0.45

Table 16 Environment = CO₂, Load = 100 N, Speed = 10 mm/s

Dewpoint (°C)	Vapour Pressure (mbar)	μ	Wear Rate (mg/m)
-20.76	0.96	2.02	21.02
-4.7	4.13	1.99	15.34
-1.46	5.44	2.16	15.58
0.23	6.21	0.97 ¹⁾	9.26
0.91	6.53	0.75 ¹⁾	6.76
2.06	7.09	1.07 ¹⁾	8.57
3.29	7.73	1.05 ¹⁾	6.36
4.19	8.24	0.174	0.0
5.49	9.02	0.952 ¹⁾	8.87
8.24	10.90	0.92 ¹⁾	6.15
10.1	12.35	0.325	0.0
10.27	12.50	0.325	0.0
12.42	14.41	0.196	0.0
15.93	18.09	0.469	0.08
16.85	19.18	0.425	0.0

1) one sided scuff

Table 17 Environment = Air, Load = 100 N, Speed = 10 mm/s

Dewpoint (°C)	Vapour Pressure (mbar)	μ	Wear Rate (mg/m)
-15.67	1.57	1.93	16.47
-2.33	5.06	1.66	9.88
-0.23	6.00	1.77	13.09
2.6	7.36	1.33	5.5
5.17	8.82	0.67	1.44
7.6	10.43	0.60	2.47
9.2	11.63	0.68	5.01
9.79	12.10	0.87	1.3
11.16	13.26	0.44	3.18
12.43	14.42	0.51	0.93
13.34	15.31	0.517	0.172
15.2	17.26	0.571	0.09

Table 18 Environment = Oxygen, Load = 100 N, Speed = 10 mm/s

Dewpoint (°C)	Vapour Pressure (mbar)	μ	Wear Rate (mg/m)
-22.3	0.82	1.17	1.87
-11.66	2.24	1.03	1.83
0	6.11	1.30	0.53
2.53	7.33	0.88	0.81
3.93	8.09	1.13	0.74
7.19	10.15	1.03	0.69
10.1	12.35	0.95	1.0
12.9	14.87	0.69	0.6
14.9	16.93	0.90	0.42
16.4	18.64	0.92	0.59

Table 19 Environment = Argon, Speed = 10 mm/s

Dewpoint (°C)	Vapour Pressure (mbar)	Scuff Load (N)	Archard Temp. (°C)	P _S (Bar)	$\frac{P_L}{P_S}$ x 10 ⁻³
0.5	6.34	11	47.3	0.105	60.3
2.5	7.31	21	57.7	0.181	40.3
4.9	8.66	33	67.28	0.285	30.38
8.95	11.44	76	91.75	0.756	15.13
11.0	13.12	76	91.75	0.756	17.35
17.2	19.61	92	98.94	0.95	20.6
21.5	25.62	195	134.9	3.10	8.26
11.5		50	78.19	0.437	26.3
21.0		100	102.3	1.10	19.09

APPENDIX N

Heated Plate Experiments

Shell Risella

Table 1 Environment = Argon, Load = 100 N, Speed = 10 mm/s, Total Gas Flow = 50 ml/s

Temp. (°C)	μ	Wear Rate (mg/min)	Duration (mins)	Comments
20	0.410	0	410	
50	0.476	0	195	
100	0.424	0.03	195	
120	0.5	0	195	
140	0.346	0	195	
160	0.419	0	195	
180	0.570	0.68	180	Pin broke on cooling
200	4.00	-	4	Pin broke
220	4.00	3.96	2	Pin broke
250	4.00	13.56	2	Pin broke

Shell Risella

Table 2 Environment = Argon, Load = 200 N, Speed = 10 mm/s, Total Gas Flow = 50 ml/s

Temp. (°C)	μ	Wear Rate (mg/min)	Duration (mins)	Comments
100	0.2	0	195	
120	0.23	0	375	
140	0.31	0.082	195	
145	0.25	0	195	
150	2.0	1.792	4	Pin broke
160	2.0	-	11.5	Pin broke
180	2.0	2.10	8	Pin broke
200	2.0	1.19	3.5	Pin broke

CSB 460

Table 3 Environment = Argon, Load = 200 N, Speed = 10 mm/s, Total Gas Flow = 50 ml/s

Temp. (°C)	μ	Wear Rate (mg/min)	Duration (mins)	Comments
100	0.237	0.302	195	
140	0.621	0.70	195	
160	2.0	0.42	72	Pin broke
180	0.60	0.24	195	
200	2.0	1.14	180	Pin broke on cooling
220	0.62	0.32	195	
240	2.0	4.08	4.5	Pin broke

EP Oil

Table 4 Environment = Argon, Load = 200 N, Speed = 10 mm/s, Total Gas Flow = 50 ml/s

Temp. (°C)	μ	Wear Rate (mg/min)	Duration (mins)	Comments
20	0.04	0.017	195	8°C Temperature rise
100	0.03	0	195	
120	0.03	0	195	
140	0.03	0	195	
160	0.02	0.03	195	
180	0.013	0	195	
200	2.0	63.5	1	Pin broke
220	2.0	9.97	2	Pin broke
250	2.0	-	57	Pin broke

Shell Risella

Table 5 Incremented Temperature Rise

Environment = Argon, Speed = 10 mm/s, Total Gas Flow = 50 ml/s

100 N Load		200 N Load	
Temp. (°C)	μ	Temp. (°C)	μ
20	0.03	20	0.33
50	0.04	50	0.34
100	0.06	100	0.40
120	0.06	120	0.50
140	0.06	140	0.36
160	0.14	160	0.33
180	0.10	180	0.34
200	0.14	200	0.34
220	0.15	220	0.34
240	0.15	240	0.47
		270	0.60

CSB 460

Table 6 Incremented Temperature Rise

Environment = Argon, Load = 200 N, Speed = 10 mm/s, Total Gas Flow = 50 ml/s

Temp. (°C)	μ
20	0.05
50	0.05
100	0.12
120	0.24
140	0.48
160	0.44
180	1.46
200	1.06
220	1.12
250	1.14

EP Oil

Table 7 Incremented Temperature Rise

Environment = Argon, Load = 200 N, Speed =
10 mm/s, Total Gas Flow = 50 ml/s

Temp. (°C)	μ
20	0.04
50	0.04
100	0.04
120	0.04
140	0.33
160	0.031
180	0.029
200	0.026
220	0.027
250	0.035

APPENDIX P

Properties of Gases

Physical Properties at 20°C

Purity

Hydrogen

$$\rho = 0.0842 \text{ Kg/m}^3$$

$$C_p = 14.27 \text{ KJ/Kg}^\circ\text{K}$$

$$\text{H}_2\text{O} < 3 \text{ vpm}$$

$$\text{CO}_2 < 2 \text{ vpm}$$

$$\text{Hydrocarbons} < 2 \text{ vpm}$$

Nitrogen

$$\rho = 1.250 \text{ Kg/m}^3$$

$$C_p = 1.039 \text{ KJ/Kg}^\circ\text{K}$$

$$\text{H}_2\text{O} < 10 \text{ vpm}$$

$$\text{O}_2 < 5 \text{ vpm}$$

Oxygen

$$\rho = 1.31 \text{ Kg/m}^3$$

$$C_p = 0.917 \text{ KJ/Kg}^\circ\text{K}$$

$$\text{H}_2\text{O} < 10 \text{ vpm}$$

$$\text{N}_2 < 10 \text{ vpm}$$

Air

$$\rho = 1.210 \text{ Kg/m}^3$$

$$C_p = 1.005 \text{ KJ/Kg}^\circ\text{K}$$

$$\text{H}_2\text{O} < 20 \text{ vpm}$$

$$\text{CO}_2 < 1 \text{ vpm}$$

$$\text{Hydrocarbons} < 3 \text{ vpm}$$

Mixed Gas (83% N , 12% CO , 5% CO)

$$\rho = 1.3226 \text{ Kg/m}^3$$

$$C_p = 0.996 \text{ KJ/Kg}^\circ\text{K}$$

$$\text{H}_2\text{O} < 10 \text{ vpm}$$

Argon

$$\rho = 1.668 \text{ Kg/m}^3$$

$$C_p = 0.5203 \text{ KJ/Kg}^\circ\text{K}$$

$$\text{H}_2\text{O} < 2 \text{ vpm}$$

$$\text{CO}_2 < 1 \text{ vpm}$$

$$\text{O}_2 < 2 \text{ vpm}$$

$$\text{N}_2 < 10 \text{ vpm}$$

$$\text{H}_2 < 1 \text{ vpm}$$

$$\text{Hydrocarbons} < 1 \text{ vpm}$$

Appendix P (cont'd)

Physical Properties at 20 C

Purity

Carbon Dioxide

$$\rho = 1.838 \text{ Kg/m}^3$$

$$C_p = 0.838 \text{ KJ/Kg}^\circ\text{K}$$

$$\text{H}_2\text{O} < 10 \text{ vpm}$$

$$\text{O}_2 < 5 \text{ vpm}$$

APPENDIX Q

Calculation of Oxide Film Depth

$$\text{Density of Fe}_2\text{O}_3 = 5.24 \times 10^3 \text{ Kg/m}^3$$

$$\text{Apparent Swept Area} = 185.13 \times 10^{-6} \text{ m}^2 \\ (\text{for two 4mm diameter pins})$$

Molecular Weight of Fe}_2\text{O}_3

$$\text{Fe} = 2 \times 56 = 112$$

$$\text{O} = 3 \times 16 = 48$$

$$\text{Total} = 160$$

Therefore oxygen is $\frac{48}{160} \times 100\%$ of the mass of Fe₂O₃

$$= 30\%$$

So for each Kg of Fe₂O₃ produced 30% will be oxygen and

1 mg of O₂ produces 3.33 mg of Fe₂O₃.

3.33 mg of Fe₂O₃ has a volume of

$$\frac{3.33 \times 10^{-6} \text{ m}^3}{5.24 \times 10^3} = 6.36 \times 10^{-8} \text{ m}^3$$

which gives a thickness of

$$\frac{0.636 \times 10^{-9} \text{ m}}{185.13 \times 10^{-6}} = 3.436 \times 10^{-6} \text{ m}$$

$$= 3.4 \text{ microns}$$

or 34,000 Å.

The time interval between passes (average) = 2 seconds

for 15 rpm

Therefore at 100 mg/min flowrate the amount of oxygen

$$\text{supplied per pass} = \frac{100}{30}$$

$$= 3.33\text{mg}$$

Appendix Q (cont'd)

which can produce 100,000 Å of thickness.

Even if only 0.1% was used, an oxide thickness of 100 Å can be produced.

Film produced for 1000 vpm at a flowrate of 20 ml/s

$$1000 \text{ vpm gives a volumetric flow of } \frac{20}{1000} \text{ ml/s}$$

$$= 20 \times 10^{-9} \text{ m}^3/\text{s}$$

$$\text{density of oxygen} = 1.31 \text{ Kg/m}^3$$

therefore the mass flowrate of oxygen is 2.62×10^{-8} Kg

$$\text{or } 0.0262 \text{ mg}$$

which from the above would give a film thickness of

$$\begin{aligned} & 34000 \times 0.0262 \text{ Å} \\ & = 890 \text{ Å} \end{aligned}$$

APPENDIX R

Temperature of Rubbing Surfaces (Archard 1958/9)

Speed Criterion

$$S_c = U_r / 2x$$

$$x = K / \rho c$$

r depends upon the applied load w.

Assuming plastic deformation:

$$r = \left(\frac{wL}{\pi p} \right)^{\frac{1}{2}}$$

Temperature Rise

From Archard, with plastic deformation and low speed
(where $S_c < 0.1$)

$$m = \mu g \left(\frac{\pi p_m}{8K} \right)^{\frac{1}{2}} L^{\frac{1}{2}} u$$

Experimental Data

For tests in argon:

$$\begin{aligned} V &= 10 \text{ mm/s} \\ K &= 76 \text{ W/m}^{\circ}\text{K} \\ \rho &= 7.9 \times 10^3 \text{ Kg/m}^3 \\ c &= 437 \text{ J/Kg}^{\circ}\text{K} \\ L &= 100 \text{ N} \\ p_m &= 2300 \times 10^6 \text{ N/m}^2 \\ \mu &= 0.6 \text{ (non-scuff)} \end{aligned}$$

For speed criterion

$$S_c = 0.026 \text{ ie. low speed criterion applies}$$

∴ for 100 N load contact temperature

$$\theta_m = \frac{0.6 \times 9.81 \times (\pi \times 2300 \times 10^6)^{\frac{1}{2}} \times 10 \times 10 \times 10^{-3}}{8 \times 76}$$

$$= 82.3$$

(PTO)

Appendix R (cont'd)

$$\begin{aligned}\text{Actual Temperature} &= \theta_m + \theta_a \\ &= 102.3^\circ\text{C}\end{aligned}$$

APPENDIX S

Load on the Cylinder Wall

From Eilon (1975), the load on a cylinder wall from a piston ring (see Figure S.1) can be expressed as follows:

$$P_m A_1 = P_1 A_3 - \mu P_1 A_2 + P_2 A_1 \quad S.1$$

and from Neale (1975) the ring pressure (P_2) can be expressed as:

$$P_2 = \frac{E n q}{7.07 D (D/d - 1)^3} \quad S.2$$

From figure S.1 the areas A_1 , A_2 , and A_3 can be expressed in terms of D , d , b and h :

$$A_1 = 2b\pi D \quad S.3$$

$$A_2 = (d-h_p) \pi (D-d) \quad S.4$$

$$A_3 = 2b\pi (D-2d) \quad S.5$$

If we assume that most piston rings are square in cross-section (Neale 1975) then:

$$b = d/2$$

ie. axial width = radial width

and if we let $\frac{d}{D} = X$ or $d = DX$

we can substitute for d and b in equations S.3 to S.5

$$A_1 = \pi D^2 X \quad S.6$$

$$A_2 = \pi (DX-h_p)(D-DX) \quad S.7$$

$$A_3 = \pi D^2 X (1-2X) \quad S.8$$

However, the ring clearance (h_p) is very small compared to the radial width (DX), therefore equation S.7 becomes:

$$A_2 = \pi D^2 X (1-X)$$

Thus if we substitute for A_1 , A_2 and A_3 into S.1 and S.2 we get

$$P_m = P_i [(1-2X) - \mu(1-X)] + P_e \quad \text{S.9}$$

$$P = \frac{E_n q}{7.07D} \left(\frac{1}{X} - 1\right)^3 \quad \text{S.10}$$

From Neale, for piston rings the ratio of radial thickness to diameter (X) varies between 0.045 and 0.029, and the ring gap (q) is between $3d$ and $4d$.

So as an approximation let

$$X = \frac{0.045 + 0.029}{2} = 0.037$$

$$\text{and } q = 3.5d = 3.5dX$$

Thus if we substitute these values into S.9 we get

$$P_m = P_i [(1-0.074) - \mu(1-0.037)] + \frac{0.13E_n}{7.07 \left(\frac{1}{0.037} - 1\right)^3} \quad \text{S.11}$$

$$\text{For Cast Iron } E_n = 104 \times 10^9 \text{ N/m}^2$$

So as a further approximation

$$P_m = P_i (1-\mu) + \frac{1.08 \times 10^5}{(1 \text{ bar})}$$

The maximum pressure in the ring wall occurs when $\mu \approx 0$ which gives

$$P_m \approx P_i + 1 \text{ bar}$$

which for compressors operating over 100 bar

$$P_m \approx P_i$$

ie. mean wall pressure \approx discharge pressure if the ring is the top piston ring.

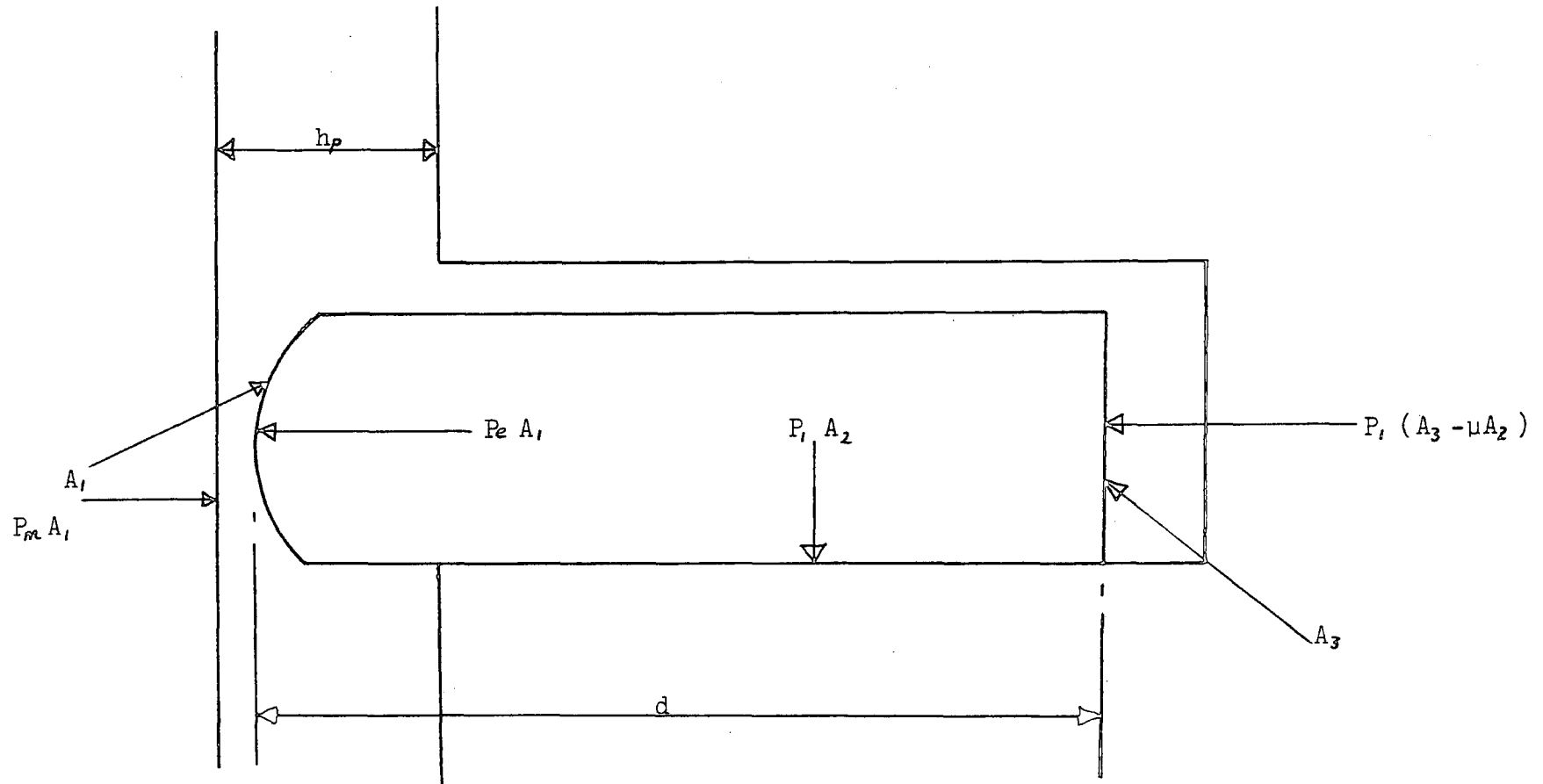


Figure S.1 Force Exerted by the Piston Ring on the Cylinder Wall

APPENDIX T

Electron Spectroscopy for Chemical Analysis (E.S.C.A.)

In electron spectroscopy for chemical analysis (E.S.C.A.) low energy electrons emitted by the specimen are analysed to provide composition information in the one to ten atom layer region near the surface. A solid sample in a high vacuum system is irradiated with a high flux of X-rays. When an X-ray photon with energy $h\lambda$ (Planck's constant multiplied by the frequency) impinges on a solid, the ejected photo-electrons (see Figure T.1) have a kinetic energy distribution made up of discrete bands reflecting the specimen's electronic structure. The experimental determination of the kinetic energy, E_k , of the photoelectrons enables the binding energy, E_b , to be calculated from the equation:

$$E_k = h\lambda - E_b \quad \text{T.1}$$

The photoelectron spectrum therefore consists of a series of peaks at discrete values of E_k corresponding to particular values of E_b . The precise location of the measured peaks identifies not only the elements present, but also their chemical environment.

The difference between the binding energy of the inner-shell electrons in a free atom and in an ion of the same element in a given chemical surrounding is called a chemical shift. An example of the shift in binding energy due to the sample chemistry is shown in Figure T.2 (Wagner et al 1976) for iron and iron oxide (Fe_2O_3).

Since X-rays cause little damage, E.S.C.A. is particularly appropriate for analysing plastics and other organic materials easily damaged by other types of radiation. However, although the spectrum is produced by the uppermost surface layers, the analysis is performed on a relatively large area.

Bibliography: M.W. Roberts (1981)
Allen and Wild (1981)

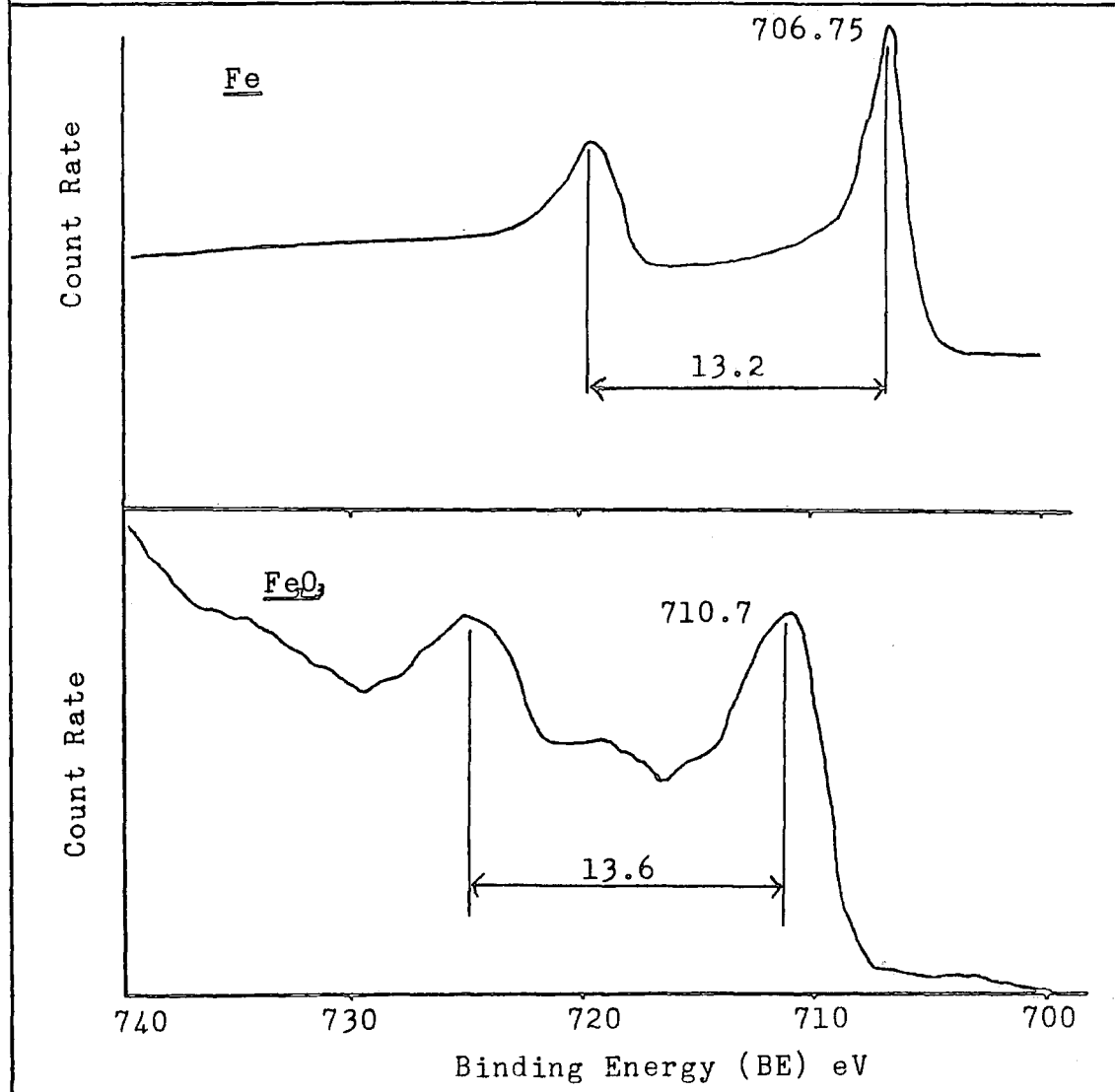
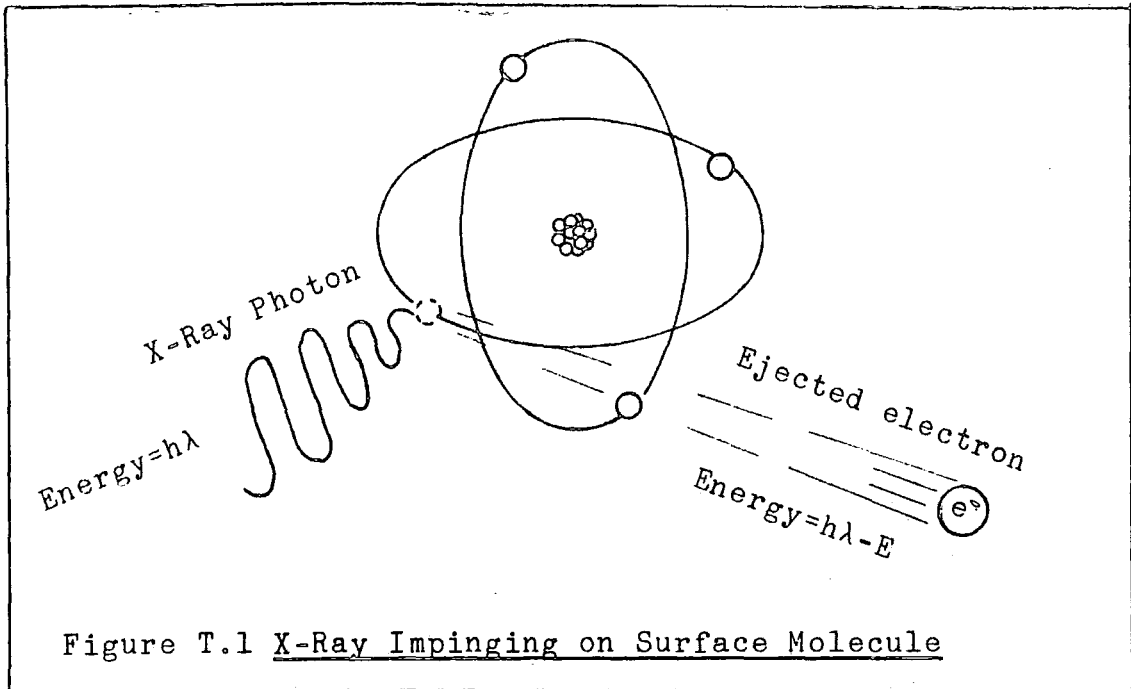


Figure T.2 The Chemical Shift Effect in E.S.C.A.

REFERENCES

- Allen G.C. and Wild R.K. (1981) "Probing the secrets of solid surfaces", C.E.G.B. Research, 11, 12-24.
- Archard J.F. (1953) "Contact and rubbing of flat surfaces", J Appl Phys, 24(8), 981-988.
- Archard J.F. (1958) "The temperature of rubbing surfaces", Wear, 2, 438-455.
- Bailey M.W. and Cameron A. (1973) "The influence of temperature and metal pairs on the scuffing of a commercial oil", Proc Inst. Mech. Engrs, 187, 757-761.
- Barnes D.J., Wilson J.E., Stott F.H. and Wood G.C. (1977) "The influence of oxide films on the friction and wear of Fe-5% Cr alloy in controlled environments", Wear, 45, 161-176.
- Bowden F.P. and Rowe G.W. (1955) "The adhesion of clean metals", P ROY SOC A, 233, 429.
- Bowden F.P. and Tabor D. (1974) "Friction (An introduction to tribology)", Heinemann Educational Books, London.
- Bowden F.P. and Young J.E. (1951) "Friction of clean metals and the influence of adsorbed films", P ROY SOC A, 208, 211.
- Campbell W.E. and Summit N.J. (1936) "Studies in boundary lubrication: Variables influencing the coefficient of static friction between clean and lubricated metal surfaces", ASME Trans, 61, 633-41.
- Davies C.B. (1951) "Influence of roughness and oxidation on wear of lubricated sliding metal surfaces", ANN NY ACAD, 53, 919-935.
- Eilon S. and Saunders A. (1957) "A study of piston-ring lubrication", Proc. Inst. Mech. Engrs, 171, 427-443.
- Godfrey D. (c 1965) "Boundary lubrication", Symposium on Lubrication and Wear, Edited by Shaw and Macks, 283-306.
- Grew W.J.S. and Cameron A. (1972) "Thermodynamics of boundary lubrication and scuffing", P ROY SOC A, 327, 47-59.
- Hale G.T. and Hodge R.N. (1969) "Safety and reliability of high pressure hydrogen compressors", Report on discussions held with Agricultural Division, Air Products Teesside, Cassel and Bain Works, ICI report MD 10342.

Hughes D.W. (1979) "A comparison of the wear characteristics of plastic-plastic contacts in continuous and intermittent tests", Final year project report, Department of Engineering, University of Durham.

Irving R. and Scarlett N.A. (1963) "Wear problems with grease lubricated rolling bearings in inert atmospheres", Inst. Mech. Engrs, Lubrication and Wear Convention, paper 29.

Jones J.A., Moore H.D. and Scarlett N.A. (1969) "Grease lubrication of ball bearings in helium", Inst. Mech. Engrs, Symposium on Lubrication in Hostile Environments, paper 1.

Jones W.R. (1982) "Boundary lubrication - Revisited", NASA report no. TM-82858.

Jones W.R. and Hady W.F. (1970) "The effect of humidity and a wettability additive on polyphenyl ether boundary lubrication of steel in air and nitrogen to 350 C", NASA report no TN D-6055.

Kragelski I.V. (1965) "Friction and Wear", Butterworths, London.

Lancaster J.K. (1962) "The influence of the conditions of sliding on the wear of electrographic brushes", Br J Appl Phys, 13, 468-476.

Lancaster J.K. and Pritchard J.R. (1981) "The influence of environment and pressure on the transition to dusting wear of graphite", J Phys D (Appl Phys), 14, 742-762.

Lloyd T. (1979) "The hydrodynamic lubrication of piston rings", Inst. Mech. Engrs, Tribology Convention 1979, 183, pt 3P, paper 5.

Marshall J.B. (1983) "A study of the effect of temperature on boundary lubrication in inert atmospheres", Final year project report, Department of Engineering, University of Durham.

Michell Instruments Ltd (1980) "Series 2000 dewpoint hygrometer", Michell Instruments Ltd, Publication Ref: 2000 - 80/2.

Montgomery R.S. (1969) "Run in and glaze formation on grey cast iron surfaces", Wear, 14, 99-105.

Moore D.F. (1975) "Principles and applications of tribology", Pergamon Press, Oxford, 144.

Moore S.L. and Hamilton G.M. (1980) "The piston ring at top dead centre", Inst. Mech. Eng. Proc, 194, 373-381.

Numerical Algorithms Group (1978) "NAG Library Routine E01ACF", Fortran library manual MK 7 vol 2, Numerical Algorithms Group.

National Centre for Tribology (1971-73) "Investigation on the effect of atmospheric environment on the lubrication of reciprocating metal contacts", Various reports from NCT Risley to ICI Billingham.

Neale M.J. (1975) "Tribology Handbook", Newnes-Butterworths, London, A31.

Rabinowicz E. (1966) "Friction and wear of materials", John Wiley and Sons, New York, London, Sydney, 109-197.

Roberts M.W. (1981) "Photoelectron spectroscopy and surface chemistry", Chemistry in Britain, 17, 510-514.

Savage R.H. and Schaeffer D.L. (1956) "Vapor lubrication of graphite sliding contacts", J Appl Phys, 27 (2), 136-138.

Scheel L.F (1961) "Gas and air compression machinery", McGraw-Hill Book Company, London, 33-57 and 210-227.

Stribeck R. (1902) "Characteristics of plain and roller bearings", Zest V.U.L., 46.

Sugishita J. and Fujiyoshi S. (1981) "The effect of cast iron graphites on friction and wear performance: II Variables influencing graphite film formation", Wear, 68 (1), 7.

Summers-Smith D. (1979) "Lubrication in inert and reducing atmospheres", Letter.

Summers-Smith D. (1975) "Lubrication of reciprocating compressors handling dry, inert and reducing gases", ICI Agricultural Division, Confidential Report No. A 20, 521.

Summers-Smith D. (1981) "Lubrication in inert and reducing atmospheres", ICI internal note 1981.

Taylor Instrument Analytics Ltd, Instruction manual for the Servmex OA.570, Taylor Instrument Publication.

Unsworth A. (1976) "Biological bearings and their replacement", Spectrum, 138, 14-16.

Wagner C.D., Riggs W.M., Davis L.E., Moulder J.F. and Muilenburg G.E. (1973) "Handbook of X-ray photoelectron spectroscopy", Perkin-Elmer Corporation, Minnesota.